CROP BASED CLIMATE REGIMES

FOR ENERGY SAVING IN

GREENHOUSE CULTIVATION

Promotor:
PROF. DR. IR. HUGO CHALLA*
hoogleraar Tuinbouwbedrijfstechnologie

Leden van de promotiecommissie:
PROF. DR. H.-P. LIEBIG
Universität Hohenheim, Stuttgart, Duitsland

DR. J. M. AASLYNG
Den Kgl. Veterinær- og Landbohøjskole, Kopenhagen, Denemarken

DR. F. BUWALDA
Praktijk Onderzoek Plant en Omgeving, Aalsmeer, Nederland

PROF. DR. IR. G.P.A. BOT
Wageningen Universiteit, Wageningen, Nederland

———————————

*Na diens overlijden vertegenwoordigd door
PROF. DR. IR. GERRIT VAN STRATEN
hoogleraar Meet-, regel en systeemtechniek

CROP BASED CLIMATE REGIMES

FOR ENERGY SAVING IN

GREENHOUSE CULTIVATION

OLIVER KÖRNER

ABSTRACT

Körner, O. Crop based climate regimes for energy saving in greenhouse cultivation. Thesis Wageningen University, Wageningen, The Netherlands, 240 pp.; English, Dutch and German summaries.

Sustainability is one of the major aims in greenhouse horticulture. According to agreements between the Dutch grower association and the government, energy consumption and the use of chemical biocides have to be reduced. More advanced greenhouse technique is beeing developed to reach the target to decrease the energy efficiency-index by 65 % between 1980 and 2010. However, this could also be achieved with existing technology by using more advanced climate regimes. The present thesis aimed at that, through designing and analysing climate regimes while employing existing climate control possibilities. Theoretical temperature and humidity regimes were designed to decrease energy consumption and a photosynthesis maximisation procedure was implemented to maximise growth.

The basis for a crop gross photosynthesis model for control purposes was created. Crop photosynthesis models were evaluated at conditions expected to occur with more sustainable climate regimes. It was shown with experimental evidence that theoretical assumptions on the temperature – CO_2 effects in a crop that are based on theoretically models scaling up leaf photosynthesis to the crop level are valid and that simplified existing models could be applied up to 28 °C. With higher temperatures new designs are needed and this can probably be achieved with an improved stomata-resistance model.

The well known temperature integration principle was modified with two nested time-frames (24-hour and six days) and a temperature dose-response function. In a year round tomato cultivation, energy consumption was predicted to decrease with up to 9 % compared to regular temperature integration.

The potential for energy saving with temperature integration is limited by humidity control when as usual fixed set points are maintained, because it counteracts temperature integration. Vents open at lower temperatures and heating is switched on at higher temperatures than required for optimal effects of temperature integration. A new approach to control relative humidity on the underlying processes (crop growth and develoment, plant water stress, calcium deficiencies and the major fungal diseases) by controlling relative humidity through maximum leaf wetness duration, minimum transpiration and transpiration integral was designed for cut chrysanthemum. This idea is based on earlier formulations to use set points for transpiration. In the current approach, general rules were formulated. From that, a control regime was designed. Simulations showed that with this humidity regime, yearly energy consumption could be reduced by 18 % (compared to a fixed setpoint of 80 % relative humidity).

When the two climate control principles, modified temperature integration and process based humidity control, were merged, annual energy consumption was predicted to decrease by more than 33 % and cut chrysanthemum plant dry weight increased with 39 % in experiments compared to a normal climate regime.

Cut chrysanthemum was used as a central crop. Here, short compact stems is one of the main quality aspects. This is commonly controlled with chemical growth retardants. An alternative is to control temperature according to the *DIF* concept (difference between average day and average night temperature). A negative *DIF* value decreases stem elongation. Therefore, temperature integration without *DIF* restriction was extensively compared to temperature integration with *DIF* restriction. Energy consumption with different settings was quantified. It was shown that an optimisation problem existed in spring and summer. For that purpose, a joined temperature integration and *DIF* regime over several days was designed and tested. The use of an average *DIF* over several days rather than a *DIF* within 24-hours was proposed. In times and climate regions when cold and warm days interchange, this approach can increase energy saving and decrease final plant stem length simultaneously. This however, was a compromise. An optimisation problem between the two regimes aiming at sustainable greenhouse horticulture remained (less energy consumption versus reduction in application of biocides). This can only be solved when detailed models for crop quality, development and growth will become available.

The regimes could be applied in commercial greenhouses with only little adjustment. The only additional expense is a computer functioning as set point generator, and a suitable interface with the existing climate computer. In addition, the achieved degrees of freedom for two main states (temperature and humidity) form a promising perspective for future optimal greenhouse climate control. The regimes, however, were based on many arbitrary assumptions. More research is needed for parameterisation.

Key words: Biocides, cut chrysanthemum, *Chrysanthemum grandiflorum*, CO_2, crop photosynthesis, *DIF*, energy saving, fungal diseases, humidity control, plant quality, simulation model, stem elongation, temperature integration.

VOORWOORD

Na meer dan vier jaar is het proefschrift dus af. Er waren weinig weken waarin ik niet over andere mogelijkheden dan het afronden van dit onderzoek heb gedacht. Steeds opnieuw weer mijzelf motiveren door te gaan, was misschien wel het moeilijkste aspect van promoveren. Ik heb dan ook geleerd dat je als eenling niet veel bereikt, dat je anderen echt nodig hebt. Zo is deze proefschrift ook als een soort groepswerk te zien. Steun heb ik van verschillende kanten ontvangen en ik heb geleerd dat er naast support op je werkplek ook steun van vrienden en bekenden broodnodig is voor een goede prestatie.

Ten eerste zou ik vooral mijn leraar prof. dr. Hugo Challa willen bedanken. Hugo was voor mij de motor achter het project, een bijna onuitputtelijke bron van wetenschappelijke kennis en inzicht, een echte sparring partner. Daarnaast was hij bovenal menselijk en begripvol. Ik vond in hem verstandige begeleider en ben dankbaar dat ik met hem dit zeer leerzame traject heb mogen doorlopen.

Tijdens het projectwerk was prof. dr. Gerrit van Straten een belangrijke discussiepartner. Gerrit heeft dan ook in de laatste weken als vertegenwoordiger van Hugo mij bij in de laatste fase van mijn proefschrift begeleid. Daar wil ik hem bijzonder voor bedanken.

Een andere inspirator is dr. Ep Heuvelink. Ep houd ik mede 'verantwoordelijk' voor het feit dat ik met dit onderzoek begon -en tot het einde heb volgehouden. Ep, onze relatie is door de jaren heen veranderd: van mijn harde doch rechtvaardige begeleider van mijn afstudeervak ben je mijn persoonlijke adviseur en vriend geworden. Je hebt mij geleerd kritisch te kijken. Ik dank je zeer voor vele discussies en je vriendschap.

Door mijn achtergrond tuinbouwplantenteelt kwam ik vaak bij de vakgroep Tuinbouwproductieketens. Voor ondersteuning uit die hoek wil ik graag prof. dr. Olaf van Kooten bedanken. Voor assistentie met het netwerk en de simulaties wil ik Menno Bakker bedanken. Voor discussies over fotosynthese metingen dank aan dr. Jeremy Harbinson. Alle medewerkers van tuinbouwproductieketens dank ik voor commentaren tijdens mijn presentaties. Mijn eigenlijke werkplek was echter bij de vakgroep Agrarische Bedrijfstechnologie. Ook hier heb ik veel steun gekregen. Kees van Asselt en Geerten Lenters hebben veel uren in het bouwen en monteren van thermokoppels en data loggers gestoken. Kees heeft zich dan ook altijd voor mijn onderzoek ingezet en hem wil ik daarvoor zeer veel dank zeggen. Sam Blaauw bedank ik voor zijn inzet bij allerlei computerzaken; bij hem kon ik altijd terecht met alle klussen en problemen. Verder wil ik Bert van 't Ooster bedanken voor de prettige samenwerking. Vooral zijn inzet bij de laatste (zware) lootjes van proefschrift heeft mij enorm geholpen. Prof. dr. Joachim Müller en dr. Wim Huisman als vakgroepsleiders wil ik voor ondersteuning en mijn werkplek bedanken. En niet te vergeten: Corrie Seves en Miranda Tap - door hun ondersteuning heb ik nu nog steeds nauwelijks kennis van administratie. Aan alle niet genoemde collegas: Dank jullie allen voor ondersteuning en de prettige werksfeer.

In het kader van het Zonnekas-project wil ik prof. dr. Gerard Bot voor zijn leiding bedanken. Rachel van Ooteghem bedank ik voor nauwe samenwerking en haar opbouwende kritiek op mijn artikelen en de aanwijzigingen (tips en slimme trucs) bij het programmeren met Matlab. Dr. Gerard Van Willigenburg ben ik dankbaar voor leerzame gedachtewisseling over simulaties aan het begin van mijn werk. Dr. Cecilia Stanghellini, dr. Eldert van Henten, en dr. Wim van Meurs en Jouke Campen bedank ik voor de open en levendige discussies. Voor berekening van energie balansen bedank ik dr. Niko van der Braak, Peter Knies en Frank Kempkes. Vooral dr. Feije de Zwart en Gert Jan Swinkels bedank ik voor het beschikbaar stellen van de kas klimaat simulator KASSIM dat uiteindelijk centraal staat in dit proefschrift. Bert Houter, die destijds bij Priva werkte, dank ik voor interessante discussies over temperatuurintegratie.

Met dank en ter herinnering aan Hugo Challa

CONTENTS

MAIN ABBREVIATIONS

A	area (m^2)
b	temperature bandwidth (°C)
BP	blueprint temperature regime
BP_{fix}	fixed temperature set point control
Ca	Calcium
CCM	climate and control model
$[CO_2]$	CO_2 concentration
CT	constant flow method
DIF	difference average day- and average night temperature (°C)
$DIF_{t_{int}}$	difference day- and night temperatures averaged over the integration interval
$DIF_{t_{int},set}$	set point difference day- and night temperatures averaged over the integration interval
DIF_{set}	set point for difference between average day and average night temperature (°C)
DSG	Dutch Solar Greenhouse
DT	average daytime temperature (°C)
E_{CO_2}	CO_2 supply
EQ.	equation
EXP.	experiment
FIG.	figure
GD	growth and development
GH	greenhouse
GM	grey mould
Γ	CO_2 compensation point
h_n	number of night hours
I_{out}	outside global radiation (W m^{-2})
IRGA	infrared gas analyser
J_{max}	maximum electron transport rate
K	greenhouse heat transmission coefficient (W m^{-2} °C^{-1})
$K_{C,25}$	Michaelis Menten constants for Rubisco carboxylation
$K_{O,25}$	Michaelis Menten constants for Rubisco oxygenation
LAI	leaf area index (-)
L_{CO_2}	CO_2 leakage
LD	long -day
LT	long-term
LW	leaf wetness
LWD	leaf wetness duration (min)
NT	average nighttime temperature (°C)
P	probability
PAR	photosynthetic active radiation (W m^{-2})
P_g	gross photosynthesis (μmol m^{-2} s^{-1})
P_{gc}	crop gross photosynthesis (μmol m^{-2} s^{-1})
P_n	net photosynthesis (μmol m^{-2} s^{-1})
P_{nc}	crop net photosynthesis (μmol m^{-2} s^{-1})
PPFD	photosynthetic photon flux density (μmol m^{-2} s^{-1})

13

PM	powdery mildew
PWS	plant water stress
$Q_{10,Rd}$	Q10 for dark respiration
R_d	dark respiration rate (μmol m^{-2} s^{-1})
R_{dc}	crop dark respiration rate (μmol m^{-2} s^{-1})
RH	relative humidity (%)
$\rho_{O_{2i}}$	O$_2$ partial pressure (mbar)
ρ_{CO_2}	CO$_2$ partial pressure(mbar)
ROD	rate of decay
r	resistance (m s^{-1})
SEM	standard error of the mean
SD	short-day
SLA	specific leaf area (cm^2 g^{-1})
STD	standard deviation
ST	short-term
SPG	set point generator
τ	transmission
t	time
t_a	actual time
t_1	time at start of the 24-hour cycle
t_{24}	time at the end of the 24-hour cycle
T_c	crop temperature (°C or K)
T_{25}	temperature at 25 °C
τ_{dif}	transmission for diffuse radiation (%)
T_h	heating temperature set point (°C)
$T_{h,\text{init}}$	initial heating temperature set point (°C)
T_{in}	inside greenhouse temperature (°C)
$\overline{T}_{\text{in}}{}'$	updated and averaged 24-hour greenhouse temperature (°C)
T_l	leaf temperature
TI	Temperature integration
$T_{\text{in,real}}$	realised greenhouse temperature (°C)
TI_{24}	24-hour temperature integration
$TI_{24,DIF}$	24-hour temperature integration with DIF
TI_{DIF}	temperature integration with DIF
$TI_{\text{n},DIF}$	nested temperature integration with DIF
T_{out}	outside temperature (°C)
$\overline{T}_{\text{day}}$	average daytime temperature (°C)
$\tau_{s,b}$	blackout-screen-factor for short-wave transmission
$\tau_{s,e}$	energy-screen-factor for short-wave transmission
$\overline{T}_{\text{targ,24}}$	target 24-hour mean temperature (°C)
T_v	ventilation temperature set point (°C)
$T_{v,init}$	initial ventilation temperature set point (°C)
V	volume

$V_{C,\max}$	maximum carboxylation rate
VPD	vapour pressure deficit between crop and air
VPD_{air}	vapour pressure deficit of the air

Subscripts

a	actual
b	boundary layer
c	crop
cal	calibrated
d	dark
day	daytime
dif	diffuse
dir	direct
fix	fixed
flex	flexible
h	heating
init	initial
i	inside
in	inside
l	leaf
max	maximum
min	minimum
n	nested
o	outside
out	outside
real	realised
RH	relative humidity
s	stomata
sun	sunlit
T	temperature
targ	targeted
v	ventilation

CHAPTER 1

GENERAL INTRODUCTION

In the recent decennia the concern about anthropogenic greenhouse gas emission affecting the Earth's climate has grown strongly[1]. The nations of the world took a significant step to protect global climate by signing the *Framework Convention on Climate Change* in 1992 and five years later in Kyoto negotiations took place on the controls of emissions of greenhouse gases[2]. Greenhouse gases allow short-wave radiation from the sun to enter the atmosphere unimpeded. When this short-wave radiation strikes the Earth's surface, some of it is reflected as long-wave radiation (heat). Greenhouse gases tend to absorb this radiation as it is reflected back from the earth towards space, trapping the heat in the atmosphere. In the last 150 years, atmospheric concentrations of several important greenhouse gases as nitrous oxide (N_2O), methane (CH_4) and carbon dioxide (CO_2) have increased by about 25 % [3]. In particular, CO_2 emissions have increased dramatically since the beginning of the industrial age largely due to burning of fossil fuels and deforestation. The inter-governmental panel on climate change (IPCC) reported that global mean surface air temperature has increased between 0.3 °C to 0.6 °C since the late 19th century and the global sea level has risen between 10 and 25 cm over the past 100 years[3]. Based on estimates from IPCC computer models, the global mean surface temperature may rise an additional 1 °C to 3.5 °C between 1990 and 2100. Among the possible changes are further increases in sea level, transformation of forest and other ecosystems, modifications of crop yield, and shifts in the geographic range of pests and pathogens[3]. To protect the Earth from heating up, atmospheric CO_2 concentration
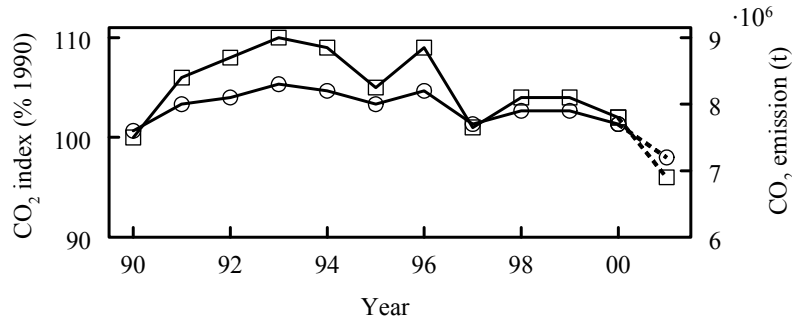
FIGURE 1. CO_2 emission (○) and index (□; based on 1990) of the greenhouse horticultural sector between 1990 and 2001. Values for 2001 were estimated (Source: Van der Knijff *et al.*, 2002 [7]).

must be reduced. Therefore, reductions of greenhouse gas emissions by an average of 6 % to 8 % from the 1990 levels between the years 2008 and 2012 was agreed between the industrial nations[2]. Some CO_2 reduction could be achieved by decreasing fossil fuel use, at little or no net cost through accelerated improvements in the efficiency of energy systems. In The Netherlands, the industry was split into subgroups for energy reduction targets. One subgroup was the agricultural sector whose emission of *greenhouse gases* was more than 10 % of the Dutch national total in 2000 [4, 5]. One third of that was CO_2. The major share of the CO_2 emission (80 %) could be directly attributed to greenhouse horticulture[4].

DUTCH GREENHOUSE HORTICULTURE AND ENERGY CONSUMPTION

Greenhouse horticulture in The Netherlands may be considered as the most intensive and sophisticated form of crop production[6]. In 2001, about 11,000 greenhouse growers used 10,159 ha for cultivation, mainly with vegetables and ornamental crops[7]. The sector has a large economical importance as it employs about 40,000 people; it has an annual return of € 3.2 billion and exports about 75 % of its produce[4]. With those values it is one of the most important export markets in the world. The Netherlands exported 14 % of the world value of horticultural production and 54 % of that was attributed to greenhouse production[8]. This strong intensification leads to environmental problems. Water and nutrient use, biocides, substrates or soil substitutes, handling material and fossil energy are the main contributing factors[9]. Most of those factors were reduced strongly in the last years by introducing new materials and cultivation procedures or large-scale implementation of biological control of pests[9]. However, the CO_2 emission governed by fossil energy consumption of this sector only recently decreased (FIG. 1) and this is a severe bottleneck in environmental friendly greenhouse production[9].

Greenhouse horticulture in The Netherlands is responsible for at least 3 % of the annual *greenhouse gas* emission. This is partly because in this sector, 85 % energy consumption is covered with natural gas and that strongly increased CO_2 emission[10]. Using other fossil energy sources does not solve this problem. With those, not only CO_2 but also CH_4, N_2O, nitrous oxide (NO_x), sulfur dioxide (SO_2) and hydrocarbons (C_xH_y) are emitted[11]. The use of natural gas has also the advantage that the exhaust can be used directly for CO_2 enrichment in the greenhouses. Although its contribution to *greenhouse gases* other than CO_2 is relatively low, the greenhouse sector, nevertheless, as one of the major contributors to CO_2 exhaust, has to contribute with a major share to the total reduction of Dutch *greenhouse gas* emission. In 1997, the Dutch greenhouse sector and the government signed the *declaration of intent on greenhouse horticulture and environment*, the successor of an earlier signed agreement from 1992 [12]. In the agreement, energy efficiency was aimed to improve with 50 % by 2000 and 65 % by 2010 relative to 1980 and to increase sustainable energy sources by 4 %[13]. However, rather than reducing total CO_2 exhaust, improving energy efficiency (energy consumption per unit produce[7]) was agreed. In 1997, general environmental aims were translated into operational and measurable targets for the sector for the period 1995 – 2010 [11, 13] and targets for reducing biocides emission were formulated, too[13]. Those targets include reductions in atmospheric emission and emissions to soil and surface water[14]. In detail, until 2010 biocides should be reduced by 72 % and 88 % for ornamentals and vegetables, respectively, relative to the mean value of the period between 1984 and 1988. A strong effort has to be taken for biocides, since those were only little reduced with new materials and cultivation procedures. Within biocides, fungicides and plant growth retardants are most important in greenhouse horticulture. Plant growth retardants are commonly used to reduce stem elongation to attain short and compact plants. This is especially targeted in potplants as e.g. kalanchoë[15, 16], poinsettia[17–19], campanula[20, 21], begonia[16, 22] or chrysanthemum[16, 23–25]. But also cut flowers as cut chrysanthemum are aimed to be rather short and compact[26, 27] and the market value is closely related to that.

To improve the environmental aspects in greenhouse horticulture measures have to be taken, which reduce the environmental impact on one side and which keep crop

TABLE 1. Energy efficiency index in greenhouse horticulture between 1980 and 2001 (Data were corrected for outside temperature differences between years).

Year	'80	'85	'90	'91	'92	'93	'94	'95	'96	'97	'98	'99	'00	'01
Energy efficiency index (%)	100	60	67	68	66	66	65	60	63	58	60	57	56	52

Source: Van der Knijff *et al.,* 2002 [7].

production on a high level in terms of mass and quality on the other side. The two major environmental impacts in greenhouse horticulture, use of fossil energy and use of chemical biocides, could be reduced by modern greenhouse techniques and more advanced climate control or by a combination of these two issues.

OPTIONS FOR ENVIRONMENTAL FRIENDLY GREENHOUSE PRODUCTION

Most environmental friendly options in greenhouse horticulture in the last years concerned improved energy efficiency. Little progress was booked in reductions of biocides[14]. Energy efficiency can either be enhanced through increase in production or in reduction in absolute energy consumption. In the last years, growers intensified the productivity through maintaining elevated CO_2 levels in greenhouses, that was achieved by natural gas combustion, hence increased energy consumption and CO_2 emission[9]. Energy efficiency was improved (TABLE 1), but CO_2 emission increased for several years (FIG. 1). Also this improvement in energy efficiency was not enough to fulfil the target for the year 2000 (50 % decrease from 1980) that was missed by 6 % [10]. Better results were attained for 2001, where the energy efficiency index decreased by 4 % compared to the previous year[7] (TABLE 1). This was attributed to both decreasing energy consumption and increasing yield per m^2 [7]. However, this was still off the target for 2000. To compensate that the energy efficiency index must decrease stronger. This cannot be achieved by increasing productivity only[9]. Energy consumption has to be reduced, too. This can probably be achieved using advanced greenhouse technique and new materials[28] as listed in TABLE 2. Climate computers, energy screens, condensers and heat buffers contributed with 3.7 % energy saving between 1991 and 2000 [10]. Of those, however, only energy-power co-generation had a significant impact on improving energy efficiency between 1994 and 1999 [4], its share was 4 % in 2001 [7]. Greenhouse technique and the degree of penetration are estimated to further improve efficiency towards 2010. When in 2010 all greenhouses will be replaced to the average estimated standard of that year with standard equipment, 14.6 % energy could be saved in comparison to 1995 [28]. With more advanced technique (i.e. if technical development is faster than predicted) up to 22.5 % energy can probably be saved[28]. This alone, however, would not be sufficient to obtain the targeted energy efficiency of 35 % in 2010 [9]. New concepts are needed that improve energy efficiency more than it is estimated to occur with expected regular increase in degree of penetration of technical equipment and the improved technique itself. New systems need to be developed[9]. There is nowadays sufficient technological basis to design low energy use systems that are able to utilise energy of the sun for heating, in combination with for example wind energy for generation of

electricity, and that are able to reduce energy loss by improved greenhouse insulation, climatisation and control, in combination with heat storage systems[9, 29–31]. In The Netherlands, these principles were the basis of a new greenhouse concept aiming at sustainable plant production[9]. This Dutch solar greenhouse concept consists of three major components: new materials with higher insulation and higher light transmission, new climatisation equipment for long term storage of heat and dehumidification with heat recovery, and advanced control concepts which exploit crop tolerances to temperature and humidity fluctuations. Ideally, the new concept should operate as a closed system, such that energy is not lost to the outer environment. In a closed greenhouse dehumidification will be one the major bottlenecks[29]. Moreover, without control, stronger temperature and humidity fluctuations can be expected than in a classical greenhouse. Should these climate parameters be kept constant, as is aimed with regular climate control, equipment with high capacity has to be installed, with high investment costs, if at all possible. To reduce technical problems maintaining fixed temperature and humidity levels and gaining maximum profit of such a system, a flexible control strategy rather than a rigid system with fixed set points should help to develop this cultivation system.

CLIMATE CONTROL

GENERAL

Greenhouse climate in The Netherlands is commonly controlled by rather rigid set points for heating and ventilation. Temperature and humidity are conservatively controlled according to a blue print regime, based on experience of the individual grower and the computer manufacturer[32]. Moreover, there are several commonly applied measures that can even increase energy consumption (TABLE 3). This suggests that there is a potential for improving the current climate control, even without considering new greenhouse technology. The ideas necessary for the sustainable greenhouse are therefore equally applicable to the current greenhouse practice. For this purpose a more sustainable climate control strategy, that focuses on optimal crop growth conditions in compliance with plant development and quality as well as prevention of plant diseases, will be developed in this thesis. This regime will also be the basis for more advanced climate control systems, that have been proposed, such as *optimal climate control*[32–34]. This aims at computing control trajectories by optimising an (economic) goal function. Ideally, in *optimal control*, the expected plant responses are explicitly taken into account[35]. However, crop modelling has not progressed far enough to allow complete modelling of development processes and other quality aspects of crop growth. Hence, even in an *optimal control* framework, it

TABLE 2. Main technical measures that are recently used for energy saving in greenhouses.

Technique [a]	Function [a]	Penetration 2001 or *2000 (%) [b]	Mean annual increase between 1990 and 2001 (%) [b]
Climate computer	Improving greenhouse climate control	96	+2.1
Condenser	Improving effectivity of the heating unit	71	+1.2
Heat-buffer	Stores heat that was generated during day to be used later on (e.g. night)	34	+2.3
Co-generation and remaining-heat	Support the combination of using the same energy for heating and power.	15	+1.3
(Movable) screens	Decreases the heat-loss factor and keeps heat longer in the greenhouse	73	+1.6
Front isolation	*same as movable screens*	77*	-0.5

Source:Tweede-Kamer, 2003 [4] [a], Van der Knijff et al., 2002 [7] [b]

TABLE 3. Commonly applied measures increasing energy consumption in greenhouses.

Measure	Purpose	Penetration 2001 or 2000 [a] (%)	Mean annual increase between 1990 and 2001 (%)
CO_2 supply	Increasing yield	83	+0.5
Minimum pipe-temperature	Improving greenhouse climate and possibilities for CO_2 supply (vents keep longer shut)	80 [a]	0
Assimilation light	Increasing yield and quality	17	+1.6

Source:Van der Knijff et al., 2002 [7], Bakker et al., 2001 [10].

will be necessary to respect certain temperature and humidity constraints, as formulated in the control regimes developed in this thesis. In this way, both the current and the future climate control system will benefit when restrictions for plant control are relaxed. This is achieved with more flexibility in both temperature and humidity control, which can respectively be attributed to energy saving and fungicide reduction.

TEMPERATURE

Greenhouse energy consumption strongly increases with increasing set points for heating temperature (TABLE 4). When non-fixed set points would be used, heating

TABLE 4. Simulation of energy consumption as function of fixed temperature set points for a complete year with cut chrysanthemum cultivation. Set point was realised with heating and ventilation of +0.5 °C and –0.5 °C from the temperature set point. The greenhouse climate and control model KASPRO[105] was applied.

Set point (°C)	10	12	14	16	18	20	22	24	26
Energy consumption (GJ)	0.43	0.56	0.73	0.94	1.20	1.51	1.88	2.27	2.65

can be shifted to times when the heat loss factor is reduced and this reduces energy consumption[30, 36]. To obtain the same crop development and yield, mean temperature must be the same as with fixed set points. Research has shown that this so-called temperature integration can be applied for many crops. Temperature integration was found applicable for ornamental plants such as roses[37–39], gerbera, kalanchoë, anthurium, Ficus benjamina[37, 40] and chrysanthemum[40–46]. Also for vegetable crops like kohlrabi[47, 48], cucumber[49, 50], tomato[51, 52] and sweet pepper[53, 54], temperature integration was applicable. With temperature integration, annual energy consumption in greenhouses was reduced by 10 % to 20 % [55–59]. This energy saving was achieved by shifting some heating to periods when the rate of heat loss from the greenhouse is reduced[55]. The concept is based on the theory, that photosynthesis increases mainly with light while development depends principally on temperature and that there is a very weak interaction between the two[47, 60]. Photosynthesis is an almost instantaneous process, whereas photoassimilate processing is a dynamic process, possibly with delay. It can be hypothesized that the plant is storing the assimilates in a carbohydrate pool[61]. On that theory, a model which links temperature to forecasted solar radiation to balance the rates of growth and development with that of photosynthesis was suggested[62, 63]. The pool capacity is however unknown and definitely differs between plants and probably between developmental stages within the same plant. Temperature integration is a simplified approach of the same theory. A certain buffering capacity is assumed that is not further quantified, but found sufficient for several days under moderate conditions[51]. The concept is based more on empirical observations. With temperature integration, the two most important boundary parameters, maximum duration of integration and the maximum allowed temperature bandwidth, are relatively unknown and need further investigation. Those parameters determine temperature flexibility and therefore improve energy saving and its use in optimal climate control.

Temperature integration in its most basic form is applied with an averaging period of 24 hours[39, 59]. This period was expanded to several days with only little negative consequences for different ornamental and vegetable crops[47, 52, 57]. The allowed temperature bandwidths in these experiments were between 2 °C and 6 °C. With a targeted mean temperature of 18 °C, the temperature can only fluctuate between a maximum of 15 °C and 21 °C. With higher tolerance, however, energy saving

strongly increases. When e.g. temperature is allowed to rise to 30 °C, then only half as much ventilation is required compared to the 27 °C leaf temperature case[64] and then night temperature can drop more and heating will be less. There is therefore an urgent need to establish the limits of the temperature and time ranges over which integration can occur without detriment to the crop[65].

Also using higher ventilation temperatures less CO_2 is needed for a given level of enrichment, with a direct effect on energy use as this was one of the most energy consuming climate control measures[7, 10]. At elevated temperature, CO_2 can be maintained at high levels to increase photosynthesis and dry matter production without the usual loss. Due to that, not only CO_2 exhaust decreases but also the economical return increases as this largely depends on CO_2 loss by ventilation[66, 67].

Just finding the maximum boundaries for temperature integration is not enough, because other factors counteract the beneficial effects of temperature integration. Some morphological plant characteristics do not react to mean temperature only but to the difference of average day and average night temperature (*DIF*)[23, 68–71]. With a positive *DIF* (higher day than night temperatures), plant length increases through internode elongation and this decreases the market quality of many ornamental crops as mentioned before. On the other hand, the *DIF* concept can be used to reduce stem and internode elongation by setting a negative *DIF*[72–74] and this can decrease the consumption of chemical growth retardants[75]. However, a targeted negative *DIF* can strongly counteract temperature integration when warm days are compensated by cool nights as it commonly occurs in spring and autumn. The disadvantages of negative *DIF* temperature regimes is therefore an increased energy use in these periods and the restriction of the degree of freedom the environmental control systems[76].

There is obviously a conflict between two different temperature regimes, temperature integration and negative *DIF*, that both aim at environmentally friendly greenhouse production. A concept is therefore needed that includes both regimes in a kind of optimisation to find the best feasible climate control settings regarding environmental friendly greenhouse climate control.

<div align="center">HUMIDITY</div>

Humidity control in commercial greenhouses is commonly applied with fixed set points of about 80 - 85 % relative humidity (RH, although humidity control is often performed with vapour pressure as set point). Heating or ventilation or both are used when greenhouse humidity exceeds this set point to reduce humidity. Humidity is controlled to attain high quality growth. High humidity conditions can induce many negative crop processes. Too high humidity can decrease pollination in fruit vegetables, as pollen grains tend to remain inside, or stick to the anthers[77, 78]; and it can lead to soft and thin leaves and surfaces that makes them susceptible for fungal

spores and which are always present in greenhouses[79]. Also in general, high humidity increases the danger of fungal and bacterial diseases. Holder and Cockshull (1990)[80], Bakker (1991)[78], and Jolliet *et al.* (1993)[81] found a lower tomato fruit yield at high humidity and leaf calcium deficiencies. High humidity can also induce calcium deficiencies in vegetable fruits, that can lead to blossom-end rot[82].

The most important reason for humidity control is actually the danger of fungal diseases. Fungicides are commonly used, but as mentioned before, their application must be reduced. Also, some fungi became already tolerant to certain fungicides, e.g. chrysanthemum white rust[83, 84]. The use of more heavy fungicides is not a desirable solution. In stead, climate control could be used to control fungi in a different way[85]. A humidity regime based on the underlying processes could be developed where relative humidity would not be controlled by a fixed value, but where actions to reduce humidity would only be taken if necessary, for example when the threshold of a certain fungal spore development rate is exceeded.

Such a control is even more important when temperature integration is applied, because humidity control is a limiting factor for that. The low fixed setpoints for humidity control used in common practice counteract the positive effect of temperature integration on energy consumption. In this situation with reduced ventilation and heating, RH increases when temperature drops and *vice versa*. Vents open at lower temperatures than required for temperature control, resulting in CO_2 and energy loss, or heating will be required to decrease relative humidity, resulting in higher energy demand, or both.

A new concept must be developed that protects plants from high humidity on the one side and that keeps freedom for temperature integration on the other. To this end, a process based humidity control regime based on underlying processes is designed for temperature integration control in this thesis.

AIM OF THE THESIS

New technological concepts are being developed that focus on a strong reduction of greenhouse energy consumption. However, with existing technology, energy saving can also be achieved. The capacity of currently existing technology should be utilised before investments in more expensive and not yet existing technology are done. Climate computers are widely spread (TABLE 2) and form the basis for a computerised greenhouse climate control. With that, energy saving has already been achieved and there is probably more capacity for a more sustainable greenhouse cultivation including energy and biocide reduction. The present thesis therefore aims at reduction of energy consumption and biocide use by designing and analysing several flexible control regimes, employing existing climate control possibilities using set points of a commercial climate computer. These strategies are, however, not

only useful for current greenhouse practice, but can also serve as a basis for future greenhouse concepts. A complete climate regime that controls plant growth, plant development and plant quality is targeted. The boundaries of current temperature integration schemes are aimed to be extended to increase energy saving and a photosynthesis maximisation procedure should be implemented to maximise growth. Because regular humidity control counteracts temperature integration, a flexible humidity regime is planned that will be combined with temperature integration. The resulting dynamic climate regime must finally be combined with a negative *DIF* regime.

With this dynamic approach, plant development should not be affected, crop growth should be maximised through photosynthesis maximisation and short-compact plants are aimed at. Simultaneously, energy consumption and biocide use should be reduced.

OUTLINE OF THE THESIS

The development of the climate regimes in this thesis is presented in two major Chapters. In **CHAPTER 2**, the basis for a crop gross photosynthesis model for the use in extreme climate conditions is created. Different regimes on dynamic climate control are designed and presented in **CHAPTER 3**. Finally in **CHAPTER 4** a general discussion on the quality and applicability of the presented climate regimes is given.

To maximise photosynthesis in temperature integration regimes, CO_2 supply should be optimised. To find the optimum of energy consumption and growth, a well performing crop photosynthesis model is needed. Present photosynthesis models were neither designed for nor validated under excessive temperature conditions. A crop photosynthesis model has therefore to be found that can be used for crop photosynthesis maximisation under extended temperature conditions. In **CHAPTER 2.1**, a simulation study is performed to compare different leaf photosynthesis models under conditions expected with a more extended temperature integration concept. Those models need to be validated before a decision on which model to be used for climate control can be taken. A crop photosynthesis measuring system is therefore designed and calibrated in **CHAPTER 2.2** for later use for experimental testing of photosynthesis models. Crop photosynthesis measurements with the model crop cut chrysanthemum on conditions with extended temperatures (up to 33 °C) are performed in **CHAPTER 2.3**. Two different leaf photosynthesis models as part of crop photosynthesis model are further compared with measured data in **CHAPTER 2.4**.

The basis for a more flexible or dynamic climate regime is build by two independent regimes for the two major greenhouse climate states regarding energy consumption and biocide use, temperature and relative humidity. In **CHAPTER 3**, independent regimes are developed and energy consumption is estimated with simulations. The regimes are then merged and tested with experiments. The restriction of a negative

DIF set point on dynamic temperature regimes is evaluated in terms of energy consumption. Possibilities of either using *DIF* or temperature integration are discussed. To relieve the *DIF* restriction on temperature integration over several days, a concept is developed, too.

The dynamic climate regime is introduced with a modified temperature regime. Temperature integration is extended to a more flexible regime in **CHAPTER 3.1**. Within this regime, the most promising crop photosynthesis model of CHAPTER 2 is used. The temperature integration regime is combined with a flexible humidity regime that calculates relative humidity set points based on underlying crop processes in **CHAPTER 3.2**. The combined regime is tested with greenhouse experiments using cut chrysanthemum as model crop in **CHAPTER 3.3**. Regular temperature integration with a 24-hour averaging period is compared in terms of energy consumption with *DIF* using simulations in **CHAPTER 3.4**. It was aimed to quantify the energy costs when applying *DIF* next to temperature integration for different seasons. Regular temperature integration with an integration period length of six days was combined with a *DIF* concept in **CHAPTER 3.5**. Simulations and greenhouse experiments are performed for that. In **CHAPTER 3.6**, different regimes are combined and a simulation study is performed to compare them to find the best regime regarding energy consumption in different seasons.

CHAPTER 2

CROP PHOTOSYNTHESIS

2.1 MODELLING TEMPERATURE EFFECTS ON CROP PHOTOSYNTHESIS

O. KÖRNER, H. CHALLA & R.J.C VAN OOTEGHEM

ABSTRACT

The climate inside a solar greenhouse (a high-tech greenhouse essentially heated by solar energy and provided with facilities for seasonal energy storage) is more dependent on outside conditions than in ordinary greenhouses. To optimise ventilation, one has to take into account that optimum temperature for canopy photosynthesis rises with increasing concentration of atmospheric CO_2. To predict canopy photosynthesis and to relate dry weight production to temperature control, a well performing model is needed. Models of canopy photosynthesis have not yet been validated at the extreme climate situations that may be expected in a solar greenhouse in summer (high irradiation, temperature and humidity). Three versions of increasing complexity of leaf photosynthesis simulation models; $M1$, $M2$ and $M2^+$ were evaluated in a canopy photosynthesis model under such conditions. The reference (SUCROS related) model, $M1$ has been extensively validated for a tomato crop under

normal greenhouse conditions, *M2* is an extension of *M1* with a more biochemical description of the underlying processes and *M2*[+] is an extension of *M2*, including a sub-model of stomatal resistance. In a crop model, the three sub-models were compared under fixed conditions and with observed climate data. There were substantial differences between the three models, especially at high temperatures and high radiation, irrespective of the CO_2 level. The biochemical model *M2* performed somewhat different from *M1*, but the strongest discrepancies were observed with model *M2*[+], due to the much higher predicted stomatal resistance compared to the values adopted in *M1* and *M2*. The results demonstrate that it is necessary to investigate the performance of greenhouse crop models under a wider range of conditions when they are to be applied in a solar greenhouse.

INTRODUCTION

Nowadays, there is sufficient technological basis to design greenhouse systems, that are able to utilise energy of the sun for heating, in combination with e.g. wind energy for generation of electricity, improved greenhouse insulation, climatisation and heat storage systems[30, 31, 86]. The Dutch Solar Greenhouse (DSG) is an approach to reduce fossil energy use in Dutch greenhouse horticulture[9]. Advanced climate control in a DSG should contribute at reduction of the required heating, heat exchange and -storage capacities, whilst maintaining yield and product quality[87].

From a technical point of view it is beneficial in a DSG to accept stronger temperature fluctuations than in regular greenhouses. Therefore air temperature should increase with radiation more than in traditional climate regimes, maintaining a high CO_2 level in the greenhouse air (as long as ventilation can be avoided), which in turn is favourable for photosynthesis, because it suppresses photorespiration[88]. In a DSG, therefore it may be anticipated that at high radiation there will be either a high CO_2 concentration that can be maintained at little or no ventilation, or atmospheric CO_2 with ample ventilation.

In this optimisation a well performing crop photosynthesis model is needed to predict production as a function of greenhouse climate. However, present tomato crop growth models are designed for and have been validated under normal, moderate greenhouse conditions[89, 90].

The SUCROS based crop photosynthesis model that is incorporated in TOMSIM[89] uses the leaf photosynthesis module *M1*, where stomatal resistance is a constant and the behaviour of several biochemical key processes has been summarised in a simplified description. This model was successfully validated under normal temperature and relative humidity conditions[89], but we wondered how this simplified version would perform under the more extreme conditions of a DSG. To answer this question the performance of a complete greenhouse crop photosynthesis model[91] was

investigated at high radiation, temperature and humidity conditions. The performance of this model with the reference leaf photosynthesis model *M1* was compared with the results of alternative leaf photosynthesis-modules, *M2* and *M2*[+]. In *M2* the simplified description of the underlying biochemical key-processes was replaced by a more process based description. *M2*[+] is the same as *M2*, but it also includes a model of the stomatal resistance r_s, instead of using a fixed r_s[92].

Steady state comparisons were made for a range of temperatures, CO_2 concentrations and radiation levels. In addition, canopy gross photosynthesis was simulated dynamically under climate conditions obtained from two identical, mechanically cooled, closed greenhouse compartments with a tomato crop, used for measuring canopy photosynthesis (data not presented in this study).

MATERIALS AND METHODS

CLIMATE DATA

CO_2 concentration was maintained at 350 and 750 µmol mol^{-1} between 22 August and 29 September 2000 for two successive days in turns to avoid photosynthetic acclimation of the tomato plants to elevated CO_2 in two identical semi-closed greenhouses at Wageningen University, The Netherlands. Day temperature was 20, 24, 28, 32 and 36 °C. CO_2 concentration inside the greenhouses was measured every 275 s by an infrared gas analyser (URAS 3G, Hartmann & Braun, Frankfurt, Germany). Pure CO_2 was injected proportionally to the difference of measured and target CO_2 concentration through a thermal mass flow controller (5850E, Brooks, Hatfield, PA, USA) with 150 g CO_2 h^{-1} maximum flow rate. The system was controlled by commercial control software (HP VEE 5.0, Hewlett Packard, Englewood, CO, USA). Air temperature and relative humidity (RH) were measured at three positions inside each greenhouse and controlled by a commercial computer system (VitaCo, Hoogendoorn, 's Gravenzande, The Netherlands). RH increased with greenhouse temperature and was between 80 % at 20 °C and 88 − 98 % at 36 °C, corresponding to 0.46 and 0.70 kPa or 0.06 kPa vapour pressure deficit (VPD). Leaf temperature was measured every 5 s, averaged over 5 minutes and stored on a data logger (DT 600, Esis, Roseville, NSW, Australia) by 10 evenly distributed type-K thermocouples ($\varnothing$ 0.025 mm) in each greenhouse. Thermocouples were attached to the bottom of sunlit leaves with tension and glue[93]. Photosynthetic photon flux density (PPFD) was measured above the canopy at 2.15 m highs with a 1 m line quantum sensor (LI–191SA, LI-COR, Lincoln, NE, USA).

TABLE 1. Maximum carboxylation rate ($V_{C,\max}$), maximum electron transport rate ($J_{\max}$), CO_2 compensation point (Γ) and dark respiration rate (R_d) for the three leaf photosynthesis modules ($M1$, $M2$ and $M2^+$). With variable leaf temperature (T_l) and temperature at 25 °C (T_{25}) in K and constants: Maximum carboxylation rate at 25 °C ($V_{C,\max,25}$), dark respiration rate at 25 °C ($R_{d,25}$), Q10 for dark respiration ($Q_{10,Rd}$), activation energy (E) for $V_{C,\max}$ (E_{VC}), $J_{\max}$ (E_J), Rubisco carboxylation (E_C), Rubisco oxygenation (E_O) and dark respiration rate (E_D), O_2 partial pressure ($\rho_{O_{2i}}$), constants for optimum curve temperature dependent electron transport rate S and H, gas constant R, Michaelis Menten constants for Rubisco carboxylation ($K_{C,25}$) and Rubisco oxygenation ($K_{O,25}$) and the quotient between maximum oxygenation and carboxylation rate ($V_{O/C}$).

	M1	*M2 / M2$^+$*
$V_{C,\max}$	$V_{C,\max,25} \cdot Q_{10,Vc}^{(T_l - T_{25})/10}$	$V_{C,\max,25} \cdot e^{E_{VC}\cdot(T_l-T_{25})/(T_l\cdot R\cdot T_{25})}$
$J_{\max}$	Optimal temperature step function	$J_{\max,25} \cdot e^{\left(E_J\cdot\frac{T_l-T_{25}}{T_l\cdot R\cdot T_{25}}\right)} \cdot \left(1+e^{\frac{(S-H)/T_l}{R}}\right) \cdot \left(1+e^{\frac{(S-H)/T_{25}}{R}}\right)^{-1}$
Γ	$42.7 + 1.68\cdot k + 0.012\cdot k^2$ $k = T_l - 298.15$	$\dfrac{\rho_{O_{2i}} \cdot V_{O/C}}{2} \cdot \dfrac{K_{C,25} \cdot e^{E_C\cdot(T_L-25)/(T_L\cdot R\cdot 25)}}{K_{O,25} \cdot e^{E_O\cdot(T_L-25)/(T_L\cdot R\cdot 25)}}$
R_d	$R_{d,25} \cdot Q_{10,RD}^{(T_l-298.15)/10}$	$R_{d,25} \cdot e^{E_D\cdot(T_l-T_{25})/(T_l\cdot R_g\cdot T_{25})}$

MODEL

Leaf photosynthesis is described by a two parameter (maximum gross photosynthesis $P_{g,\max}$ and leaf photochemical efficiency α_l), negative exponential light-response curve[94]. From this, canopy photosynthesis was derived, based upon the calculated sunlit and shaded leaf area index[95] (LAI) and integrated over canopy height with three point Gaussian Integration[96]. As explained before, three leaf photosynthesis models ($M1$, $M2$ and $M2^+$) were compared. In $M1$ descriptive formulae are used to calculate the initial slope α and light-saturation value $P_{g,\max}$ [97, 98]. In $M2$ the original biochemical based equations[97] were used (TABLE 1). Instead of a constant stomatal resistance, used in $M1$ and $M2$, stomatal resistance in $M2^+$ is modelled as a function of leaf temperature, ambient CO_2, short-wave radiation absorption by the canopy, LAI and VPD[92].

CANOPY LIGHT RESPONSE CURVES

Light response curves were fitted to the results of simulated canopy gross photosynthesis obtained with climatic data from the greenhouse experiments. To this end maximum canopy gross photosynthesis ($P_{gc,\max}$) and canopy photochemical

TABLE 2. Fitted values for maximum gross photosynthesis, $P_{gc,max}$ (µmol CO_2 m^{-2} s^{-1}), and photochemical efficiency, α_c (mmol CO_2 {mol photons}$^{-1}$), for modules $M1$ and $M2^+$. Parameters were fitted with P_{gc} simulations for one hour consisting of 5 min input values of leaf temperature, RH and outside global radiation at 350 ± 30 and 750 ± 30 µmol mol^{-1} at 24, 28, 32 and 36 °C air temperature.

Model	Parameter	CO_2 350 µmol mol^{-1}				CO_2 750 µmol mol^{-1}			
		Temperature (°C)							
		24	28	32	36	24	28	32	36
$M1$	α_c	53.1	52.3	50.4	67.0	61.6	64.4	57.0	60.9
	$P_{gc,max}$	37.0	39.7	42.7	33.6	57.1	56.9	93.4	90.1
$M2^+$	α_c	52.0	52.4	50.0	64.0	61.3	63.8	58.7	60.0
	$P_{gc,max}$	29.9	29.6	26.1	18.2	47.8	47.4	46.9	34.5

efficiency (α_c) in the negative-exponential equation (EQ. 1) as used by Heuvelink (1996)[6] were estimated by non-linear least squares iteration using the PROC NLIN procedure of SAS 6.12 [99].

$$P_{gc} = P_{gc,max} \cdot (1 - e^{\frac{-\alpha_c \cdot PPFD}{P_{gc,max}}})$$

[1]

RESULTS

SIMULATION OF P_{gc} WITH STEADY STATE CLIMATE CONDITIONS

P_{gc} with $M1$ and $M2$ responded only slightly to temperature between 20 °C and 34 °C (FIG. 1), but with $M2^+$, there was a strong response in this range. P_{gc}, however, exhibited an optimal temperature response in all three sub-models. $M1$ had a 6 °C long optimum plateau between 26 and 32 ºC for all radiation intensities tested (FIG. 2), $M2$ and $M2^+$ responded in an optimal point. At higher ambient CO_2 concentration, the P_{gc} response to temperature was steeper in all three sub-models and the optimum temperature for P_{gc} increased only slightly with increasing CO_2. However, the response pattern of P_{gc} to temperature was clearly different between $M1$ and $M2$. With $M1$ there were discontinuities that were not observed with the biochemical based $M2$. When stomatal behaviour was incorporated in the model ($M2^+$), the stomatal resistance was higher and this had pronounced consequences for the temperature response of P_{gc}. Maximum P_{gc} was observed at lower temperatures and there was a much stronger decrease with increasing temperature than in the other
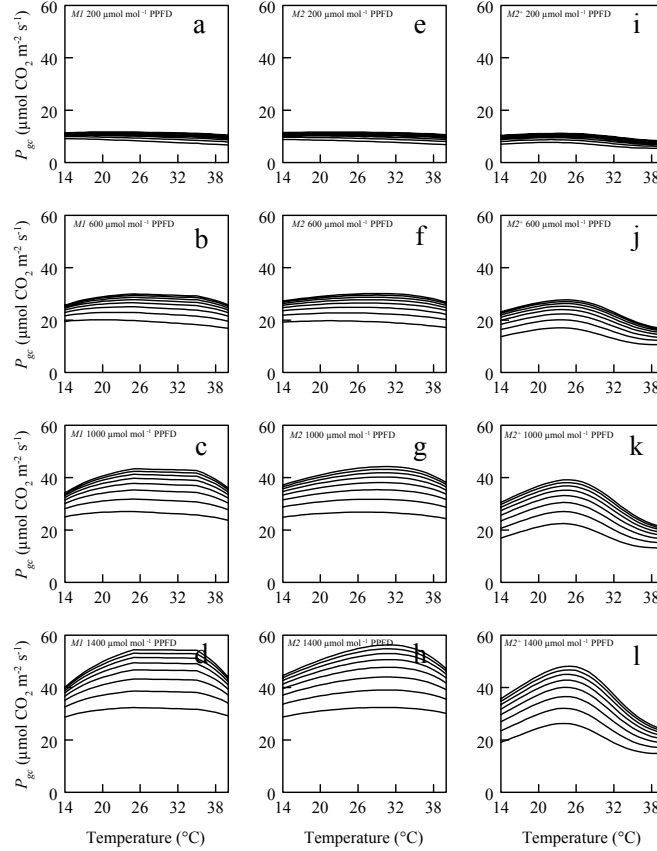
FIGURE 1. Simulated crop gross photosynthesis (P_{gc}) as function of temperature. Eight CO_2 concentrations (300 – 1000 µmol mol^{-1}, lines) and four photosynthetic photon flux densities (PPFD) are compared (200 (a, e, i), 600 (b, f, j), 1000 (c, g, k) and 1400 µmol mol^{-1} (d, h, l)) with *M1* (a – d), *M2* (e – h) and *M2*$^+$ (i – l). LAI was 3 and a fixed sine of solar elevation of 0.8; fraction of diffuse radiation of 0.5; constant relative humidity of 80 %, scattering coefficient for photosynthetic active radiation = 0.15 and leaf extinction coefficient of diffuse light = 0.8) were applied.

modules considered. For all CO_2 radiation levels tested, P_{gc} was lower with *M2*$^+$ than with *M1* and *M2*.

SIMULATION OF P_{gc} WITH OBSERVED CLIMATE CONDITIONS

Simulations with *M1* and *M2*$^+$ using observed climatic data and fitted light response curves (parameters in TABLE 2) are illustrated in FIG. 2. In all cases fitted P_{gc} was higher with *M1* than with *M2*$^+$. This difference increased with radiation and with temperature. At higher temperatures the response of P_{gc} to radiation with *M2*$^+$ was more linear than with *M1*. $P_{gc,max}$ increased with temperature up to 32 °C with *M1* at both CO_2 levels. With *M2*$^+$, on the other hand, $P_{gc,max}$ decreased over the whole range from 24 to 36 °C at 350 µmol mol^{-1} CO_2 and from 28 to 36 °C at 750 µmol mol^{-1} CO_2. The overall level of P_{gc} was higher at elevated CO_2 in both models,
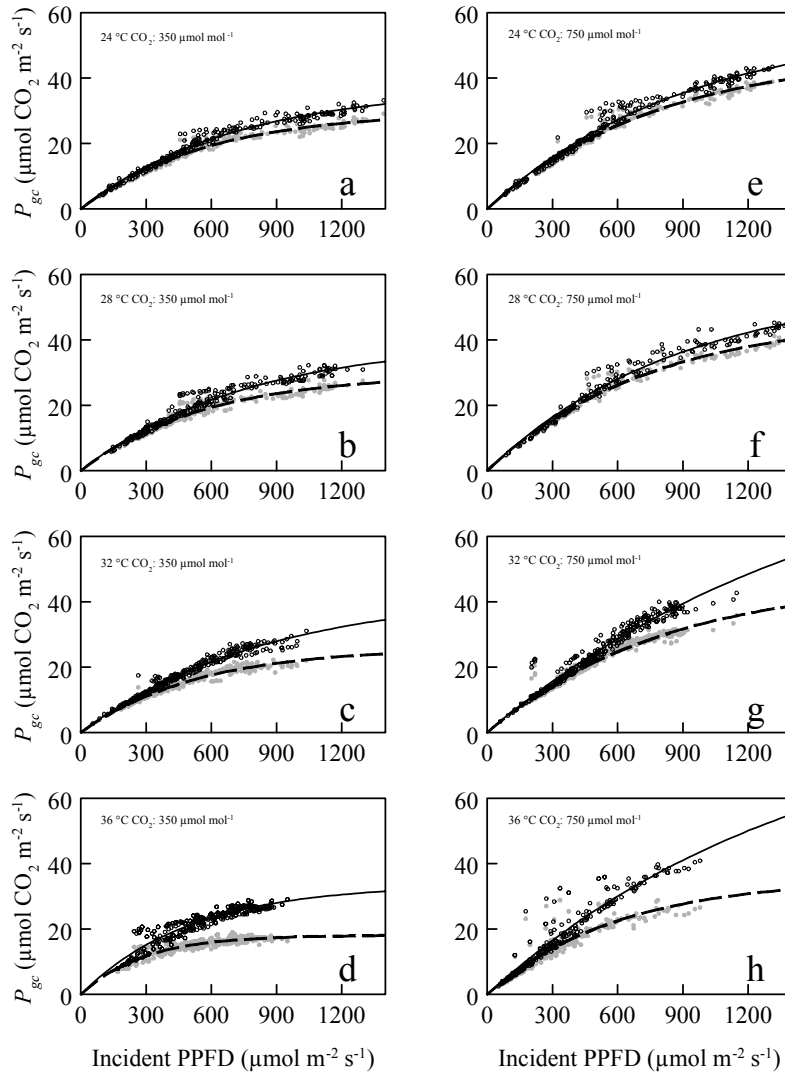
FIGURE 2. Simulated P_{gc} on climate data achieved from crop assimilation experiment at 350 ± 30 µmol mol^{-1} (a-d) and 750 ± 30 µmol mol^{-1} (e - h) at 24 (a, e), 28 (b, f), 32 (c, g) and 36 °C (d, h) for *M1* (○) and *M2*$^+$ (●) as function of photosynthetic photon flux density (PPFD). P_{gc} was simulated for a one-hour interval, consisting of 5 min input values of leaf temperature, relative humidity and outside global radiation. Negative-exponential functions (EQ. 1) with $P_{gc,max}$ and α_c were fitted by to the data (lines) (TABLE 2).

where the relative difference between the two was the same as at ambient CO_2 concentration. The photochemical efficiency was slightly higher for almost all situations tested.

DISCUSSION

The performance of the three models differed considerably in the situations tested. Especially the incorporation of r_s to the model resulted in different response to increasing temperature and CO_2. Stomatal resistance, with the model used in this study, appeared to have a major impact on canopy gross photosynthesis and its response to temperature. In $M2^+$ the increase of P_{gc} with ambient CO_2 and temperature was less than expected from literature[e.g. 100]. In that case it was a combined effect of quantum yield and light saturated photosynthesis, where the second parameter can be compared to $P_{gc,\text{max}}$ in our model and the first may be approximately scaled to α_c. They did not include r_s in their model, but adopted a fixed quotient of 0.7 between ambient and intercellular CO_2 concentration. However, also with $M2$ with fixed r_s, the response of P_{gc} to temperature and CO_2 was not as pronounced[101]. Our results, however, are in agreement with Cannell and Thornley (1998)[100], who also reported that canopy gross photosynthesis shows less CO_2 - temperature interaction than leaf photosynthesis. This probably is due to low light levels inside the canopy (i.e. light limited photosynthesis). The DSG is planned to be equipped with a energy friendly dehumidification unit[9], which will affect temperature and vapour pressure. Due to relatively low ventilation rate and relaxed climate control in the DSG[87], VPD, a factor that affects r_s according to the used model[102] in $M2^+$, is likely to vary as well. As we have seen, variations in r_s may influence the canopy photosynthesis rate strongly and therefore those have to be taken into account in crop photosynthesis models.

Based on the comparison of the performance of the three model versions in the present study, it can be concluded that, although $M1$ performs well under standard conditions, it may not be able to adequately predict extreme situations encountered in the DSG. Both incorporation of more detailed biochemical processes and behaviour of stomata would be needed for model based climate control. Experiments on canopy photosynthesis are needed to verify whether the crop photosynthesis model improvements observed by simulations can also be observed in comparison with measurements.

2.2 Crop photosynthesis measurement system

O. Körner, M. Hulsbos, A. van 't Ooster, H. Gijzen & H. Challa
Design and calibration of a measuring-system for
crop photosynthesis for model validation
(submitted)

ABSTRACT

Photosynthesis is the best described part of the crop system. From that knowledge, crop photosynthesis models have been designed. These models were often validated with data measured on single leaves; plants or very small crop stands of only few plants. Larger systems have been designed, but were mostly not feasible for elevated CO_2 concentrations and different non-commercial greenhouse climates. For advanced model based climate control, models have to be designed and validated for a larger climate range. For measuring crop net CO_2 exchange, a well performing measuring system is therefore necessary. This, however, is difficult to design. A detailed description including design and system-calibration as well as described approach to use data for crop model-validation is still missing. The aim of this research was therefore to design and calibrate a net CO_2 exchange system that can be used for crop model validation. The system was aimed to measure crop photosynthesis at a range of CO_2 concentrations and different constant temperatures, various constant

photosynthetic photon flux densities (PPFD) and natural light. The measuring system was re-build from two identical free-standing semi-closed greenhouses of 44 m² floor area each. The greenhouses were sealed against air filtration to the possible maximum. Leakage and unwanted CO_2 sources were quantified with three tracer gases in the empty shelters (SF_6, N_2O and CO_2). CO_2 dosage was controlled by software and measuring devices and proportionally supplied according to the difference between set point and measured concentration. Net CO_2 exchange of the crops was calculated as difference between dosage and leakage. An error analysis was performed to find system requirements allowing a maximum system error of 5 %. Sample number in averaging time and variation in CO_2 concentration had the highest impact on total variation. To resemble an endless crop canopy for model validation, CO_2 net exchange measurements were recalculated with a geometric crop photosynthesis model taking light penetration into the sides of the crop into account. The complete system (measurements and simulation) was tested with a vegetative growing cut chrysanthemum crop. Under the investigated circumstances with constant low PPFD levels of 85 and 160 µmol m^{-2} s^{-1} and under natural light conditions from 0 to 600 µmol m^{-2} s^{-1} PPFD at 970 µmol mol^{-1} CO_2 the system functioned well within the 5 % error range.

INTRODUCTION

Due to the recent development in climate control for energy saving, greenhouse climate (i.e. temperature and humidity) is allowed to fluctuate much more than with conservative rigid climate regimes. Temperature integration regimes[39, 57, 103] and process based humidity control[104] permit flexibility in greenhouse climates. These regimes are mainly based on independent rules and control is not optimised. In order to control heating, ventilation and CO_2 dosage optimally, well performing models predicting energy consumption and crop performance are necessary. Physical greenhouse climate models could be used to optimise energy consumption[e.g.105]. Crop performance on the other hand has to be predicted by more biological based models. One of the major issues in that perspective is to optimise the ratio between CO_2 supply and crop gross photosynthesis (P_{gc}). For that, well performing models are necessary. Those must be designed and validated for dynamic climate conditions as they prevail with modern climate control regimes. The models predictive quality and their ability to account for CO_2 effects should be thoroughly tested by comparing simulations with an extensive set of representative measurements[106]. Repeating measurements on CO_2-exchange at various climate conditions (i.e. light, CO_2, temperature and humidity) would then be needed. This type of measurements were mostly done on leaves[100, 107–110] or single plants in a chamber[111–115] and were then scaled up to the crop level. An important shortcoming of such measures is that some

important conditions as light interception, microclimate, crop size and developmental stage do not sufficiently resemble those of full grown crops[106]. Therefore, photosynthesis measurements with larger plant canopies were performed[89, 106, 116–121]. Those experiments, however, were mostly done in poorly sealed commercial greenhouses at ambient CO_2 concentrations and conservative climate conditions, or measurements were restricted to short-term periods and often done in a single greenhouse only (i.e. no replications). Most small canopy gas-exchange systems where described without calibration. Van Iersel and Bugbee (1999)[114] described set-up and calibration of a multi-chamber gas-exchange system. This system, however, is only suitable for six small pot plants and does not represent larger crop canopies. A larger scale system with a several square meter crop canopy was not elaborately described. A properly sealed and well performing large scale CO_2 gas-exchange system that is able to create a wide range of climate conditions irrespectively outside global radiation is needed. A net CO_2 exchange measuring system with two identical greenhouses with 44 m^2 floor area suitable for variable climate conditions (i.e. different CO_2 levels, temperatures and irradiances) was designed and calibrated. To validate P_{gc} models per m^2 crop, nevertheless, a modified model version is necessary. Most crop photosynthesis models[e.g. 91] assume an endless flat canopy, but no greenhouse for measuring net CO_2 exchange that is capable to detect low photosynthesis levels is large enough to represent that. Simulated P_{gc} per m^2 crop using a regular model would underestimate measured values, because radiation penetrating into the sides of the crop stand is not taken into account with those models. When validating models, refinements in terms of crop architecture in the gas exchange measurement system are needed[89]. The crop was therefore evaluated as a block rather than a flat infinite canopy. A model to calculate leaf photosynthesis for 4000 points in a 3-dimensional grid was implemented. The complete system was explained and constant low and dynamic P_{gc} levels were investigated.

MATERIALS AND METHODS

TECHNICAL EQUIPMENT

A semi-closed greenhouse system for measuring CO_2 net exchange[89, 122] was designed. For that, two identical day-lit greenhouse compartments with 44 m^2 net floor area (5.8 x 7.5 m) Netherlands (FIG. 1). The total net volume of one system (greenhouse + basement) was 270 m^3. Electric heating and direct mechanical cooling with in the rooms under the compartments controlled temperature and humidity. CO_2 concentrations from the compartments and the walkway in front of the basement below the compartments (assumed CO_2 source) were measured by one infrared gas
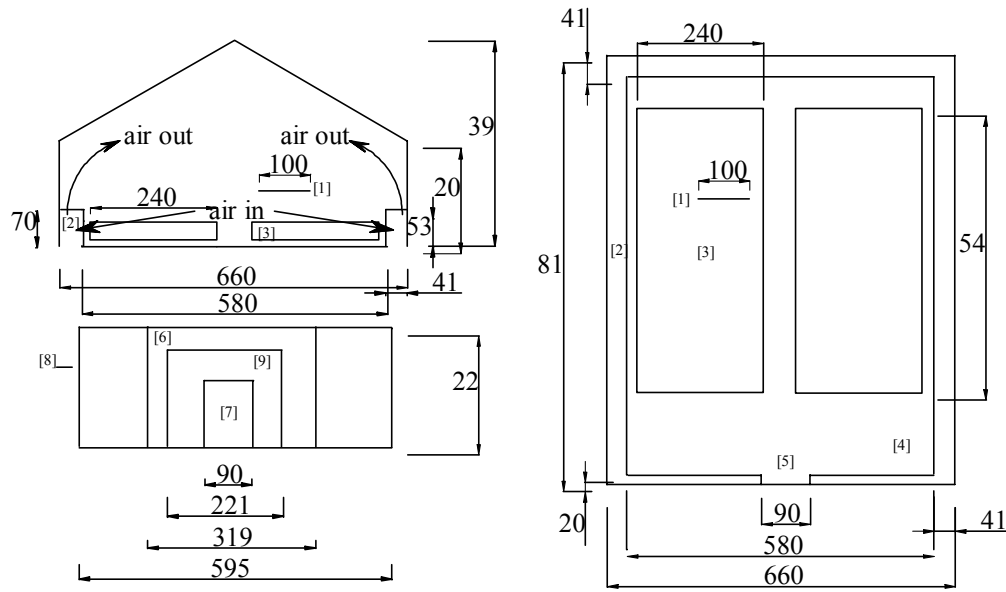
FIGURE 1. Semi-closed greenhouse system set-up for measuring chrysanthemum crop CO_2 exchange (PPFD line quantum sensor [1], air conditioning in/outflow [2], planting containers [3], ground area [4], compartment door [5], basement [8], air conditioning unit [6], door to basement below the compartment [7], entrance unit [9]).

analyser (IRGA; URAS 3G, ABB, Hartmann & Braun, Frankfurt, Germany). A multiplexer-sample-unit (Hewlett Packard, Palo Alto, CA, USA) switched between the three channels according to their sequence. Air was transported from a measuring point with an under-pressure pump through a teflon sample line ($\varnothing$ 4 mm). Before the air entered the IRGA, it was dried in a condenser. Greenhouse samples were mixtures of four sampling points above the crop canopy.

Measurements with generated smoke into the air-conditioning unit of the empty shelters revealed an under-pressure in the basement below the greenhouse compartment (see FIG. 1). Air was clearly drawn from the walkway in front of the basement through openings to the inner semi-closed system. Air apparently left the greenhouse through the glass-cover. Therefore, two sample points in the walkway in front of each basement were used to measure outside-system CO_2 concentration.

Pure CO_2 was injected into the air conditioning unit proportionally to the difference between setpoint and measured CO_2 concentration using a thermal gas mass flow controller (5850E, Brooks, Veenendaal, The Netherlands) with a maximum flux rate of 450 g CO_2 h^{-1} (2.84 mmol CO_2 s^{-1}; TABLE 1). Sampler, analyser and mass-flow controller were controlled by a data-logger connected to a computer with a software program written with commercial control software (HP VEE 5.0, Hewlett Packard, Englewood, CO, USA).

TABLE 1. Proportional dosage of CO_2 as function of difference between CO_2 set point and measured concentration ($\Delta[CO_2]_{set}$) inside the semi-closed system.

$\Delta[CO_2]_{set}$	$1-4$	≤ 6	≤ 8	≤ 10	≤ 13	≤ 16	≤ 19	≤ 24	≤ 29
Valve-opening (%)	2.2	4.8	6.5	8.2	10.9	13.6	16.3	21.0	25.7
CO_2 supply (mmol s^{-1})	0.06	0.14	0.18	0.23	0.31	0.39	0.46	0.60	0.73
$\Delta[CO_2]_{set}$	≤ 34	≤ 39	≤ 44	≤ 49	≤ 59	≤ 69	≤ 79	≤ 89	> 90
Valve-opening (%)	30.6	35.6	40.7	46.0	56.9	68.3	80.4	93.0	100
CO_2 supply (mmol s^{-1})	0.87	1.01	1.16	1.31	1.62	1.94	2.28	2.64	2.84

Retractable metal roof-covers could be used independently to cover the complete greenhouses from outside radiation. For experiments under controlled light conditions, this and two independent controlled groups of assimilation lamps (SON-T AGRO, Philips, Eindhoven, The Netherlands) to achieve 0, 85 or 160 µmol mol^{-1} photosynthetic photon flux density (PPFD) were installed in each greenhouse.

Greenhouse climate (air temperature and relative humidity) was measured at two positions in the greenhouse with dry and wet-bulb PT–500 thermometers (Hoogendoorn, Vlaardingen, The Netherlands). A third electronic device measured temperature and humidity for climate control performed with a commercial setpoint controller (VitaCo, Hoogendoorn, Vlaardingen, The Netherlands). Direct and diffuse global radiation was measured with two solarimeters (Kipp and Sons, Delft, The Netherlands) on the roof of the building next to the greenhouses (FIG. 2). PPFD was measured in the greenhouses with a height adjustable 1-m line quantum sensor
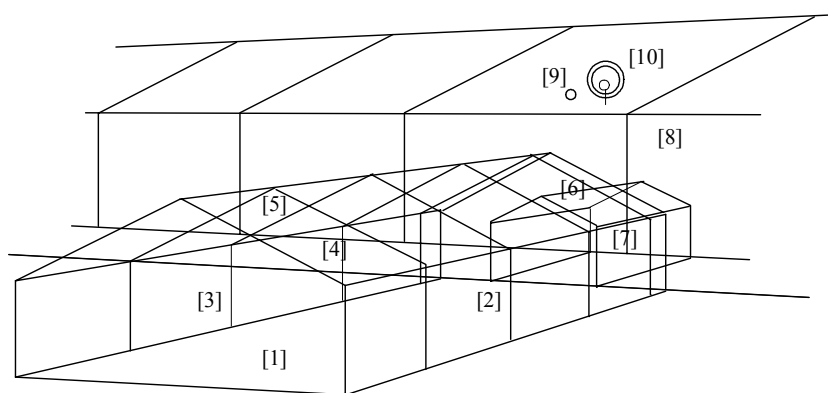
FIGURE 2. Semi closed greenhouse with front wall [1], eastern side wall [2], western side wall [3], eastern roof pane [4], western roof pane [5], greenhouse back-wall [6], connecting room between building and greenhouse with measurement equipment [7], concrete building back-wall [8] and the measuring devices for radiation (solarimeter for direct radiation [9] and solarimeter for diffuse radiation measurements [10]).

(to measure PPFD just above crop canopy) in each greenhouse (LI–191SA, LI-COR, Lincoln, NE, USA).

MEASURING NET CO_2 EXCHANGE

Mean CO_2 net exchange of a greenhouse crop ($\overline{P_{nc}}$, µmol CO_2 s^{-1}) was calculated as difference between CO_2 supply and CO_2 consumption between two time points[123] (t_2 and t_1) and the change in CO_2 amount stored in the system.

$$\overline{P_{nc}} = \left(\int_{t_1}^{t_2} E_{CO_2} dt - \int_{t_1}^{t_2} L_{CO_2} dt - \rho \cdot V \cdot \left([CO_2]_{t_2} - [CO_2]_{t_1} \right) \right) \cdot (t_2 - t_1)^{-1} \qquad [1]$$

This equation contains CO_2 supply rate (E_{CO_2}, µmol CO_2 s^{-1}), CO_2 leakage or unwanted source or sinks (L_{CO_2}, µmol CO_2 s^{-1}), CO_2 concentration inside the compartment ($[CO_2]$, µmol CO_2 mol^{-1} air), density of greenhouse air ρ (mol m^{-3}) and volume of the measuring system V (m^3). Crop gross photosynthesis (P_{gc}, µmol CO_2 s^{-1}) could be calculated by adding daytime crop dark respiration ($R_{dc,}$, µmol CO_2 s^{-1}) to P_{nc}.

$$P_{gc} = P_{nc} + R_{dc} \qquad [2]$$

R_{dc} was determined at night by measuring net CO_2 exchange without radiation (PPFD=0) at constant temperature (T_d, ±0.5 K) ($R_{dc,T}$). To calculate temperature dependency of R_{dc}, $R_{dc,T}$ was substituted in a temperature dependent respiration function[97].

$$-\left(\int_{t_1}^{t_2} E_{CO_2} dt - \int_{t_1}^{t_2} L_{CO_2} dt - \rho \cdot V \cdot \left([CO_2]_{t_2} - [CO_2]_{t_1} \right) \right) \cdot (t_2 - t_1)^{-1} = R_{dc,T} \quad \begin{array}{l} \forall \;\; PPFD = 0 \\ \forall \;\; T_{l,d} = \text{const.} \end{array} \qquad [3]$$

$$R_{dc} = R_{dc,T} \cdot e^{E_d \cdot (T_{l,i} - T_{L,d})/(T_{l,i} \cdot R \cdot T_{l,d})} \qquad [4]$$

EQ. 4 contains leaf temperature during light ($T_{l,i}$, K), leaf temperature during darkness ($T_{l,d}$, K) gas constant (R) and activation energy (E_d, J mol^{-1})[97]. To attain accurate P_{nc} measurements, the dynamic parameters E_{CO_2}, L_{CO_2} and $[CO_2]$ have to be determined with acceptable accuracy and their variation must be known.

SYSTEM VARIATION AND ERROR ANALYSIS

All technical equipment has certain accuracy. The total variation of the system can only be as small as the cumulative accuracy of all involved devices. The theoretically

expected accuracy could be determined by calibrating the measuring devices directly used for CO_2 exchange measurements such as mass flow controller and IRGA. The total variance of CO_2 net exchange ($s_{P_{nc}}^2$) can then be calculated from theoretical variances such as that of CO_2 supply (s_E^2), $[CO_2]$ measurement ($s_{[CO_2]}^2$) and others. This was done with error analysis[124].

When only one measuring time point is analysed and assuming that the volume was measured without error, $s_{P_{nc}}^2$ could be calculated with EQ. 5.

$$s_{P_{nc}}^2 = s_E^2 + s_L^2 + s_\rho^2 \cdot \left(\frac{V \cdot d[CO_2]}{t_{i+1} - t_i} \right)^2 + s_{d[CO_2]}^2 \cdot \left(\frac{V\rho}{t_{i+1} - t_i} \right)^2 + s_t^2 \cdot \left(\frac{\rho V \cdot d[CO_2]}{(t_{i+1} - t_i)^2} \right)^2 \quad [5]$$

with sample-interval time ($t_{i+1} - t_i$), variances for CO_2 leakage (s_L^2), CO_2 concentration difference between two measurements ($s_{d[CO_2]}^2$), air density (s_ρ^2) and sample time (s_t^2). The total variance of a series of CO_2 samples (measuring time points) can be determined from time integrals for CO_2 supply ($\int E_{CO_2}$), CO_2 leakage ($\int L_{CO_2}$) and CO_2 storage ($Q = \rho \cdot V \cdot [CO_2]_2 - [CO_2]_1$) and their and their variances ($s_{\int E_{CO_2}}^2$, $s_{\int L_{CO_2}}^2$, s_Q^2).

$$s_{P_{nc}}^2 = \frac{s_{\int E_{CO_2}}^2 + s_{\int L_{CO_2}}^2 + s_Q^2}{(t_2 - t_1)^2} \quad [6]$$

The maximum allowed variance ($s_{P_{nc} \max}^2$) can be calculated from the maximum allowed absolute error for CO_2 uptake measurement ($\delta_{P_{nc} \max}$). $\delta_{P_{nc} \max}$ was derived from a more relative error of 5 % for all P_{nc} levels[124].

LEAKAGE, UNWANTED CO_2 SOURCES, SCRUBBERS AND BUFFERS

In the perfect case, a gas exchange system is airtight and no unwanted CO_2 source or sink exist inside the system. In that case, L_{CO_2} would be zero or a controlled parameter. However, a perfectly airtight greenhouse is difficult to realise. Certain leakage is indispensable, because an amount of air equal to the amount of CO_2 gas that is supplied to the greenhouse (up to ~ 250 l h^{-1}) needs to exit. Also gas expands with increasing temperature and a perfectly airtight greenhouse would burst. Furthermore, CO_2 sources other than the pure supply and sinks other than plants could be present inside the system. Using inert material in case of a newly built system would overcome most of these problems. In our case, however, greenhouses were re-build from old structures. To detect leakage ventilation and unwanted CO_2 source, general mass balance equation was applied[125]. The rate of change in time (t) of inside gas concentration ($[x_i]$, µmol mol^{-1}) for a perfectly mixed air was used as starting point.

$$V\rho\frac{d[x_i]}{dt} = -f_v(t)([x_i]-[x_o]) + \sum f_p(t) + \sum f_u(t) - \sum f_{ad/abs} - f_{cv}(t,T_i,[x_i]) \qquad [7]$$

with concentration of outside gas ($[x_o]$), leakage ventilation (f_v, μmol s^{-1}), controlled gas source rate (f_p, μmol s^{-1}), uncontrolled gas sources (f_u, μmol s^{-1}), gas adsorption and absorption ($f_{ad/abs}$, μmol s^{-1}) and losses due to chemical reaction (f_{cv}, μmol s^{-1}).

To investigate f_v independently from other CO_2 sinks or sources, the tracer gases sulphur hexafluoride (SF_6) and nitrous oxide (N_2O) were used with gas chromatography. With these gases, ad- and absorption and internal sources as well as chemical decay were minimised. Using SF_6 and N_2O, the only tracer gas source was assumed to be f_p (SF_6 is manmade and does not exist naturally and N_2O has a low and very stable concentration in nature). The constant-flow method (CT) was applied with both gases. With this procedure, a constant gas flux that stabilised the gas concentration inside the greenhouses at a relatively constant high concentration level (within the possible range for the measuring equipment) was introduced over a time interval of 19 hours. Constant gas injections of 158 and 41 μmol s^{-1} (SF_6 and N_2O, respectively) for greenhouse 1, and 149 and 44 μmol s^{-1} for greenhouse 2 were applied, respectively. As soon as the gas concentration was stabilised (0.0033 μmol SF_6 mol^{-1} air and 65 μmol N_2O mol^{-1} air), air was sampled into a cylinder to get a representative sample over the complete period. Gas samples of 20 ml were taken at three different times to check the stability of the gas concentration.

As no uncontrolled gas source, no absorption or adsorption and no chemical decay exists with SF_6 and N_2O, f_v can be calculated directly from gas supply.

$$f_v = \frac{f_p}{x_i - x_o} \qquad [8]$$

To estimate, the uncontrolled CO_2 source (f_{u,CO_2}), measurements with CO_2 as tracer gas were performed, too. For that, three CT measurements (with supply of 0, 0.21 and 0.83 mmol CO_2 s^{-1}) were performed. Because f_v was determined by SF_6 and N_2O at the same time, the remaining part of leakage was f_{u,CO_2} and was predicted from the CO_2 balance[89].

$$L_{CO_2} = -f_{u,CO_2} + f_v \cdot ([CO_2]_i - [CO_2]_o) \qquad [9]$$

Inside greenhouse CO_2 concentration ($[CO_2]_i$, μmol mol^{-1}) was determined from four different sampling points in each compartment. Outside CO_2 concentration ($[CO_2]_o$, μmol mol^{-1}) was measured in the corridor in front of the basement below the compartments (FIG. 1). The corridor was the assumed inlet leakage location,

because of an under-pressure in the basement and overpressure in the greenhouse compartment.

To check these measurements, a second procedure was applied. Three rate of decay (ROD) measurement (350, 600 and 1000 µmol mol^{-1} as starting points) were performed with CO_2. With ROD, a certain start gas concentration is achieved. After that, supply is stopped and the change in gas concentration in time is recorded. ROD is based on the first two right-hand terms in Eq. 7 and can be re-formulated for CO_2.

$$\ln \frac{[CO_2]_i - [CO_2]_o}{[CO_2]_{i,t=0} - [CO_2]_o} = \frac{f_{v,CO_2}}{V\rho}(t - t_0)$$ [10]

f_v can then determined graphically by plotting $t - t_0$ versus the natural logarithm of the CO_2 gas-ratio (left hand side Eq. 10), since $-f_v/V\rho$ is the slope of the curve. For this method, outside CO_2 concentration must be constant. In addition, outside CO_2 concentration data must be increased with the difference in CO_2 concentration that results from f_{u,CO_2}.

The existence of a CO_2 buffer ($f_{ad/abs,CO_2}$) was only suspected in water (liquid H_2O can take up 38.8 mmol l^{-1} CO_2 at 1013 Pa and 20 °C). CO_2 could be absorbed and relieved from free water inside the greenhouse according to pressure and concentration. The speed of CO_2 dissolving in water at different concentrations is unknown. Measurements of CO_2 concentrations were therefore performed in dry greenhouses and with a water layer of 5 – 10 cm at constant climate conditions. Different constant CO_2 supply rates (0, 0.63 and 2.39 mmol CO_2 s^{-1}) were stepwise applied for 50 minutes in both situations. Chemical decay of CO_2 (f_{cv,CO_2}) was neglected. This because the atmosphere has a slow CO_2 decay function, and decay can be assumed zero within the time unit used in of measurements (minutes).

RESPONSE AND REACTION TIMES

Although there is hardly any delay in photosynthetic plant response to environmental conditions, time delay between a plant reaction and its measurement is from utmost importance in dynamic climate conditions. The response time for a gas-exchange system can be calculated for small units (i.e. for single or few plants) by the air-flow through the system and its volume[114]. In the present system, there is no one directional air-flow as it is common in small acrylic plastic chambers[113, 114, 126, 127]. The air in the present system is assumed to be mixed perfectly very fast. The air conditioning unit was located in the basement and air was drawn from and blown into the greenhouse part of the semi-closed system with high speed. Air inlets were present across the full length of all side-walls (FIG. 1). Air outlets were projected beneath those openings ensuring a high air mixing rate. When a smoke generator was used in the basement, the complete greenhouse was completely foggy within less than

15 seconds. However, the mixed air had to be transported to the measuring system and analysed. Due to that, a transport-delay and a measuring delay existed. The transport-delay was due to CO_2 sample pipe-length and the measuring delay was the response time for the IRGA after a switch between two compartments. If these delay times would not be obeyed, determined CO_2 concentration in the IRGA would be partly from the preceding measurement. This would contribute to inaccuracy in the measured photosynthesis response. Both delays were determined by alternated supply of CO_2 concentrations (345 and 1000 µmol mol^{-1}), either at begin of the measuring lines in the greenhouses or directly to the IRGA.

CO_2 DYNAMICS

To attain an overall system check and to test whether the mass balance (EQ. 1) can be used as such, the system was checked for a first order response. In response to a step function, a straight line of the logarithm of the CO_2 gas-ratio in time would proof a clear first order response function.

CO_2 concentration is the major state variable to the mass balance. Timely variations in CO_2 concentration setpoint had to be limited to prevent effects on measured P_{nc}. With a constant light source and constant climate set points (constant P_{nc} assumed), CO_2 supply would fluctuate only little between t_1 and t_2. However, CO_2 uptake can fluctuate with natural light conditions when semi-cloudy sky conditions prevail. This can lead to timely variations in CO_2 concentration and supply. When different air-samples had to be averaged over time in order to obey the committed 5 % maximum error a maximum acceptable PPFD deviation between two measurements had to be determined.

EXPERIMENTS

To test the complete system, CO_2 gas exchange measurements were performed with a vegetative growing cut chrysanthemum crop (*Chrysanthemum grandiflorum* cv. Reagan Improved) obtained from a commercial propagator (Fides Goldstock Breeding, Maasland, The Netherlands) under conditions with natural radiation and with constant low light source. Plants were transplanted on 13 March 2002 in six containers of 1.8 x 2.4 m in perlite at a density of 64 plants per m^2 in one greenhouse (GH_1). GH_1 was assumed to resemble both greenhouses. During measurements, a fully-grown chrysanthemum crop was achieved (LAI > 4, stem length 1.1 m – 1.5 m). Plants were then placed in two groups of three containers of 13 m^2 (5.4 x 2.4 m) each group. The crop canopy of each group exceeded the size of the containers by 12.5 cm on three sides. The area of one group was therefore ca. 14.5 m^2 ([5.4 + 0.125] x [2.4 + 2 x 0.125]), i.e. 29 m^2 for the whole canopy. Between the two groups a corridor of 60 cm width was created for maintaining plants.

A green net installed at the inner side-borders of the canopy protected the plants from side radiation from the corridor. Daylength of 19 hours (4.55 a.m. – 11:55 p.m.) was induced with assimilation lamps (SON-T AGRO, SGR 200, Philips, The Netherlands). During this period, light was switched on when outside global radiation fell below 300 W m^{-2} and off again when it rose above 400 W m^{-2}. Day and night temperatures were set to 20 °C and 19 °C, respectively, and relative humidity to 85 %. CO_2 gas exchange measurements were performed between 26 April and 22 May 2002. CO_2 concentration was either set to 450 or 1000 µmol mol^{-1}. To test the system performance at low photosynthetic conditions, measurements at constant low light conditions were performed (26 April – 12 May 2002) with two different photosynthetic levels using 85 µmol m^{-2} s^{-1} and 160 µmol m^{-2} s^{-1} PPFD. The light were switched on between 4.55 a.m. and 11:55 p.m. while the retractable roof was closed. CO_2 set point was 450 µmol mol^{-1} and temperature was set to 19 °C during night and 20 °C during day and relative humidity was set to 85 %.

Natural light measurements were performed between 16 May and 22 May 2002. Greenhouse temperature and relative humidity was set as with constant light treatments. CO_2 concentration was set to 1000 µmol mol^{-1} (16 May – 22 May). Neither screen nor supplementary lighting was applied.

SIMULATIONS

For simulations, leaf photosynthesis was scaled up to the crop level with a geometric radiation absorption model. Photosynthesis of separate leaves was determined with photochemical efficiency (α_l) and maximum leaf gross photosynthesis ($P_{g,\max}$) of the negative exponential light response curve[94]. $P_{g,\max}$ and α_l were calculated with several biochemical key processes for leaf CO_2 assimilation[97] that have been summarised in a simplified description[98, 128]. A homogeneous distribution of CO_2, temperature and humidity inside the canopy was assumed such that $P_{g,\max}$ and α_l were the same for the whole canopy.

A model was developed that calculated diffuse and direct photosynthetic active radiation (PAR, W m^{-2}) absorbed by individual leaves inside the block-shaped plant stand. A rectangular 3-dimensional grid of 4000 points (P_{xyz}; 20 points along width, 20 points along depth, and 10 points along the height of the block) was adopted.

Diffuse and direct PAR were first determined outside the greenhouse[129] (PAR_{difOut}, PAR_{dirOut}). Transmission was then determined separately for PAR_{difOut} and PAR_{dirOut}. Transmission of direct PAR (τ_{dir}) was calculated depending on elevation and azimuth of the sun, the angle of incidence on roof or wall and the transmission curve of roof or wall and the presence of non-transparent construction parts[130]. The interception of any beam reflected by the wall behind the greenhouses was taken into account, too. It was assumed that neighbouring greenhouses fully intercept direct

photosynthetic active radiation (PAR) and that the intensity of diffuse PAR coming from neighbouring houses was the same as that of the unobstructed sky. Transmission of diffuse PAR (τ_{dif}) was assumed constant according to measurements performed at an overcast sky. Absorption of diffuse and direct PAR was calculated for each point independently. Absorption of a single (direct) PAR beam was calculated from path length through the canopy, leaf area traversed, average projection of leaves into the direction of the beam, reflection and scattering for shaded and sunlit leaves[96] and similar to the model for hedgerow canopies[131]. Intensity of absorption of a direct PAR beam at each point in the block was calculated by multiplying PAR_{dirOut} by the transmission-value of the specific direct PAR beam (through either the cover of the phytotron, the front or back wall, or the sides). Absorption of diffuse PAR was calculated by averaging absorbed intensities of numerous single beams coming from 6400 different angles from whole hemisphere. PAR_{difOut} intensity was equal for all directions. Gross assimilation was then separately calculated from absorbed total PAR fluxes for shaded and sunlit leaves[96] ($PAR_{shd,abs}$ and $PAR_{sun,abs}$, respectively) to yield shaded and sunlit photosynthesis ($P_{g,shd}$ and $P_{g,sun}$, respectively).

$$\left[P_{g,sun,P}\begin{pmatrix} x_1...x_{20} \\ y_1...y_{20} \\ z_1...z_{10} \end{pmatrix} \right] = P_{g,\max} \cdot (1 - e^{\frac{-\alpha_l \cdot \left[PAR_{shd,abs,P}\begin{pmatrix} x_1...x_{20} \\ y_1...y_{20} \\ z_1...z_{10} \end{pmatrix} \right]}{P_{g,\max}}}) \tag{11}$$

$$\left[P_{g,sun,P}\begin{pmatrix} x_1...x_{20} \\ y_1...y_{20} \\ z_1...z_{10} \end{pmatrix} \right] = P_{g,\max} \cdot (1 - e^{\frac{-\alpha_l \cdot \left[PAR_{sun,abs,P}\begin{pmatrix} x_1...x_{20} \\ y_1...y_{20} \\ z_1...z_{10} \end{pmatrix} \right]}{P_{g,\max}}}) \tag{12}$$

Shaded leaves intercepted diffuse light and the scattered part of direct light and sunlit leaves intercepted in addition to that also the direct light beam. Leaves were assumed to have the so-called near-planophile vertical leaf angle distribution. For that, a scattering coefficient ($\sigma = 0.15$) and an extinction coefficient for diffuse radiation ($K_{dif} = 0.8$) were used. P_{gc} was calculated by summing up rates of CO_2 assimilation for every single point in the grid. Measured and simulated P_{gc} values were fitted by non-linear least squares iteration. (PROC NLIN, SAS ver. 8.0, SAS Institute Inc., Cary, NC, USA) to the negative-exponential light response curve for canopies with maximum canopy gross photosynthesis ($P_{gc,\max}$) and canopy photochemical efficiency[89] (α_c).

$$P_{gc} = P_{gc,\max} \cdot \left(1 - e^{\frac{-\alpha_c \cdot PPFD}{P_{gc,\max}}} \right) \tag{13}$$
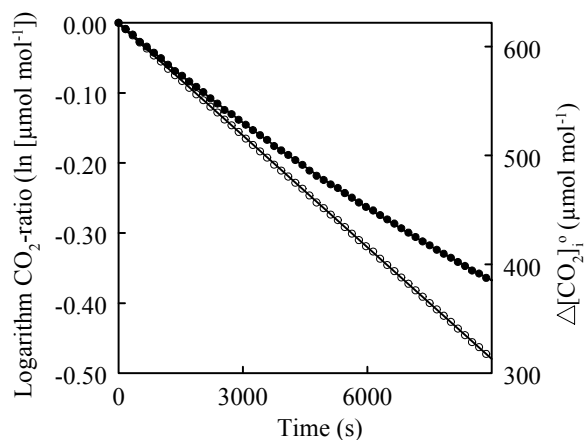
FIGURE 3. Decay of the difference between inside and outside CO_2 concentration ($\Delta[CO_2]_i^o$; ●) with negative exponential curve fit (R^2=1.0), and the natural logarithm of the gas-ratio ($\ln\left(\Delta[CO_2]_i^o \middle/ \left([CO_2]_{i,t=0} - [CO_2]_o\right)\right)$; ○) with linear curve fit ($R^2 = 1.0$).

RESULTS

ERROR ANALYSIS AND CO_2 DYNAMIC

The measuring system worked well in combination with the mass balance equation (FIG. 3). A linear fit to the logarithm of the gas-ratio was found. The equation could be used without adjustment. The error estimates of one CO_2 sample moment had different effects on the total variance. Increasing the partial variances separately by factor 2 increased $s_{P_{nc}}^2$ by factor 2.5 for CO_2 concentration, 1.27 and 1.17 for CO_2 leakage and supply. The system was less sensitive in variation in CO_2 dosage than in CO_2 concentration. Keeping CO_2 concentration constant within 5 % error range was of major importance. The highest impact on data variations, nevertheless, had the number of time points used for calculating CO_2 assimilation. The overall measuring error of the complete system could rise to 50%, when only one measuring time point was used. Using more than one measuring point reduced the error strongly and the
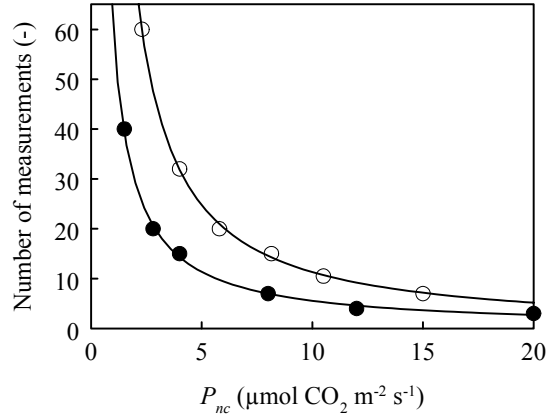
FIGURE 4. Number of necessary measuring points as function of net photosynthesis to attain an overall measuring error of 5 % ($\bigcirc$) or 10 % ($\bullet$). Data were arbitrarily chosen and calculated according to the errors.

targeted threshold of 5 % could be achieved. The number of necessary measurements (N) to comply with 5 % error decreased exponentially with P_{nc} (FIG. 4, EQ. 14).

$$N = 152.12 \cdot P_{nc}^{-1.1286} \qquad [14]$$

At very low actual CO_2 assimilation rates of 5 μmol m^{-2} s^{-1}, 25 measuring time points had to be used to obey the 5 % error. In our system, the interval time between two measurements was 5 minutes. Therefore, an average over more than 2 hours was necessary at very low assimilation levels. At rather low net assimilation levels of 15 μmol CO_2 m^{-2} s^{-1} only 40 minutes were necessary. These levels are attainable with ca. 200 and 500 μmol m^{-2} s^{-1} PPFD at ambient CO_2 concentration (350 μmol mol^{-1}) with a non-block crop (FIG. 5). At higher radiation and CO_2 levels to reach e.g. 30 μmol CO_2 m^{-2} s^{-1} net assimilation (with ca. 900 μmol m^{-2} s^{-1} PPFD and 750 μmol CO_2 mol^{-1} air) only 4 time points and therefore a mean over 20 minutes would be enough.

When calculating the number of necessary measurements, the actual net CO_2 exchange per m^2 crop area (A) could be used. Substituting EQ. 1 in EQ. 14 results in:

$$N = 152.12 \cdot \left(\left(\left(\int_{t_1}^{t_2} E_{CO_2} - \int_{t_1}^{t_2} L_{CO_2} - \rho \cdot V \cdot \left([CO_2]_{t_2} - [CO_2]_{t_1} \right) \right) \cdot (t_2 - t_1)^{-1} \right)^{-1.1286} \bigg/ A \right) \qquad [15]$$

More than one measuring time point, however, could lead to a different error, when light level or CO_2 concentration fluctuate, because photosynthetic light response is not linear (FIG. 5).
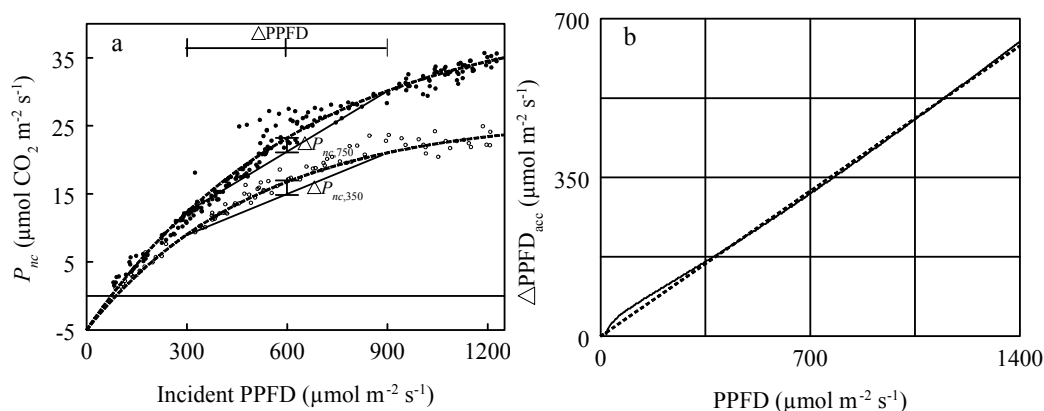
FIGURE 5. a) Simulated crop net photosynthesis (P_{nc}) with a non-block model (CHAPTER 2.1) at 350 ± 30 ($\bigcirc$) and 750 ± 30 ($\bullet$) μmol mol^{-1} CO_2 and 24 ± 2 °C. Measured climate data were input (5-minute averages of CO_2 concentration, RH, temperature and outside global radiation). Lines (---) were fitted according to EQ. 2 and EQ. 13 ($P_{nc,max}$ = 31.35 and 47.01 μmol CO_2 m^{-2} s^{-1}, α_c = 0.062 and 0.072 μmol CO_2 mol^{-1} photon for 350 and 750 μmol mol^{-1} CO_2, respectively). With example of acceptable PPFD deviation of 600 ± 300 μmol m^{-2} s^{-1} (ΔPPFD) and resulting P_{nc} differences for 350 and 750 μmol mol^{-1} CO_2 ($\Delta P_{nc,350}$ and $\Delta P_{nc,750}$). **b)**. Calculated accepted deviation from mean photosynthetic photon flux density (ΔPPFD) in the greenhouse at a range from 0 to 1400 μmol m^{-2} s^{-1} PPFD with at an acceptable error of 5 % (—) and linear fit (---), R^2=0.998.

$$\Delta\text{PPFD}_{acc} = 0.457 \cdot \text{PPFD} \qquad\qquad\qquad [16]$$

The acceptable deviation from the mean radiation level (ΔPPFD_{acc}) at 1000 μmol CO_2 m^{-2} s^{-1} increased almost linearly with radiation. This effect is almost independent from CO_2 concentration (FIG. 5).

REACTION TIMES AND CYCLE DURATION

The reaction time of the IRGA was found to be 40 s (TABLE 2) and the acceptable delay time of the measuring lines was 30 s. A total delay time of 70 s was therefore necessary for measurements (TABLE 3). The switch-time between two sampling points was 2 s. When both semi-closed systems were used for measurements, three locations had to be sampled (both greenhouses and inlet leakage location). One cycle duration for CO_2 measurement was then 216 s for both greenhouses and 144 s when only one greenhouse was used. A second cycle continuously measured CO_2 supply, PPFD, direct and diffuse global radiation outside the greenhouse and greenhouse climate (temperature and RH). This cycle used 14 s. Both cycles were independently averaged to 5 minutes.
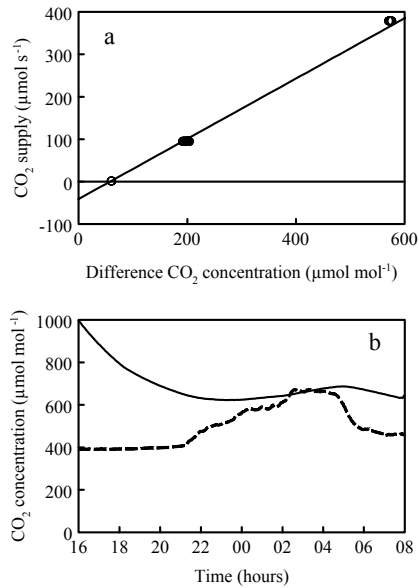
FIGURE 6. a) CO_2 leakage as function of CO_2 concentration-difference between greenhouse and outside (greenhouse 2); Inside and outside CO_2 concentration was at four times constant (± 1 μmol mol^{-1}) over 30 minutes (inside CO_2 concentration 450, 583, 590 and 970 μmol mol^{-1}; CO_2 supply = 0.70; **b)** Inside (———) and outside (– – –) CO_2 concentration as function of time during a rate of decay measurement (greenhouse 2).
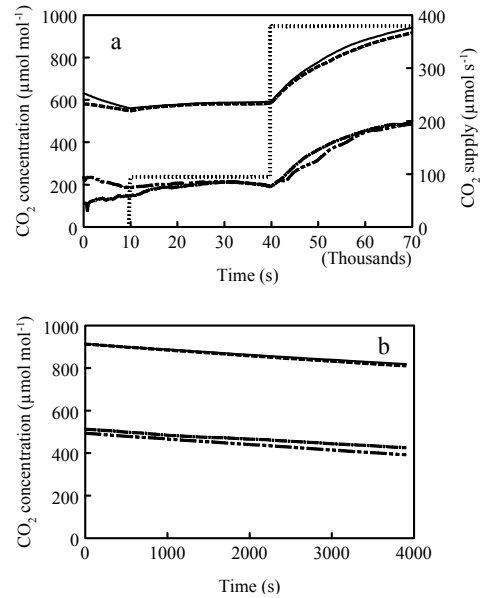
FIGURE 7. a) CO_2 concentration in greenhouse with dry (———) and wet floor (– – –, 5 – 10 cm water layer) and difference between inside and outside CO_2 concentration for dry (— — —) and wet (— — — —) conditions with various CO_2 supply-rates (····); and **b)** CO_2 concentration during ROD for dry (———) and wet floor (– – –) and difference between inside and outside CO_2 concentration for dry (— — —) and wet (— — — —) conditions.

LEAKAGE, CO_2 SOURCES AND BUFFERS

Measurements on leakage and CO_2 sources were performed for both greenhouses individually. For leakage measurements with greenhouse 2, the N_2O measuring system was out of order and only SF_6 and CO_2 were available. Leakage was determined to 0.7 mol air greenhouse^{-1} s^{-1} for both greenhouses (TABLE 4). The ROD measurements agreed well with CT data. Only little differences existed between the three gases (CO_2, SF_6 and N_2O) used in CT leakage measurements. When CO_2 was used as tracer gas, CO_2 concentration inside the greenhouse and in the walkway in front of the basement (leakage inlet location) had to be constant (± 1 μmol CO_2 mol^{-1} air). This constancy was achieved four times during the measurements for at least 30 minutes. A line was calculated that determined leakage (FIG. 6). The uncontrollable source f_{u,CO_2} was found to be constant in both greenhouses with 30 and 41 μmol CO_2 greenhouse^{-1} s^{-1}, respectively (TABLE 4). The slope of the line was f_v = 0.70 mol air s^{-1} per greenhouse. Greenhouse CO_2 concentration depended on CO_2 concentration of the walkway. When greenhouse CO_2 concentration was

TABLE 2. CO_2 concentration measured directly with the IRGA (URAS 3G) depending on reaction time and alternating dosage of two different calibrated CO_2 concentration ($[CO_2]_{cal}$) for determining the delay-time of the IRGA with standard deviation (STD) of 10 measurements. The bold fields indicate the acceptable concentration.

$[CO_2]_{cal}$	Reaction time (s)			
	20	30	40	50
$1000 \pm 3*$	893.6 ± 9.0	994.5 ± 0.38	998.5 ± 0.34	999.4 ± 0.21
$345 \pm 3*$	444.8 ± 2.1	356.4 ± 0.94	347.7 ± 0.36	345.9 ± 0.16

* Variation according calibration report IRGA 09.01.02 (ABB Automation, Delft, The Netherlands)

TABLE 3. CO_2 concentration measured with the IRGA (URAS 3G) depending on reaction time and alternating supply of two different calibrated CO_2 concentration ($[CO_2]_{cal}$) to determine the IRGA delay-time and sample lines with standard deviation (STD) of four different measurements. The bold fields indicate the acceptable concentration.

$[CO_2]_{cal}$	Reaction time (s)				
	50	60	70	80	100
$345 \pm 3*$	352.2 ± 4.9	347.6 ± 1.8	346.0 ± 0.8	345.3 ± 0.4	345.1 ± 0.2
$1000 \pm 3*$	991.6 ± 3.3	997.0 ± 1.4	998.3 ± 0.7	998.8 ± 0.5	999.1 ± 0.5

* Variation according calibration report IRGA 09.01.02 (ABB Automation, Delft, The Netherlands)

subject to ROD mesurements, CO_2 concentration clearly increased when CO_2 concentration of the walkway increased (FIG. 6). This supports the earlier findings that leakage was mainly located in the connection between basement-door and walkway outside the system. The existence of a water layer in the greenhouses did not have a distinct buffering or supplying effect on the aerial CO_2 concentration (FIG. 7). No effect of wind speed on leakage rate could be found either (data not presented). L_{CO_2} ($\mu mol\ s^{-1}$) could then be determined for greenhouse system 1 and 2 (GH$_1$ and GH$_2$, respectively).

$$L_{CO_2,GH_1} = -30 + 0.7 \cdot \left([CO_2]_i - [CO_2]_o \right)$$ [17]

$$L_{CO_2,GH_2} = -41 + 0.7 \cdot \left([CO_2]_i - [CO_2]_o \right)$$ [18]

FINAL MODEL FOR P_{nc}

Greenhouse net CO_2 exchange could be formulated for both greenhouses. The number of measurements used in one averaging time-unit (t_{av}) depended on the actual level of net CO_2 assimilation (i.e. N) respecting D_{PPFD}.
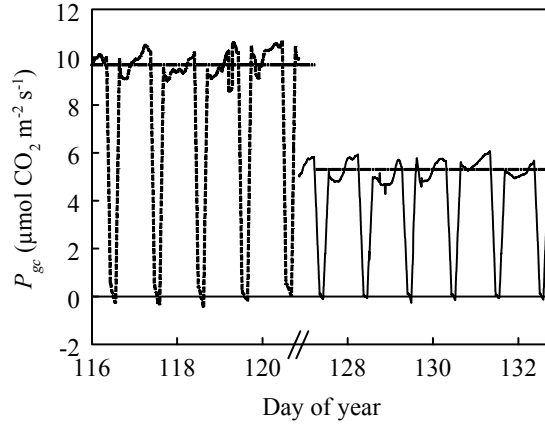
FIGURE 8. Measurements of crop gross photosynthesis (P_{gc}) with constant light level of 85 μmol m^{-2} s^{-1} PPFD (——) and 160 μmol m^{-2} s^{-1} PPFD (---) in cut chrysanthemum with overall daytime mean (— – —). P_{gc} was calculated from net CO_2 gas exchange of the day (P_{nc}) and net CO_2 gas exchange during the following night (R_d). CO_2 concentration was 445 μmol mol^{-1}.

$$P_{nc,\mathrm{GH_1}} = \left(\int_{t_1}^{t_2} E_{CO_2}\,dt + \int_{t_1}^{t_1} \left(-30 + 0.7 \cdot \left([CO_2]_i - [CO_2]_o\right)\right) - \rho \cdot V \cdot \left([CO_2]_{t_2} - [CO_2]_{t_1}\right) \right) \cdot (t_2 - t_1)^{-1} \quad [19]$$

$$P_{nc,\mathrm{GH_2}} = \left(\int_{t_1}^{t_2} E_{CO_2}\,dt + \int_{t_1}^{t_1} \left(-41 + 0.7 \cdot \left([CO_2]_i - [CO_2]_o\right)\right) - \rho \cdot V \cdot \left([CO_2]_{t_2} - [CO_2]_{t_1}\right) \right) \cdot (t_2 - t_1)^{-1} \quad [20]$$

PHOTOSYNTHESIS AND CLIMATE AT CONSTANT LOW LIGHT CONDITIONS

CO_2 gas exchange with two constant low PPFD levels of 85 and 160 μmol m^{-2} s^{-1} showed that the system responded rather stable to a constant light source (FIG. 8). P_{gc} fluctuated only little from the daytime means of 5.3 and 9.7 μmol m^{-2} s^{-1} (STD = 0.35 and 0.37 μmol m^{-2} s^{-1}).

It was generally observed that temperature dropped in the afternoon to slightly lower values. Temperature range during day was between 20 °C and 21 °C. Relative humidity was rather constant with a mean of 87.5 % (±0.5 %). RH increased during night to values more than 95 % and temperature dropped with a lower set point to an average of 19.5 °C. CO_2 concentration in the morning was higher than the set point. Greenhouse CO_2 concentration increased during the dark period through crop respiration. Also outside CO_2 concentration (inlet leakage location) had a distinct influence on that. When assimilation light was switched on, a stable CO_2 concentration of 445 μmol mol^{-1} (±2 μmol mol^{-1} was reached after 2 or 3 hours for 160 and 85 μmol m^{-2} s^{-1} PPFD and maintained until the light was switched off.

TABLE 4. Parameters of leakage measurements to determine the CO_2 leakage rate (f_v , mol air s^{-1} greenhouse^{-1}) and the uncontrolled CO_2 source (f_{u,CO_2} , µmol CO_2 s^{-1} greenhouse^{-1}) with constant flow technique (CT) for greenhouse 1 and greenhouse 2 (GH$_1$ and GH$_2$, respectively) for three different gases (N$_2$O, SF$_6$ and CO_2).

		Tracer gas		
		SF$_6$	N$_2$O	CO_2
GH$_1$	f_v	0.70	-	0.70
	f_{u,CO_2}		0.69	30
GH$_2$	f_v	0.71		0.70
	f_{u,CO_2}	-	-	41

PHOTOSYNTHESIS AND CLIMATE WITH NATURAL LIGHT CONDITIONS

Climate in the semi-closed greenhouse with natural light conditions was less stable than with a constant light source. During night, temperature was rather constant at 20 °C (STD = 0.3). During day, however, maintaining a stable low temperature was difficult to achieve when outside radiation was high. When outside radiation increased to values higher than 700 W m^{-2}, greenhouse temperature also increased. The capacity of the climate control installation was obviously insufficient. A constant 20 °C temperature was only maintained when radiation was less than that (data not presented); e.g. on 18 May 2002, radiation was always lower than 700 W m^{-2}, mean air temperature in the greenhouse was 20 °C (STD = 0.7 °C). Greenhouse CO_2 concentration was somewhat lower than the set point (1000 µmol mol^{-1}) during night (995 µmol mol^{-1}), but constant (±1 µmol mol^{-1}). During daytime, CO_2 concentration fluctuated between maximum and minimum peak levels of 930 and 992 µmol mol^{-1} and a mean CO_2 level of 971 µmol mol^{-1} (STD = 14.3) was maintained during 18 May. With increasing radiation and therefore increasing photosynthesis rate, CO_2 concentration slightly decreased. When temperature was in constant, P_{gc} was well predicted (FIG. 9). Greenhouse temperature decreased relatively slower than radiation and due to that P_{gc} data at a certain range of PPFD could be attained. However, only a small set of data was available with elevated constant temperatures and the complete range for fitting a light response curve was not available. When radiation was low and temperature could be kept constant, a better fit to the light response curve could be attained (FIG. 10). The relative response differed between high and low PPFD values. P_{gc} was relatively lower with low than with high PPFD. This was also predicted with the block-shaped crop model (FIG. 10). Increasing temperature lead to a higher photosynthesis rate between 300 and 600 µmol m^{-2} s^{-1} PPFD (compare FIG. 9 and FIG. 10). Simulations employing the block-model agreed very well with measurements with constant temperatures (FIG. 11). The block-model
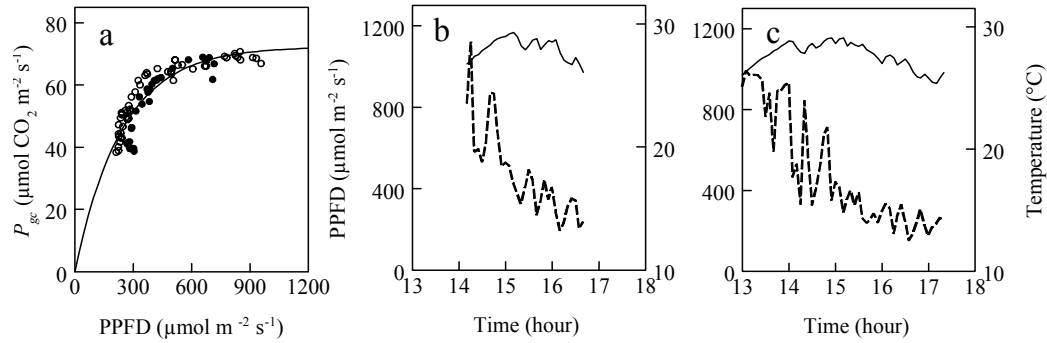
FIGURE 9. **a)** Measured crop gross photosynthesis (P_{gc}) with fitted negative exponential light response curve (—) for cut chrysanthemum during two days (20.05.02, ● and 21.05.02, ○) with mean-, maximum-, minimum temperature and STD of 28.0, 29.3, 26.1, 0.9 °C and 27.6, 29.1, 25.4, 1.06 °C for 20.05. and 21.05., respectively. Average CO_2 concentration was 948 (STD = 14.4) and 948 (STD = 11.5) for 20.05. and 21.05., respectively; **b)** and **c)** 5-min averages of greenhouse temperature (—) and PPFD (---) for the used measuring period from 20.05 and 21.05, respectively.

strongly improved the fit between measurements and simulations compared to a model that does not take the sides of a crop into account. When measurements were taken with natural light, sides of the crop were about 50 % of the complete crop surface. When this was not taken into account (using a non-block model) simulated P_{gc} was underestimated by 28 %. This relationship was almost linear ($R^2 = 0.99$), but percentage underestimation slightly decreased with higher assimilation rate. Then, the ratio between direct and diffuse radiation increased and parts of the crop sides were probably shaded and this resulted in a relative decrease of the block-shaped model. The block-model overestimated P_{gc} measurements only slightly (FIG. 12) and there was a linear relationship, too ($R^2 = 0.99$).

DISCUSSION

The aim of the present research was to develop a system that was capable to measure low and high crop photosynthesis rates at various climate conditions and to show the
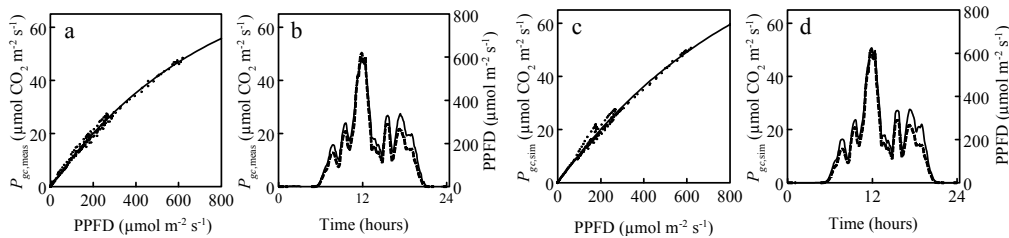
FIGURE 10. Measured (a, b) and simulated (c, d) crop gross photosynthesis ($P_{gc,\ meas}$ and $P_{gc,\ sim}$, respectively) for cut chrysanthemum at 971±14 µmol CO_2 mol^{-1} air and 20.3±0.7 °C (18.05.02) as function of PPFD with fitted light response curve (a, c); and P_{gc} (—) and PPFD (---) in time (b, d).
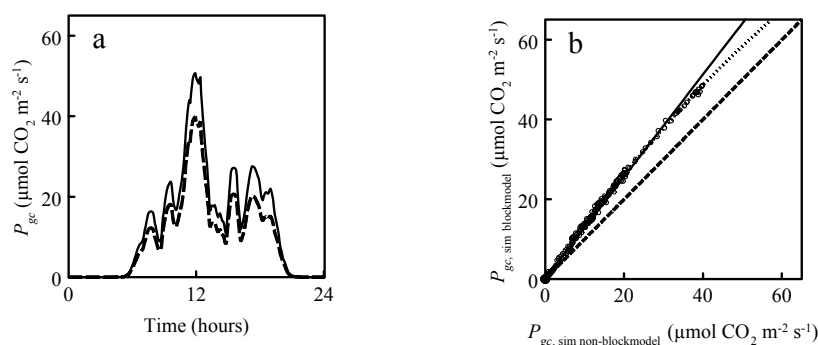
FIGURE 11. a) Simulated crop gross photosynthesis (P_{gc}) with the adjusted block model (—) and normal model (---) for cut chrysanthemum at 1000 µmol mol^{-1} CO_2 concentration and 20.3, STD = 0.7 °C); **b)** Simulated P_{gc} with block-model ($P_{gc,\ \mathrm{sim\,blockmodel}}$) compared to simulated P_{gc} with a normal non-block model ($P_{gc,\ \mathrm{sim\,non\text{-}blockmodel}}$), with linear regression (—; $P_{gc,\ \mathrm{sim\,blockmodel}} = 1.282 \cdot P_{gc,\ \mathrm{sim\,non\text{-}blockmodel}}$; $R^2 = 0.99$), polynomial fit (---).
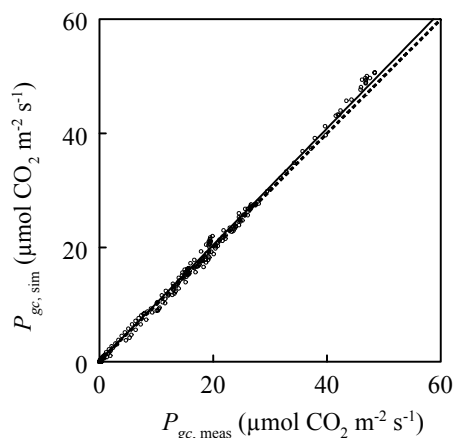
FIGURE 12. Measured and simulated crop gross photosynthesis ($P_{gc,\ \mathrm{meas}}$ and $P_{gc,\ \mathrm{sim}}$, respectively) for cut chrysanthemum at 971 µmol mol^{-1} CO_2 concentration and 20.3, STD = 0.7 °C); with linear regression (—; $P_{gc,\ \mathrm{sim}} = 1.02 \cdot P_{gc,\ \mathrm{meas}}$; $R^2 = 0.99$) and $P_{gc,\ \mathrm{sim}} = P_{gc,\ \mathrm{meas}}$ (---).

options for crop photosynthesis model validation. System design, calibration and performance were illustrated and measured data fitted well with the applied model. Since the leaf photosynthesis module in the model was validated within a greenhouse tomato crop canopy under regular climate conditions as also applied here[89], the probability of the validity of the measurements is high (even though crop was different). A direct comparison with measured and reported crop photosynthesis cannot be made, because the sides of the crop influence crop photosynthesis per square-meter. It has been illustrated that the block-shape model was important when comparing measured greenhouse photosynthesis with simulations. When larger greenhouses were used for measurements[e.g. 106], the sides of the crops are relatively less important and regular model versions (i.e. no three dimensional block-shape)

could be validated or compared with regular models[e.g. 132]. However, the sides of the crop become more important when units are smaller as they accounted between 37 % and 50 % of the complete crop surface during the measurements. The maximum acceptable measuring error for the measuring system (P_{nc}) was set to 5 %. The system performed well inside this error range when certain rules were followed. Because we aimed to create a system for the use in model validation for further application in climate control, the highest possible accuracy should be realised. Long data sets had to be used to comply with the 5 % error rule with low light levels. This was not problematic when constant light conditions were applied with photosynthetic artificial lighting. Then, CO_2 concentration and irradiation were constant and with constant temperature also P_{nc}. Under these circumstances, long averaging periods are not a concern. However, when natural low light conditions prevail long periods must be used, too. Then radiation probably fluctuates. This, however, would only lead to a small error increase if given rules are obeyed. The chosen maximum system error was low compared to a reported average error of 10 % in a crop photosynthesis system that used 192 m^2 greenhouses[106]. In addition, in that system only variation in CO_2 concentration was possible since climate control was not designed for various climate conditions. The major use of the present system is its application in measuring crop photosynthesis with many different greenhouse climate conditions for model validation. This because future greenhouse controllers should mainly be based on models to maximise profit and minimise energy consumption[133, 134] and those models need to be validated. Many photosynthesis driven crop growth models are partly based on poorly designed and validated temperature responses and are therefore only designed for rigid climate regimes. Those models have been successfully validated for e.g. tomato[6] or chrysanthemum[135] but it is questionable if they are applicable for flexible climate regimes. Flexible greenhouse temperature regimes partly based on photosynthesis models have already been developed[103, 136] but those were either based on leaf photosynthesis responses or P_{gc} models were not validated for applied temperature conditions. The presented system can contribute to improve that and support the development of improved greenhouse climate controllers. Crop gross photosynthesis data for the use in model validation (i.e. respecting the 5 % error) that were achieved with measurements under natural light conditions were difficult to attain. Only few occasions could be used for further analysis, because greenhouse temperature fluctuated with outside radiation. Under those conditions, however, some data could be used where temperature was constantly low. Also data attained with high temperature conditions could be used, though this was not targeted. The present system was not able to keep a low temperature when radiation increased to a high level. The cooling unit had obviously insufficient effective capacity. This could however be achieved with a more advanced cooling machine and with the present system measurements at higher constant temperatures of e.g. 26 °C and higher would be possible.

CONCLUSIONS

The present crop photosynthesis measuring system can be used to quantify photosynthesis in a canopy. The system was able to detect low and high photosynthetic rates within an error range of 5 %. With those measurements, crop photosynthesis models can be validated. For that, the presented light-interception model for a canopy is needed. Without taking light interception of the canopy block sides into account, an underestimation of photosynthesis resulted. The bottle-neck in the present measuring system was climate control of the experimental greenhouse. When this is improved, measurements at a range of temperatures are possible and crop photosynthesis models can then be validated for a wide range of climate conditions.

2.3 QUANTIFICATION OF TEMPERATURE AND CO_2 EFFECTS ON CHRYSANTHEMUM CROP PHOTOSYNTHESIS

O. KÖRNER & H. CHALLA

ABSTRACT

Temperature that maximises photosynthesis rises with radiation and CO_2 concentration. This has been thoroughly investigated for leaves but not for a canopy. Using this knowledge to maximise photosynthesis with climate control, well performing crop photosynthesis prediction models are necessary. CO_2 gas exchange measurements have been performed in two identical semi closed greenhouses with a 29 m^2 cut chrysanthemum crop. The effects of CO_2 (400, 700 and 1000 µmol mol^{-1}) and temperature (23, 28 and 33 °C) were studied. Data were fitted to the negative exponential light response curve for canopies ($P_{gc} = P_{gc,max} \cdot (1 - \exp(\alpha_c \cdot PPFD / P_{gc,max}))$). With the estimated parameters of this equation (maximum crop gross photosynthesis, $P_{gc,max}$, and crop photochemical efficiency, α_c), P_{gc} was predicted at 300, 600, 900 and 1200 µmol m^{-2} s^{-1} photosynthetic photon flux density (PPFD) for the three applied temperatures. A quadratic curve was fitted to the predicted P_{gc}-temperature responses to determine temperature that maximised photosynthesis at the different PPFD levels.

Temperature for maximum P_{gc} for all PPFD levels was below 23 °C with 400 µmol mol^{-1} CO_2. At higher radiation levels, temperature for maximum photosynthesis rose with elevated CO_2. An increase in temperature for maximising P_{gc} from 400 to 1000 µmol mol^{-1} CO_2 of at least 1 °C, 3.5 °C and 4.5 °C at 600, 900 and 1200 µmol m^{-2} s^{-1} PPFD, respectively, was predicted. This is far less as reported from literature for light saturated leaves in tomato when CO_2 concentration increased from 350 to 1200 µmol mol^{-1} (13 °C). The values reported here can probably be compared with tomato. When those value were approximated to an increase from 350 to 700 µmol mol^{-1}, 10 °C temperature shift was assumed. When this was scaled up to the crop level (leaf area index of 8), the temperature shift decreased to 4 °C at 500 µmol mol^{-1} PPFD but maintained the 10 °C shift at 2000 µmol mol^{-1} PPFD. Non-published data with a tomato crop revealed that a shift of at least 8 °C was possible between 400 and 1000 µmol mol^{-1} CO_2 at 1200 µmol m^{-2} s^{-1} PPFD. The probable lower shift found here is probably due to the incomplete temperature range for 400 µmol mol^{-1} CO_2. CO_2 – temperature interaction in a crop are probably well described in models for crop photosynthesis. Further investigations with a broader temperature range are necessary.

INTRODUCTION

In the last 20 years, more flexible temperature regimes were designed for energy saving in greenhouses[30, 55, 57, 61, 136]. With those regimes, vents open at higher temperatures than with common rigid regimes. This leads to two important differences: temperature is increasing with irradiation to a much higher extend and it is possible to increase greenhouse CO_2 concentration without the usual ventilation loss. This creates an interesting situation for optimisation of greenhouse climate, because high CO_2 will only be maintained at little or no ventilation, a situation that also results in a high temperature inside the greenhouse.

At common cultivation temperatures gross photosynthesis is relatively insensitive to temperature and photosynthesis response to temperature was assumed unaffected between 15°C and 25°C in greenhouse crop models[137]. However, outside the common temperature range, temperature affects photosynthesis rate[138]. This becomes more pronounced when either light or intercellular CO_2 level increase[88, 100, 139]. The underlying process is based on temperature and CO_2 response of ribulose biphosphate carboxylase / oxygenase (Rubisco). The ratio of carboxylation and oxygenation of Rubisco decreases with increasing temperature[140]. Elevated CO_2 concentration suppresses photorespiration and temperature that maximises photosynthesis increases[88, 101, 141–143]. When temperature that maximises photosynthesis is taken into account for ventilation control, energy consumption can be reduced and economical return can increase[64], because this largely depends on CO_2 loss by ventilation[66, 67].

This approach has been applied in climate control[136], but only leaf photosynthesis models were used, whereas crop photosynthesis shows less CO_2 – temperature interaction than leaf photosynthesis[100, 101]. On the other hand, leaf photosynthesis responses to temperature were thoroughly investigated (overview presented by Cannell and Thornley, 1998). A wide range in measured temperature optimum increase of light saturated leaf photosynthesis was found with different species. Using this information for modelling crop photosynthesis, resulted in large variations in CO_2 – temperature interaction[100]. However, this variation was probably due to the large difference of the investigated crops with e.g. pine, eucalyptus and tomato. The leafy greenhouse crop tomato had the largest shift in optimum temperature of light-saturated leaf photosynthesis of 13 °C between 350 and 1200 µmol mol^{-1} CO_2 [144]. When those value were approximated to an increase from 350 to 700 µmol mol^{-1}, 10 °C temperature shift was assumed[100]. When this was scaled up to the crop level (leaf area index of 8), the temperature shift decreased to 4 °C at 500 µmol mol^{-1} PPFD but maintained the 10 °C shift at 2000 µmol mol^{-1} PPFD.

However, the large variations in response of modelled crop photosynthesis to temperature and CO_2 leads to uncertainties in predicting crop photosynthesis at higher than commonly applied temperatures in present crop photosynthesis models. We aimed to investigate the predicted values with experimental evidence, because a well-validated model is necessary for optimal greenhouse climate control[145]. In the present research cut chrysanthemum was used to experimentally quantify the response of crop photosynthesis to temperature above the commonly applied levels. In another paper, these measurements will be used for validation of a crop photosynthesis model for the use in optimal ventilation control in cut chrysanthemum greenhouses.

MATERIALS AND METHODS

MEASURING CO_2 NET EXCHANGE

CO_2 net exchange was measured in a semi-closed greenhouse system[122] as presented in CHAPTER 2.2. Two identical greenhouses were used at Wageningen University, The Netherlands. The greenhouses (GH$_1$ and GH$_2$) had 44 m^2 ground cover (5.8 m x 7.5 m) and a total volume (incl. air conditioning unit) of 270 m^3. CO_2 concentration was measured with an infrared gas analyser (IRGA, Uras 3G, Hartmann & Braun, Frankfurt, Germany). The IRGA was calibrated once a week with standard CO_2 concentrations of 0, 350 and 1000 µmol mol^{-1} (Hoek Loos, Dieren, The Netherlands). The major part of the system consisted of the IRGA, a thermal gas mass flow controller for CO_2 flux (5850E, Brooks, Veenendaal, The Netherlands), a multiplexer-sample unit (HP3852, Hewlett Packard, Palo Alto, CA, USA) and a control computer with commercial software (HP-VEE, Hewlett Packard, Englewood,

CO, USA). Sample-air was drawn from the greenhouses and the in-let leakage location (location where outside air enters the system, determined before experiment started) in a timely sequence controlled by the multiplexer-sample unit through the control software. Air was dried in a condenser and CO_2 concentration was determined by the IRGA. The control computer decided on the percentage opening of the CO_2 mass flow controller valve based on the difference between measured CO_2 concentration and set point (PI-controlled). Leakage rate was predicted from CO_2 balance[89] as function of a determined constant CO_2 source and difference between inside and outside-system CO_2 concentration (see CHAPTER 2.2). Measured values of CO_2 concentration, CO_2 supply, PPFD, direct and diffuse global radiation outside the greenhouse and greenhouse climate (temperature and RH) were averaged over 5 minutes and logged (HP 3852, Hewlett Packard, Palo Alto, CA, USA).

The complete system was calibrated and thoroughly described in CHAPTER 2.2. The maximum measuring error was kept below 5 %, calculated as described in CHAPTER 2.2 [124]. The error was high when photosynthesis level was low. Averaging several measuring moments reduced the error strongly. In the present experiment, data were averaged over 60 min.

CO_2 net exchange of a greenhouse crop (P_{nc}, μmol CO_2 s^{-1}) was calculated as difference between CO_2 supply and CO_2 consumption between two time points and the change in the amount of CO_2 stored in the system[123]. P_{gc} was calculated by adding crop dark respiration (R_{dc}) to P_{nc}. R_{dc} was determined by measuring net CO_2 exchange during the first hour of the night period (temperature set point was the same as during day-time) that was assumed to be representative for the whole day. Day-time R_{dc} was recalculated with a temperature dependent respiration function[97] since daytime temperature was not perfectly constant and could differ from temperature used for nighttime respiration measurements.

PLANTS AND CLIMATE CONDITIONS

Chrysanthemum cuttings (*Chrysanthemum* Indicum group), cultivar *Reagan Improved*, were rooted in peat-blocks at 20 °C on a heated bench and covered with foil on 12 March 2001 at Wageningen University. The block-rooted cuttings were transplanted in two greenhouses on 23 March 2001 at a density of 64 plants per m^2 in six containers (in each greenhouse) of 0.5 x 1.8 x 2.4 m (height, widths and length, respectively) with perlite (according to procedure described in CHAPTER 2.2). Two groups of three containers of 13 m^2 (5.4 x 2.4 m) were formed. The crop canopy of each group exceeded the size of the containers by about 12.5 cm on three sides. The area of the whole canopy was therefore 28.5 m^2. Between the two groups a corridor of 0.8 m width was kept for maintaining the plants and a green gaze protected the

TABLE 1. Climate settings in greenhouses 1 and 2 (GH_1, GH_2) during the CO_2 exchange measurements with cut chrysanthemum.

| Day of year | GH₁ | | GH₂ | |
| | Temperature | CO_2 | Temperature | CO_2 |
	(°C)	($\mu mol\ mol^{-1}$)	(°C)	($\mu mol\ mol^{-1}$)
125 – 127	23	1000	23	400
128 – 130	23	700	23	1000
131 – 133	23	400	23	700
134 – 136	28	1000	28	400
139 – 141	28	700	28	700
142 – 144	28	400	28	1000
145 – 147	33	1000	33	400
148 – 150	33	700	33	700
151 – 153	33	400	33	1000

plants from side radiation from the corridor. Plants were grown with natural long day (neither assimilation lamps nor screen was used) in the first three weeks after transplanting. From 13 April onwards, 11-h short-day was applied induced by movable metal roof covers on top of the greenhouses between 7 p.m. and 8 a.m.

Plants were irrigated through drip-irrigation pipes below the surface with nutrient solution. Nutrient solution was checked every three days for pH and electrical conductivity (EC) (Cyberscan pH 10 and Cyberscan Con 10, Eutech Instruments, Singapore) and maintained at pH 5 and 1.5 dS m^{-1} (EC). Dry and wet bulb air temperature was measured at the top of the canopy at two places in the greenhouses in boxes with two PT–500 thermometers (Hoogendoorn, Vlaardingen, The Netherlands), and water vapour pressure deficit of the air (VPD) was calculated from that. Climate was controlled with a commercial greenhouse climate computer (VitaCo, Hoogendoorn, Vlaardingen, The Netherlands). One extra climate-measuring box was installed in each greenhouse directly connected to the climate computer. PPFD was measured in the greenhouses with a height adjustable 1-m line quantum sensor (LI–191SA, LI-COR, Lincoln, NE, USA) installed 0.15 m above crop canopy.

Before treatments started, greenhouse climate was maintained at 18 °C and was between 75 % and 90 % relative humidity (RH) day and night and pure CO_2 was supplied to a lower threshold concentration of 350 µmol mol^{-1} CO_2. CO_2 supply stopped during night and increased to the equilibrium between CO_2 increase through dark respiration and leakage. Between 25 April and 04 May, a three-daily rhythm of daytime CO_2 concentration of 400, 700 and 1000 µmol mol^{-1} was applied. After that, experimental treatments started (Table 1). Plants were then in generative flower development stage. Compartments were opened every three days to maintain plants
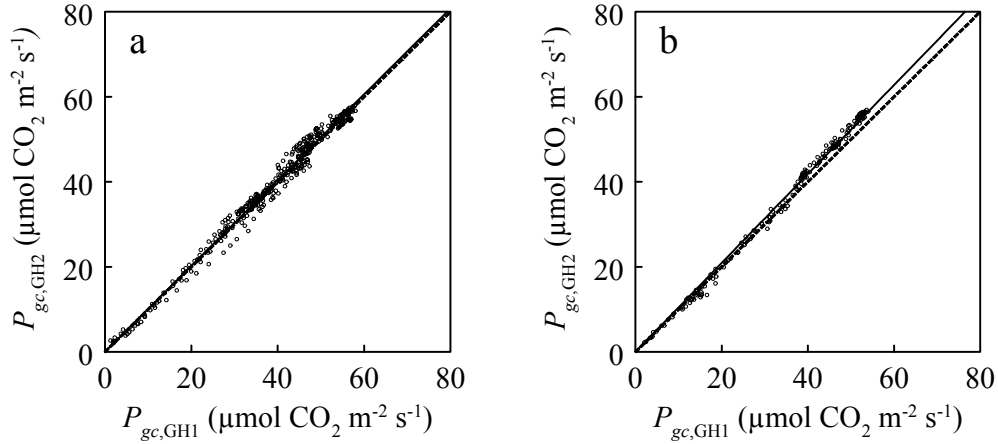
FIGURE 1. Comparison of crop gross photosynthesis (P_{gc}) between greenhouse 1 (GH₁) and greenhouse 2 (GH₂) between **(a)** day of the year 138–141 with 700 μmol mol⁻¹ CO_2 concentration and 28 °C temperature and **(b)** day of the year 149 – 150 with 700 μmol mol⁻¹ CO_2 concentration and 33 °C temperature. Broken lines (---) represent $P_{gc,GH2} = P_{gc,GH1}$, continuous lines (—) represent linear regression (a) $P_{gc,GH2} = 1.010 \cdot P_{gc,GH1}$ (R^2=0.999); (b): $P_{gc,GH2} = 1.046 \cdot P_{gc,GH1}$ (R^2=0.999).

and adjust the line quantum sensors. Once a week 10 evenly distributed and randomly selected plants were sampled in each greenhouse. Leaf area (LI–3100, LI-COR, Lincoln, NE, USA), plant dry weights (drying oven at 105 °C for two cycles of 16 hours) and plant heights were determined. During measurements, a fully-grown chrysanthemum crop with LAI of 6 was attained . Stem length increased from averages of 75, 95, 103 and 105 cm for 05, 11, 21 and 28 May, respectively.

DATA SELECTION

Hysteresis (i.e. lower photosynthetic rate in the afternoon than in the morning at the same PPFD[146]) was observed in the afternoon during some days. Therefore, only data before 12-h solar time were used for analyses during days when hysteresis occurred. In addition, data were only used when the system error was smaller than 5 % as calculated in CHAPTER 2.2. Data were selected within a temperature margin of ±1 °C (hourly means) from set points (i.e. 23, 28 or 33 °C).

DATA ANALYSIS

Data analyses were performed with the statistical software package SAS (ver. 8.0)[147]. Comparisons between data sets taken at the same time in different greenhouses was performed with the *paired samples t-test*. Measured P_{gc} was fitted with PPFD to the two parameter (crop maximum photosynthesis, $P_{gc,max}$ and crop photochemical efficiency, α_c) negative exponential light response curve for canopies[6] with non-linear least square iteration.

TABLE 2. Realised average greenhouse temperature (T; °C) and vapour pressure deficit (VPD; kPa) during day for the two greenhouses (GH_1 and GH_2) that were used for data analysis at different temperature treatments with standard deviation of 5-minute averages.

Greenhouse		Temperature set point (°C)		
		23	28	33
GH_1	T	23.17 ± 0.47	28.03 ± 0.51	32.86 ± 0.56
	VPD	0.38 ± 0.09	0.56 ± 0.1	0.89 ± 0.15
GH_2	T	23.5 ± 0.55	27.7 ± 0.76	32.73 ± 0.76
	VPD	0.55 ± 0.13	0.66 ± 0.11	1.02 ± 0.12

$$P_{gc} = P_{gc,\max} \cdot \left(1 - e^{\frac{\alpha_c \cdot PPFD}{P_{gc,\max}}} \right) \qquad [1]$$

Fitted values for α_c and $P_{gc,\max}$ were used to estimate P_{gc} for constant PPFD levels of 300, 600, 900 and 1200 µmol m^{-2} s^{-1} at the different temperatures and CO_2 levels. To determine the temperature that maximises P_{gc}, quadratic equations were fitted to the predicted P_{gc}-temperature responses (PROC NLIN, SAS 8.0)[147].

GREENHOUSES COMPARISON

Transmission for diffuse radiation in both greenhouses has been found to be identical throughout the experiment (59 %). For that purpose, PPFD outside the greenhouse was calculated with a factor converting global radiation to photosynthetic active radiation (PAR, W m^{-2}) (0.47 [98], and a factor converting PAR to PPFD (µmol m^{-2} s^{-1}; 4.57 [148]). Direct comparisons of P_{gc} measurements in both greenhouses under the same climatic conditions at the same time (temperature, CO_2 and radiation) was done once before the treatments started (18 °C, 700 µmol mol^{-1} CO_2) and two times during the experiment for a duration of three days at 700 µmol mol^{-1} CO_2 and 28 °C or 33 °C (FIG. 1). Highly significant differences in measured P_{gc} were observed between the two greenhouses (all P < 0.001). However, differences were small at 18 °C and 28 °C (1 % in both cases). The difference was higher at 33 °C with an average of 4.6 % lower P_{gc} in GH_1 than in GH_2. Because all differences were smaller than the chosen maximum threshold error of 5 % (CHAPTER 2.2), data of both greenhouses could be merged for light response curve estimation. For estimating the effect of CO_2 concentrations on P_{gc} at the same temperature, nevertheless, greenhouses had to be compared directly. Since the measured differences were constant ($R^2 = 0.99$ in all cases), data of GH_1 were corrected by the observed differences between the greenhouses.

TABLE 3. Realised CO_2 concentration (μmol mol^{-1}) for two greenhouses used for data analysis.

Greenhouse		Temperature set point		
		23	28	33
GH$_1$	400	400 ± 3	401 ± 5	413 ±12
	700	687 ± 7	705 ± 10	691 ± 15
	1000	964 ± 12	1007 ± 14	1005 ± 15
GH$_2$	400	382 ± 8	403 ± 9	408 ± 22
	700	700 ± 4	700 ± 9	690 ± 11.5
	1000	988 ± 7	989 ± 8.2	1009 ± 18

RESULTS

GREENHOUSE CLIMATE CONDITIONS

Greenhouse temperature fluctuated with radiation in some cases. Especially GH$_2$ was difficult to control (data not presented). However, data could be selected from either of the greenhouses with constant temperatures (±1 °C, TABLE 2). Variation in greenhouse climate (light, temperature, VPD and CO_2 concentration) was probably the major reason for data variation. VPD increased with temperature and was slightly higher in GH$_2$. Realised CO_2 concentration was somewhat different from the set points but was rather constant (TABLE 3). Certain variation, however, is difficult to control in a semi-closed greenhouse as variable outside radiation conditions largely determine inside greenhouse conditions. Although data varied, analyses could be performed on the effect of temperature and CO_2 on P_{gc} at different light intensities by selecting data with as less as possible variation while reducing the measuring error to < 5 % (CHAPTER 2.2).

CROP GROSS PHOTOSYNTHESIS MODEL

Hourly P_{gc} measurements were plotted as function of PPFD (FIG. 2). Data generally responded according to the negative exponential light response curve (EQ. 1) and were well described by this equation with coefficient of multiple determination (R^2) between 0.85 and 0.95 (TABLE 4).

CO_2 EFFECT ON CROP GROSS PHOTOSYNTHESIS

CO_2 concentration had a strong effect on P_{gc} (FIG. 2) and this effect absolutely decreased with increasing CO_2 level. P_{gc} increased with about 50 % when CO_2

TABLE 4. Fitted parameters (mean ± standard error) of the negative exponential light response curve for crops (maximum gross photosynthesis, $P_{gc,max}$, µmol CO_2 m^{-2} s^{-1} and incident photochemical efficiency, α_c, mmol CO_2 {mol photons}$^{-1}$) with estimated R^2 at three different CO_2 concentration (400, 700 and 1000 µmol mol^{-1}) and three different temperatures.

CO_2	400			700			1000		
	Temperature (°C)								
	23	28	33	23	28	33	23	28	33
α_c	95.1	74.5	62.2	119.1	92.0	82.5	117.6	97.8	95.1
	±2.3	±1.0	±1.1	±2.8	±1.3	±1.2	±1.9	±1.9	±1.1
$P_{gc,max}$	44.2	45.5	47.8	62.6	81.4	73.0	73.0	99.8	72.2
	±0.8	±0.5	±0.8	±1.2	±2.3	±1.5	±1.3	±3.9	±0.8
R^2	0.89	0.87	0.85	0.91	0.93	0.93	0.92	0.95	0.86

concentration increased from 400 to 1000 µmol mol^{-1} CO_2 (data not presented). The effect of CO_2 on P_{gc} could be attributed to both α_c and $P_{gc,max}$ but was different with different temperatures applied. At 23 °C, $P_{gc,max}$ increased between 400 and 1000 µmol mol^{-1} CO_2, whereas α_c did not increase when CO_2 was higher than 700 µmol mol^{-1}. This was in contrast to measurements at 33 °C where α_c increased between 400 and 1000 µmol mol^{-1} CO_2 but not $P_{gc,max}$, which only increased to 700 µmol mol^{-1}. At 28 °C, both $P_{gc,max}$ and α_c increased with increasing CO_2 level to 1000 µmol mol^{-1}.

TEMPERATURE EFFECT ON CROP GROSS PHOTOSYNTHESIS

Temperature had a distinct influence on P_{gc} when radiation and CO_2 concentration were high. When either of the two was low, the temperature effect on P_{gc} was low, too (FIG. 3). This was due to a contrasting effect of $P_{gc,max}$ and α_c. As CO_2 concentration, temperature affected both α_c and $P_{gc,max}$ (TABLE 4), but contrary to CO_2, α_c decreased with temperature (35 % from 23 °C to 33 °C at 400 µmol mol^{-1} CO_2). The decrease was stronger at a lower CO_2 level, which was probably due to decreasing photorespiration at higher CO_2 concentrations[149] and was also reported earlier[100].

However, at higher CO_2, temperature had a much stronger effect on $P_{gc,max}$ than on α_c. When temperature increased, $P_{gc,max}$ changed only little at 400 µmol mol^{-1} CO_2 (a slight increase with increasing temperature; TABLE 4). However, $P_{gc,max}$ had a peak at 28 °C (in the range measured) with 700 and 1000 µmol mol^{-1} CO_2. The peak was more pronounced with higher CO_2 concentration.

Using the fitted values for $P_{gc,max}$ and α_c to calculate P_{gc} at different PPFD levels
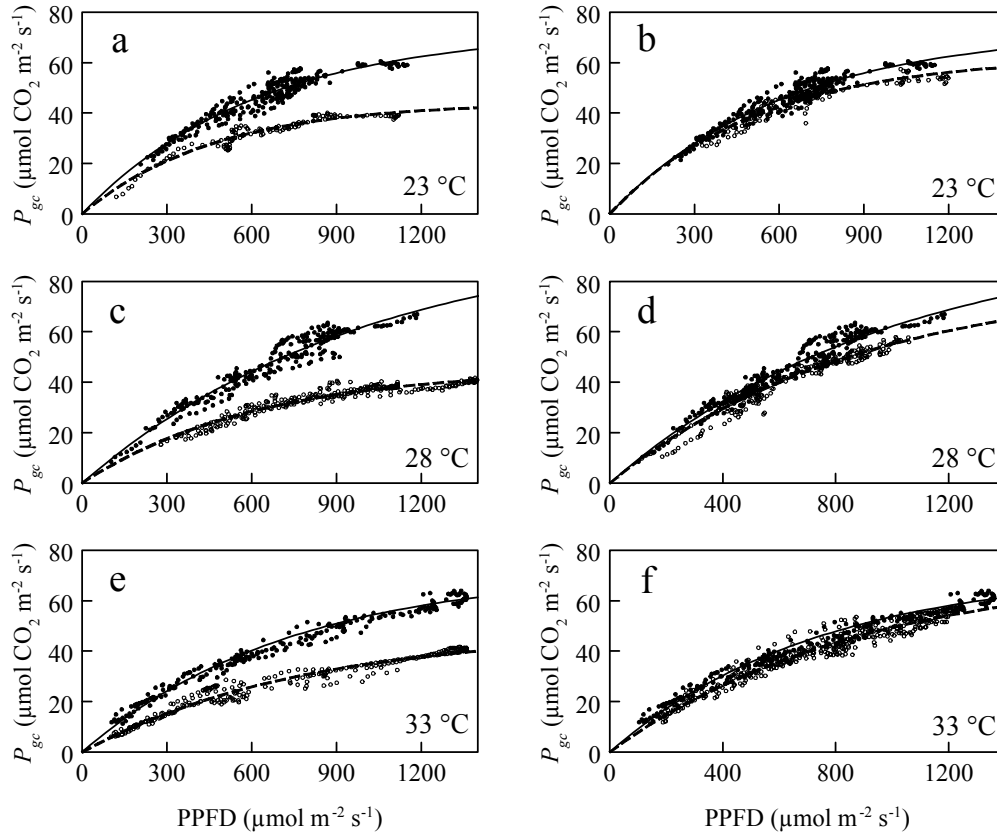
FIGURE 2. Comparison of the influence of CO_2 concentration of 400 (---, ○) and 1000 (—, ●) μmol mol^{-1} (a, c, e), and 700 (---, ○) and 1000 (—, ●) μmol mol^{-1} (b, d, f) on crop gross photosynthesis (P_{gc}) at different temperatures of 23 °C (a, b), 28 °C (c, d) and 33 °C (e, f). Points are average P_{gc} values over one hour plotted against one-hour averages of PPFD. Data were fitted with the negative exponential light response curve for crops.

revealed that values around 27 °C maximised P_{gc} when PPFD was higher than 900 μmol m^{-2} s^{-1} at CO_2 concentrations $\geq$ 700 μmol mol^{-1} (FIG. 3, TABLE 5). With 400 μmol mol^{-1} CO_2, P_{gc} approximately linearly decreased with increasing temperature. This was due to the combined effect of decreasing α_c and constant $P_{gc,max}$ at 400 μmol mol^{-1} CO_2. Because temperature had a stronger effect on $P_{gc,max}$ than on α_c, and the CO_2 effect was stronger for $P_{gc,max}$ than for α_c, higher CO_2 levels increased P_{gc} to a maximum level and decrease thereafter. This was observed when PPFD was 900 μmol m^{-2} s^{-1} or higher (FIG. 3). Temperature that maximised P_{gc} was below 23 °C with up to 300 μmol m^{-2} s^{-1} for all CO_2 concentrations. With higher radiation, an obvious shift to higher optimum temperatures was observed (TABLE 5). The shift from 400 to 1000 μmol mol^{-1} CO_2 was at least 1 °C, 3.5 °C and 4.5 °C at 600, 900 and 1200 μmol m^{-2} s^{-1} PPFD.
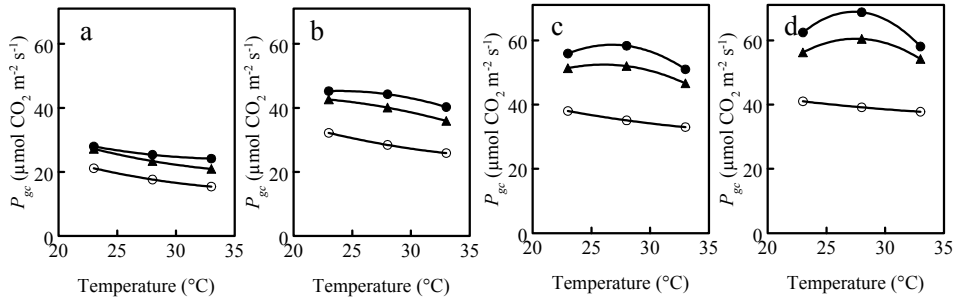
FIGURE 3. Crop gross photosynthesis (P_{gc}) as function of temperature with CO_2 concentration of 400 ($\circ$), 700 ($\blacktriangle$) and 1000 µmol mol^{-1} ($\bullet$) and photosynthetic photon flux density (PPFD) of 300 (a), 600 (b), 900 (c) and 1200 (d) µmol m^{-2} s^{-1}. Points were calculated from fitted negative exponential light response curves and fitted with quadratic functions. Standard errors are smaller than symbols in all cases.

TABLE 5. Temperature (°C) that maximises photosynthesis calculated from quadratic responses to temperature and CO_2 concentration at different PPFD levels and CO_2 concentrations as used in FIG. 3

CO_2 (µmol mol^{-1})	PPFD (µmol m^{-2} s^{-1})			
	300	600	900	1200
400	< 23	< 23	< 23	< 23
700	< 23	< 23	26.0	27.5
1000	< 23	23.9	26.5	27.4

DISCUSSION

Validity of measurements are supported comparing the calculated light use-efficiency at moderate temperature (23 °C) to 0.08 and 0.11 mol CO_2 {mol photon}$^{-1}$ (with 350 and 1000 µmol mol^{-1} CO_2, respectively) for the same temperature with a cucumber crop[106]. These values were also comparable to other crops[89, 120, 150]. However, measured P_{gc} in the present CO_2 gas exchange system cannot be compared directly to literature. The sides of the crops affect photosynthesis to a large extend as was reported in CHAPTER 2.2. Since crop size also increased during measurements, light interception and accordingly P_{gc} increased with the duration of the experiment. Therefore, when measurements at different temperatures were compared the error of an older and bigger crop with high temperatures was included. For detailed data analysis, a canopy radiation distribution model as presented in CHAPTER 2.2 is needed. However, the present data can be used as first approximation of P_{gc} response to temperature at various climatic conditions. Measured P_{gc} responded to the temperature-CO_2 interactions with different radiation levels as expected from theory[100, 101]. Major general conclusions drawn from simulations[100] can be supported by the experimental results: A. Elevated CO_2 increases P_{gc} more at warm than at cool

temperatures and this was due to a large combined CO_2 response of both α_c and $P_{gc,\text{max}}$; B. Elevated CO_2 raised the temperature optimum of canopy photosynthesis, due to an upward shift in the optimum temperature for $P_{gc,\text{max}}$; C. Large upward shifts in the temperature optimum of canopy photosynthesis in response to elevated CO_2 only occur at both warm temperatures and high irradiances. In the present research, temperature control was rather successful as data could be selected that were in the range of ±1 °C. The effect of VPD, nevertheless, may have affected photosynthesis. A VPD increase from 0.5 to 1.0 kPa decreased leaf photochemical efficiency by 15 %, 6 % or 4 % with 400, 800 and 1200 µmol mol^{-1} CO_2 [151] and this was in the same range as the observed values. In respect to the reported decrease in photochemical efficiency with VPD probably only measurements at 400 µmol mol^{-1} CO_2 were significantly affected. Optimum temperature for photosynthesis higher than 23 °C at low radiation would probably be possible, because a lower VPD would increase photochemical efficiency[151]. This would then reduce the temperature shift. A non-constant VPD with different temperature treatments is, however, difficult to avoid in large-scale photosynthesis measurements. This was earlier reported and led to strong variability in measured P_{gc}[106]. Climate variations, however, can be included when data are used for model validation. Although in a canopy this effect would probably be less, because of higher humidity levels in the lower part of the canopy, the model that best describes P_{gc} at high temperature should therefore include a stomata model.

There was probably little shift in the temperature optimum at low radiation as suggested[100], but due to the missing data < 23 °C, this could not be proven. At higher radiation levels, nevertheless, a clear shift could be shown. This was probably a combining effect of α_c and $P_{gc,\text{max}}$ since the opposing effect of α_c and $P_{gc,\text{max}}$ on photosynthesis is more pronounced in a crop than with leaves only[100]. The major difference between leaf-and crop parameters is that for a canopy of LAI > 3, a substantial portion of the leaf area will be shaded and $P_{gc,\text{max}}$ decreases compared to the leaf case when the area is normalised[106]. Therefore, also at saturated light level at the top of the canopy, response to temperature will not solely be determined by $P_{gc,\text{max}}$[101]. The influence of α_c increases in deeper regions of the canopy with low radiation levels and this leads to a smaller temperature – CO_2 effect in a canopy.

Low radiation levels were little effective. Radiation had to be 900 µmol mol^{-1} PPFD to yield in a distinct temperature optimum clearly higher than 23 °C. This was because in elevated but non-saturating CO_2 concentrations (as 700 µmol mol^{-1} and probably 1000 µmol mol^{-1}) the decline in α_c with increase in temperature decreased as also reported from leaf quantum yield[100] (φ). φ is used in the non-rectangular hyperbola[152] and is analogous to α_l, although based on absorbed rather than incident radiation[153].

Similar measurements as reported here were performed with a tomato crop (data not presented). Optimum temperatures at high radiation and CO_2 differed only little from the here reported data with cut chrysanthemum. This suggests that greenhouse crops respond similar to temperature – CO_2 interaction. With the tomato crop, temperature optimum at 400 µmol mol^{-1} CO_2 was below 20 °C. A shift of at least 8 °C (to 28 °C) was possible when CO_2 concentration increased to 1000 µmol mol^{-1} at 1200 µmol m^{-2} s^{-1} PPFD. The lower shift found with cut chrysanthemum is probably due to the incomplete investigated temperature range for 400 µmol mol^{-1} CO_2. The reported predicted shift when upscaling leaf photosynthesis to the crop level was almost the same with LAI of 2 or 8 [100]. The temperature shift was rather low at 500 µmol mol^{-1} PPFD (4 °C) and high (10 °C) at 2000 µmol mol^{-1} PPFD. These values are probably realistic and CO_2 – temperature interaction in a crop are probably well described in models for crop photosynthesis. However, further investigations with a broader temperature range are necessary.

CONCLUSIONS

The opposing effects of α_c and $P_{gc,max}$ on temperature – CO_2 interactions in a crop canopy results in different responses compared to the leaf level with regular radiation prevailing in temperate greenhouses. The approach using a leaf photosynthesis model to optimise temperature control in greenhouses[136] probably overestimated the temperature that maximises photosynthesis. For climate control in cut chrysanthemum when maximising photosynthesis, temperature should be lower than 23 °C with low radiation (< 300 µmol m^{-2} s^{-1} PPFD). With increasing radiation, greenhouse temperature may also increase to maximise P_{gc}, but then CO_2 concentration must be elevated. When temperature becomes higher than 28 °C, photosynthesis decreases even at high CO_2 and radiation.

For a better understanding of the measured data, a light interception model that takes the block-shape of the crop intro account should be used. This is especially important because the crop was higher with higher temperature treatments and this may have affect measured data due to the side effect. Then, crop gross photosynthesis models can be compared to the data and validated models could be applied for climate control.

The present research helped to support the theory about temperature – CO_2 interactions on crop photosynthesis in cut chrysanthemum with experimental evidence. Present results with cut chrysanthemum compared with unpublished data from tomato suggest that crop photosynthesis reaction to temperature is similar for greenhouse crops with similar optimum growth temperature. Present models that scale up leaf photosynthesis to the crop level are probably realistic. These two preliminary conclusions, however, have to be investigated in more detail.

2.4 SIMULATING CROP GROSS PHOTOSYNTHESIS AT HIGH TEMPERATURES

O. KÖRNER & R.J.C. VAN OOTEGHEM

ABSTRACT

In greenhouse climate control optimisation of CO_2 enrichment while targeting photosynthesis maximisation can be achieved with the recent development in flexible temperature regimes. For that, well performing photosynthesis models are needed. Present crop photosynthesis models in greenhouse horticulture are often based on simplified temperature responses that are suitable for conventional applied (i.e. conservative) greenhouse temperatures. These models were not designed for high temperatures as they can occur with modern and future climate control. In present leaf photosynthesis models, the stomata resistance is considered constant, while it is known to vary with greenhouse climate. In this study, a biochemical based leaf photosynthesis model calculating leaf photochemical efficiency (α_l) and maximum leaf gross photosynthesis at light saturation ($P_{g,\max}$) of the negative exponential light response curve was tested with regular and high temperatures. The basic model (*M2)* had a fixed stomata resistance. It was connected to a simple stomata model to yield $M2_{r_s}$. These two leaf photosynthesis models (*M2* and $M2_{r_s}$) were implemented in a

crop model and compared by simulation. Crop gross photosynthesis was simulated at conditions with fixed light, CO_2 and temperature. The models were also compared to cut chrysanthemum crop, photosynthesis measurements at 23 °C, 28 °C and 33 °C at 400, 700 and 1000 µmol mol^{-1} CO_2 as reported in CHAPTER 2.3. Only small differences were observed at 23 °C. At 28 °C, *M2* had a better prediction of crop gross photosynthesis (P_{gc}). At higher temperatures, this model overestimated P_{gc}. Then, $M2_{r_s}$ had a good prediction of P_{gc}, only slightly underestimating it. Prediction of temperature that maximises photosynthesis was good with $M2_{r_s}$ (<1 °C difference) at photosynthetic photon flux density of 900 µmol m^{-2} s^{-1} or higher but overestimated when stomata resistance was constant in *M2* (>2 °C difference). Neither of both models was the best at all climate conditions. A stomata resistance model showed a good effect, but a better model approach is still needed.

INTRODUCTION

Modern greenhouse climate control aims at optimal crop growth and performance with low energy consumption. Temperature regimes were designed that allow greenhouse temperature to rise more than with common rigid regimes in order to reduce energy consumption[55, 136]. These regimes are mainly based on empirically observed plant responses to temperature and only simple models are applied to calculate temperature that maximises photosynthesis at prevailing climate conditions[136]. The aim is then to increase crop growth through crop photosynthesis maximisation while saving energy through refraining from ventilation[103]. For that, models are needed with a good predictive quality at higher than regular temperatures that also accurately predict temperature that maximises photosynthesis. At temperatures created by regular climate controllers, crop photosynthesis is primarily a function of irradiation and CO_2 concentration as it is relatively unsusceptible to temperature. Outside those conditions, nevertheless, photosynthesis rate is affected by temperature[138] and then also vapour pressure deficit has a strong influence on photosynthesis through its impact on stomatal conductance (CHAPTER 2.1). Then, for optimal greenhouse climate control models are needed that accurately predict photosynthesis[145]. Present crop photosynthesis models were not designed for climate conditions beyond the regular applied temperatures created by conservative rigid temperature regimes, and a simplified temperature-response function is commonly used in models[137]. Models that completely depend on biochemical equations[97] result in a curvilinear relationship that is probably more realistic (CHAPTER 2.1). However, at high temperatures stomata resistance is increased through higher vapour pressure deficit and higher temperature[92]. The biochemical model could therefore be improved by coupling it with a stomata conductance model. This was done for soybean and rose leaves[154, 155]. The photosynthetic response to temperatures between approx. 17 °C and

28 °C was then well predicted at different CO_2 levels[155]. However, it is questionable if models can predict photosynthesis with a low error at higher temperatures. For those conditions, models need to be validated on a crop level. With leaves only, important conditions as light interception, microclimate, crop size and stage are not taken into account[156]. For crop photosynthesis model validation, leaf photosynthesis models need to be implemented in a crop model environment and thoroughly validated with various measurements in a larger plant stand. For that purpose, CO_2 exchange measurements with a chrysanthemum crop with temperatures between 23 °C and 33 °C and different CO_2 levels were discussed in CHAPTER 2.3. In the present research, those measurements were used to validate two leaf photosynthesis models (with and without stomata conductance) as part of a crop model. We used the biochemical model with basic parameters[97] and a semi-empirical stomata resistance model that was parameterised for a tomato crop[92]. The aim of this paper was a first evaluation of the response of the basic biochemical model combined with a stomata model at high temperatures in a crop. Measured climate of a semi-closed greenhouse was used to simulate crop gross photosynthesis (P_{gc}). Crop photochemical efficiency and maximum crop photosynthesis were estimated from these simulations. P_{gc} at constant climate conditions was simulated with those parameters as performed for measured P_{gc} in CHAPTER 2.3 and compared to those measurements.

MODELS

A leaf photosynthesis model with fixed stomata resistance ($M2$) was coupled with a simple stomata resistance model to obtain the model $M2_{r_s}$. The two models ($M2$ and $M2_{r_s}$) were compared with each other and with measurements. The models computed the two parameters of the negative exponential light-response curve ($P_g = P_{g,\max} \cdot (1 - \exp(\alpha_l \cdot \text{PPFD} / P_{g,\max}))$): maximum gross photosynthesis at light-saturation ($P_{g,\max}$, μmol m^{-2} s^{-1}) and leaf photochemical efficiency as initial slope of the curve (α_l, mol CO_2 {mol photon absorbed}$^{-1}$))[94]. Original biochemical based equations[97] were used. α_l was calculated from potential photochemical efficiency in absence of oxygen (α_0, mol CO_2 {mol photon absorbed}$^{-1}$, TABLE 1) corrected for photorespiration, CO_2 concentration ($[CO_2]$, μmol mol^{-1}), and CO_2 compensation concentration[89, 98] (Γ, μmol mol^{-1}).

$$\alpha_l = \alpha_0 \cdot \frac{\max([CO_2], \Gamma) - \Gamma}{\max([CO_2], \Gamma) + 2\Gamma} \qquad [1]$$

Γ was computed from leaf temperature (T_l, K; assumed to be equal to air temperature), temperature at 25 °C (T_{25}, K), O_2 partial pressure inside the

TABLE 1. Parameters and values as used for simulations in the two different leaf photosynthesis models $M2$ and $M2_{r_s}$

	Meaning	Value	Unit	Model
E_J	Activation energy maximum electron transport rate	37	kJ mol^{-1}	all
E_C	Activation energy Rubisco carboxylation	59.356	kJ mol^{-1}	all
E_O	Activation energy Rubisco oxygenation	35.948	kJ mol^{-1}	all
E_{R_d}	Activation energy dark respiration	66.405	kJ mol^{-1}	all
E_{VC}	Activation energy carboxylation rate	58.520	kJ mol^{-1}	all
r_{b,CO_2}	boundary layer resistance for CO_2 diffusion	136	s m^{-1}	all
S	Constant I. for optimum curve temperature dependent maximum electron transport rate	0.71	kJ mol^{-1} K^{-1}	all
H	Constant II. for optimum curve temperature dependent maximum electron transport rate	220	kJ mol^{-1}	all
$R_{d,25}$	dark respiration at 25 °C	1.1	µmol CO_2 m^{-2} s^{-1}	all
K_{dif}	Extinction coefficient for diffuse radiation	0.8	-	all
θ	degree of curvature of CO_2 response of light saturated net photosynthesis	0.7	-	all
R	gas constant	8.314	J mol^{-1} K^{-1}	all
α_0	Leaf photochemical efficiency in absence of oxygen	0.0875	mol CO_2 {mol photon}$^{-1}$	all
$V_{c,max,25}$	maximum carboxylation rate at 25 °C	97.875	µmol CO_2 m^{-2} s^{-1}	all
$J_{max,25}$	maximum electron transport rate at 25 °C	210	µmol m^{-2} s^{-1}	all
$K_{O,25}$	Michaelis-Menten constant Rubisco oxygenation	155	mbar	all
$K_{C,25}$	Michaelis-Menten constant Rubisco carboxylation	310	µbar	all
r_{min,H_2O}	minimum internal resistance for H_2O	82	s m^{-1}	$M2_{r_s}$
$\rho_{O_{2i}}$	O_2 partial pressure inside stomata	210	mbar	all
σ	scattering coefficient	0.15	-	all
r_{s,CO_2}	stomata resistance for CO_2 diffusion	80	s m^{-1}	$M2$
T_{25}	temperature in Kelvin at 25 °C	298.15	K	all
$V_{O/C}$	$V_{O,max} / V_{C,max} = K_O / K_C$ =constant	0.21	-	all

stomata ($p_{O_{2i}}$, mbar) that was assumed to be constant, the *Michaelis-Menten* constants for Ribulose-biphosphate carboxylation and oxygenation at 25 °C ($K_{C,25}$, µbar; $K_{O,25}$, mbar) with their activation energies (E_C, E_O, J mol^{-1}), the quotient between maximum oxygenation and carboxylation rate ($V_{O/C}$) and the gas constant (R, J mol^{-1} K^{-1}) [97]. Parameter-values are given in TABLE 1.

$$\Gamma = \frac{p_{O_{2i}} \cdot V_{O/C}}{2} \cdot \frac{K_{C,25} \cdot e^{E_C \cdot \frac{T_l - T_{25}}{T_l \cdot R \cdot T_{25}}}}{K_{O,25} \cdot e^{E_O \cdot \frac{T_l - 25}{T_l \cdot R \cdot 25}}} \qquad [2]$$

$P_{g,max}$ was determined by adding leaf dark respiration (R_d, µmol m^{-2} s^{-1}) to maximum net photosynthesis ($P_{n,max}$, µmol m^{-2} s^{-1}). $P_{n,max}$ was calculated as function

of maximum net photosynthesis rate limited by CO_2 (P_{n,CO_2}, µmol m^{-2} s^{-1}), maximum endogenous photosynthetic capacity (P_{mm}, µmol m^{-2} s^{-1}) and a parameter for degree of curvature of CO_2 response of light saturated net photosynthesis (θ). P_{n,CO_2} was calculated from $[CO_2]$, Γ, density of CO_2 (ρ_{CO_2}) and total resistance for CO_2 diffusion (r_{CO_2}, m s^{-1}). r_{CO_2} was calculated by summing up boundary layer resistance, stomata resistance and carboxylation resistance to CO_2 diffusion (r_{b,CO_2}, r_{s,CO_2}, r_{c,CO_2}, m s^{-1}, respectively).

$$P_{n,max} = \frac{P_{n,CO_2} + P_{mm} - \sqrt{\left(P_{n,CO_2} + P_{mm}\right)^2 - \left(4 \cdot \theta \cdot P_{n,CO_2} \cdot P_{mm}\right)}}{2 \cdot \theta} \qquad [3]$$

$$P_{n,CO_2} = \frac{\left(\max\left([CO_2]-\Gamma\right)-\Gamma\right) \cdot \rho_{CO_2}}{r_{CO_2}} \qquad [4]$$

P_{mm} was calculated from actual maximum electronic transport rate at 25 °C ($J_{max,25}$, µmol m^{-2} s^{-1}), activation energy (E_J, J mol^{-1}) and constants for optimum curve temperature dependent electron transport rate (S, H; TABLE 1) and T_l according to Farquhar *et al.* (1980)[97]. R_d was calculated from respiration at 25 °C ($R_{d,25}$, µmol m^{-2} s^{-1}), activation energy (E_{Rd}, J mol^{-1}) and T_l.

$$P_{mm} = 0.25 \cdot J_{max,25} \cdot e^{\left(E_J \cdot \frac{T_l - T_{25}}{T_l \cdot R \cdot T_{25}}\right)} \cdot \left(1 + e^{\frac{(S-H)/T_l}{R}}\right) \cdot \left(1 + e^{\frac{(S-H)/T_{25}}{R}}\right)^{-1} \qquad [5]$$

$$R_d = R_{d,25} \cdot e^{E_{Rd} \cdot \frac{T_l - T_{25}}{T_l \cdot R \cdot T_{25}}} \qquad [6]$$

r_{b,CO_2} and r_{c,CO_2} were the same in both models. r_{c,CO_2} was calculated from the effective *Michaelis-Menten* constant of Ribulose-biphosphate carboxylase/oxygenase (Rubisco) for CO_2 at O_2 partial pressure of 210 mbar[98] and maximum carboxylation rate ($V_{c,max}$, µmol m^{-2} s^{-1}); r_b was assumed to be constant[89] (TABLE 1).

$$r_{c,CO_2} = K_c \cdot \left(1 + \frac{p_{O_{2i}}}{K_O}\right) \cdot p_{O_{2i}} \cdot M_{CO_2}^{-1} \cdot V_{c,max}^{-1} \qquad [7]$$

$$V_{c,max} = V_{c,max,25} \cdot e^{E_{VC} \cdot \frac{T_l - T_{25}}{T_l \cdot R \cdot T_{25}}} \qquad [8]$$

In *M2* also r_{s,CO_2} was constant[89], in *M2$_{r_s}$* r_{s,CO_2} was modelled as proposed for a greenhouse tomato canopy[92]. The model determines r_{s,CO_2} of the average leaf in the

canopy as simplification. Microclimatic differences inside the canopy were not taken into account. r_{s,CO_2} was determined from four functions ($f(x)$) computing the influence of the major climate variables on crop stomata resistance: Short-wave radiation absorbed by the canopy (I_c, W m^{-2}; EQ. 10), crop temperature (T_c, K, assumed to be equal to air temperature; EQ. 11), CO_2 concentration ($[CO_2]$, µmol mol^{-1}; EQ. 12) and water vapour pressure deficit (VPD; EQ. 13). The functions were calculated with leaf area index (LAI), minimum internal resistance for H_2O diffusion (r_{min,H_2O}, m s^{-1}) and VPD (mbar). A ratio of 1.6 : 1 was used between resistance to CO_2 diffusion and resistance to H_2O diffusion[157].

$$r_{s,CO_2} = r_{min,H_2O} \cdot f(I_c) \cdot f(T_c) \cdot f([CO_2]) \cdot f(\text{VPD}) \cdot 1.6 \qquad [9]$$

$$f(I_c) = \frac{I_c/(2 \cdot \text{LAI}) + 4.3}{I_c/(2 \cdot \text{LAI}) + 0.54} \qquad [10]$$

$$f(T_c) = 1 + 0.022593 \cdot (T_c - 297.662)^2 \qquad [11]$$

$$f([CO_2]) = \begin{cases} 1 & if \ \ I_c = 0 \\ 1.49 & if \ \ [CO_2] \geq 1100 \ \ \mu mol \ \ mol^{-1} \\ 1 + 6.08 \cdot 10^{-7} \cdot ([CO_2] - 200)^2 & if \ \ I_c > 0 \ \ \& \ \ [CO_2] < 1100 \ \ \mu mol \ \ mol^{-1} \end{cases}$$
$$[12]$$

$$f(\text{VPD}) = 4/(1 + 255 \cdot e^{-0.5427 \cdot \text{VPD}})^{0.25} \qquad [13]$$

MATERIALS AND METHODS

PLANTS AND CLIMATE CONDITIONS

Cut chrysanthemum (*Chrysanthemum grandiflorum*) was used as model crop. Measurements on crop CO_2 exchange measurements were performed with a fully-grown crop with LAI of 6 and plant heights between 75 cm and 105 cm as described in CHAPTER 2.3. Experiments were conducted in a semi-closed CO_2 exchange system with two independent controlled greenhouses as described in CHAPTER 2.2. Inside the greenhouses, the crop was placed in two groups of three containers with a net crop area of 28.5 m^2. Three different temperatures (23 °C, 28 °C and 33 °C) and three different CO_2 levels (400, 700 and 1000 µmol mol^{-1}) were applied for three consecutive days each treatment. CO_2 net exchange was measured from the difference between CO_2 supply and uptake by the plants with the mass balance equation[123].

Leakage of the measuring system was taken into account. P_{gc} was calculated by adding crop dark respiration (R_{dc}, µmol m^{-2} s^{-1}) to crop CO_2 net exchange. R_{dc} was determined by measuring net CO_2 exchange during the first hour of the night period (temperature set point was the same as during day-time) which was assumed to be representative for the whole day. Day-time R_{dc} was recalculated with a temperature dependent respiration function[97]. P_{gc} data were averaged over one hour (measurements were taken every 5 min). Data were selected that reduced the system error to less than 5 % (CHAPTER 2.2).

SIMULATING CROP PHOTOSYNTHESIS WITH FIXED CLIMATE

For fixed climate conditions the same procedure as described in CHAPTER 2.1 was applied. Both leaf photosynthesis modules were implemented in the simulation environment MATLAB® (version 6.0, MathWorks, Natick, MA, USA) and scaled up to the crop level based upon the calculated sunlit and shaded LAI[95] and integrated over canopy height with three point Gaussian Integration[96]. A flat canopy was assumed (i.e. no side lighting).

SIMULATING CROP PHOTOSYNTHESIS WITH MEASURED CLIMATE IN A BLOCK

To compare measurements of block-crop to simulation in a day-lit phytotron (i.e. to be able to validate the crop photosynthesis models), a model was developed that calculated diffuse and direct photosynthetic active radiation (PAR, W m^{-2}) absorption by leaves inside the plant stand (CHAPTER 2.2). Then also side lighting was taken into account. Both leaf photosynthesis models were implemented in Visual Fortran (ver. 6.6, Compaq Computer Corporation) and scaled up with this geometric model.

The plant stand was assumed to have the shape of a block, i.e. to be rectangular in the 3 dimensions. Inside the plant stand a rectangular 3-dimensional grid of points (P_{xyz}) was adopted with in total 4000 points (20 along width, 20 along depth, and 10 along the height of the block). Intensity of absorption of a beam of direct PAR at each point in the block was calculated by multiplying direct PAR outside the greenhouse by the transmission of the direct PAR beam (through either the cover of the phytotron, the front or back wall, or the sides), by the fractional absorption by leaves in the path of the beam from point of entrance in the block to each point P_{xyz}. Absorption of diffuse PAR at P_{xyz} was calculated by averaging absorbed intensities of numerous single beams coming from 6400 different angles from the whole hemisphere. Transmission of single beams by the greenhouse cover and walls was set constant according to measurements performed at overcast sky. Transmission of the direct PAR beam by roof panels or wall of the greenhouse τ_{dir} was calculated dependent on elevation and azimuth of the beam, whether the beam was entering roof or wall, and angle of incidence on roof or wall[130], i.e. from shades cast by construction elements (running

either vertical or horizontal) transmission of the elements averaged over the whole pane or wall was calculated. This was multiplied by transmission of the glass to yield τ_{dir}. In addition to interception of PAR beams by the greenhouse cover and walls, also diffuse and direct PAR interception by the building running at the northern side of the series of greenhouses. It was assumed that neighbouring houses could intercept direct PAR, and that the intensity of diffuse PAR coming from neighbouring houses was the same as that from the unobstructed sky. Path lengths of transmitted single beams of PAR in the plant stand were calculated from simple geometry. Absorption of the single PAR beam was calculated from path length, leaf area traversed, average projection of leaves into the direction of the beam, reflection and scattering, for shaded and sunlit leaves[96] and similar to the model for hedgerow canopies[131]. Crop photosynthesis was then calculated by summing up rates of CO_2 assimilation for every single point in the grid from separate calculations for sunlit and shaded leaves[96]. Leaves were assumed to have the so-called near-planophile vertical leaf angle distribution. For that, a scattering coefficient (σ) and an extinction coefficient for diffuse radiation (K_{dif}) were used (TABLE 1).

Simulations were performed for days when crop CO_2 exchange measurements were done as described in CHAPTER 2.3 (day 125–153 of the year). Simulations were only performed during times when measured P_{gc} was suitable for analysis, based on the system error and hysteresis (i.e. 1. days when hysteresis occurred only data to 12 h solar time were used; 2. data when the measuring error was < 5 %). Solar time was used for simulations and only data until 4 p.m. solar time were used. Input to the simulations were measured climate data of greenhouse temperature, CO_2 concentration, relative humidity (only $M2_{r_s}$), outside global radiation averaged over 5 min and the 3-dimensional size and position of the canopy. The corridor between the two groups of plants was not taken into account for simulations, but photosynthesis per square-meter was calculated for net plant size.

DATA ANALYSIS

Maximum canopy gross photosynthesis ($P_{gc,max}$, μmol m^{-2} s^{-1}) and canopy photochemical efficiency (α_c, mol CO_2 {mol photon absorbed}$^{-1}$) in the negative-exponential equation for crops were estimated by non-linear least square iteration (PROC NLIN, SAS 8.0)[147]. Photosynthetic photon flux density (PPFD, μmol m^{-2} s^{-1}) and P_{gc} were input to the iteration process.

$$P_{gc} = P_{gc,max} \cdot (1 - e^{\frac{-\alpha_c \cdot PPFD}{P_{gc,max}}}) \qquad [14]$$
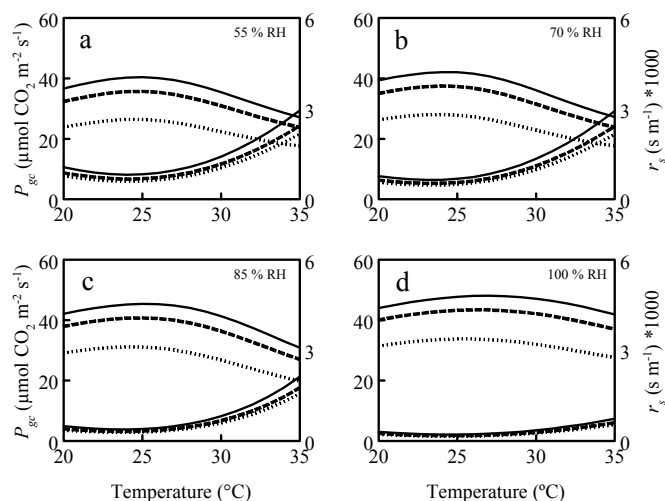
FIGURE 1. Simulated crop gross photosynthesis (P_{gc}, upper lines) and stomata resistance for CO_2 diffusion (r_s, lower lines) with the model $M2_{r_s}$ for a flat canopy at four different relative humidity levels (55 %, a; 70 %, b; 85 %, c and 100 %, d) as function of temperature at 400 (---), 700 (– – –) and 1000 (—) μmol mol^{-1} CO_2 at PPFD of 1200 μmol m^{-2} s^{-1}. LAI was 3 and a fixed sine of solar elevation of 0.8; fraction of diffuse radiation of 0.5.

With these estimated values for α_c and $P_{gc,max}$, P_{gc} was predicted for constant PPFD levels of 300, 600, 900 and 1200 μmol m^{-2} s^{-1} at the different temperatures and CO_2 levels as it was performed in CHAPTER 2.3 for measured P_{gc}. Predictions were then used for comparison with measured responses that were also predicted through fitting the negative exponential equation. Quadratic equations were used to fit the P_{gc}-temperature responses to find the temperature that maximises photosynthesis at the prevailing climate conditions.

RESULTS

FIXED CLIMATE

As a constant stomata resistance was used in $M2_{r_s}$, this model was not susceptible to variations in relative humidity (RH). Then, only PPFD, CO_2 and temperature determined photosynthesis. However, in $M2_{r_s}$, the impact of relative humidity on VPD was such that simulated P_{gc} increased with RH (FIG. 1). Comparing the two models directly at the same constant climate conditions (using RH of 90 % for $M2_{r_s}$) shows that only small differences existed at regular temperatures between 20 and 25 °C (FIG. 2). With higher temperatures, $M2$ resulted in a much higher P_{gc} prediction.
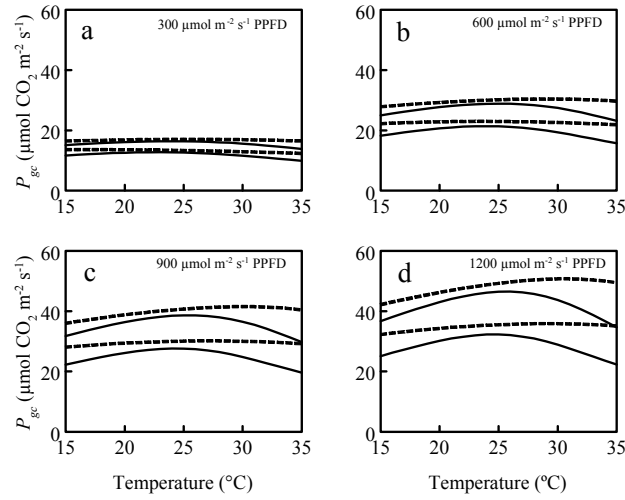
FIGURE 2. Simulated crop gross photosynthesis (P_{gc}) for a flat canopy with $M2$ (– – –) and $M2_{r_s}$ (—
)as function of temperature at 400 (lower lines) and 1000 μmol mol^{-1} CO_2 (upper lines) and four
photosynthetic photon flux densities (PPFD) of 300 (a), 600 (b), 900 (c) and 1200 μmol m^{-2} s^{-1} (d).
LAI was 3 and a fixed sine of solar elevation of 0.8; fraction of diffuse radiation of 0.5; constant
relative humidity of 90 % (for $M2_{r_s}$).

MEASURED CLIMATE

RH during the measuring period showed rather constant values (80 – 87 %; TABLE 2).
Increasing temperature, however, increased VPD and this affected photosynthesis
prediction with $M2_{r_s}$ (see EQ. 13). Also the temperature function (EQ. 11) increased
stomata resistance and therefore decreased quality of P_{gc} prediction (FIG. 1). At
almost regular climate conditions with 23 °C, only small differences between the two
models were observed and the measurements were well described at 400 μmol mol^{-1}
CO_2 (FIG. 3). When CO_2 was elevated, $M2_{r_s}$ slightly underestimated measured P_{gc}.
This was probably because $M2_{r_s}$ had a generally lower P_{gc} calculation due to the
high stomata resistance. When temperature increased, predictions were less good with
$M2$ (FIG. 3). With higher photosynthesis rates (high light and elevated CO_2), the
difference between the two models increased. Then, $M2$ overestimated measured P_{gc}
and $M2_{r_s}$ underestimated it. At 33 °C observations were qualitatively similar to 28
°C, but the differences were more pronounced (FIG. 3) and the stomata model was a
rather good tool to limit photosynthesis prediction. When simulated P_{gc} was used to
predict α_c and $P_{gc,max}$ response curve (TABLE 3), it shows the same results from a
different perspective (FIG. 4). Then, fixed climate situations could be created to
directly compare P_{gc} simulated with the two models and measured P_{gc} in
greenhouses. With low photosynthesis rates at 400 μmol mol^{-1} CO_2 and low
irradiation, the two models resulted basically in the same P_{gc} prediction at all
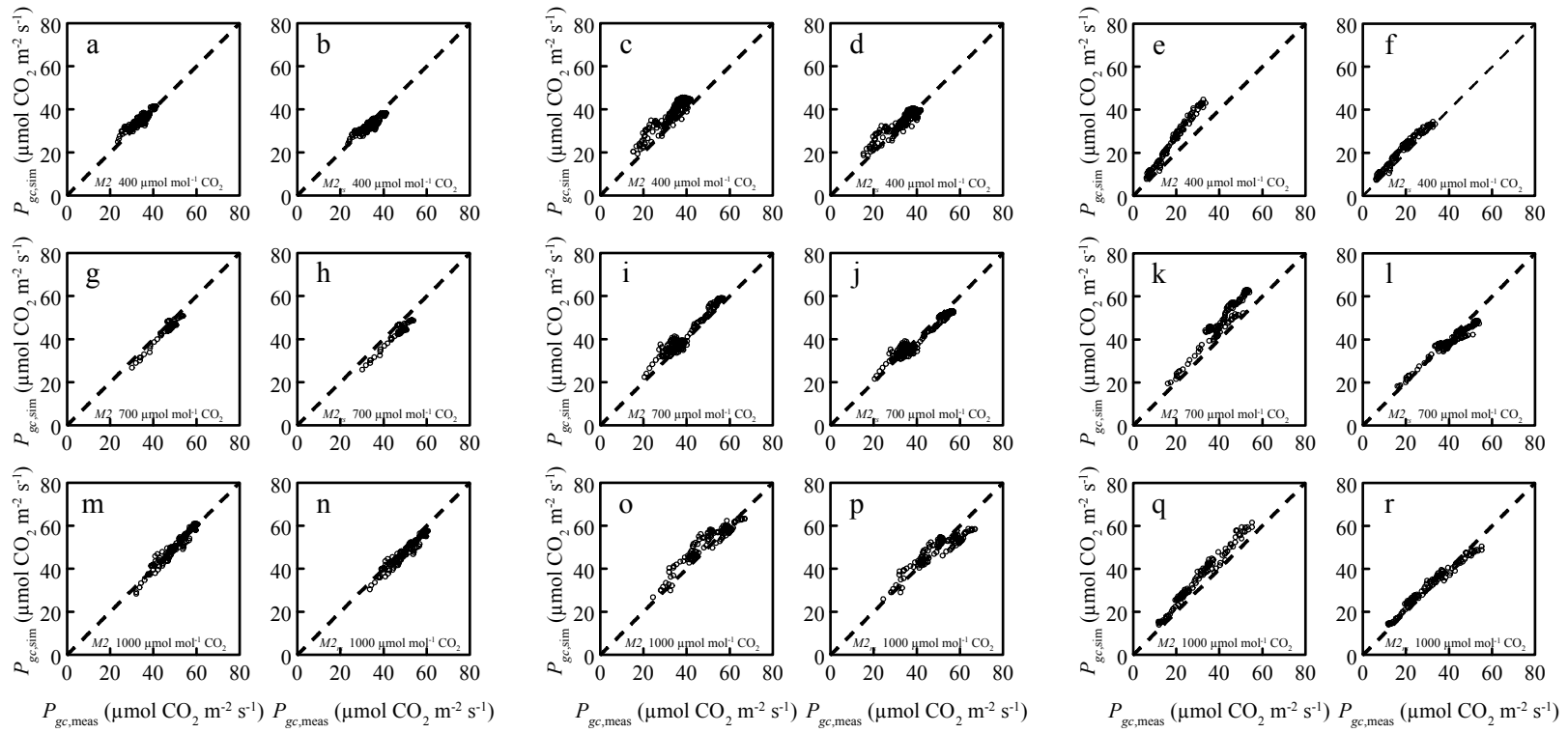
FIGURE 3. Measured ($P_{gc,\text{meas}}$) and simulated ($P_{gc,\text{sim}}$) crop gross photosynthesis with at 23 °C (a, b, g, h, m, n; first two sub-figure columns), 28 °C (c, d, i, j, o, p; sub-figure columns 3 and 4), 33 °C (e, f, k, l, q, r; last two sub-figure columns) at 400 (a – f), 700 (g – l) and 1000 (m – r) µmol mol^{-1} CO_2 concentration (m-r) with the two leaf photosynthesis models implemented in a crop model (*M2*; a, g, m, c, i, o, e, k, q; sub-figure columns 1, 3 and 5) c; *M2*$_{r_s}$; b, h, n, d, j, p, f, l, r; sub-figure columns 2, 4 and 6).

TABLE 2. Averaged realised greenhouse relative humidity (RH, %) and vapour pressure deficit (VPD, kPa) during simulations with standard deviation over 5 min. averages.

						Temperature			
		23			28			33	
CO_2	400	700	1000	400	700	1000	400	700	1000
RH	80.2	85.4	86.0	84.1	83.0	82.0	79.9	82.0	80.3
	±4.1	±3.3	±1.4	±1.9	±2.9	±7.7	±2.6	±2.4	±2.9
VPD	0.58	0.42	0.4	0.60	0.64	0.66	1.0	0.91	0.96
	±0.10	±0.06	±0.03	±0.08	±0.12	±0.23	±0.13	±0.11	±0.13

TABLE 3. Parameters (mean ± standard error) of the negative exponential light response curve for crops (maximum gross photosynthesis, $P_{gc,max}$, µmol CO_2 m^{-2} s^{-1} and incident photochemical efficiency, α_c, mmol CO_2 {mol photons}$^{-1}$) for measured climate-data simulated with the two leaf photosynthesis models (*M2* and $M2_{r_s}$) inside a crop photosynthesis model with estimated R^2 at three different CO_2 concentration ($[CO_2]$) of 400, 700 and 1000 µmol mol^{-1} and three different temperatures.

$[CO_2]$		400			700			1000		
					Temperature (°C)					
		23	28	33	23	28	33	23	28	33
	α_c	102.8	93.5	81.7	111.2	105.9	93.0	118.8	117.4	92.7
M2		±2.7	±1.8	±2.4	±3.6	±1.3	±2.1	±2.3	±2.9	±1.6
	$P_{gc,max}$	44.9	48.7	49.3	66.3	75.2	86.1	73.9	80.9	95.2
		±0.8	±0.5	±1.6	±1.9	±1.0	±2.9	±1.2	±2.4	±2.3
	R^2	0.92	0.87	0.85	0.93	0.89	0.94	0.94	0.94	0.90
	α_c	100.5	90.6	78.7	110.1	106.6	93.1	118.8	116.1	89.5
$M2_{r_s}$		±2.7	±1.7	±2.3	±3.9	±1.4	±1.8	±2.3	±3.0	±1.4
	$P_{gc,max}$	40.6	42.0	34.8	61.1	62.1	54.7	66.5	70.8	65.5
		±0.6	±0.3	±0.6	±1.7	±0.9	±0.8	±1.0	±1.9	±0.9
	R^2	0.91	0.85	0.79	0.93	0.87	0.90	0.93	0.93	0.86

temperatures. In this range, the measured P_{gc} was well described by the models. Differences occurred when high temperatures where applied. At 28 °C and very high PPFD of 1200 µmol m^{-2} s^{-1}, $M2_{r_s}$ underestimated measured P_{gc}. A good fit was obtained with *M2*. At higher temperatures, nevertheless, *M2* overestimated measured P_{gc}. This overestimation was more pronounced with high CO_2 concentration and high irradiation. The additional stomata conductance model counteracted this, resulting in a better estimation for almost all combinations of CO_2

TABLE 4. Temperature (°C) that maximises photosynthesis at 1000 µmol mol^{-1} CO_2 at different PPFD levels calculated from quadratic responses to temperature – CO_2 concentration as used in FIG. 3 for measured data and with the two leaf photosynthesis models ($M2$, $M2_{r_s}$)

Model	PPFD (µmol m^{-2} s^{-1})			
	300	600	900	1200
Measured	< 23	23.9	26.5	27.4
$M2$	25.8	26.4	27.6	29.5
$M2_{r_s}$	25.4	25.8	26.2	26.6

and PPFD at 33°C, although $M2_{r_s}$ tended to underestimate measured P_{gc}. However, the degree of underestimation is generally less than the overestimation by $M2$. Strongest discrepancies occurred at the highest temperatures and PPFD levels. At 1200 µmol m^{-2} s^{-1} PPFD and 700 or 1000 µmol mol^{-1} CO_2, P_{gc} was underestimated by 6.6 and 5.3 µmol m^{-2} s^{-1} with $M2_{r_s}$ and overestimated by 8.4 and 7.5 µmol m^{-2} s^{-1} with $M2$. To be able to apply one of the models for climate control, the prediction of temperature that maximises P_{gc} is of importance (CHAPTER 2.3). The same procedure to find this value as has been performed with measured P_{gc} (CHAPTER 2.3) was done with results of both models. Then, $M2_{r_s}$ resulted in the better estimation (TABLE 4). In general, only small differences between both models and measurements were observed up to 28 °C. Discrepancies were most distinct with higher temperatures. Then, the application of a stomata conductance model had its highest benefit.

DISCUSSION

The major aim of this research was to evaluate whether a pure biochemical leaf photosynthesis model[97] with a low fixed stomata resistance that was reported and successfully validated within a simplified temperature response model for a tomato crop[6] was able to predict crop photosynthesis at higher than regularly applied greenhouse temperatures. A simple stomata resistance model also calibrated for a tomato crop[92] was thought to improve the photosynthesis prediction (CHAPTER 2.1). It was shown that at regularly applied temperatures both models showed the same good prediction to the measurements. At 23 °C crop photosynthesis was well predicted by the simplified model[137] (data not presented) and this supports the validity of the model at regular climate conditions. However, none of the two models was successful to predict photosynthesis within an error of 5 % when temperature, radiation and CO_2 were high. Either photosynthesis was overestimated by the basic biochemical model or it was underestimated through the too strong back-regulation by the stomata resistance model. Improvement of at least one of the two models is needed.
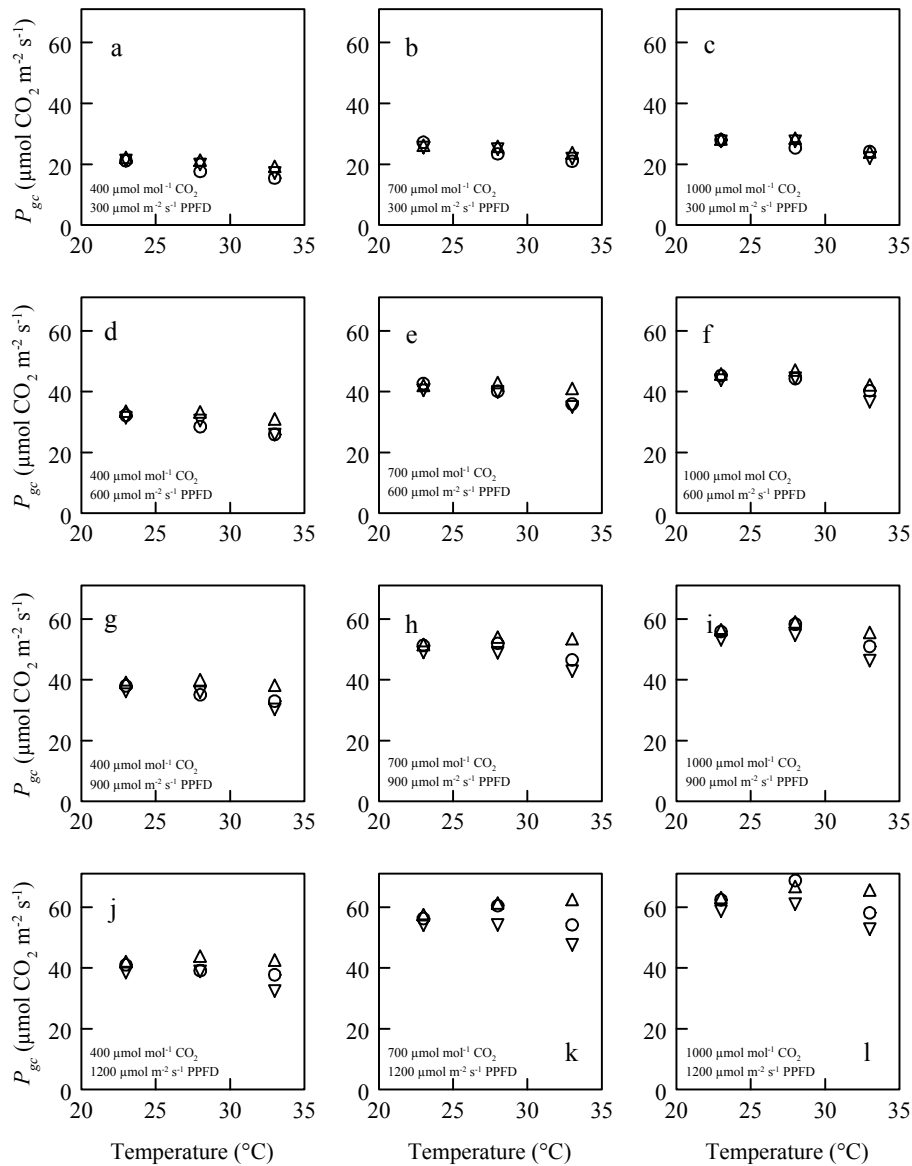
FIGURE 4. Measured crop gross photosynthesis (P_{gc}, ○) and P_{gc} simulated with the two different leaf photosynthesis modules $M2$ (△), and $M2_{r_s}$ (▽) at the three different temperatures used (23, 28 and 33 °C) and the three CO_2 levels applied (400, a, d, g. j; 700, b e, h, k and 1000, c, f, I, l) for four different PPFD levels (300, a-c; 600, d-f; 900, g-i and 1200, j-l; μmol m^{-2} s^{-1}). When bars larger than symbols indicate the standard error.

It is, however, questionable if the used parameter values were correct for cut chrysanthemum. This refers to both the biochemical equations of the basic model and the stomata model. First, because the temperature dependency of C3 photosynthesis varies among species[158], and second, because stomata model parameters were calibrated for a tomato crop and those are probably crop specific. The original model was parameterised for a leaf temperature of 25 °C and its accuracy decreases beyond

that[159]. Bernacchi *et al.* (2001)[159] proposed a generic temperature response of six temperature dependent parameters within the model of Farquhar *et al.* (1980)[97]. Simulations with fixed climates revealed a stronger temperature dependency with that model compared to *M2* (data not presented). When the stomata model of Stanghellini (1987)[92] was included in both models, photosynthesis at 28 °C was higher with the model of Bernacchi *et al.* (2001)[159] than $M2_{rs}$, and lower at 33 °C. Underestimation of measured photosynthesis at 33 °C would be even stronger. Adjusting stomata model parameters could reduce this underestimation. When either the temperature or the VPD function would be adjusted in the model[92], P_{gc} could probably be well predicted at the temperatures considered. In the present approach, the modelled stomata resistance was probably too high such that it accounted for a too strong reduction in P_{gc}. This is also evident since in well adapted plants stomata play a relatively small part in determining the rate of photosynthesis, comprising less than about 20 % of the total photosynthetic limitation[160]. In our simulations the stomata influence at high temperatures and high PPFD was much more than that. A better stomata resistance model could help. However, significant uncertainty about the physiological controls of stomata responses and their interactions exist[160]. A negative correlation of net photosynthesis and stomata conductance was reported by Jarvis and Davies (1998)[161] but models implemented the contrary[162]. The design of non-empirical stomata models remains difficult and due to that, most stomata models are empirical or semi-empirical[e.g. 163]. But then, parameters need to be calibrated extensively. This could be improved with a combination of the findings of Jarvis and Davies (1998)[161] and the proposal that stomatal function is linked to any carbon fixing substrate pool (Farquhar and Wong, 1984)[164]. Utilising photosynthesis capacity to approximate the pool size could yield in a simple model of stomatal function determining sub-stomatal CO_2 concentration[161].

It could be hypothesised that a combination of the biochemical approach of Bernacchi *et al.* (2001)[159] and a stomata model as suggested by Jarvis and Davies (1998)[161] could be successful to predict photosynthesis at high temperatures. With the presented model including the stomatal resistance module, photosynthesis maximisation with ventilation and CO_2 control[103, 136] could be achieved within an error of 1 °C at higher PPFD levels. However, this does not denote the actual absolute deviation between measured and simulated photosynthesis. A better fit between actual and predicted P_{gc}, however, is needed for the more advanced concept of *optimal climate control*[145].

CONCLUSIONS

Present leaf photosynthesis models need to be designed for high temperature conditions when application in modern climate control is aimed for. When using the

biochemical approach of Farquhar *et al.* (1980)[97], a stomata model is necessary that reduces photosynthesis at high temperatures. Stomatal resistance models can strongly improve prediction of crop photosynthesis at high temperatures but the strength of back-regulation has to be adjusted by the model parameters. A generic approach can improve that, but is difficult to design. This, however, could yield a well performing photosynthesis model for high temperature conditions. For current application, the presented and tested biochemical model including predicted stomata resistance has closest prediction considering the whole temperature. This model can be used for control. For future application with optimal climate control, a better model is probably needed.

CHAPTER 3

CLIMATE REGIMES

3.1 A MODIFIED TEMPERATURE INTEGRATION REGIME

O. KÖRNER & H. CHALLA
Design for an improved temperature integration concept in greenhouse cultivation
Computers and Electronics in Agriculture 39, 39 – 59

ABSTRACT

The ability of crops to tolerate temperature deviations from the average set point could play an important role in energy saving greenhouse climate regimes. This principle is used in the so called temperature integration procedure, which is based on empirical knowledge and uses fixed maximum and minimum temperatures. More dynamic flexible boundaries depending on the underlying crop processes would probably increase the potential for energy saving in greenhouses. Therefore our aim was to improve the temperature integration concept by introducing dynamic temperature constraints. Processes with a fast temperature response (e.g. photosynthesis or stress) were decoupled from developmental processes with a slow response time. A modified temperature integration procedure was designed combining the usual long-term integration over several days and fixed boundaries for daily average temperature with short-term integration over 24 hours with flexible temperature limits. Because the optimum temperature for canopy photosynthesis rises

with increasing concentration of atmospheric CO_2, this aspect was included in ventilation control. Because plants react not only to extreme temperatures but also to their duration, a dose concept was applied to stress-related temperature constraints. The desired mean temperature for the subsequent 24 hours was calculated once in 24 hours. Within this 24-hour cycle, temperature set points for heating and ventilation were optimised in relation to the fast crop processes. The temperature regime was tested by simulations. Greenhouse climate, energy consumption and crop photosynthesis were simulated for complete years and different parameter settings for tomato as model crop. With the modified regime compared to regular temperature integration, with the same ±2 ºC long-term temperature bandwidth 4.5 % (normal secure settings) or up to 9 % (extreme settings) more energy could be saved (on a yearly basis). Crop gross photosynthesis could increase by approximately 2.5 %.

INTRODUCTION

To achieve a certain target temperature, greenhouses in The Netherlands are usually heated with a central boiler and cooled by ventilation. Set points for heating and ventilation with a narrow bandwidth (i.e. 1 – 2 °C) are set according to a blueprint regime, based on the experience of the individual grower and the computer manufacturer[165]. Due to daily weather variations, heating and ventilation may alternate several times a day, leading to extra fossil energy consumption. Reduction of the amount of fossil energy used per unit produce and associated reduction of CO_2 emission is recently one of the major issues in greenhouse cultivation in moderate temperate climates such as in The Netherlands.

Climate control is necessary for attaining high crop growth, yield and quality, the major targets for the growers. Extreme temperatures may induce stress and associated damage to the plasmatic structures or the photosynthetic apparatus of the plant[142, 166]. Less extreme sub-optimal temperatures may delay plant development and affect other plant characteristics such as dry matter distribution.

Climate regimes based on temperature integration[167] that allow temperature fluctuations while respecting proper plant development and crop growth have been developed. Using temperature integration a certain mean temperature is maintained within upper and lower limits over specified time intervals. Intervals such as night time[168], complete 24-hour cycles[39, 41] and periods of several days[52] have been successfully applied for a large variety of greenhouse crops. The maximum integration interval and temperature bandwidth for high quality crops are still fairly unknown. The concept in fact is based on empiricism and lacks physiological background. Fixed temperature bandwidths and integration intervals are commonly used. In regular temperature integration regimes fast (minutes) and slow (days) plant processes are not a matter of concern. Taking these into account could probably

increase energy saving while maintaining crop yield and quality. Processes with a slow response time (e.g. plant development) probably respond primarily to average temperatures over prolonged periods and processes with a quick response (e.g. photosynthesis) may allow more extreme temperature deviations without losses in quality and growth[169, 170].

A more flexible temperature regime based on temperature integration could also improve the performance of optimal greenhouse climate control, because there is more freedom to generate optimal temperature trajectories outside the normal range. We therefore designed a regime with a wider short-term temperature bandwidth while maintaining the restrictions of long-term temperature integration over several days. The aim of this study was to describe and explain such a new temperature regime and to investigate its potential for energy saving and productivity. Therefore, the regime was tested with a greenhouse climate and crop photosynthesis model. Simulations were performed with different parameter settings for tomato to investigate the effects on greenhouse climate, energy consumption and photosynthesis as an indicator of crop growth.

OUTLINE OF THE REGIME

BASIS

The target greenhouse day and night temperature in common practice is usually not fixed. Temperature set points are modified automatically, such that e.g. ventilation temperature increases with instantaneous radiation or total daily radiation according to grower's experience, based on rules of thumb[165]. Increasing the bandwidth between ventilation and heating set points while controlling mean rather than instantaneous temperature is a further development of this blueprint regime and called temperature integration. Temperature integration is based on the assumption that within the limits considered the crop responds linearly to temperature. Maximum, minimum and mean temperature and averaging period are the key parameters for temperature integration. Freedom for temperature fluctuations, i.e. the possibilities for temperature to freely fluctuate due to the environment without being controlled by heating or ventilation, increases with longer averaging period and increasing temperature bandwidth. With a relatively short averaging period of 24 hours, a cool day has to be compensated directly by a warm night or *vice versa*. Temperature integration over longer periods of several days enables compensation of warm or cold spells during one of the following days and higher energy savings are possible[60]. Whatever length of averaging period is used, mean temperature has to be attained within certain margins while actual heating can be shifted to periods of lower costs[36]. Theoretically, three extreme (and many in-between) situations are possible with this regime. During sunny days and cold nights

greenhouses heat up during daytime and cool down at night. In the most favourable conditions, greenhouse temperature stays above the heating set point and no energy for heating will be needed. With cold days, heating can be shifted to nighttime under energy screens, which saves large amounts of energy[39]. In that case, more energy can be saved with increasing temperature compensation possibilities. Cold days can then be compensated later by warmer periods and there is no need to compensate high day temperatures during the following night when the integration period is longer than one day (e.g. the day after, with an integration period of two days). No temperature compensation during night is possible when mean daytime greenhouse temperature is the same as the desired 24-hour mean temperature.

<div align="center">SCHEME</div>

The regular temperature integration regime has a fixed averaging period, which is usually between 4 and 8 days. In this approach the existence of fast and slow plant processes is not considered. However, taking this distinction into account, new possibilities for energy saving become available. The regular concept of temperature integration was therefore modified to a system of two nested temperature integration regimes with different averaging periods, short-term (ST) (dedicated to fast plant processes) and long-term (LT) (dedicated to slow plant processes). LT corresponds to the averaging period of several days in regular temperature integration; ST correspondents to a 24-hour period (FIG. 1). For ST, a target short-term temperature range rather than a fixed target temperature is used as control criterion. Temperature is allowed to fluctuate within this range but the average temperature should comply with the requirements of the LT regime (FIG. 2). Temperature course *a* is with regular temperature integration; in *b* the temperature boundaries are relaxed to short-term boundaries while mean temperature is maintained. The cases *c* and *d* have different mean temperatures but are both within the acceptable range. The ST limits are adjusted if 24 hour mean temperature exceeds the LT temperature integration boundaries. Extreme temperatures are avoided by setting two thresholds on either side of the acceptable range. One threshold represents the absolute limit for temperature, after passing the other threshold stress may occur depending on the temperature dose. In fact, the effects of temperature extremes increase with duration and level of extremes and hence depend on the dose[171]. We assume an exponential response between the two threshold levels.

A further element of the improved climate regime under consideration is optimisation of temperature for crop gross photosynthesis. Temperature for maximum gross photosynthesis increases with CO_2 concentration, as illustrated with model simulations according to CHAPTER 2.1 (FIG. 3). Therefore, there is a benefit in
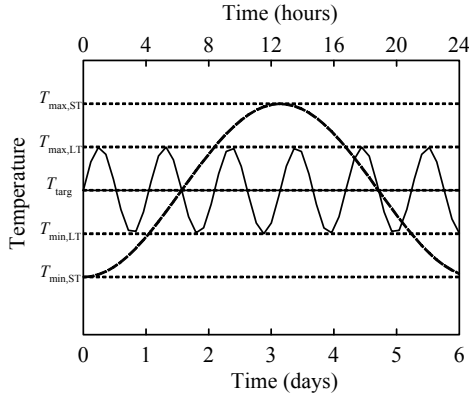
FIGURE 1. Modified temperature integration regime with short-term (ST) -nested into long-term temperature integration regime (LT) as a function of time, with ST (—) in hourly scale (24 h) and LT (---) in days. With target mean temperature (T_{targ}); maximum and minimum temperatures for long-term control ($T_{max,LT}$ and $T_{min,LT}$), and short-term control ($T_{max,ST}$ and $T_{min,ST}$).
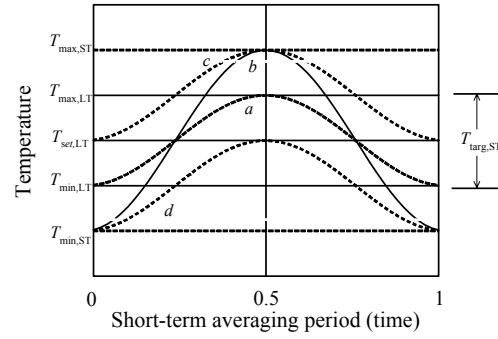
FIGURE 2. Principle of temperature control during a short-term averaging period, with target for long-term temperature integration control ($T_{set,LT}$) and boundaries for the long- and short term averaging periods ($T_{max,LT}$, $T_{min,LT}$ and $T_{max,ST}$, $T_{min,ST}$, respectively). $T_{targ,ST}$ is the target mean temperature range after the short-term period. The curves a-d represent short-term temperature regimes. The means of a and b equal $T_{set,LT}$, while those of c and d equal $T_{max,LT}$ and $T_{min,LT}$, respectively.

allowing greenhouse air temperature to rise with radiation more than required for LT control, to prevent ventilation and associated drop in CO_2 concentration and due to photorespiration[88]. Introduction of photosynthesis optimisation will lead to a high CO_2 concentration that can be maintained at little or no ventilation, or atmospheric CO_2 with ample ventilation.

MATERIALS AND METHODS

TECHNICAL IMPLEMENTATION

The proposed regime was implemented in a simulation model of the greenhouse crop system developed in the technical software environment MATLAB® (version 6.0, MathWorks, Natick, MA, USA) using greenhouse tomato as model crop. This programme, including a crop photosynthesis module, functioned as the set point generator. Greenhouse air temperature, relative humidity and CO_2 concentration inside the greenhouse and outside global radiation were input with a fixed time step of 5 minutes. The set point generator was coupled with a greenhouse climate and control model[105] (CCM). Set points for heating, ventilation and CO_2 concentration
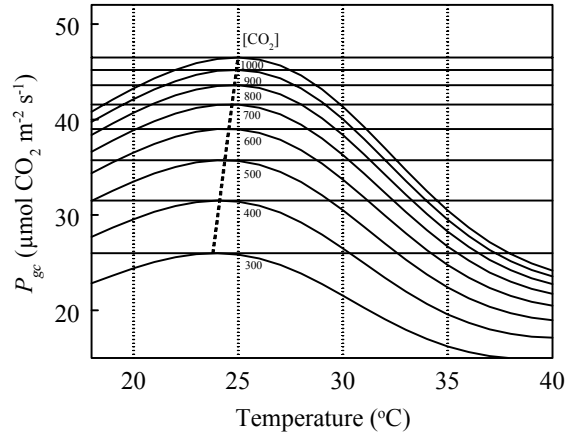
FIGURE 3. Example of simulated tomato crop gross photosynthesis (P_{gc}) as a function of temperature and CO_2 concentration at 800 W m^{-2} outside global radiation; greenhouse transmission for direct and diffuse short wave radiation of 70 %; fixed sine of solar elevation of 0.8; fraction of diffuse radiation of 0.5; constant relative humidity of 80 % and a scattering coefficient for photosynthetic active radiation = 0.15; leaf extinction coefficient of diffuse light = 0.8. Maximum P_{gc} for each CO_2 concentration is indicated by the diagonal line (---).

were calculated by the set point generator and sent as input to the CCM. The CCM returned simulated greenhouse climate (relative humidity, air temperature and CO_2 concentration), while using the received set points for control of heating and ventilation. The inner greenhouse climate was controlled by a replica of commercially available climate controllers. The CCM provided simulations for a 2 ha Venlo-type greenhouse with single glass cover with a diffuse short-wave radiation transmission of 78.5 %. Transmission of direct sunlight was calculated as a function of azimuth and elevation of the sun[172]. The CCM controlled greenhouse climate through heating and ventilation, and simulated energy consumption with a 2-minute time step. Energy input to the greenhouse was calculated taking incoming solar short-wave radiation into account (no assimilation lamps were used) and required direct heat supply from the heating unit. Heat was provided by a natural gas fired hot water boiler (maximum of 94 °C). Natural gas consumption was simulated with a heat content of 35.17 MJ per m^{-3} natural gas. Energy losses were calculated from radiative, convective and latent heat fluxes through the greenhouse cover and conduction through the ground below the greenhouse. Energy loss from heating pipes was calculated by sensible heat flux through convection to the greenhouse air and by radiative heat exchange to greenhouse elements and the crop. Radiative heat exchange processes were governed by the *Stefan-Boltzmann* equation. An effective sky temperature (T_{sky}) as the temperature of a black hemisphere exchanging thermal radiation with the greenhouse cover was calculated[105]. Latent heat loss by crop transpiration was calculated and natural ventilation was computed[92, 173]. An energy saving screen was used that reduced short-wave transmission to the crop canopy by 70 % when it was closed. Air exchange between the compartment beneath and above

the screen was simulated by convective heat flux through openings in the fabric[105]. Validations of the CCM in four semi-commercial Venlo-type greenhouse compartments of 192 m^2 ground cover with a full-grown rose stand have been performed[105]. Greenhouse climate on a short time scale (minutes) was well predicted and simulated and measured annual energy consumption differed only by 2 %. In addition, simulations done with the CCM agreed well with reported gas consumption calculated with the regularly validated greenhouse climate model *Pregas*[174, 175]. Natural gas consumptions for commercial year-round tomato cultivation without screen were 2.15 and 2.16 GJ m^{-2} year^{-1} for *Pregas* and CCM, respectively.

REFERENCE CLIMATE REGIME

Two reference temperature regimes were used for comparison. The heating set points were 18 °C and 19 °C and ventilation set points were 19 °C and 20 °C for night and day, respectively. The first reference regime (blueprint, *BP*) was according to commercial practice and included adaptation of temperature set points in relation to instantaneous radiation and daily radiation. Daytime ventilation set points increased linearly with outside global radiation (0.5 K per 100 W m^{-2} between 400 to 800 W m^{-2}) and nighttime ventilation and heating set points increased linearly with daily global radiation sum (0.25 K per 1 MJ m^{-2} d^{-1} between of 6 and 16 MJ m^{-2} d^{-1}). In the second reference temperature regime (*BP$_{fix}$*) night- and daytime heating and ventilation temperature set points were fixed, as is uncommon in commercial practice.

SPECIFICATION OF THE LONG-TERM TEMPERATURE INTEGRATION REGIME

The averaging period for temperature integration was six days. A *post hoc* procedure for temperature integration was used, i.e. deviations from mean target temperature were compensated afterwards rather than using an optimal forecasted temperature trajectory for determining temperature set points. Deviations of mean temperature of the preceding 5 days were compensated during the last 24-hours of the averaging period. Temperatures before 5 days were no longer taken into account. Within the 24 hours of day 6 of the integration interval there were several constraints, A. constraints to attain the target average temperature over the full integration period, B. constraints to avoid extreme temperatures and C. constraints for optimisation of crop gross photosynthesis. The target 24-hour mean temperature ($T_{targ,24}$) at day 6 (d) of the averaging period (t_{int}) was obtained from the difference between the sums of the 24-hours means of desired temperatures ($\overline{T}_{des}$) over t_{int} and previous realised temperatures ($\overline{T}_{real}$) over the preceding five days ($t_{int} - 1$).

$$T_{targ,24}(d) = \sum_1^{t_{int}} \overline{T}_{des} - \sum_1^{t_{int}-1} \overline{T}_{real}$$ [1]

SPECIFICATION OF THE SHORT-TERM TEMPERATURE REGIME

The ST averaging period was 24 hours. First, the greenhouse temperature without control (i.e. neither ventilation nor heating through temperature set points) for ST was estimated at the start of each new averaging period (0:00 h) with a simple K-value model (EQ. 2). In semi-commercial greenhouses this equation described greenhouse temperature well (De Zwart, IMAG, Wageningen, pers. communication).

$$T_{in} = T_{out} + \frac{1}{3} \cdot \tau_{dif} \cdot \frac{I_{out}}{K} \qquad [2]$$

with inside greenhouse temperature (T_{in}, °C), outside temperature (T_{out}, °C), fraction of greenhouse transmission for diffuse short-wave radiation (τ_{dif}), outside global radiation (I_{out}, W m^{-2}) and overall greenhouse heat transmission coefficient (K, W m^{-2} °C^{-1}). K was set to 4 and 8 W m^{-2} °C^{-1}, respectively, with and without energy screen.

EQ. 2 was compared to simulations with the CCM with relative passive heating and ventilation temperature set points of 10 °C and 34 °C, respectively. Relative humidity set point was 85 %. Hourly mean temperatures of the CCM were on average underestimated by 2.5 °C, 3.4 °C, 1.3 °C and 0.7 °C in spring, summer, autumn and winter, respectively. This was sufficient for the purpose of planning. The equation was only used for a rough estimation of greenhouse temperature in the next 24 hours without concern about temperature control, although the absolute ST temperature thresholds ($T_{max,ST}$, $T_{min,ST}$) were respected to avoid temperature extremes. Once the planning for the next 24 hours had been made, the greenhouse environment during simulation was actively controlled by heating and ventilation. As EQ. 2 was only used for planning, the actual greenhouse mean temperature was continuously updated with realised temperature.

We used the lazy-man weather prediction[165], where weather at day d was assumed to be the same at day d–1. 24-hour mean greenhouse temperature at day d was updated every 5 min with the actual greenhouse temperatures. To protect the crop against excessive high or low temperatures due to radiation or too strong compensation, maximum and minimum heating (24 °C, 10 °C) and ventilation temperatures (34 °C, 14 °C) were set initially, and adapted during cultivation (EQ. 3, EQ. 4 and FIG. 4).

$$dose_{max} = \frac{\left(T - T_{max,rel}\right) \cdot e^{160 \cdot \left(\frac{1}{T_{max,abs}} - \frac{1}{T}\right)}}{T_{max,abs} - T_{max,rel}} \cdot \left(t_{dose_{max}} \cdot t_{sample}\right)^{-1} \qquad [3]$$

$$dose_{min} = \frac{\left(T_{min,rel} - T\right) \cdot e^{-30 \cdot \left(\frac{1}{T_{min,abs}} - \frac{1}{T}\right)}}{T_{min,rel} - T_{min,abs}} \cdot \left(t_{dose_{min}} \cdot t_{sample}\right)^{-1} \qquad [4]$$
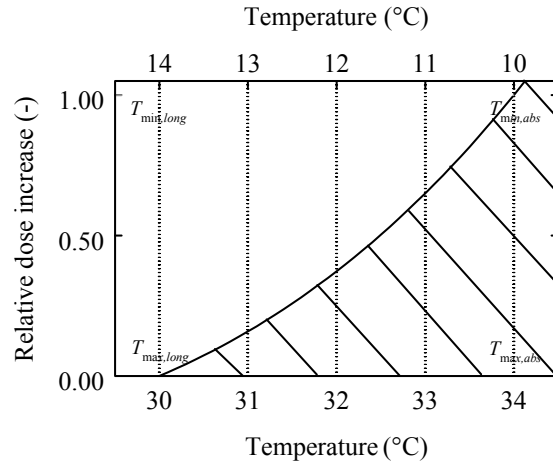
FIGURE 4. Principle of temperature dose without time factor. An example is given for relative maximum temperature ($T_{max,rel}$); relative minimum temperature ($T_{min,rel}$); absolute maximum temperature ($T_{max,abs}$) and absolute minimum temperature threshold ($T_{min,abs}$) which are 30, 14, 34 and 10 °C, respectively.

with upper and lower relative thresholds ($T_{max,rel}$ and $T_{min,rel}$, °C), upper and lower absolute thresholds ($T_{max,abs}$ and $T_{min,abs}$, °C), greenhouse air temperature (T, °C), dose for maximum and minimum temperature boundaries ($dose_{max}$ and $dose_{min}$), sample time (t_{sample}, min) and maximum and minimum exposure at $T_{max,abs}$ or $T_{min,abs}$ ($t_{dose_{max}}$ or $t_{dose_{min}}$, min); $t_{dose_{max}}$ and $t_{dose_{min}}$ were set 30 minutes for standard conditions. Single values taken each t_{sample} were integrated over time. If the integrated value exceeded 1, the corresponding relative threshold was held for the duration of a refresh time of 6 hours and was then reset. This was due to regeneration of plant tissue at non-extreme temperatures.

Crop gross photosynthesis (P_{gc}) was calculated based on leaf photosynthesis and radiation distribution within the canopy[96]. Leaf photosynthesis was described with the two parameter (maximum gross photosynthesis and photochemical efficiency), negative exponential light-response curve [94]. Biochemical based equations were used as described in CHAPTER 2.1 [175].

The upper threshold for greenhouse CO_2 concentration was 1000 µmol mol^{-1} and set when vents were closed. Temperature giving rise to maximum gross photosynthesis at 1000 µmol mol^{-1} (under prevailing light conditions) was used as ventilation set point. CO_2 set point was 350 µmol mol^{-1} when vents were open or when outside global radiation was below the threshold of 40 W m^{-2}.

SET POINTS

Temperature in a commercial control system is controlled by set points for heating and ventilation. Heating set point (T_h) was obtained according to EQ. 5 and

ventilation set point (T_v) according to EQ. 6. Default values were absolute extreme temperatures thresholds (i.e. $T_{max,abs}$ or $T_{min,abs}$).

$$T_h = \max\begin{pmatrix} T_{min,ST} & T_{min,dose} \end{pmatrix} \qquad [5]$$

$$T_v = \min\begin{pmatrix} T_{max,ST} & T_{max,dose} & T_{max,phot} \end{pmatrix} \qquad [6]$$

with minimum and maximum temperature according to the dose concept ($T_{min,dose}$ and $T_{max,\underline{dose}}$, respectively); minimum and maximum temperature determined in the ST loop ($T_{min,ST}$ and $T_{max,ST}$, respectively); and temperature for maximum photosynthesis ($T_{max,phot}$).

SIMULATIONS

Greenhouse tomato cultivation was simulated for a crop grown as usual in practice in The Netherlands. However, a 365 day cultivation period with planting date 1 January ignoring the normal 2 – 3 weeks interruption for cleaning and replanting was used. A representative one-year reference climate data set for De Bilt[177] (The Netherlands, lat. 52 °N) was used for simulations on yearly dynamics of greenhouse climate, energy consumption and crop growth. The reference year consisted of a typical Dutch climate data set with hourly values of air temperature, relative humidity, direct and diffuse global radiation, CO_2 concentration, wind speed, wind direction and soil temperature. An energy screen was used and controlled as in commercial practice. For dehumidification, the screen was opened to a maximum of 4 %. Gas was burned

TABLE 1. Simulated regular and modified temperature integration regimes with P_{gc} optimal (+) and non-optimal (0). With maximum time for dose response (t_{dose}) in minutes and the set point for relative humidity in % (RH_{set}).

Temperature integration regime (bandwidth)	Regime settings			Abbreviation
	t_{dose}	P_{gc} - optimisation	RH_{set}	
	0	+	85	$MTI_{T_{abs}\,0\pm2...\pm6}$
		+	85	$MTI_{\pm2...\pm6}$
			99	$MTI_{\pm2...\pm6\_RH99}$
Modified	30	0	85	$MTI_{\pm2...\pm6\_nonoptP_{gc}}$
($\pm2, \pm4, \pm6$ °C)			99	$MTI_{\pm2...\pm6\_nonoptP_{gc}\_RH99}$
	180	+	85	$MTI_{T_{abs}\,180+2\,+6}$
	360	+	85	$MTI_{T_{abs}\,360+2\,+6}$
Regular	-	0	85	$RTI_{\pm2...\pm6}$
($\pm2, \pm4, \pm6$ °C)	-	0	99	$RTI_{\pm2...\pm6\_RH99}$

for CO_2 supply with the heater. Excess heat was stored in a heat buffer of 120 m^3. When the buffer was completely filled, CO_2 supply stopped. Target mean greenhouse temperature was 19 °C for all simulations. Different settings for the modified and the regular temperature integration regime (TABLE 1) were compared to each other and to the two reference climate regimes BP and BP_{fix}. Relative humidity set points were 85 % or 99 % for separate simulations and controlled by ventilation.

The same back-regulation (FIG. 5, EQ. 7 and EQ. 8) was used for all simulations with temperature integration. Minimum and maximum average target temperature were set according to the difference between realised and target mean temperature and *vice versa*. The offset-factors f_h and f_v (heating and ventilation) were proportional to the deviation from the mean target temperature ($\Delta \overline{T}$) and controlled its realisation.

$$f_h = x + \left((x \cdot t_{int}) - (x \cdot t_{int}) \cdot e^{\frac{\Delta \overline{T}}{r_h}} \right)$$ [7]

$$f_v = y + \left((y \cdot t_{int}) - (y \cdot t_{int}) \cdot e^{-\frac{\Delta \overline{T}}{r_v}} \right)$$ [8]

EQ. 7 and EQ. 8 contain length of averaging period (t_{int}), maximum allowed absolute positive and negative deviation from the target temperature (i.e. half temperature bandwidth, x and y, respectively) and factors for the strength of back regulation for heating and ventilation (r_h and r_v, respectively). The stronger the back regulation (i.e. the lower r_h or r_v), the more conservative the system is. To achieve the targeted mean temperature over the averaging period, low r_h and r_v values have to be used for

TABLE 2. Annual mean temperature and mean temperature per month for simulated climate regimes.

Regime	Annually	Month											
	-	Jan	Feb	Mar	Apr	May	Jun	Jul	Aug	Sep	Oct	Nov	Dec
						Mean temperature (°C)							
BP	20.3	18.4	18.7	19.2	20.6	21.1	22.7	22.2	22.8	21.1	19.6	18.7	18.3
BP_{RH99}	20.4	18.4	18.6	19.2	21.0	21.3	22.9	22.3	23.2	21.3	19.6	18.7	18.4
BP_{fix}	20.0	18.4	18.6	19.0	20.2	20.6	22.1	21.7	22.3	20.7	19.4	18.6	18.3
$RTI_{\pm2}$	19.6	18.8	18.9	18.9	19.5	19.7	21.1	20.7	21.4	19.9	19.0	18.8	18.7
$RTI_{\pm4}$	19.3	18.7	18.8	18.8	19.1	19.3	20.3	20.3	20.7	19.5	18.7	18.7	18.7
$RTI_{\pm6}$	19.2	18.7	18.7	18.7	18.9	19.3	20.1	20.2	20.5	19.4	18.7	18.5	18.7
$MTI_{\pm2}$	19.4	19.0	18.9	18.9	19.4	19.4	20.1	20.3	20.5	19.5	19.0	18.8	19.3
$MTI_{\pm4}$	19.3	18.8	18.6	18.8	19.2	19.5	20.2	20.3	20.5	19.5	18.7	18.7	19.0
$MTI_{\pm6}$	19.3	18.7	18.4	18.8	19.1	19.5	20.3	20.4	20.6	19.5	18.7	18.5	19.0

low temperature bandwidths. In our simulations r_h and r_v were set to 1.7, 2.9 and 4.7 for ±2 °C, ±4 °C and ±6 °C temperature bandwidth, respectively.

RESULTS

GENERAL REGIME BEHAVIOUR AND ENERGY SAVING

Mean temperature for the reference regime was lower when the temperature set points were independent of radiation (TABLE 2). Since these influences accounted for an increase in energy consumption of 0.8 % (data not presented), energy consumption of BP_{fix} was used for comparisons to the different temperature integration regimes. The yearly mean temperatures varied with about 1 °C between temperature integration and blueprint regimes. The blueprint regimes had higher temperatures in summer and this accounted for the higher yearly mean temperatures. Monthly mean temperatures differed only slightly in winter, spring and autumn. During these seasons energy consumption in greenhouses is highest. Therefore, energy saving of the temperature integration regimes compared to BP_{fix} (FIG. 6) was not due to a lower mean temperature. In the modified regime more energy was saved than with regular temperature integration (FIG. 6). Energy saving increased with temperature bandwidth in all cases evaluated. This increase, however, was less than proportional to temperature bandwidth. Yearly greenhouse energy saving increased by up to 23 % compared to the blueprint regime (temperature bandwidth of ±6 °C). Compared to regular temperature integration energy saving increased relatively with 14 % (3 % absolute) (FIG. 6). The set point for relative humidity highly influenced energy saving. Without humidity control (i.e. set point relative humidity of 99 %), energy saving increased for all investigated cases compared to the control with a set point of 85 % (FIG. 6).

This increase was fairly insensitive to temperature bandwidth. Energy consumption was mainly reduced between early spring and late autumn (FIG. 7). During the first two months of cultivation (i.e. January and February), energy consumption for both regular and modified temperature integration regime even exceeded the blueprint regime very slightly.

The implemented control for temperature integration was too rigid since no optimal temperature trajectory was calculated for the future, and back-regulation (EQ. 7 and EQ. 8) was too strong during winter months (FIG. 8). In this period temperature integration pays when shifting heating to night under energy screens[55]. This was not implemented in the control and heating set point alternated between its highest and lowest limits (i.e. 24 °C and 10 °C). The difference in energy saving between the two
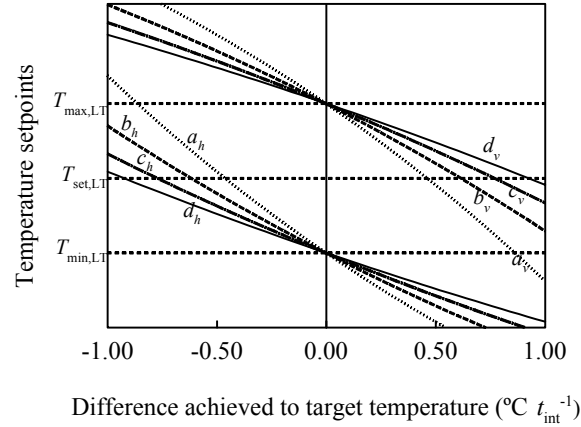
FIGURE 5. Maximum *v* (ventilation) and minimum *h* (heating) temperature as a function of the difference between mean greenhouse temperature and target mean temperature over the integration interval t_{int}. Lines indicate different levels of back-regulation (*a* highest, *d* lowest). With target mean temperature for 24 hours according to the long-term temperature averaging period $T_{targ,LT}$ and upper and lower temperature boundaries according to long-term temperature averaging period $T_{max,LT}$ and $T_{min,LT}$, respectively.

energy saving regimes was most extreme at the lower temperature bandwidth. The larger the temperature bandwidth, the more similar were the yearly energy consumption patterns.

CROP GROSS PHOTOSYNTHESIS MODULE

In the modified climate regime, crop gross photosynthesis was higher than with the reference regime and regular temperature integration (TABLE 3). P_{gc} with the modified regime increased with temperature bandwidth from ±2 °C to ±4 °C

TABLE 3. Percentage crop gross photosynthesis (P_{gc}) increase with regular and modified temperature integration (*RTI*, *MTI*) in comparison to the fixed blueprint regime (BP_{fix}) (A). Percent difference P_{gc} and energy consumption ($E_{cons.}$) influenced by non − maximised P_{gc} in *MTI* ($MTI_{\_nonoptP_{gc}}$) (B).

Temperature bandwidth (°C)	A		B	
	Increase in comparison to blueprint (BP_{fix})		Increase in comparison to $MTI_{\_nonoptP_{gc}}$	
	RTI	*MTI*	*MTI*	
	P_{gc}	P_{gc}	P_{gc}	$E_{cons.}$
±2	2.1	3.5	0.2	0.8
±4	2.0	3.9	0.4	1.6
±6	1.8	3.8	0.4	1.2
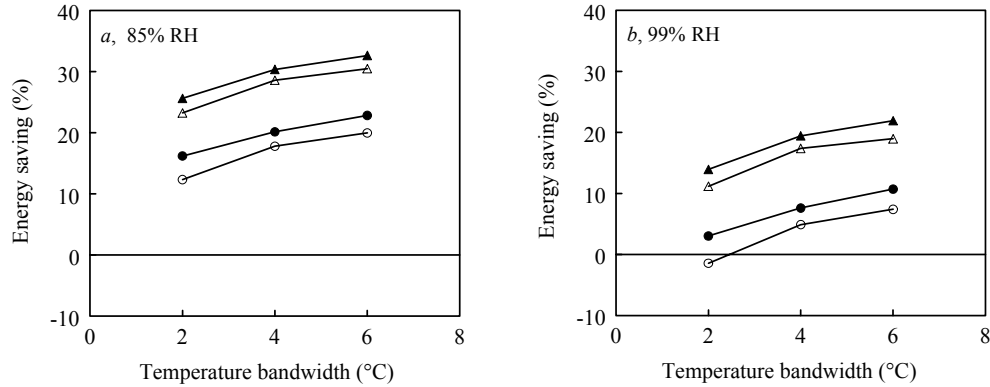
FIGURE 6. Simulated yearly energy saving of regular temperature integration with 85 % and 99 % relative humidity set point (O, $\triangle$, respectively), and modified temperature integration ($t_{dose_{max}}$ and $t_{dose_{min}}$ = 30 minutes) with 85 % and 99 % relative humidity set point ($\bullet$, $\blacktriangle$, respectively) compared to BP_{fix} with 85 % and 99 % relative humidity set point (*a*, *b*).

and stabilised after that; regular temperature integration had its highest P_{gc} at temperature bandwidth of ±2 °C and continuously decreased thereafter. The control algorithm was probably the reason for that. As mentioned above, temperature integration control was not implemented optimally. With increasing freedom for temperature compensation, periods of extreme high temperatures were either compensated by short periods of extreme low temperatures or by long periods of low temperatures. Photosynthesis increase at high temperature periods was later overcompensated by very low or long lasting low photosynthesis levels (data not presented). Comparing simulations with and without the optimising photosynthesis module proved that energy consumption and crop gross photosynthesis slightly increased when applying the maximisation procedure (TABLE 3).

<div align="center">TEMPERATURE-DOSE RESPONSE MODULE</div>

Increasing the duration of absolute maximum and minimum temperatures (T_{abs}) increased energy saving and P_{gc} (FIG. 9 a). The modified regime with ±2 °C temperature bandwidth increased energy saving by 4.5 % (T_{abs} = 30 minutes) or 9 % (T_{abs} = 360 minutes) compared to regular temperature integration. The percentage energy saving was higher with larger maximum temperature bandwidths over the complete range (FIG. 9 b). The increase in energy saving decreased with increasing maximum duration and decreased stronger with larger temperature bandwidths. Percentage difference in P_{gc} between the different maximum temperature bandwidths did not change significantly with permissible duration for the absolute temperature extreme.
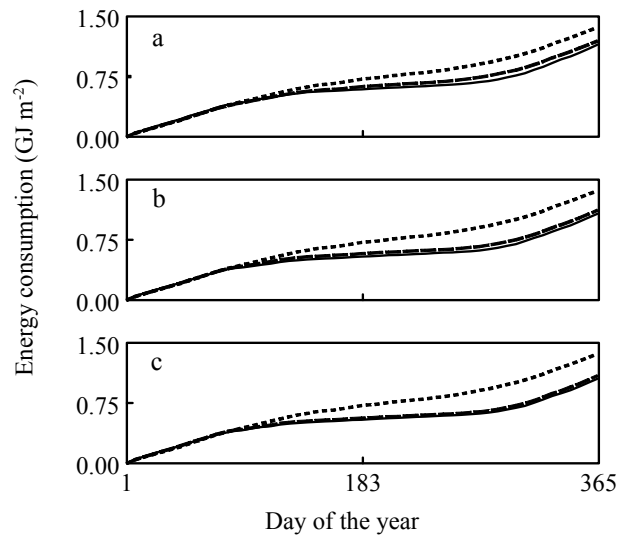
FIGURE 7. Simulated cumulative energy consumption (GJ m^{-2}) of a blueprint temperature regime (----, upper line), regular temperature integration (– – –, middle line) and modified temperature integration (—, lower line) with temperature bandwidths of ±2 °C (a), ±4 °C (b) and ±6 °C (c). A six-day averaging period for tomato crop cultivation in The Netherlands according to a reference climate year was used (RH set point 85 %).
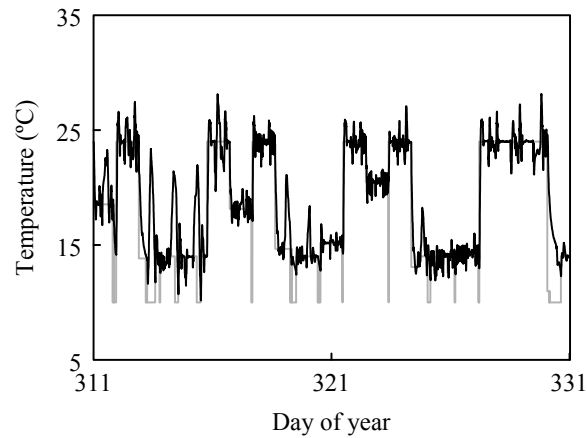
FIGURE 8. Simulated heating set point (grey line) and greenhouse temperature (black line) during 21 typical autumn days for the modified temperature integration regime with standard settings and LT temperature bandwidth of ±2 °C.

105
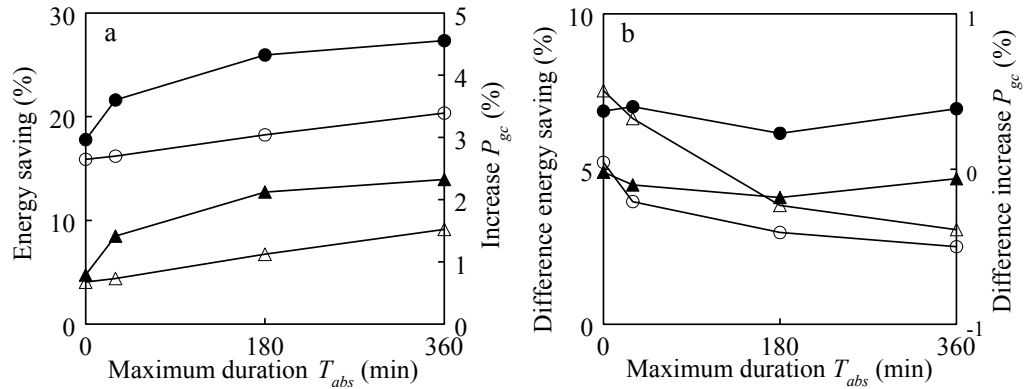
FIGURE 9. a) Energy saving (white symbols) and increase of crop gross photosynthesis P_{gc} (black symbols) for ±2 °C temperature bandwidth compared to blueprint regime (○, ●) and to common temperature integration with ±2 °C temperature bandwidth (△, ▲) as a function of maximum exposure at the absolute temperature limit (t_{dose} and T_{abs}, respectively). **b)** Differences in energy saving (white symbols) and crop gross photosynthesis (black symbols) between temperature bandwidths of ±4 °C and ±2 °C (△, ▲) and between temperature bandwidths of ±6 °C and ±2 °C (○, ●) as a function of maximum exposure at the absolute temperature limit (t_{dose} and T_{abs}, respectively).

DISCUSSION

A conceptual design for a more advanced temperature integration control was shown. Simulations indicated that energy consumption could be reduced further with the new regime. Energy consumption, nevertheless, was evaluated with simulations. As mentioned earlier, the greenhouse climate and control model agreed closely with measured gas consumption[105]. Less than 0.5 % deviation from a commercial greenhouse climate model[175] was found, too. This supports the validity of the greenhouse simulation model for comparing simulated energy consumption. The most crucial part in temperature integration is achieving the desired mean temperature without losses in crop development, quality and / or growth. Yearly mean temperatures of both evaluated temperature integration regimes, nevertheless, was lower than with the reference temperature regimes. This was due to summer situations when temperature integration was able to compensate warm days by cooler nights, whereas in the reference regimes the temperature would not drop below 18 °C. An overall more constant yearly week-average temperature course for temperature integration regimes was the result of that, too. This could probably result in better tomato fruit yield since tomato cultivation is optimal around a mean temperature between 18 °C and 19 °C. Higher temperature enhances early fruit growth at the expense of vegetative growth[178]. The proposed modified temperature integration regime enabled an additional increase in absolute energy saving of up to 9 % compared to the regular regime. This maximum energy saving was only possible with the most extreme setting for temperature-dosage (i.e. 360 minutes). These settings, in fact, should give rise to crops with high quality and yield. It was reported that

cucumber plants could repeatedly bridge a period of 360 minutes at 8 °C during a period of 24-hour if the temperature rises to 20 °C after that[169]. In the modified regime the temperature increased only to 14 °C after a cool period. The reported findings[169], however, indicate that the applied 30 minutes at 10 °C for the standard settings in the proposed modified temperature integration regime was safe and that the most extreme dose of 360 minutes at 10 °C may be feasible. The combination of the lowest long-term temperature bandwidth (±2 °C) with the longest permissible exposure to the absolute temperature threshold, yielded the highest relative increase in energy saving compared to regular temperature integration. This was due to the increase in freedom for instantaneous temperature fluctuation, which was most beneficial at safe long-term settings. The implemented control algorithm for the modified regime gives already most of its freedom for temperature fluctuation at low long-term bandwidths. This is due to the strong effect of the nested-time regime. Regular temperature integration with higher temperature bandwidths of ±4 °C and ±6 °C buffers many short-term fluctuations already. With smaller bandwidths, however, instantaneous temperature is almost constantly controlled and this control decreased with the modified regime. Regular temperature integration with small bandwidth was very close to the reference regime and therefore energy saving was low.

Energy consumption increased when applying the photosynthesis maximisation procedure. Photosynthesis on the other hand increased only slightly. Compared to the reference regime and regular temperature integration, nevertheless, photosynthesis with modified temperature integration increased much more. This was most probably due to less window opening and longer time at high CO_2 dosage (data not shown). To increase the positive effect of photosynthesis maximisation the procedure could probably be improved, because the control was too rigid.

The proposed regime could probably be improved with better parameter estimation, e.g. a deeper insight into plant physiology could improve the exponential model for temperature-dose response. Also the crop photosynthesis model was not properly validated for extreme temperature conditions. However, a theoretical photosynthesis model evaluation study has been performed (CHAPTER 2.1) and the one applied here was promising. In addition, a better greenhouse climate model for calculating subsequent 24-hour greenhouse temperature could probably improve the climate control possibilities. The application of simple models, however, was sufficient for the aim of the present research to show and evaluate the new design of a temperature integration regime.

A high freedom in temperature set point determination has been achieved and this makes the regime valuable for optimal climate control. However, before implementing this regime as a module into an optimal climate control programme, it should further be improved by longer greenhouse climate predictions than 24 hours (i.e. several days) and by calculating an optimal temperature trajectory for this period.

The longer the period is for which conditions are predicted and analysed the greater are the opportunities for optimal control[36].

Highest energy saving was attained when no humidity control was used. An improvement of humidity control as e.g. based on the underlying processes rather than an overall low relative humidity set point could therefore most probably increase energy saving and possibilities for optimal climate control. Until now energy saving strategies have mainly been focussed on temperature and more advanced humidity control was mainly developed in relation to disease control[179]. For an overall approach, one should take both advanced temperature and advanced humidity control into account.

CONCLUSIONS

The presented modified temperature integration regime is a promising starting point for further development. The distinction between short- and long-term processes in temperature integration lead to an increase in energy saving compared to a regular temperature integration regime. The modified regime increased crop photosynthesis slightly. A more advanced CO_2 control could probably improve this. With more knowledge about the hard limits in time and quantity for short temperature drops and increases, with this system energy saving and options for optimal climate control could probably increase. Humidity control, furthermore, is still limiting energy saving possibilities with temperature integration. A more advanced flexible humidity control concept based on the underlying processes rather than using fixed values could probably help to further decrease energy consumption and give more freedom for optimal climate control.

ACKNOWLEDGEMENTS

3.2 PROCESS BASED HUMIDITY REGIME

O. KÖRNER & H. CHALLA
Process based humidity control regime for greenhouse crops
Computers and Electronics in Agriculture (in press)

ABSTRACT

Modern greenhouses in the Netherlands are designed for efficient use of energy. Climate control traditionally aims at optimal crop performance. However, energy saving is a major issue for the development of new temperature regimes. Temperature integration (*TI*) results in fluctuating and often high relative humidity (RH) levels in modern, highly insulated greenhouses. At high temperature, water vapour pressure deficit (VPD) is usually high and RH consequently low and *vice versa*. Relatively low fixed set points (80 – 85 % RH) for air humidity as is common practice, may strongly influence the efficiency of *TI*, because heating and / or ventilation actions are required to control humidity rather than temperature. This requires much energy. Fluctuating RH may affect crop performance in several ways. Too low VPD may reduce growth due to low transpiration and associated physiological disorders. Water vapour pressure above the dew point leads to condensation on the relative cooler plant tissue and this may give rise to diseases. High VPD, on the other hand, may

induce high stomatal resistance and plant water stress. The aim of the present research was the design of a process-based humidity control concept for a reference cut chrysanthemum crop cultivated with *TI*. RH control set points were generated as function of underlying processes. Greenhouse performance with this humidity regime and different temperature regimes were simulated with respect to greenhouse climate, energy consumption and photosynthesis. Compared to a fixed 80 % RH set point, annual energy consumption of a year round cut chrysanthemum cultivation could be reduced by 18 % for *TI* with ±2 °C temperature bandwidth as well as for regular temperature control. For separate 12-week cultivations with planting date 01 March, energy saving could increase up to 27 % or 23 % for *TI* and regular temperature control, respectively.

INTRODUCTION

Future greenhouse systems in moderate climates will have to be energy efficient. Greenhouses will have decreased transmission for long-wave- and increased transmission for short-wave-radiation compared to common shelters[9]. Improved heat insulation will lead to more fixation of solar energy. For optimal use of these greenhouse systems and for maximum energy saving and optimal crop growth, climate regimes should be designed especially for this type of greenhouses[9]. For this purpose, the temperature integration principle (*TI*) could be used. With *TI*, mean temperature is controlled rather than instantaneous temperature, allowing temperature fluctuations within a certain bandwidth[167]. However, when applying *TI* (especially in highly insulated greenhouses) humidity is a limiting factor for energy saving. With *TI*, heating and ventilation are minimised leading to more temperature fluctuations. In this situation with reduced ventilation and heating, relative humidity (RH) increases when temperature drops and *vice versa*. Water vapour pressure deficit between greenhouse air and crop (VPD) may affect transpiration and consequently absolute air humidity. The low fixed set points for humidity control used in common practice (80 – 85 % RH) counteract the positive effect of *TI* on energy consumption. Vents will open at lower temperatures than required for temperature integration or heating will decrease relative humidity or both. This problem will be even more pronounced in future highly insulated greenhouses[180].

Humidity control, nevertheless, is very important for achieving high quality crop yield. Without humidity control, high RH levels may lead to loss of crop quality due to fungal diseases, leaf necrosis, calcium deficiencies and soft and thin leaves[181]. Crop growth may decrease[182], anatomical changes may occur and plant development can be disturbed or delayed[183, 184]. High humidity conditions can further hamper pollination in fruit vegetables, as pollen grains tend to remain inside, or stick to the

anthers[77, 78] and vase life in ornamental plants may be shortened[85]. Too low RH conditions on the other hand (high VPD), can lead to plant water stress.

By using flexible humidity constraints, significant reductions in energy consumption could be realised[85]. To this end dynamic humidity ranges should be established for different underlying humidity-related crop processes. The constraints formulated in this way together determine the acceptable range. In this research, such a humidity regime is proposed. A first design with roughly estimated parameters was introduced to show the possibilities of such a regime. Processes were identified and constraints were formulated on the basis of literature for the case of cut chrysanthemum. Processes related to plant water stress, calcium deficiencies, crop growth and development and major airborne fungal diseases were distinguished. The regime was investigated in simulations with a greenhouse climate and control model[105]. The effect of the regime on energy consumption, greenhouse climate and crop photosynthesis with different temperature integration regimes was evaluated.

HUMIDITY REGIME

The regime is based on the response of crop processes that are affected by greenhouse atmospheric humidity (plant water stress, calcium deficiencies, crop growth, crop development and fungal diseases). These processes by their nature react to different aspects of atmospheric humidity, either to VPD, to absolute or to relative humidity. Fungal diseases probably react to a combination of relative humidity and leaf wetness. Leaf wetness (i.e. condensation) occurs when temperature drops below the dew point. This value depends on absolute humidity. Plant water stress and calcium deficiencies are related to transpiration whose climate determinants are VPD, radiation and CO_2 concentration (i.e. on stomatal conductance). Crop growth and development are probably also mainly affected by an indirect effect of VPD on transpiration.

CROP GROWTH AND DEVELOPMENT

Humidity affects growth of greenhouse crops mainly through its impact on leaf size and light interception rather than through a direct impact on photosynthesis by increased stomatal conductance at low VPD[185]. Leaf area can either increase or decrease under long-term high humidity exposure[185]. Increased leaf area was found in cucumber[186] or chrysanthemum[184] and leaf area decreased in tomato[80]. Due to that, tomato fruit yield also decreased when exposed to 28 days at 0.15 kPa VPD[80]. The smaller leaf area was associated with low calcium concentrations in the leaf laminae and calcium deficiency symptoms[80, 187]. Holder and Cockshull (1990)[80] concluded that the cost of reducing humidity to VPD greater than 0.3 kPa was likely to exceed any economic gain. However, crop growth in cut chrysanthemum is relatively

insensitive to a continuous atmospheric vapour pressure deficit (VPD$_{air}$) between 0.1 kPa and 1.2 kPa [184]. This was also supported by Mortensen (2000)[183], who did not find any significant dry weight increases with chrysanthemum long-term exposure to 0.155 kPa. But in chrysanthemum, plant development can be affected by low VPD conditions. Applying a continuous VPD$_{air}$ of 0.1 kPa or 0.155 kPa delayed flower development of cut chrysanthemum by 4 – 5 or 3 – 4 days[183, 184]. The delays, however, are cultivar dependent[184]. Although humidity conditions < 0.2 kPa VPD are likely to occur in chrysanthemum cultivation when short-day is induced with blackout screens or during winder at reduced ventilation[184], those investigations concerned continuous high humidity situations and that is much more extreme than would probably ever be encountered in commercial growing[184].

The underlying processes leading to delayed flower development in cut chrysanthemum exposed to low VPD are obscure[184]. Although the response of crop growth to humidity is probably based on more underlying processes as transpiration and calcium transport, an overall rule was applied combining growth and development as first general protection. Because plants are able to compensate unfavourable climate conditions, a mean VPD for control in greenhouse conditions was applied. A simple rule with a 24-hour VPD integral with upper and lower boundary was used for that. Since the literature review on effects of humidity on greenhouses crops[151] revealed that for most greenhouse crops, growth and development are unaffected between 0.3 and 1.0 kPa VPD, and only one of six tested cut chrysanthemum cultivars delayed flower development when continuously exposed to 1.1 kPa VPD[184], the two boundaries for the 24-hour VPD integral were chosen as 0.3 and 1.1 kPa to maintain crop growth and development at a high level.

PLANT WATER STRESS AND CALCIUM DEFICIENCIES

Increasing VPD enhances potential crop transpiration (λE) and xylem water flux and therefore import of calcium ions into leaves. A too high VPD in combination with high radiation leads to higher λE than the plants can handle[188]. With too high potential λE water loss may exceed water uptake. This discrepancy between water uptake through the roots and transpiration from the leaves may occur at VPD levels higher than 1 kPa[151]. Then, plant water potential may decrease below the acceptable range and plants may start wilting. Permanent leaf-damage may occur (especially in combination with high radiation). A transpiration integral with upper and lower boundary to adequately deal with this problem was suggested[189]. Transpiration related disorders, could then be controlled by integrating λE. Plants integrate long high humidity periods without negative consequences, whereas plant water stress can occur in minutes or hours.

A minimum and maximum transpiration mean was set to control plant water stress and calcium deficiencies. A lower boundary on 24-hour transpiration mean was

defined to prevent calcium deficiencies. To prevent plant water stress, an upper threshold on the 1-hour mean transpiration was applied. To set boundaries, two λE extremes were calculated with climate conditions that may occur when *TI* is applied with large temperature bandwidths as presented in CHAPTER 3.1. Equations derived by Stanghellini (1987)[92] were used for that. The upper boundary was established for a situation with 30 °C, 65 % RH and high irradiation radiation, the lower boundary for 14 °C, 93 % RH and low irradiation. This corresponded to 12 and 300 J m^{-2} s^{-1} λE at LAI of 3, respectively. When λE exceeded the lower threshold, transpiration had to reach the threshold within one hour. When λE exceeded the upper threshold, this had to occur within five minutes. Forecasted transpiration was checked for that. If the requirement could not be met, a transpiration set point was chosen such that satisfied the integral requirement.

FUNGAL DISEASES

In commercial chrysanthemum production in greenhouses grey mould (*Botrytis cinerea*), powdery mildew (*Erysiphe cichoracearum*) and chrysanthemum white rust (*Puccinia horiana*) are the major air-borne plant pathogenic fungi. For control of fungi, relative humidity and leaf wetness duration (LWD), the time integral of leaf wetness are most important[190].

Chrysanthemum white rust: Chrysanthemum white rust (*Puccinia horiana*) causes pale areas on the upper leaf surface, with powdery orange pustules or spots directly beneath on the undersides of the leaves. Severely infected plants are much weakened and fail to bloom properly. High humidity over 90 % and a film of moisture appear to be necessary for germination of both teliospores and basidiospores[191]. However, no new infection occurs at LWD less than 5 hours[192] and at least 2 – 3 hours LWD is necessary for penetration of existing infections[191]. Basidiospores, nevertheless, are very sensitive to desiccation[193] and the survival of spores is both time and dose dependent[194]. *P. horiana* spores survive for 5 minutes at 80 % RH and for one hour at 90 % RH[194]. Assuming a greenhouse temperature of 20 °C, this corresponds to 0.48 and 0.25 kPa VPD as a more direct measure of desiccation. These values were used for control in this regime. LWD was restricted to three hours followed by a VPD dependent desiccation time (as dose-response) using an arbitrary exponential function fitting the two mentioned control values[194].

Grey mould: Grey mould is caused by *Botrytis cinerea*. It attacks ornamentals as chrysanthemum[195], roses and gerbera[79] as well as vegetables as tomato[196]. In Dutch greenhouse environment, conidia of *B. cinerea* are always present[79]. The fungus sporulates on infected tissues under high RH conditions. Usually *B. cinerea* does not

invade healthy green tissue such as leaves and stems unless an injured or dead area is present. However, lower leaves in the canopy are often attacked and then the fungus can spread. The spores contain little water and need to absorb it from the environment[197] and due to that condensation provokes spore germination[197, 198]. It is, however, difficult to predict at what RH level spores germinate and infect plants[197]. Free moisture is probably necessary for fast germination and infection, and a minimum LWD may provoke growth and development. As with chrysanthemum white rust, spores are sensitive to desiccation and die after longer periods of low RH[197]. After short periods (about 2 hours) spores continue germinating when humidity gets very high again[197]. However, relative humidity > 93 % is at least necessary for spore development and infection can occur with RH higher than 95 % [199]. To control *B. cinerea* in chrysanthemum, first a long-term relative humidity boundary of 93 % must be respected[85, 174] and secondly LWD must stay below a certain limit. The same LWD threshold as for chrysanthemum white rust was used. In addition, a long-term integral of RH was applied. RH was not allowed to be higher than 93 % for maximum of 48 successive hours. When this happened, RH was set to 85 % until 4 hours (arbitrarily) below 93 % RH were achieved.

Powdery mildew: Chrysanthemum powdery mildew is caused by *Erysiphe cichoracearum* with its anamorph *Oidium chrysanthemi* DC. Conidia of the family *Erysiphales* consist of   50 % – 70 % of water and can germinate and infect without dew and condensation is not required for growth[200]. Once infection occurs it develops rapidly under dry conditions[201]. However, water sprays or rain reduces powdery mildew in roses[202] and squash[203]. In fact, dew after sporulation may kill spores due to lack of oxygen, but spores may become more resistant when LWD is too short[204]. Different species of powdery mildew differ widely in their ability to germinate in water[205] and survival greatly depends on intensity of conidia adhesion to the plant tissue[206]. However, to include this as a first approximation into control, a minimum LWD of one hour was applied in each 24-hour cycle to kill possible *Oidium chrysanthemi* spores.

MATERIALS AND METHODS

DETERMINATION OF RH SET POINT

The processes affected by humidity control (calcium deficiencies, plant water stress, crop growth and development, chrysanthemum white rust, powdery mildew and grey mould) all require a separate, process related RH window. A 24-hour course of greenhouse temperature was calculated once a day (0:00 h) with a simple greenhouse model as reported in CHAPTER 3.1 and weather forecast according to the
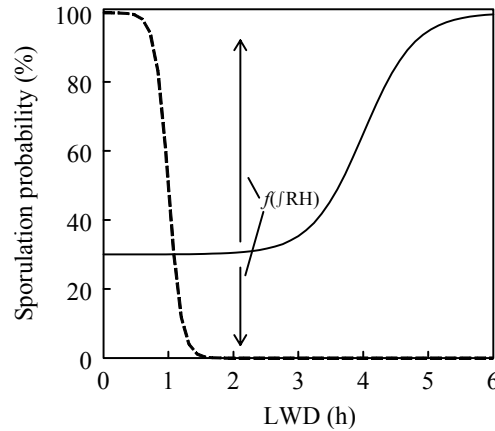
FIGURE 1. Theoretical example of the relationship between leaf wetness duration (LWD) and sporulation probability for powdery mildew (*Oidium chrysanthemi*) (---) and chrysanthemum white rust (*Puccinia horiana*) or grey mould (*Botrytis cinerea*) (—). Applied models were arbitrarily chosen respecting only the boundaries. Powdery mildew: $100/(1 + \exp((t - P_{50})/x))$, t is time in hours, P_{50} is time of reduction to 50 % sporulation probability and x is a form parameter. Chrysanthemum white rust and grey mould: $P_{RH} + (100 - P_{RH})/(1 + \exp(-(t - P_{50,LWD})/x))$, P_{RH} is the threshold probability that is determined by the relative humidity integral ($\int RH$) and $P_{50,LWD}$ is the time reduction to 50 % of the LWD influence.

lazy-man weather prediction[165]. Future and recorded climate data were used for control. Humidity in greenhouses is commonly controlled by set points for RH or vapour pressure deficit. From that decisions on ventilation or heating or a combination of these two measures are made by the climate computer. In the present approach, set points for RH were created and used as input for a climate computer. Set points were clustered into lower and upper RH thresholds (RH_{set}^{-} and RH_{set}^{+}, respectively). Lower thresholds deal with humidity related problematic processes that are susceptible to low humidity conditions such as powdery mildew (*PM*), plant water stress (*PWS*), and the maximum level for growth and development (*GD*$_{max}$). Upper thresholds deal with humidity related problematic processes that are susceptible to high humidity conditions such as chrysanthemum white rust (*WR*), Calcium deficiencies (*Ca*), grey mould (*GM*) and minimum level for growth and development (*GD*$_{min}$). Powdery mildew and plant water stress can occur at relatively low humidity conditions and chrysanthemum white rust, grey mould and calcium deficiencies can occur at high RH conditions. Developmental delay and growth reductions can occur under both circumstances. Conflicts between humidity requirements of different processes may occur. Sporulation probability for powdery mildew, for instance, is reduced by setting a minimum LWD and for chrysanthemum white rust (and grey mould) by setting a maximum LWD (FIG. 1). In addition, also spore survival requirements are conflicting, and depend on desiccation time of these two fungi (FIG. 2). Solving these problems would lead to conflicting climate set points. To cope

115
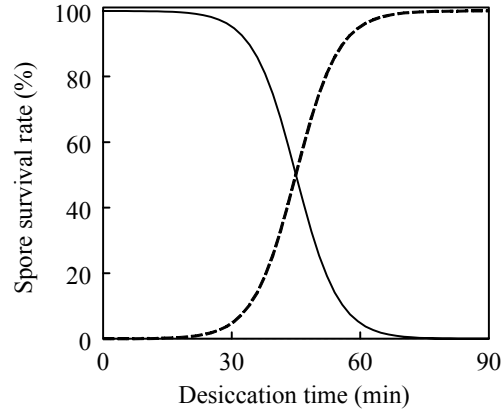
FIGURE 2. Theoretical example of spore survival rate as function of desiccation time for chrysanthemum white rust (*Puccinia horiana*) (—) and powdery mildew (*Oidium chrysanthemi*) (---). Applied models are for constant VPD conditions of the form $100/(1+\exp(-(t-L_{50})/x))$ and $100/(1+\exp((t-L_{50})/x))$ for chrysanthemum white rust and powdery mildew, respectively; t is time in minutes, L_{50} is time of 50 % survival rate and x is a form parameter. Parameters were chosen arbitrarily but respecting the boundaries.

with that conflict, priorities were given to different processes. To implement control of humidity including the rules for all processes, the two clusters of rules were distinguished. RH_{set}^{+} is dealing with maximum relative humidity constraints and RH_{set}^{-} with minimum constraints. For priority assignment, an approach according to response times was used[207]. Plant water stress has the fastest response time as it is controlled with a 1-hour integral and is to be compensated within 5 minutes. This is controlled first. Then, because high humidity conditions and a relatively short minimum leaf condensation (i.e. short response time) are necessary to control powdery mildew, this process was controlled second and maximum VPD integral for growth and development was third. Active dehumidification follows only after control measures for plant water stress, powdery mildew and maximum VPD for growth and development have been taken. Constraints for those processes have equal priority.

Constraints for each cluster were determined first (EQ. 1), where lower constraints had priority over upper constraints (EQ. 2). Default values for RH_{set}^{-} and RH_{set}^{+} were respectively 70 % and 99 %. With these rules, RH was set to 99 % until a complete LWD of one hour was achieved for powdery mildew control in each 24-hour cycle. The upper threshold for growth and development had second order priority as this was controlled after plant water stress and powdery mildew. Processes of RH_{set}^{+} had third order priority, because all processes of RH_{set}^{-} were controlled first. Therefore, e.g. desiccation-time for chrysanthemum white rust was immediately applied after control for RH_{set}^{-} was terminated. An overview of the different processes and their constraints is illustrated in TABLE 1.

$$RH_{set}{}^- = \max\left(RH_{set,PM}, RH_{set,LWS}, RH_{set,GD\,\max}\right)$$
$$RH_{set}{}^+ = \min\left(RH_{set,WR}, RH_{set,GM}, RH_{set,Ca}, RH_{set,GD\,\min}\right)$$

[1]

$$RH_{set} = \max\left(RH_{set}{}^+, RH_{set}{}^-\right)$$

[2]

<div align="center">CALCULATION OF MICROCLIMATE</div>

In a fixed time sequence, static values of different microclimate parameters were calculated from greenhouse climate data. To this end, crop transpiration (i.e. latent heat of evaporation, λE), crop temperature (T_c), dew point temperature of the greenhouse air (T_{dp}) and LWD were the most important factors. Within a greenhouse, λE normally is the major process contributing to accumulation of water vapour in the greenhouse atmosphere. λE increases with LAI, T_c, VPD (Pa), and net short wave radiation[189].

λE (W m^{-2}) of a canopy was obtained by a simplified approximation of the Penman-Monteith equation[208] for a greenhouse tomato crop[92].

$$\lambda E \sim \frac{12 \cdot \text{LAI}}{3 + r_{i_{H_2O}}/r_{b_{H_2O}}}\left(\frac{I_c}{40} + \frac{T_h - T_{air}}{3} + \frac{\text{VPD}}{\gamma}\right)$$

[3]

EQ. 3 contains internal and external resistance to H$_2$O ($r_{i_{H_2O}}$, $r_{b_{H_2O}}$, s m^{-1}), short-wave radiation on the top of the canopy (I_c, W m^{-2}), temperature of surfaces and greenhouse air (T_h and T_{air}, K) and the psychrometric constant (γ, Pa K^{-1}). The symbol $\sim$ denotes to a rough approximation of this relationship. The internal resistance (stomatal) was calculated as function of temperature, CO$_2$ concentration (μmol mol^{-1}) and RH; and the boundary layer resistance (external) was assumed constant and calculated from the specific heat capacity of the air, the density of the air and the convective heat transfer coefficient between greenhouse air and canopy (Stanghellini, 1987)[92]. T_c was calculated as proposed by Stanghellini (1987)[92] for a tomato crop, based on the energy balance separated for day and night. The night equation was used whenever I_c was lower than 10 W m^{-2}.

$$T_c - T_{air} \sim \begin{cases} 0.006 \cdot I_c + 0.08 \cdot \left(T_h - T_{air}\right) - 0.25 \cdot \dfrac{\text{VPD}_{air}}{\gamma} & if \quad I_c \geq 10 \quad \text{W} \quad \text{m}^{-2} \\[3mm] 0.16 \cdot \left(T_h - T_{air}\right) - 0.1 \cdot \dfrac{\text{VPD}_{air}}{\gamma} & if \quad I_c < 10 \quad \text{W} \quad \text{m}^{-2} \end{cases}$$

[4]

Equations that were used to calculate λE and T_c were originally designed for a dense stand of a tomato crop and were only a rough approximation to the sample crop

TABLE 1. Humidity related crop processes in cut chrysanthemum process based humidity control, their controlling factors (vapour pressure deficit, VPD; relative humidity, RH; leaf wetness duration, LWD and latent heat of evaporation λE), control criteria and applied priority for set point determination.

Process	Control factors and criteria				Priority
	VPD (kPa)	RH (%)	LWD (h day^{-1})	λE (J m^{-2} s^{-1})	
Growth	$\int 24h \geq 0.3$ $\int 24h \leq 1.1$	-	-	-	3/4
Development	$\int 24h \geq 0.3$ $\int 24h \leq 1.1$	-	-	-	3/4
Water Stress	-	-	-	$\int 1h \leq 300$	1
Ca deficiencies	-	-	-	$\int 24h \geq 12$	4
White rust	desiccation	-	≤ 3	-	4
Grey mould	-	$\int 48h \leq 93$	≤ 3	-	4
Powdery mildew	-	-	≥ 1	-	2

cut chrysanthemum as used here. However, since T_c may vary with the position of leaves within the canopy three leaf layers of equal partial LAI were distinguished to represent this heterogeneity in the chrysanthemum crop. To estimate T_c and leaf condensation in different layers of the crop, the *Beer-Lambert Law* was applied[209]. It was assumed that only I_c changed with LAI while VPD$_{air}$, T_h and T_{air} were the same at all locations in the crop.

T_{dp} (°C) was calculated by a function containing RH (%), saturated vapour pressure of the crop ($VP_{sat,c}$, Pa) and constants in similarity to Zolnier *et al.* (2000)[210].

$$T_{dp} = 237.3 \cdot \log_{10}\left(\frac{VP_{sat,c} \cdot \text{RH}/100}{610.78}\right)\bigg/\left(7.5 - \log_{10}\left(\frac{VP_{sat,c} \cdot \text{RH}/100}{610.78}\right)\right) \qquad [5]$$

It was assumed that condensation occurred when the difference between crop- and dew point temperature was smaller than 1.5 K[211, 212].

Because the distinction between a completely wet and a completely dry leaf layer was important with this regime (i.e. relationship between LWD and desiccation time for powdery mildew and white rust control) a state variable, leaf wetness (LW) was introduced that could assume only three states (wet, intermediate and dry).

$$\text{LW} = \begin{cases} -1 & if \quad T_c - T_{dp} \geq 2 \\ 0 & if \quad 1.5 < T_c - T_{dp} < 2 \\ +1 & if \quad T_c - T_{dp} < 1.5 \end{cases} \qquad [6]$$

Leaf wetness was set according to that and integrated over time to LWD for three levels in the crop separately. If one layer exceeded a specific threshold, RH set point for this process decreased. The strength of decrease depended on the number of wet leaf layers. For e.g. *Botrytis cinerea*, RH set point was calculated from setting $T_c - T_{bp}$ to 0.75, 1.5 and 2.25 for one, two and three wet layers, respectively. The highest RH that satisfied this value was calculated and used as partial set point.

TECHNICAL IMPLEMENTATION

The humidity control regime was implemented in the software environment MATLAB® (version 6.0, MathWorks, Natick, MA, USA) and used in simulations with a greenhouse climate and control model[105] with cut chrysanthemum as test crop. A one year reference climate data set for De Bilt[177] (The Netherlands, lat. 52 °N) was used for simulations on greenhouse climate, energy consumption and crop growth for a whole growing season. The model consisted of a typical 1-ha Venlo-type greenhouse with a single glass cover (transmission for diffuse radiation of 78.5 %) with blackout screen. A set point controller was implemented that used the set points calculated by the MATLAB® programme in five minute intervals. Greenhouse air temperature, RH and CO_2 – concentration inside the greenhouse and outside global radiation were input to the model. RH set points were calculated by the humidity control regime and sent together with set points for temperature control as input for simulation to the greenhouse climate model. The control system in the greenhouse model used the set points and the model returned simulated realised greenhouse climate (RH, temperature and CO_2 concentration). CO_2 set point was 1000 µmol mol^{-1} when vents were closed and 350 µmol mol^{-1} when vents were open or when the outside global radiation was below the threshold of 40 W m^{-2}. Crop gross photosynthesis was calculated based on leaf photosynthesis and radiation distribution within the canopy[96]. Leaf photosynthesis was described by the two parameter (maximum gross photosynthesis and photochemical efficiency), negative exponential light-response curve[94] and applied as reported in CHAPTER 2.1 [175].

SIMULATIONS

Cultivation of cut chrysanthemum was simulated with set points according to common practice in the Netherlands (blueprint) and with flexible humidity and temperature regimes (TABLE 2). Targeted mean temperature over the six-day averaging period was set to 19 °C. The blueprint consisted of initial set points of 18.5 °C and 19.5 °C for heating and ventilation, respectively, and influences through global radiation. Daytime ventilation set points increased linearly with outside global radiation level (0.5 K per 100 W m^{-2} between 800 and 1200 W m^{-2}) and

TABLE 2. Performed simulations with cut chrysanthemum in a 1-ha greenhouse; simulations were performed for each climate regime, year round (planting date 01 January) and five separate cultivations with different planting dates (01 February, 01 March, 01 April, 01 May, 01 June).

RH (%)	Temperature control			
	Regular	TI with temperature bandwidth (°C)		
		±2	±4	±6
70	BP_{70}	$TI_{\pm2,70}$	$TI_{\pm4,70}$	$TI_{\pm6,70}$
80	BP_{80}	$TI_{\pm2,80}$	$TI_{\pm4,80}$	$TI_{\pm6,80}$
90	BP_{90}	$TI_{\pm2,90}$	$TI_{\pm4,90}$	$TI_{\pm6,90}$
99	BP_{99}	$TI_{\pm2,99}$	$TI_{\pm4,99}$	$TI_{\pm6,99}$
Flexible	BP_{flex}	$TI_{\pm2,flex}$	$TI_{\pm4,flex}$	$TI_{\pm6,flex}$

TABLE 3. Percent energy saving for year-round cut chrysanthemum with different temperature regimes combined with the process based humidity control compared to the same temperature regimes with fixed relative humidity set points of 70, 80, 90 and 99 %; with regular temperature control (Regular) and temperature integration with 6-day averaging period and different temperature bandwidths of ±2 °C, ±4 °C and ±6 °C ($TI_{\pm2}$, $TI_{\pm4}$, $TI_{\pm6}$).

RH set point (%)	Temperature control			
	Regular	$TI_{\pm2}$	$TI_{\pm4}$	$TI_{\pm6}$
70	31.6	31.9	29.7	27.8
80	18.2	18.8	17.4	16.0
90	1.9	3.7	1.5	-0.6
99	-0.9	-0.1	−2.2	−4.9

TABLE 4. Crop gross photosynthesis for year-round cut chrysanthemum with different temperature regimes with different RH set points compared to the same temperature regimes with a fixed RH set point of 80 %; with temperature integration with ±2 °C, ±4 °C, ±6 °C temperature bandwidth ($TI_{\pm2}$, $TI_{\pm4}$, $TI_{\pm6}$) and normal temperature regime (Regular).

RH set point (%)	Temperature control			
	Regular	$TI_{\pm2}$	$TI_{\pm4}$	$TI_{\pm6}$
70	-0.3	-0.3	-0.3	-0.04
80	-	-	-	-
90	1.3	1.5	1.7	2.6
99	2.0	2.1	2.9	4.0
Flexible	1.8	1.9	2.3	3.3

nighttime heating and ventilation set points increased linearly with daily global radiation sum (0.25 K per 1 MJ m^{-2} d^{-1} between 12 and 16 MJ m^{-2} d^{-1}). Temperature integration was applied over a six-day averaging period according to the procedure for *regular temperature integration* as described in CHAPTER 3.1. Two types of

TABLE 5. Simulations on cumulative energy consumption (MJ m^{-2}) for a 12-week cut chrysanthemum cultivation with different planting dates for a regular temperature regime (Regular) and temperature integration with 6-day averaging period and ±4 °C temperature bandwidth ($TI_{\pm4}$) with fixed (80 %) and process based humidity regime.

| Planting date | Climate regime | | | |
| | Regular | | $TI_{\pm4}$ | |
	RH fixed (80 %)	RH process-based	RH fixed (80 %)	RH process-based
01 February	416	332	387	307
01 March	267	205	222	161
01 April	148	113	110	83
01 May	79	66	64	60
01 June	58	55	59	59

simulations were performed on crop growth, greenhouse climate and energy consumption. First, a year round cultivation starting 01 January was simulated.

Short-day was induced with blackout screens. For this, 25 % of the greenhouse area was assumed under long-day and 75 % under short-day (day-time 6:00 a.m. – 0:00 and 8:00 a.m. – 7:00 p.m., respectively). During long-day, an energy saving screen (SLS 10 plus, Ludvig Svensson, Kinna, Sweden) was applied between 7 p.m. and 8 a.m. when sunset was earlier than 7 p.m. or between sunset and 8 a.m. when sunset was later than that. In addition to that, twelve separate cultivations were simulated with monthly plantings. For simplification, the cultivation period was 12 weeks independent of the season. Long-day was maintained during the first three weeks and short-days between week 4 and 12 after planting. Simulations were performed for a regular temperature regime and for *TI* with different temperature bandwidths with fixed 70 %, 80 %, 90 % and 99 % relative humidity set points.

RESULTS

ENERGY SAVING AND CROP GROSS PHOTOSYNTHESIS

Yearly energy consumption was strongly reduced with increasing RH set points up to 99 % for all temperature integration regimes. Increasing temperature bandwidths decreased energy consumption. With set points in the range 90 % and 99 % RH the effect of RH on energy consumption was small compared to RH < 90 % (FIG. 3).

Applying process based humidity control reduced energy consumption compared to a humidity regime with fixed RH set points of about 90 % (TABLE 3). Applying *TI*, energy saving with the process based humidity regime compared to the same regime
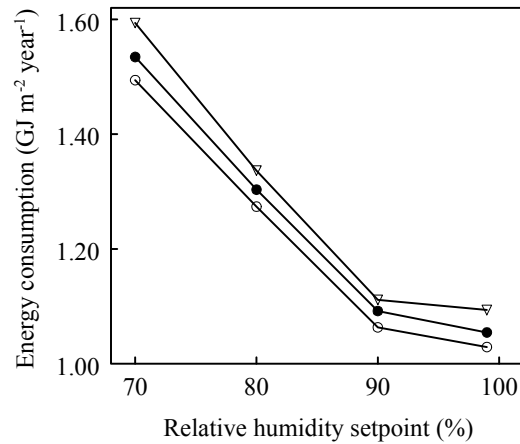
FIGURE 3. Energy consumption as function of fixed relative humidity set point for simulations with the blueprint regime (∇) and six-day temperature integration with a bandwidth of ± 4 °C ($\bigcirc$) and ± 6 °C ($\bullet$).

with a fixed humidity set point of 80 % RH decreased with increasing temperature bandwidths. However, combining the process based humidity regime with *TI* yields in increasing energy saving with increasing bandwidth compared to a blueprint regime (data not presented). Yearly crop gross photosynthesis with process based humidity control increased compared to a fixed RH set point of 80 % as commonly used in practice between 1.8 % and 3.3 % depending on temperature control (TABLE 4).

In year round cut chrysanthemum cultivation most energy was saved with the process bases humidity regime during the first weeks of cultivation in winter (FIG. 4). In summer, energy consumption did not significantly differ between a fixed RH set point of 80 % and a flexible RH control. The same was observed with simulations of separate 12-week cultivations with *TI* (TABLE 5). In summer plantings (May and June), the new humidity regime had no or marginal consequences on *TI*. This was less pronounced with the blueprint temperature control. The highest absolute savings on energy consumption were obtained in winter but in spring relative savings were highest, e.g. 27 % for *TI* with planting in March. Applying the process based humidity regime with regular temperature control resulted in yearly energy saving of 18 % compared to a fixed RH set point of 80 % and only a little difference to a set point of 90 % RH (TABLE 3, FIG. 4). Combining the process based humidity regime with a 6-day *TI* regime (with e.g. temperature bandwidth of ± 4 °C) increased energy saving compared to regular temperature control with 80 % RH set point up to 40 % during one 12-week cultivation period in spring (TABLE 5).
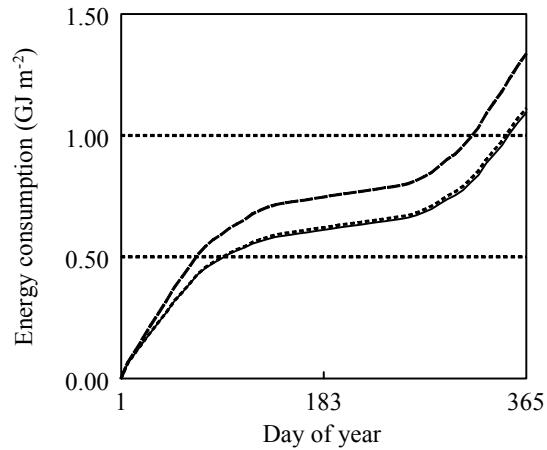
FIGURE 4. Yearly cumulative energy consumption (GJ m^{-2}) for a year round cultivation of cut chrysanthemum in a common 1 ha greenhouse with regular temperature control with fixed relative humidity set point of 80 % (– – –, upper line), 90 % (---, middle line) and process based humidity regime (—, lower line).
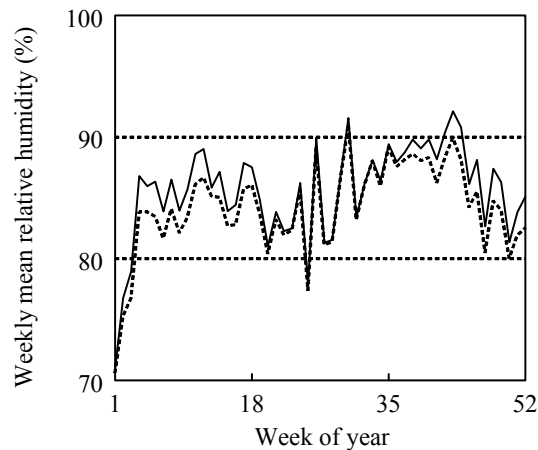
FIGURE 5. Weekly mean relative humidity for simulations of greenhouse climate for year round cut chrysanthemum cultivation with normal temperature control with fixed relative humidity set point of 80 % (—) and process based humidity regime (---).

GENERAL BEHAVIOUR OF THE GREENHOUSE CLIMATE

In winter, average relative humidity with a year round chrysanthemum crop was slightly higher in the process based humidity control regime compared to a regime with a fixed set point of 80 % RH for all investigated temperature controls (FIG. 5). In summer, weekly mean relative humidity did not differ for any temperature control. Instantaneous relative humidity in winter, nevertheless, fluctuated much more and

123

TABLE 6. Monthly average percent daytime (short-day) lee vent-opening (V) and average daytime greenhouse CO_2 concentration ($[CO_2]$) for regular temperature control and temperature integration with 6-day averaging period and temperature bandwidths of ±4 °C with fixed relative humidity set point of 80 % and process based humidity control for year round cultivation.

	Climate regime							
	Normal				$TI_{\pm4}$			
	RH fixed (80 %)		RH process-based		RH fixed (80 %)		RH process-based	
Month	V	$[CO_2]$	V	$[CO_2]$	V	$[CO_2]$	V	$[CO_2]$
	(%)	ppm	(%)	ppm	(%)	ppm	(%)	ppm
1	4.3	524	0.2	799	2.6	530	0.1	753
2	7.1	485	2.8	740	5.7	471	0.5	743
3	19.3	483	15.0	680	11.1	470	5.9	773
4	29.2	442	24.6	571	31.3	431	26.7	590
5	42.4	421	39.3	465	40.4	397	37.6	467
6	51.8	416	49.4	434	70.4	379	69.8	382
7	56.0	418	53.6	434	65.1	379	64.9	381
8	60.7	423	59.7	434	71.9	383	71.5	386
9	40.3	435	34.3	497	53.1	404	52.0	436
10	22.8	463	16.3	602	21.6	435	17.3	621
11	8.8	489	2.5	725	9.5	471	5.1	742
12	5.5	557	0.2	849	5.8	551	0.2	852

was often very high (i.e. condensation) with the process based humidity regime (FIG. 6 and FIG. 7). Ventilation was reduced and average CO_2 concentration was higher for the process based humidity regime for normal temperature control and *TI* (TABLE 6).

DISCUSSION

With the new humidity regime simulated energy consumption decreased strongly. Simulated energy consumption was in the same order of magnitude as in commercial practice in The Netherlands. Simulated yearly energy consumption for a normal temperature regime with a fixed RH set point of 80% was 1.34 GJ m^{-2} year^{-1} and reported values from practice were 1.41 and 1.55 GJ m^{-2} year^{-1} [174, 175]. The small discrepancy supports the validity of the greenhouse simulation model for comparing energy consumption. The new regime gave rise to a strong reduction in energy consumption compared to a regular humidity regime, in particular during winter. During this season, temperature control has little effect on ventilation because low outside global radiation and temperature do not heat up greenhouses above the temperature ventilation set point. Therefore, humidity control is basically the only

FIGURE 6. Instantaneous relative humidity values (i.e. 5-minute averages) for day 40 – 41 after planting for normal temperature regime with fixed 80 % relative humidity set point (——) and process based humidity control (- - -) for 4 separate 12-week cultivations of cut chrysanthemum with different planting dates 01 January, (a), 01 March (b), 01 May (c) and 01 July (d).

cause for ventilation. When humidity levels are above the set point, opening of ventilators lead to extra energy consumption for maintaining temperature. Reduced ventilation was therefore the major cause of energy saving in winter. Temperature- and humidity controls interact in ventilation towards the summer. When outside global radiation and temperature increase, greenhouse temperature control gets stronger impact on the rate of ventilation and the role of humidity control diminishes. *TI* in summer contributes only little to yearly energy saving, because greenhouses heat up during daytime but do not cool down at night. A low night temperature, nevertheless, is indispensable to compensate for the high day temperatures. Because cut chrysanthemum is partly cultivated under darkening screens temperature will not drop much during the night. With *TI*, there is more night ventilation than in normal temperature control, because elevated day temperatures have to be compensated during the night. Therefore, process based humidity control had an impact on energy saving during summer when temperature was controlled normally and not when it was controlled by *TI*.The described humidity regime is a first approach to control greenhouse humidity according to their underlying processes concerning crop requirements. Parameter values were chosen from empirical results or arbitrarily in many cases (e.g. transpiration set points) and were not validated. Results rather indicate the value of such a regime for future climate control rather than being quantitatively correct. The system was not controlled optimally and before strong conclusions on the value of the new regime could be made, greenhouse experiments are necessary. First experimental results for complete cultivations with cut chrysanthemum in spring and autumn controlled by the process based humidity
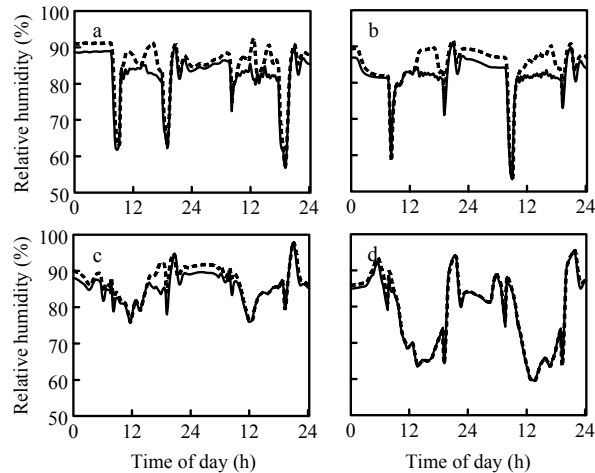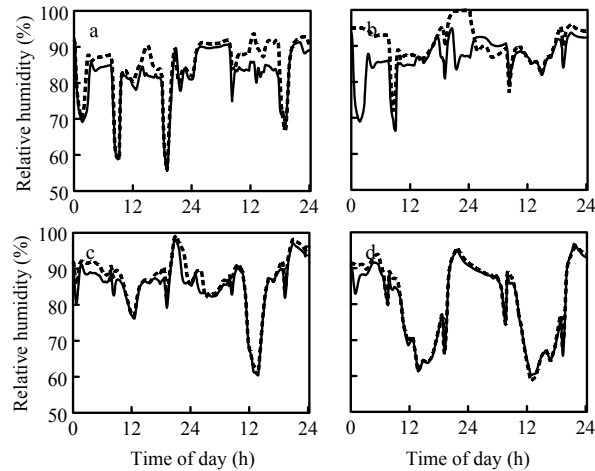
FIGURE 7. Instantaneous relative humidity values (i.e. 5-minute averages) for day 40 – 41 after planting for temperature integration with 6-day averaging period and temperature bandwidths of ± 6 °C with fixed 80 % relative humidity set point (—) and process based humidity control (---) for 4 separate 12-week cultivations of cut chrysanthemum with different planting dates 01 January, (a), 01 March (b), 01 May (c) and 01 July (d).

regime combined with temperature integration with different bandwidths (CHAPTER 3.1) did not show any negative consequences on plant growth, development or quality. There is little doubt that the approach of controlling greenhouse humidity according to the response of individual processes that are affected by humidity is promising in terms of energy saving.

ACKNOWLEDGEMENTS

3.3 TEMPERATURE INTEGRATION AND PROCESS BASED HUMIDITY CONTROL IN CUT CHRYSANTHEMUM

O. KÖRNER & H. CHALLA
Evaluation of an energy saving climate regime for cut chrysanthemum
(submitted)

ABSTRACT

Due to international agreements, energy efficiency in Dutch greenhouse horticulture has to be increased from 1980 until 2000 or 2010 by 50 % or 65 %, respectively. Besides alternative greenhouse techniques energy saving climates are a valuable tool to reach that target. Simulations have shown that a modified temperature integration regime with a six-day averaging period and increased set point flexibility was able to reduce annual energy consumption compared to a regular temperature integration regime by up to 9 %. The commonly applied fixed set point for relative humidity of 80 % – 85 % strongly reduced the potential for energy saving with this regime. Therefore, a more flexible humidity control regime was developed. Simulations have also shown that yearly energy consumption could be reduced by 18 % compared to a fixed set point of 80 % relative humidity. When joining the two regimes (temperature integration and humidity control) more energy saving was predicted. Quantification of energy saving, however, was only based on simulations and plant responses were

only discussed theoretically. Therefore, the joint regime was applied in two experiments with cut chrysanthemum investigating the effect on plant development and growth. Different temperature bandwidths for temperature integration (±2 °C, ±4 °C, ±6 °C and ±8 °C) were compared with the joint regime. Crop development was only delayed with ±8 °C temperature bandwidth. The best regime with respect to plant development, growth, quality and energy saving (±6 °C temperature bandwidth) was compared in a spring experiment with a climate regime used in commercial practice. Energy consumption was 23.5 % lower with the joint regime than with the regular regime. No negative consequences of high humidity were observed, but a strong increase in dry weight of all plant organs. Total plant dry weight was 39 % higher than in the regular regime.

INTRODUCTION

In The Netherlands agreements were made to increase energy efficiency in greenhouse horticulture from 1980 until 2000 or 2010 by 50 % or 65 %, respectively[213]. The target for the year 2000, however, was missed by 6 % [10]. Therefore more energy must be saved in the future. Modern greenhouse technique and equipment such as climate computers, energy screens and condensers with heat storage facilities already contributed with 3.7 % energy saving between 1991 and 2000 [10]. Future technical innovation will probably be able to further increase energy saving. When all greenhouses from 1995 would be replaced in 2010, 14.6 % energy could be saved in comparison to 1995 [28]. This alone, however, would not be enough to reach the target for energy saving and efficiency. Instead of applying the more expensive technical solution intelligent energy efficient control regimes should be applied in combination with modern greenhouse design.

Temperature integration (*TI*) could be used. *TI* in its simplest form controls the 24-h average temperature rather than fixed set points for heating and ventilation[39, 41, 167, 214]. Because many greenhouse crops are able to integrate longer periods than 24-hours more energy could be saved. The averaging period was extended to longer period of several days[52, 57]. *TI* in this form, however, could be optimised further (CHAPTER 3.1), because fast (minutes) and slowly responding (days) plant processes are not considered. Controlling greenhouse climate with independent short and long-term processes was suggested[133, 207]. Processes with a slow response time (e.g. plant development) respond primarily to average temperatures over prolonged periods and processes with a quick response (e.g. photosynthesis) may allow more extreme temperatures without losses in quality and growth[169, 170]. *TI* has therefore been refined to a nested short and long-term integration interval system in CHAPTER 3.1. A decrease in yearly energy consumption of up to 9 % compared to regular *TI* was predicted with tomato.

The potential for energy saving with *TI* is limited by humidity control when as usual fixed set points are maintained, because it counteracts *TI*. Vents open at lower temperatures and heating is switched on at higher temperatures than required for optimal effects of *TI*. A humidity regime with flexible set points for cut chrysanthemum with e.g. maximum leaf wetness duration, minimum transpiration and a transpiration integral[151, 207] has been designed (CHAPTER 3.2). Simulations showed that with this humidity regime, yearly energy consumption could be reduced by 18 % (compared to a fixed setpoint of 80 % relative humidity).

When these two climate control principles modified *TI* and the process based humidity regime were merged, energy reduction increased further[215]. For separate 12-week cut chrysanthemum cultivations with plantings 01 January, 01 February or 01 March, simulations indicated respectively 12 %, 30 % or 40 % energy saving. In these simulations, no optimal heating / screen combination[55] was applied.

Energy consumption was obtained from simulation studies that needed confirmation in greenhouse experiments where also plant responses could be taken into account. The aim of the present research was therefore to verify the simulations and evaluate crop responses with the joint climate regime in greenhouse experiments to show the practical value of these regimes. In two experiments with cut chrysanthemum (spring and autumn) different temperature bandwidths (±2 °C, ±4 °C, ±6 °C and ±8 °C) with the modified *TI* were compared using the joint regime and a regime with common rigid set points.

MATERIALS AND METHODS

PLANTS AND CLIMATE CONDITIONS

Two experiments (EXPT. 1 and EXPT. 2) were performed in four almost identical greenhouse compartments (12.8 m x 12.0 m) within a multi-span Venlo-type greenhouse at Wageningen University, The Netherlands (lat. 52 °N). The four compartments (A, B, C and D) were adjacent to each other in an ascending row from west (A) to east (D). Greenhouse compartments A, B and C consisted of one outside wall (south) and greenhouse compartment D of two outside (east and south) and two inside walls. The east wall of compartment D was whitened for EXPT. 2 and had a normal light transmittance in EXPT. 1.

Ca. 24,000 block-rooted cut chrysanthemum plants 'Reagan Improved' obtained from a commercial propagator (Fides Goldstock Breeding, Maasland, The Netherlands) were transplanted on 24.08.2001 (EXPT. 1) and 06.02.2002 (EXPT. 2) at a density of 64 plants m^{-2}. In each greenhouse compartment there were eight parallel soil beds (each 1.13 x 10.25 m). Compartments were heated with upper and lower heating

circuits as common in Dutch commercial practice for cut chrysanthemum[216]. The lower heating circuit was located on the grid that was lifted when appropriate for plant growth. To prevent plant damage maximum pipe temperature of the lower circuit was set to 38 °C. The upper circuit (located on the side walls and overhead below the screen) was the main heating system with a max. temperature of 80 °C. Air samples were continuously taken from above the crop canopy for measuring CO_2 concentration with an infrared-gas analyser (Advance Optima Uras 14, ABB, Hartmann & Braun, Frankfurt, Germany). Pure CO_2 was supplied when concentration was below the set point. Air temperature and relative humidity (RH) were measured just above the crop canopy (10 – 20 cm) with dry and wet bulb PT–500 thermometers. Every five minutes data were automatically recorded by a commercial climate control system (VitaCo, Hoogendoorn, Vlaardingen, The Netherlands).

RH was controlled by heating and ventilation in EXPT. 1 and by ventilation only in EXPT. 2. Heating of the lower circuit was used in the first two hours after screen-folding in the morning when RH exceeded the set point (EXPT. 1). Lee-side vents opened proportional to the difference between measured RH and set point to a maximum of 10 % (EXPT. 1 and EXPT. 2).

Four tensiometers were distributed in each compartment. Water was supplied according to demand. A sprinkler system located under the screens was used until flowers started to open colour. After that, irrigation pipes placed on each soil bed were used. The plants were treated with 18-hour long day (LD) until the 16th leaf on the plants was unfolded followed by short day (SD) of 11 hours using blackout screens. Blackout screens were completely unfolded irrespective of the greenhouse climate during the whole night. In EXPT. 2, assimilation light (SON-T AGRO, Philips, Eindhoven, The Netherlands) with 9.6 W m^{-2} photosynthetic active radiation (PAR) was used throughout the light period when outside global radiation fell below 150 W m^{-2} and switched off again at 200 W m^{-2}. No assimilation light was used in EXPT. 1, instead incandescent lamps were used for day-length control. As common practice in Dutch cut chrysanthemum cultivation, the top flower was pinched.

Leaf temperature of sunlit and shaded leaves in the canopy was continuously measured in the two middle greenhouse compartments by 10 evenly distributed K-type thermocouples ($\varnothing$ 0.025 mm), averaged over 5 minutes and stored on a data logger (DT 600, Esis, Roseville, NSW, Australia). Thermocouples were attached to the bottom of the leaves with tension and glue[93]. Energy consumption of the two middle greenhouse compartments (B and C) was calculated from water flux in the heating pipes measured with electromagnetic flowmeters (MagMaster, ABB Kent-Taylor Ltd., Cambridgeshire, England) and difference between in- and outflux temperature to the greenhouse compartments (isolated PT–100 thermometers mounted on the heating-pipes with thermoconductive gel). Measurements were

TABLE 1. Climate treatments applied in two greenhouse experiments (EXPT. 1, EXPT. 2) in four greenhouse compartments (GH) each with 6-day temperature integration (*TI*) with long-term temperature bandwidths (*b*), process based humidity regime (*PB*) and blueprint regime (*BP*).

GH	EXPT. 1		EXPT. 2	
	Temp.	RH	Temp.	RH
A	$TI \pm 4\,°C$	*PB*	*BP*	80 %
B	$TI \pm 2\,°C$	*PB*	$TI \pm 6\,°C$	*PB*
C	$TI \pm 8\,°C$	*PB*	*BP*	80 %
D	$TI \pm 6\,°C$	*PB*	$TI \pm 6\,°C$	*PB*

performed every 10 s, averaged over 5 min and stored in a data-logger (Hewlett Packard, Palo Alto, CA, USA) between day of year $261 - 311$ and $38 - 108$ for EXPT. 1 and 2, respectively.

Important external quality parameters for cut chrysanthemum are stem and internode length, number of leaves per plant and leaf size, flower number and size[26]. To evaluate the effect of the climate regimes on external quality, 24 or 12 evenly distributed and randomly selected plants (EXPT. 1 and 2, respectively) were harvested weekly per greenhouse compartment. The two border soil-beds and 2 m at each side of a bed were not used for sampling. Areas clearly influenced by inhomogeneity in soil structure or nutrient supply were not used either. From each plant, fresh- and dry weight (drying oven at 105 °C for two cycles of 16 hours) of leaves, stems and flowers, stem length, leaf- and flower number were measured. Leaf area of each plant was determined with a leaf area meter (LI 3100, LI-COR, Lincoln, NE, USA). Twice a week plants were checked for fungal diseases and humidity related disorders.

CLIMATE CONTROL AND TREATMENTS

During the first five days after transplanting in EXPT. 2, heating and ventilation temperature were set to fixed values of 18.5, 19.5 °C and 19.5, 20.5 °C for day and night for all compartments, respectively; RH was set to a maximum of 80 %. In EXPT. 1, treatments started the second day after transplanting. During treatments, climate was controlled either with the joint regimes (*JT*) or with a blueprint regime according to commercial practice (*BP*; TABLE 1). *BP* consisted of heating and ventilation temperature set points of 18.5, 19.5 °C and 19.5, 20.5 °C for day and night, respectively. Daytime ventilation set point increased by 0.5 K per 100 W m^{-2} between 600 and 1000 W m^{-2} outside global radiation. Nighttime heating and ventilation setpoints were increased by 0.5 K per 1 MJ m^{-2} day^{-1} global daily radiation sum of the preceding light period between 7 and 12 MJ m^{-2} day^{-1}.

Temperature: In *JT, TI* with an integration interval of six days was applied. Each 24 hours were treated independently and nested within the six-day averaging period. The 6-day boundaries were calculated from targeted 6-day mean temperature (T_{targ}), the allowed long-term temperature bandwidths (*b*; ±2, ±4, ±6 or ±8 °C) and a proportional back regulation (CHAPTER 3.1). A receding horizon of 1 day was used, i.e. the preceding 5-day period was evaluated at the beginning of each new day and compensated at day six of the averaging period. Temperature history older than 5 days was not taken into account. T_{targ} depended on that of a reference regime, it was either calculated from set points of an imaginary blueprint regime (EXPT. 1) or from realised greenhouse temperatures in *BP* compartments (EXPT. 2).

A target average 24-h temperature with a temperature window rather than a fixed average target temperature as in regular *TI* was used as control criterion (CHAPTER 3.1). Maximum ventilation and minimum heating set point were applied (34 °C and 10 °C). Too extreme temperatures were avoided by soft boundaries that were treated with temperature-time dose-response as explained in CHAPTER 3.1. Two types of thresholds (absolute and relative) represented the limits, an exponential response was assumed between them. A maximum duration (30 min) at maximum and minimum set points was set and temperature was recorded for dose response after passing a relative boundary (14 °C or 30 °C for heating and ventilation, respectively). Heating and ventilation temperatures for the dose response were initially set to the absolute thresholds and adjusted after dosage was completed. The relative boundary was then hold for the duration of a refresh time of 6 h and was then reset. Temperature was allowed to fluctuate within this range provided that the 24-h average temperature remained within the 6-day boundaries. For that, greenhouse temperature during the next 24 hours was simulated with forecasted weather and a simple static greenhouse model as used in CHAPTER 3.1 and CHAPTER 3.2. Weather forecast was supplied by a meteorological company (Meteo Consult, Wageningen, The Netherlands) using the Dutch software package *Weerbeeld* (ver. 6.4.1, Meteo Consult, Wageningen, The Netherlands) through an internet connection. The mean forecasted temperature was updated with realised temperature every 5 minutes and used as control criterion.

Because integration capacity in chrysanthemum depends on plant development stage[217] and temperature fluctuations during flower initiation can delay flower development[68, 218], a development stage dependent temperature control[56] was applied in *JT*. *TI* was applied during LD in both experiments with *JT*. Since time to visible flower bud is particularly critical to temperature variation during SD[218], temperature with *JT* in EXPT. 1 was then set as with *BP* in this period.

Because the first stages in chrysanthemum flower development are already completed when the first flower bud is visible[219] and flower development is probably not sensitive to temperature variations, the procedure was changed for EXPT. 2.

The duration of the first initiated flower primordia from pinched chrysanthemum plants could be determined to 8.7 days with a regression model using the prevailing temperatures[219]. This agrees well with the reported 8 – 10 days[220]. However, cut chrysanthemum plants were not pinched before short-day was applied, and vegetative plant growth is still going on for 6 – 8 days until flower induction starts[221]. Because flower initiation of the plant is probably an ongoing process, we assumed the first 14 SD sensitive to temperature variations. During this period, temperature fluctuation was restricted by a 6-day temperature bandwidth of ± 1 °C, but could still fluctuate in the short-term. It's magnitude was restricted by the long-term (CHAPTER 3.1). Caution was in particularly given with SD temperature during night. Although flower development depends on 24-hour mean temperature[41], flower initiation was reported delayed with night temperatures lower than 16 °C or higher than 24 °C [17]. Therefore, also short-term fluctuations were restricted during night while flowers initiated. Heating set point was restricted to > 18 °C and a fixed margin between heating and ventilation temperature of 1 °C was set.

Relative humidity: RH was controlled with a process based humidity regime (*PB*) within *JT* (CHAPTER 3.2), i.e. set points were calculated according to separate plant affecting processes as Ca-deficiencies, plant water stress, crop growth, crop development and airborne fungal diseases (powdery mildew, chrysanthemum white rust and grey mould). Decisions on climate control against fungal diseases were mainly based on calculated leaf wetness duration[190] (LWD, i.e. time integral of leaf condensation). Leaf wetness was determined from predicted crop temperature[92] and measured RH. Leaves were assumed to be wet when the difference between predicted dew point and crop temperature was less than 1.5 °C [211, 212].

CO_2: CO_2 concentration set point was either 1000 or 350 µmol mol^{-1}, depending on ventilation. Set point was 1000 µmol mol^{-1} when vents were closed. CO_2 set point was 350 µmol mol^{-1} when vents were open or when outside global radiation was below 40 W m^{-2}. Temperature giving rise to maximum crop gross photosynthesis (P_{gc}) at 1000 µmol mol^{-1} (under prevailing light conditions) was used as a secondary set point for ventilation with *JT* (CHAPTER 3.1), hence the ventilation set point was recalculated when vents opened. Leaf photosynthesis was calculated as described in CHAPTER 2 according to biochemical equations[97] including stomata resistance as function of radiation absorbed by the canopy, leaf temperature and vapour pressure deficit[92]. Leaf photosynthesis was scaled up to P_{gc} based on radiation distribution within the canopy[96].
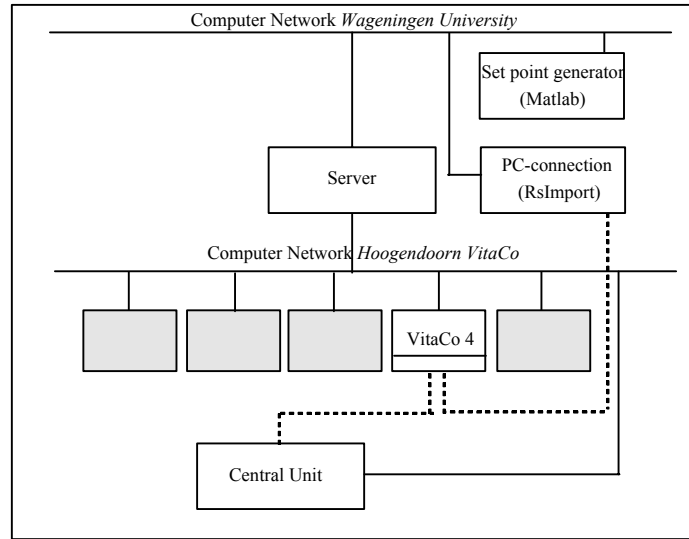
FIGURE 1. Network system at Wageningen University to control greenhouse climate with a commercial VitaCo climate computer connected via RS-Import 1.0 (Hoogendoorn, Vlaardingen, The Netherlands) with the set point generator programmed in the control software MATLAB, with direct computer to computer connections (---) and network connections (—).
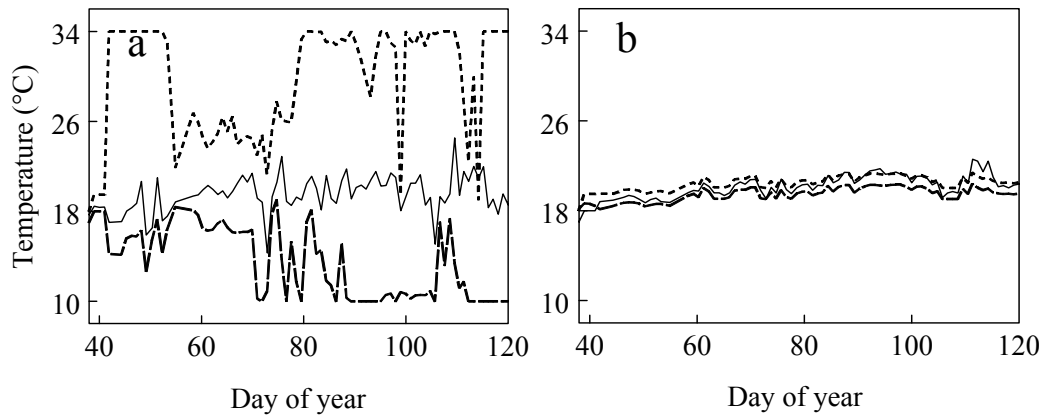
FIGURE 2. 24-hour average greenhouse temperature (—), heating set points (– – –) and ventilation set points (----) for the joint climate regime (a) and the blueprint regime (b) in EXPT. 2.

CLIMATE CONTROL IMPLEMENTATION

The climate regimes *JT* and *BP* were implemented in the technical software environment MATLAB® (version 6.0, MathWorks Inc., Natick, MA, USA). The control algorithm was used as set point generator and coupled to a commercial greenhouse climate computer (VitaCo, Hoogendoorn, Vlaardingen, The Netherlands)

via the internal computer network of Wageningen University (FIG. 1). The greenhouse climate computer controlled climate by heating and ventilation. It further recorded temperature, RH and CO_2 concentration every 5 min. In the same sequence, climate data were supplied to a shared computer network drive by the climate computer and read by the set point generator programme. Set points were then sent to an intermediate computer. The connection to the climate computer was done by exclusively designed software (RsImport, ver. 1.0, Hoogendoorn, Vlaardingen, The Netherlands). Set points were used by the climate computer for climate control in the same way as set points that are input to the system.

RESULTS

GENERAL REGIME BEHAVIOUR AND GREENHOUSE CLIMATE

Temperature with *BP* was rigid controlled with a small margin between heating and ventilation temperature (FIG. 2). This was in strong contrast to *JT*. With *JT*, fluctuation of 24-hour mean temperature increased with increasing long-term temperature bandwidth (FIG. 3) and greenhouse set points were reduced (FIG. 4 and 5). In periods with relatively high solar radiation in autumn (e.g. day 240 – 244 of the year), greenhouse temperature in *JT* was mainly controlled through ventilation. Higher temperature levels were observed when temperature bandwidth (*b*) was large. Then, greenhouse temperature could fluctuate almost freely with little control in *JT* (*b* = ±6 °C or ±8 °C; FIG. 4). During a cold period in late October temperature was mainly controlled by heating (FIG. 5), but ventilation was controlled to maximise P_{gc}. RH control was probably the reason to open vents in first place; the secondary control was then continuously calculating the optimum temperature for maximum P_{gc} (FIG. 5, day 302).

Although ventilation was stronger reduced with higher temperature bandwidth leading to a higher CO_2 concentration (FIG. 6), mean temperature over the complete

TABLE 2. Average greenhouse temperature and relative humidity (T, RH) and average daytime (8 a.m. – 6 p.m.) CO_2 concentration ($[CO_2]$) for four different temperature bandwidths (*b*) for the joint climate regime (*JT*) in EXPT. 1, and in the blueprint regime (*BP*) and *JT* in EXPT. 2.

	Experiment						
	EXPT. 1				EXPT. 2		
	$JT \pm 2$	$JT \pm 4$	$JT \pm 6$	$JT \pm 8$	BP	$JT \pm 6$	LSD[a]
T	19.68	20.02	19.61	19.63	20.3	19.6	0.16
RH	86.6	86.7	88.4	89.9	74.2	85.1	8.56
$[CO_2]$	646	648	678	723	438	705	55.8

[a] LSD: Least significant difference for EXPT. 2 data (Student's t-test; α=0.05)
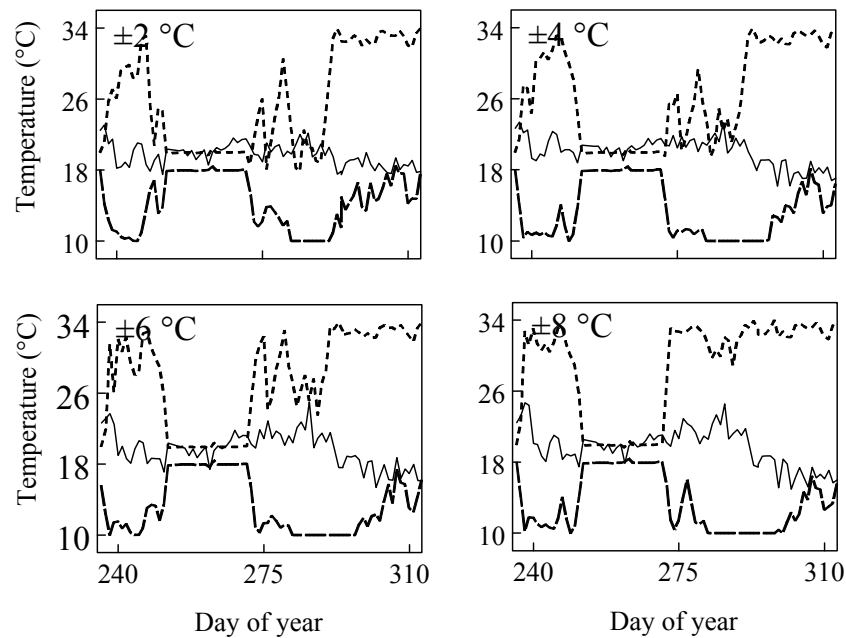
FIGURE 3. 24-hour averages of greenhouse temperature (—), heating set point (– – –) and ventilation set point (----) for the joint climate regime (*JT*) with four different temperature bandwidths (±2, 4, 6 and 8 °C) in cut chrysanthemum cultivation (EXPT. 1).

TABLE 3. Number of hours with leaf wetness (LW) per week (a) and number of times LWD exceeded 3 hours (b) for blueprint regime (*BP*) and joint climate regime (*JT*) in EXPT. 2. Leaves were assumed to be wet when the difference between calculated dew point temperature[210] and crop temperature[92] was < 1.5 °C [211, 212] or when the top-to-bottom sprinkler irrigation system was applied.

Regime		Week											
		1	2	3	4	5	6	7	8	9	10	11	12
BP	a	1	1	1	1	1	1	1	0	0	0	0	0
	b	0	0	0	0	0	0	0	0	0	0	0	0
JT	a	1	1	1	5	7	7	45	60	55	51	25	16
	b	0	0	0	0	0	1	12	18	15	16	7	2

TABLE 4. Leaf-number, flower-number, leaf area index (LAI) and specific leaf area (SLA, $cm^2 \; g^{-1}$) for cut chrysanthemum with the joint climate regime (*JT*) for different temperature bandwidths (*b*) in EXPT. 1 at day 77 after transplanting. Data are presented with standard error of the mean of 24 plants in each treatment.

b	Number		LAI	SLA
	Leaves	Flower		
±2	30.8 ± 0.3	10.3 ± 0.4	4.6	368
±4	30.9 ± 0.3	11.3 ± 0.3	4.7	363
±6	31.6 ± 0.3	11.5 ± 0.3	5.0	374
±8	31.5 ± 0.3	12.4 ± 0.4	4.6	352
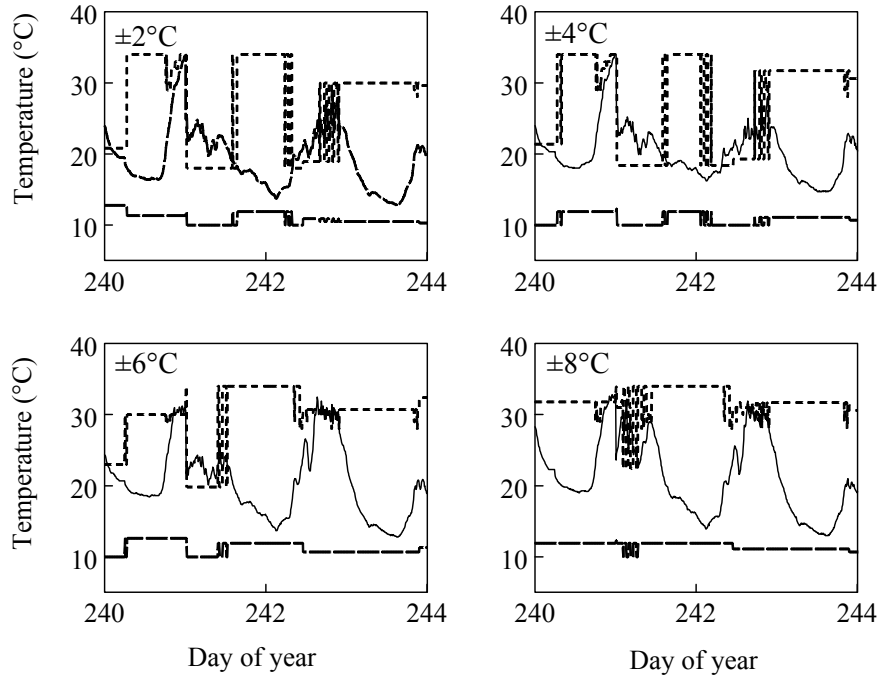
FIGURE 4. Realised greenhouse temperature (—), heating set points (– – –) and ventilation set point (----) for four temperature bandwidths (±2 °C, ±4 °C, ±6 °C and ±8 °C) in cut chrysanthemum cultivation (EXPT. 1) with the joint climate regime (*JT*) between day of year 240 and 244
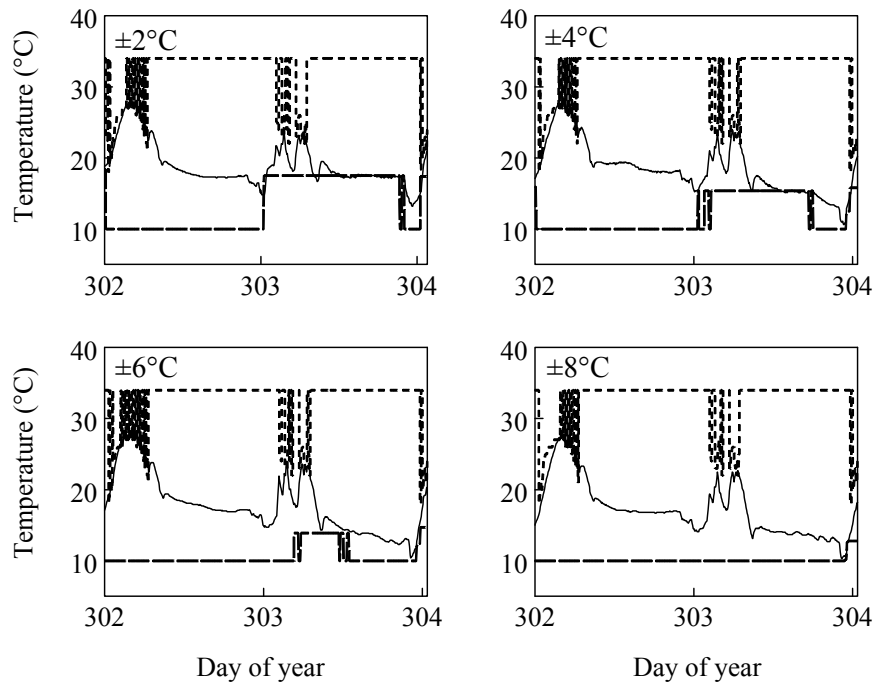
FIGURE 5. Realised greenhouse temperature (—), heating set points (——) and ventilation set point (----) for four different temperature bandwidths (±2 °C, ±4 °C, ±6 °C and ±8 °C) in cut chrysanthemum cultivation (EXPT. 1) with the joint climate regime (*JT*) between day of year 302 and 304.

137
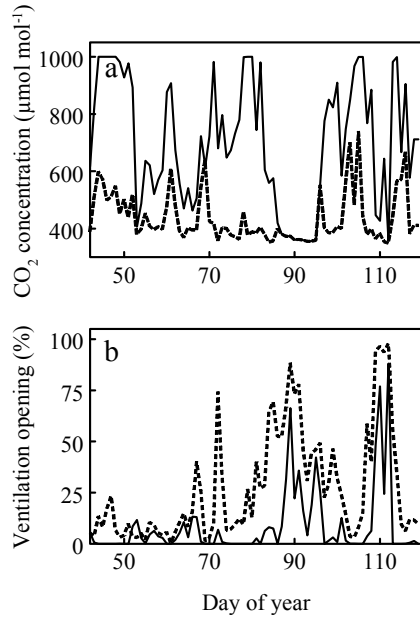
FIGURE 6. 24-hour average CO_2 concentration for joint regime (*JT*) (—) and blueprint (*BP*) (– – –) (a) and lee-side ventilation opening for *JT* (—) and *BP* (---) (b) with EXPT. 2.
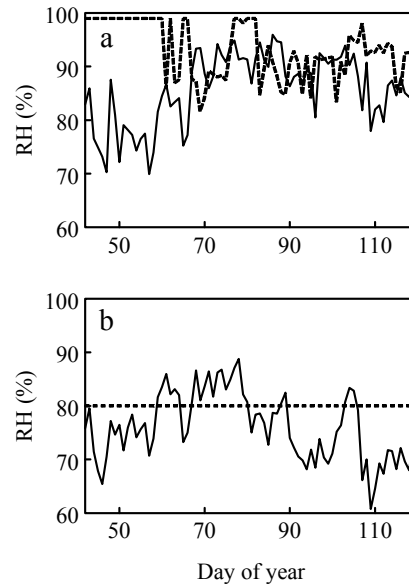
FIGURE 7. 24-hour average relative humidity (RH) (—) and RH set points (---) for joint climate regime (a) and blueprint (b) with EXPT. 2.

cultivation period differed only little within *JT* (TABLE 2). The higher mean temperature of $b = \pm 4$ °C was probably based on the relative location of greenhouse compartment A next to a tropical experimental compartment. However, this was not the case with *BP* in the same compartment during EXPT. 2, *BP* had a 0.7 °C higher average temperature over the complete cultivation period than *JT*. This was due to the fixed lower heating set point of 18.5 °C. From mid March, the *BP* greenhouse warmed up to almost 25 °C and this could not be compensated as in *JT* (data not presented). A gradually increasing 24-h mean temperature could be observed (FIG. 2). When *b* increased, ventilation was diminished and RH increased (TABLE 2). Due to the process based humidity regime this led only to ventilation when absolutely necessary (FIG. 7), e.g. when predicted leaf condensation exceeded the maximum allowed LWD according to the *PB* rules (TABLE 3). For that purpose, leaf temperature was predicted by a simple model (CHAPTER 3.2). Only little deviation between measured and predicted leaf temperature was observed for shaded leaves (FIG. 8). The variation was higher for sunlit leaves, where predictions underestimating measured values in low temperature ranges. This led to overestimating of leaf condensation in sunlit leaves during night (cold period) and humidity control would have act sooner as it should.
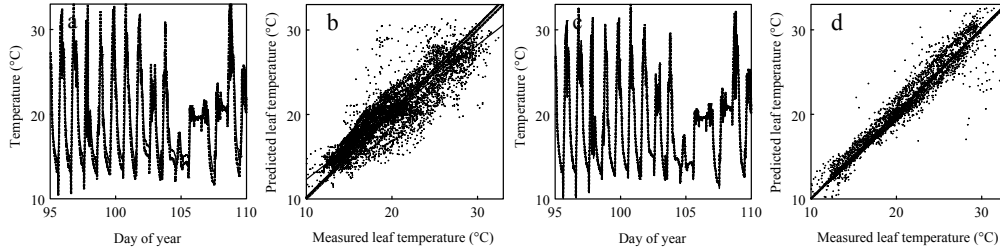
FIGURE 8. Measured (——) and predicted (– – –) leaf temperature (5-minute means) for sunlit leaves (a) and shaded leaves (c) during 15 days with the joint regime (*JT,* EXPT. 2) with ($b = \pm 6$ °C); plot measured (T_m) versus predicted (T_p) leaf temperature for sunlit leaves (b; $T_m = Tp$ (– – –), $T_p = 0.80 \cdot T_m + 4.4$ (——), $R^2 = 0.82$; $T_p = 1.017 \cdot T_m$ (— – —), $R^2 = 0.76$) and shaded leaves (d; $T_m = T_p$ (– – –), $T_p = 1.007 \cdot T_m + 0.04$ (——), $R^2 = 0.95$; $T_p = 1.005 \cdot T_m$ (— – –), $R^2 = 0.95$).

CROP PERFORMANCE

When P_{gc} was real-time simulated with the same LAI for both treatments (LAI was common input to the P_{gc} control module), the high observed daytime CO_2 concentration in *JT* controlled climates resulted in a 8.5 % higher cumulative P_{gc} compared to the *BP* regime (data not presented). Growth analysis, however, showed a stronger increase in dry weight of all plant organs with *JT* compared to *BP* (FIG. 9).

After 83 days of cultivation, total dry weight was about 39 % higher for *JT* controlled plants. This was probably due to a higher light interception of *JT* treated plants with higher LAI (FIG. 10). Leaf number was only little different throughout the complete cultivation period with *JT* and *BP*. The individual leaves where therefore larger in *JT*, but specific leaf area was higher with *BP* than with *JT* (430 and 370 cm^2 g^{-1}, respectively). This difference was only pronounced after 28 March (data not presented). Flower dry weight did not change with *b* in EXPT. 1 but was 25 % higher with *JT* than with *BP* in EXPT. 2 (FIG. 9). Since flower number was equal with *JT* and *BP*, individual flowers had in average 25 % more dry weight. However, relatively more stem- and leaf- than flower dry-matter was produced. In EXPT. 1, slightly higher
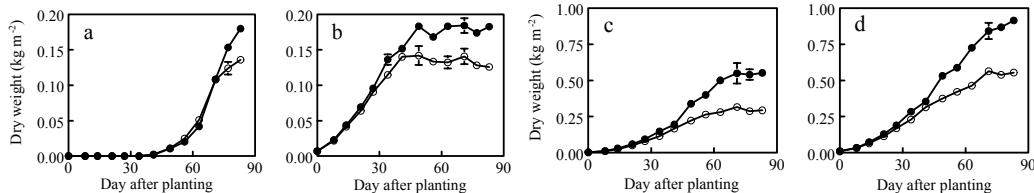
FIGURE 9. Dry weight for a blueprint regime (○) and joint climate regime (●) of flowers (a), leaves (b), stems and side stems (c) and total plant (d) in a spring cultivation of cut chrysanthemum (EXPT. 2) as a function of time, bars larger than symbols indicate standard errors of the mean of two greenhouses.
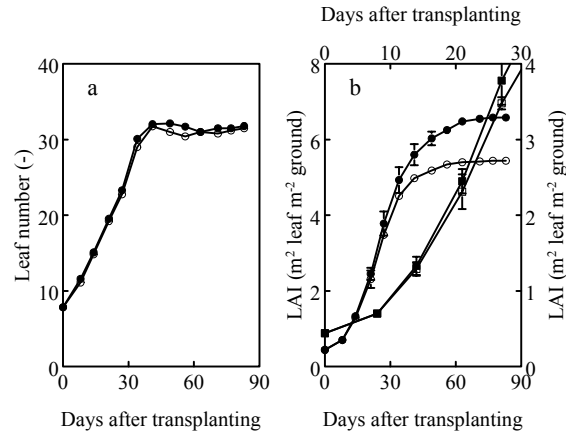
FIGURE 10. Number of formed leaves (a) and leaf area index (LAI) (b) for the blueprint regime (○) and joint climate regime (●) during the complete cultivation period and focus on LAI during the first 30 days of cultivation for the blueprint and joint climate regime (□, ■; EXPT. 2) as a function of time, bars larger than symbols indicate standard error of the mean of two greenhouses.

flower and leaf numbers were observed with higher temperature bandwidth in *JT* (TABLE 4). The biggest plants with longest stems and leaf area were achieved with a temperature bandwidth of ±6 °C. Those were also the heaviest where flowers contributed most to that (FIG. 11). With ±8 °C plant development was delayed by 4 – 5 days (but not at other bandwidths, data not presented). Temperature sums after cultivation with $b = \pm 6$ °C or ±8 °C were only slightly different (FIG. 12). This shows that the overall temperature sum alone did not affect plant development. Differences in temperature-sum could be observed between the developmental stages. During the vegetative stage, temperature sum had probably no or only little influence on leaf unfolding as basically no difference in leaf number between ±6 °C and ±8 °C temperature bandwidths was observed (TABLE 4). Temperature was only slightly lower with $b = \pm 8$ °C during flower initiation compared to ±2 °C and ±6 °C. Therefore, developmental delay was probably based during flower development. This stage can be further divided in three phases: visible bud to disbud, disbud to colour, and colour to flower[68]. Each phase has a different temperature optimum[68]. Since no
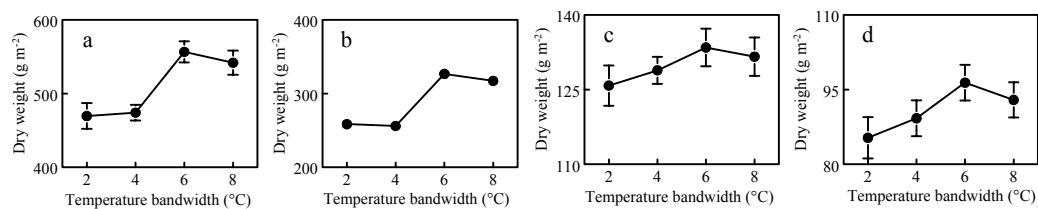
FIGURE 11. Dry weights of the whole plants (a), stems (b), leaves (c) and flowers (d) at regular harvest at day 77 after transplanting of EXPT. 1 for four different temperature bandwidths with the joint climate regime; standard error of the mean of 24 plants are smaller than symbols in all cases.
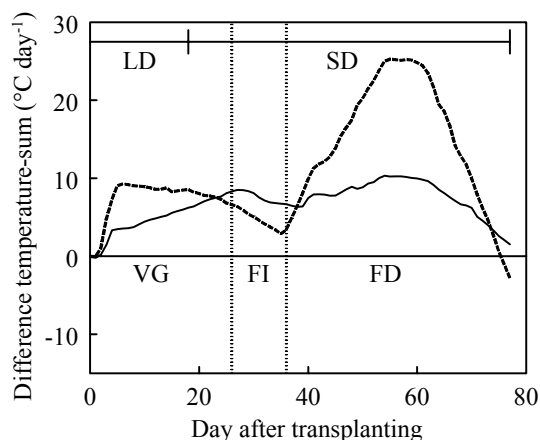
FIGURE 12. Difference in temperature-sum (°C-days) between joint climate regime (*JT*) with 6-day temperature bandwidths of ±8 and ±6 °C (—) and ±8 and ±2 °C (– – –) during the complete cultivation period with long-day and short-day (LD and SD, respectively) divided in vegetative growth (VG), flower induction (FI) and flower development (FD).

detailed investigation for different flower phases was performed here, phases could only be assigned roughly according to the reported average duration for each phase[68] (TABLE 5). Temperature was not optimal with any bandwidth, but differences between them were small in the first two phases. Mean temperature decreased with temperature bandwidth during the last two phases and this was probably the reason for the developmental delay of *JT* with ±8 °C temperature bandwidth. Although the difference in temperature-sum between *BP* and *JT* in EXPT. 2 increased during SD to 48 °C – days (TABLE 6), no final developmental delay was observed. Neither had a difference of 11 °C – days after vegetative development (LD+8) obvious influence on leaf unfolding. However, with *JT* flower development was slightly delayed in the first part of flower development but developmental speed increased later on relative to *BP* (data not presented, but supported by flower dry weight increase in FIG. 9). This was

TABLE 5. Mean temperatures (°C) of flower development phases for *JT* in EXPT. 1 according to Karlsson *et al.* (1989)[68]. Phases were divided in: start of short-day to visible bud (I), from visible bud to disbud (II), from disbud to colour (III) and from colour to flower (IV). Average time to complete the phases was assumed 40 % (I), 35 % (II), 10 % (III) and 15 % (IV) of total time to flower[68] resulting in 23.6, 20.7, 5.9 and 8.9 days. Optimum temperature was 21.3, 20.3, 23.1 and 19.1 °C for phase I, II, III and IV, respectively.

b	Flowering phase			
	I	II	III	IV
±2	20.25	19.79	18.75	18.33
±4	20.64	20.32	17.82	17.7
±6	20.23	20.37	17.41	16.96
±8	20.30	20.49	16.88	16.32

TABLE 6. Temperature sums (°C day^{-1}) after end of the long-day period (LD), after long-day period plus eight days (LD+8) and after short-day period (SD) for joint climate regime (*JT*) and blueprint regime (*BP*) in EXPT. 2

	Period during cultivation		
Treatment	LD	LD+8	SD
BP	315	466	1590
JT	304	455	1542
LSD[a]	3.0	2.2	11.0

[a] LSD: Least significant difference (Student's t-test; $\alpha=0.05$)

TABLE 7. Mean temperatures (°C) of flower development phases for *JT* and *BP* in EXPT. 2 according to Karlsson *et al.* (1989)[68] (a) and difference in temperature sum to optimum temperature (°C day^{-1}) (b). Phases were divided in: start of short-day to visible bud (I), from visible bud to disbud (II), from disbud to colour (III) and from colour to flower (IV). Average time to complete the phases was assumed 40 % (I), 35 % (II), 10 % (III) and 15 % (IV) of total time to flower[68] resulting in 26, 22.8, 6.5 and 9.8 days. Optimum temperature was 21.3, 20.3, 23.1 and 19.1 °C for phase I, II, III and IV, respectively. Data are presented with standard error of the mean of two compartments each.

		Flowering phase			
		I	II	III	IV
BP	a	20.00 ± 0.02	21.04 ± 0.01	20.65 ± 0.05	20.59 ± 0.06
	b	33.80	16.87	15.93	14.60
JT	a	19.65 ± 0.03	20.22 ± 0.03	20.09 ± 0.04	19.87 ± 0.11
	b	42.90	1.82	19.57	7.6

probably due to the more optimal mean temperature with *BP* until the flower bud was visible and the opposite during the following flower development phase (TABLE 7). The *PB* regime within *JT* did not cause any fungal disease or visible calcium deficiencies or any other problems in any treatment (data not presented).

TABLE 8. Measured energy consumption (MJ m^{-2}) for the joint climate regime (*JT*) for two different bandwidths in EXPT. 1 (*b* = ±2 °C or ±8 °C) and EXPT. 2 (*b* = ±6 °C) and blueprint regime (*BP*) in EXPT. 2.

Experiment	Measuring period (DOY)	Energy consumption (MJ m^{-2})		Energy saving (%)
		JT ± 2 °C	*JT* ± 8 °C	
EXPT. 1	244 – 324	94	79	15.9
		BP	*JT* ± 6 °C	
EXPT. 2	38 – 108	251	192	23.5

TABLE 9. Temperature-sums of upper and lower heating circuits (°C day^{-1}) for the joint climate regime (*JT, b* = ±6 °C) and blueprint regime (*BP*) for cultivation of cut chrysanthemum after 5th day of cultivation in EXPT 2. Only data were used when heating was switched on, otherwise temperature was assumed 0 °C.

Regime	Lower circuit	Upper circuit
JT	824	523
BP	1589	1052
LSD[a]	578	594

[a] LSD: Least significant difference (Student's t-test; α=0.05)

ENERGY CONSUMPTION

Energy consumption was 23.5 % lower with *JT* (temperature bandwidth of ±6 °C) compared to *BP* in EXPT. 2 (TABLE 8). This was also distinct from temperature-sum of the heating pipes of both regimes (TABLE 9). With a narrow temperature bandwidth of ±2 °C, energy consumption was 15.9 % higher than with ±8 °C (TABLE 8).

DISCUSSION

It could be shown with experiments that the joint climate regime with modified temperature integration and process based humidity control was able to reduce energy consumption while crop growth strongly increased compared to a blueprint regime. Energy saving was as expected with the combined regime during this season[215]. When the same duration was used for simulations with a reference climate year as in EXPT. 2, 29 % energy was saved (data not presented). The difference to the measured 23.5 % was acceptable for the purpose of regime to approval. Energy saving could be achieved with the connection of two sub-regimes for temperature and humidity control. The purpose of the first, *TI*, is either to shift heating periods when the heat loss factor is reduced[36, 55] or to use the greenhouse as solar collector more than with common climate regimes by extending the ventilation set point. Then, one can refrain from heating during cooler periods to achieve the targeted mean temperature. In the present case, temperature rose to 29 °C beginning of February and dropped to 12 °C in the same 24-hour period. This led to a 24-h mean temperature of 18.9 °C. With regular temperature integration with the same bandwidth (±6 °C), temperature would have been restricted to 14 °C and 26 °C. However, maximum energy saving could be achieved when compensation would not be necessary. Such a regime was applied in Denmark[136], but plant development was delayed in winter[222]. In the present regime, developmental delay was only observed with extreme settings and this was

probably due to the non-optimal mean temperature during flower development. The control system was obviously not able to control mean temperature with $b = \pm8$ °C. A stronger temperature compensation would have been necessary. With ±6 °C temperature bandwidth, nevertheless, no developmental delay was observed and energy was saved while a strong increase in dry matter could be achieved. Similar findings with chrysanthemum were reported with a *free* dynamic climate control system (without temperature compensation) optimising photosynthesis in small acrylic-plastic containers placed in a greenhouse[127, 223]. Also in roses, a dry matter increase of more than 40 % was achieved in late spring with the same control for greenhouses[136]. However, energy consumption for heating was then increased compared to a reference regime[136]. When the system was applied in winter (January to March), no dry matter increase was found but heat energy was reduced slightly. This depended on the system settings. High energy saving was possible but only with a simultaneous decrease in dry matter production[136].

Chrysanthemum fresh weight increase of 16 % and energy saving was reported when temperature integration ($b = \pm4$ °C) was applied with a constant CO_2 set point of 350 µmol mol^{-1}[40]. Since CO_2 was kept low in that research and therefore no P_{gc} optimisation was performed, higher photosynthesis levels due to less ventilation and consequently higher CO_2 concentration can only partly explain the strong increase in plant weight with the *JT* climate in the present experiment. Although it was reported that CO_2 enrichment alone can increase fresh yield of chrysanthemum with up to 37 % [224], a higher light interception of the *JT* treated plants was probably the main reason for more growth. With higher LAI, light interception was higher and due to that photosynthesis and growth. This was only important for the first ~30 days, because LAI with 3 already intercepts 90 % radiation[225] and there is only little P_{gc} increase after that[226]. Initial plant size was higher and this partly resulted in the final difference. A positive *DIF* (difference between average day and average night temperature) was probably the reason for that. With positive *DIF* internodes elongate and longer stems can be expected [e.g. 23] and leaves act the same. This was supported by Hendriks *et al.* (1990)[227], who reported that positive *DIF* led to longer poinsettia plants with bigger leaves and bracts than combinations with zero or negative *DIF*. Increase in leaf area may also be supported through high RH[183, 228]. Dry matter allocation was, however, negatively influenced as dry matter percentage allocated to flowers was lower with *JT* than with *BP*. This was also observed with *TI* experiments[40], but in contrast to Cockshull (1982)[229]. This author reported that proportion dry matter allocated to chrysanthemum flowers remained constant irrespectively environmental condition. A positive *DIF* could have been the reason as it results in a higher percentage stem dry matter compared to a negative *DIF*[230]. The observed decrease in flower dry matter percentage was therefore based on the

strong increase in stem dry matter with *JT* (53 % and 60 % with *BP* and *JT*, respectively).

CONCLUSION

When applying the joint climate regime energy saving and crop yield increase are possible at the same time, while plant development is not delayed. Dry matter increase was probably a combination of regular *TI* behaviour in spring, when greenhouses heat up during day and cool down during night attaining a positive *DIF* and accordingly larger leaves. In a young stage, this can be very advantageous compared to a common climate regime with fixed set points and zero *DIF*. Compared to existing dynamic regimes for energy saving including P_{gc} maximisation[136] also plant development is controlled and this is an important economical issue. In chrysanthemum, different developmental stages are however the bottleneck with dynamic climate controls. In commercial cut chrysanthemum practice all development stages are grown in one greenhouse and therefore application of this dynamic regime is only possible when also the growing system changes such that homogeneous compartments are used for cultivation. A different solution would be to select or to breed new genotypes that are more robust against temperature fluctuations. A combination of modern greenhouse structures, dynamic climate control regimes and new cultivars will probably be the best solution for future environmentally friendly greenhouse production. However, the evaluated regimes form a promising basis for future climate controllers and can also be extended to other greenhouse crops.

ACKNOWLEDGEMENTS

3.4 *DIF* AND 24-HOUR TEMPERATURE INTEGRATION: A SIMULATION STUDY TO QUANTIFY ENERGY CONSUMPTION

O. KÖRNER, M.J. BAKKER & E. HEUVELINK
Temperature regimes for energy saving and stem length control:
a simulation study to quantify energy consumption
(submitted)

ABSTRACT

A combined greenhouse climate and control model was used to study energy consumption in year round cut chrysanthemum. Temperature was either controlled for energy saving with 24-h temperature integration (TI_{24}) or TI_{24} was restricted by a negative *DIF* regime ($TI_{24,DIF}$) for stem length control (*DIF* = difference between average day and average night temperature). Energy consumption was reduced by both regimes compared to a blueprint regime according to commercial practice when in winter heating was shifted to nighttime using a screen. With increasing weather fluctuations in spring and autumn, weekly energy reduction could increase to more than 60 % for TI_{24} with ±6 °C temperature bandwidth. With $TI_{24,DIF}$ in the same period, only 37 % or 17 % less energy was used than with a blueprint regime (–6 °C and –12 °C *DIF*, respectively). In general, $TI_{24,DIF}$ reduced energy demand compared

to the blueprint, but energy saving was higher with TI_{24} without *DIF* restrictions. The decision whether to apply TI_{24} or $TI_{24,DIF}$, the actual cultivation period is the most important criterion. Controlling stem length with negative *DIF* in spring and autumn has the highest additional costs, almost no negative *DIF* control is possible in summer, and during winter TI_{24} and $TI_{24,DIF}$ result in an almost similar greenhouse climate.

INTRODUCTION

For environmental and financial reasons reducing energy consumption is becoming more important in greenhouse horticulture. The greenhouse industry is aiming for low energy greenhouse concepts with no or minimal reduction in growth, yield quality. External quality for ornamental crops (e.g. chrysanthemum) is mainly determined by internode- and stem-length, leaf number and flower attributes[26]. To obtain good yields and high quality, high amounts of energy are used in commercial practice. Environmental unfriendly chemical growth inhibitors are used to reduce internode length and to achieve short compact plants[75] and rigid regimes are applied to control greenhouse air temperature. To diminish environmental impact, greenhouse heating and use of chemicals should be reduced[231, 232] while achieving high quality crops with intelligent climate regimes.

For example, leaf unfolding rate and flower development rate are responding to 24-hour mean temperature[72, 233] and temperature integration[41, 167] can be applied. With temperature integration heating set-point can be lowered when the heat loss factor for a greenhouse is high and heating set point can be increased when heat loss is low. In this way mean temperature can be attained at its desired level while heating is shifted to periods of lower costs[36]. For example, temperature integration with heating using energy screens during winter nights can help to reduce energy consumption in winter[39, 55]. The highest relative energy savings with temperature integration, however, can be achieved in spring and autumn, when greenhouses heat up naturally by solar radiation during the day. Consequently, no or only marginal heating during the night is then required.

The *DIF* concept[73] (difference between average day temperature, DT, and average night temperature, NT) is a further advanced temperature control method on 24-hour basis, and can be used to control stem elongation. Negative *DIF* treatment (i.e. NT > DT) results in shorter internodes and more compact plants[74].

However, applying negative *DIF* or regular temperature integration can result in opposite temperature strategies. The disadvantages of a negative *DIF* regime include the decreased freedom for temperature fluctuation in temperature integration with an averaging period of 24 hours[76] (TI_{24}) and therefore increased energy consumption compared to TI_{24}. TI_{24} aims at minimising climate control actions (temperature may

freely alter between heating and ventilation set-point), whereas *DIF* regimes may counteract that. *DIF* regimes integrate 24-hour temperature, too, but the difference between average day and average night temperature is imposed. A *DIF* setting limits TI_{24} and is therefore to be distinguished as TI_{24} with *DIF* ($TI_{24,DIF}$). During cold periods with cold days and nights, heating during the night using an energy screen is always more beneficial, and applying negative *DIF* in the same time is not conflicting. However, TI_{24} during mild sunny days may yield in higher DT than NT, and heating (if needed) is shifted to nighttime. Compared to TI_{24}, therefore, $TI_{24,DIF}$ either does not change temperature settings or it eliminates energy saving options during times of highest saving margins in spring and autumn.

Simulations with $TI_{24,DIF}$ and TI_{24} with various settings were performed to quantify and evaluate the energy demands of achieving short compact chrysanthemum plants by applying negative *DIF* compared to 24-hour temperature integration.

MATERIALS AND METHODS

MODEL

Greenhouse climate was simulated with a detailed greenhouse climate and control model[105] (CCM). The climate part of the CCM consisted of three sub-models: a thermal model, a vapour model and a CO_2 model. The CCM provided simulations for a modern 1-ha Venlo-type greenhouse with a single glass cover with transmission for diffuse short-wave radiation (τ_{dif}) of 78.5 %. Direct transmission of the greenhouse cover (τ_{dir}) was calculated as a function of azimuth and elevation of the sun[172]. The CCM controlled greenhouse climate through heating and ventilation, and simulated energy consumption based on the balance of energy in- and output fluxes to the greenhouse with a 2-minute time step. A representative one year reference climate data set for De Bilt (The Netherlands, lat. 52 °N) was used for that[177]. Outside climatic data were provided as hourly values of air temperature, relative humidity, water vapour pressure deficit, direct and diffuse global radiation, CO_2 concentration, wind speed and wind direction.

The CCM calculated energy input to the greenhouse resulting from incoming solar short-wave radiation (no assimilation lamps were used) and from direct heat supply from the heating unit by burning natural gas to heat water in a boiler to a maximum of 94 °C. Heating was performed with lower and upper heating pipes as common in cut chrysanthemum commercial practice in The Netherlands. Gas was also burned for CO_2 dosage and CO_2 concentration was set to a minimum of 400 µmol mol^{-1} greenhouse air. For that, an energy ratio of 35.17 MJ m^{-3} gas was used[234]. A short term heat storage tank of 120 m^3 with a several layer system[235] was used and filled when more gas was burned for CO_2 dosage than necessary for simultaneous heating;

CO_2 dosage was stopped when the heat storage tank was completely filled with water of 94 °C.

Energy losses were derived from radiative, convective and latent heat fluxes from the greenhouse cover and from conduction through the greenhouse ground. The radiative exchange processes between the greenhouse cover and the crop canopy were calculated using the *Stefan-Boltzmann* law. For that, a sky temperature was introduced expressing the temperature of a black hemisphere that is exchanging thermal radiation with the greenhouse cover[105].

Energy losses through natural ventilation were calculated[173] with wind speed and vent opening as determining factor. Latent heat production by crop transpiration was calculated according to Stanghellini (1987)[92]. A cut chrysanthemum crop with a constant leaf area index (LAI) of 3 was assumed. Energy losses from latent heat were either calculated by direct mass transfer to the outside air or by phase changes through condensation on the glass wall and the resulting convection losses influenced by the temperature of the greenhouse cover, outside air temperature and wind speed[130].

Two types of screens were used in the simulations (energy saving screen and blackout screen), where only one of the screens was used at the same time. When a screen was completely unfolded, short-wave transmission was reduced with a screen factor ($\tau_{s,e}$ = 0.3, $\tau_{s,b}$ = 0.0 for energy and blackout, respectively). When screens were unfolded, air exchange between the compartment beneath and above the screen was simulated by convective heat flux through openings in the fabric[236].

The CCM was coupled to a set point generator (SPG) via a data-file sharing system. Climatic set points (heating and ventilation temperature, relative humidity and CO_2) were generated by the SPG implemented in the control software environment MATLAB® (version 6.0, MathWorks, Natick, MA, USA). In a simultaneous 2-model simulation (CCM / SPG), set points for heating and ventilation were calculated by the SPG and sent as input for simulation to the CCM with a fixed time step of 5 minutes. The CCM returned simulated realised greenhouse climate (RH, temperature and CO_2 concentration) to the SPG, while using the received set points.

<center>TEMPERATURE REGIMES</center>

Four temperature regimes were simulated and compared with each other (TABLES 1 and 2) based on fixed set points for day and night (BP_{fix}), common blueprint temperature control according to commercial practice (BP), temperature integration with a 24-hour averaging period (TI_{24}), and TI_{24} restricted by a targeted negative DIF ($TI_{24,DIF}$).

TABLE 1. Temperature regimes used for simulations of greenhouse climate and energy consumption based on two sided temperature bandwidth (b), and initial heating and ventilation temperature set points ($T_{h,init}$ and $T_{v,init}$). Targeted 24-hour mean temperature range with TI_{24} for calculation of $T_{h,init}$ and $T_{v,init}$ was 18.5±0.5 °C.

Regime	b	$T_{h,init}$ (minimum)	$T_{v,init}$ (maximum)
	(°C)	(°C)	(°C)
BP_{fix}	-	18.0	19.0
BP	-	18.0*	19.0**
$TI_{24} \pm 2$	2	16.5	20.5
$TI_{24} \pm 4$	4	14.5	22.5
$TI_{24} \pm 6$	6	12.5	24.5
$TI_{24} \pm 8$	8	10.5	26.5

*Linear increase during nighttime with daily global radiation sum (0.25 K per 1 MJ m^{-2} d^{-1} between 12 and 16 MJ m^{-2} d^{-1}). **Linear increase during daytime with outside global radiation (0.5 K per 100 W m^{-2} between 800 to 1200 W m^{-2}).

Fixed set points and blueprint regime: BP_{fix} for day and night with 1 °C margin between heating and ventilation were simulated (TABLE 1). In practice, however, the temperature regime is established according to the grower's experience and expectations of optimal crop growth, yield, quality etc.[207] and possibilities to implement this in a climate computer[237]. A blueprint regime (BP) is the result of that. In this regime daytime ventilation set points increased linearly with outside global radiation level (0.5 K per 100 W m^{-2} between 800 to 1200 W m^{-2}) and nighttime heating and ventilation set points increased linearly with daily global radiation sum (0.25 K per 1 MJ m^{-2} d^{-1} between 12 and 16 MJ m^{-2} d^{-1}).

24-hour temperature integration: A temperature integration procedure with a 24-hour averaging period (TI_{24}) was applied. To achieve comparable mean temperatures with TI_{24} as in BP and BP_{fix}, the same 24-hour mean target temperature range ($\overline{T}_{targ,24}$) of 18.5 °C with the same margin of ±0.5 °C was used as for heating and ventilation temperature in BP_{fix} and BP (TABLE 1). During each 24-hour cycle, temperature could fluctuate freely between the calculated heating and ventilation temperatures (T_h, T_v). To calculate the initial T_h ($T_{h,init}$) and T_v ($T_{v,init}$), the 24-hour target temperature and temperature bandwidth (b) were used (TABLE 1).

$$T_{v,init} = \overline{T}_{targ,24} + b \qquad [1]$$

$$T_{h,init} = \overline{T}_{targ,24} - b \qquad [2]$$

T_h and T_v were recalculated every 5 minutes. For that a receding horizon of 24 hours was applied. Subsequent 24-hourly greenhouse temperatures ($T_{in}(t_1..t_{24})$) with $T_{h,init}$ and $T_{v,init}$ as heating and ventilation set points were estimated with a simple equation (EQ. 4) at the beginning of each new 24-hour period (t_1, 8:00 a.m.). Greenhouse temperature was calculated without climate control actions (i.e. closed vents and no heating) as a function of outside global radiation (I_{out}, W m^{-2}), outside temperature (T_{out}, °C), diffuse transmission of the greenhouse cover (τ_{dif}) and overall greenhouse heat transmission coefficient (K, W m^{-2} °C^{-1}). K was assumed to be 4 or 8 W m^{-2} °C^{-1} with unfolded and folded screen, respectively.

$$T_{in}(t_1..t_{24}) = \begin{cases} T_{h,init} & if \quad T_{out}(t_1..t_{24}) + \frac{1}{3} \cdot \tau_{dif} \cdot \frac{I_{out}(t_1..t_{24})}{K(t_1..t_{24})} < T_{h,init} \\ T_{out}(t_1..t_{24}) + \frac{1}{3} \cdot \tau_{dif} \cdot \frac{I_{out}(t_1..t_{24})}{K(t_1..t_{24})} & if \quad T_{v,init} > T_{out}(t_1..t_{24}) + \frac{1}{3} \cdot \tau_{dif} \cdot \frac{I_{out}(t_1..t_{24})}{K(t_1..t_{24})} > T_{h,init} \\ T_{v,init} & if \quad T_{out}(t_1..t_{24}) + \frac{1}{3} \cdot \tau_{dif} \cdot \frac{I_{out}(t_1..t_{24})}{K(t_1..t_{24})} > T_{v,init} \end{cases}$$ [3]

T_{in} was updated each five minutes and averaged to $\overline{T}_{in}{}'$ at the actual time (t_a), with hourly means of realised greenhouse temperature logged in five minute sequence ($T_{in,real}$) from start of the 24-hour cycle (t_1).

$$\overline{T}_{in}{}' = mean\left[T_{in,real}(t_1..t_a), \quad T_{in}(t_{a+1}..t_{24}) \right]$$ [4]

T_h and T_v were then determined to achieve $\overline{T}_{targ,24}$ at the end of each 24-hour cycle (t_{24}). The initial temperature set points were used as long as $\overline{T}_{in}{}'$ was inside the targeted temperature bandwidth ($\overline{T}_{targ,24} \pm 0.5$ °C); otherwise heating or ventilation temperature set points were restricted to $\overline{T}_{targ,24} \pm 0.5$ °C.

$$T_v = \begin{cases} T_{v,init} & if \quad \overline{T}_{in}{}' \leq \overline{T}_{targ,24} + 0.5 \\ \overline{T}_{targ,24} + 0.5 & if \quad \overline{T}_{in}{}' > \overline{T}_{targ,24} + 0.5 \end{cases}$$ [5]

$$T_h = \begin{cases} T_{h,init} & if \quad \overline{T}_{in}{}' \geq \overline{T}_{targ,24} - 0.5 \\ \overline{T}_{targ,24} - 0.5 & if \quad \overline{T}_{in}{}' < \overline{T}_{targ,24} - 0.5 \end{cases}$$ [6]

When $\overline{T}_{in}{}'$ was smaller than $\overline{T}_{targ,24} - 0.5$, the possibility of shifting heating to nighttime under the screen for energy saving[39] was taken into account. Then, simulations where performed to determine the energetically optimal subsequent 24-hour course for T_h (taking maximum and minimum temperature with TI_{24} into account). For that, only temperature set points were taken into account, window aperture or heating due to set points for RH and interactions with temperature set points were neglected.

<u>24-hour temperature integration with negative *DIF*</u>: 24-hour mean temperature control as used in TI_{24} was applied for $TI_{24,DIF}$. Different negative *DIF* set points (DIF_{set}) of –2 °C, –4 °C, –6 °C, –8 °C, –10 °C, –12 °C and –16 °C *DIF* were used in addition. DIF_{set} was achieved by cooling the greenhouse through ventilation during daytime (number of daytime hours, h_d, was 11). Specific set points (TABLE 2) were applied to decrease temperature in order to achieve the desired *DIF* and $\overline{T}_{targ,24}$. During night, $\overline{T}_{targ,24}$ of 18.5 °C with an allowed deviation of ±0.5 °C (as used in *BP*, BP_{fix} and TI_{24}) had priority above *DIF* (night temperature compensated day temperature when necessary to achieve the desired 24-hour mean temperature). Under those conditions, T_h and T_v were computed according to the lower part of equations 7 and 8; set points during night were continuously (every 5 min.) adjusted to $T_{in,real}$ according to the procedure applied in TI_{24}. T_h and T_v were first calculated for daytime. The nighttime hours were used to compensate average daytime temperature.

$$T_h \rightarrow \begin{cases} T_h = (\overline{T}_{targ,24} - 0.5) + \dfrac{DIF_{set}}{24/(24 - h_d)} & if \quad t = \text{daytime} \\[3mm] (\overline{T}_{targ,24} - 0.5) - \sum_{t_1}^{t_a} \dfrac{T_{in,real}}{24} + T_h \cdot \dfrac{24 - t_a}{24} = 0 & if \quad t = \text{nighttime} \end{cases} \qquad [7]$$

$$T_v \rightarrow \begin{cases} T_v = (\overline{T}_{targ,24} + 0.5) + \dfrac{DIF_{set}}{24/(24 - h_d)} & if \quad t = \text{daytime} \\[3mm] (\overline{T}_{targ,24} + 0.5) - \sum_{t_1}^{t_a} \dfrac{T_{in,real}}{24} + T_v \cdot \dfrac{24 - t_a}{24} = 0 & if \quad t = \text{nighttime} \end{cases} \qquad [8]$$

SIMULATIONS

Energy consumption of cut chrysanthemum was simulated for temperature regimes of *BP*, BP_{fix}, TI_{24} and $TI_{24,DIF}$. Simulations were performed for a complete year round cut chrysanthemum greenhouse cultivation, starting January 01, 8:00 a.m. The greenhouse was assumed to be completely filled with plants the whole year through. Empty spaces resulting from harvesting were not taken into account. For simplification, a constant 12-week cultivation period with a constant three week short-day period was assumed, regardless season. To calculate energy consumption, 25 % of the greenhouse area was assumed to be under long-day and 75 % under short-day conditions. For that, two independent simulations were performed with either short-day or long-day conditions. Short-day was induced by a blackout screen unfolded between 7 p.m. and 8 a.m.; during the long-day period, an energy saving screen (SLS 10 plus, Ludvig Svensson, Kinna, Sweden) was applied between 7 p.m. and 8 a.m. when sunset was earlier than 7 p.m. or between sunset and 8 a.m.

TABLE 2. Daytime set points for heating and ventilation temperature (T_h and T_v) when applying 24-hour temperature integration with different negative DIF settings (DIF_{set}) ($TI_{24,DIF}$) during short-day period of 11 hours day-length. Targeted 24-hour mean temperature range for calculation of T_h and T_v was 18.5±0.5 °C, corresponding to set points for a zero DIF treatment when T_h = 18 °C and T_v = 19 °C.

Regime	Daytime settings (°C)		
	DIF_{set}	T_h	T_v
	(°C)	(°C)	(°C)
$TI_{24,DIF} - 2$	−2	16.92	17.92
$TI_{24,DIF} - 4$	−4	15.83	16.83
$TI_{24,DIF} - 6$	−6	14.75	15.75
$TI_{24,DIF} - 8$	−8	13.67	14.67
$TI_{24,DIF} - 10$	−10	12.58	13.58
$TI_{24,DIF} - 12$	−12	11.5	12.5
$TI_{24,DIF} - 16$	−16	9.33	10.33

when sunset was later than that. Relative humidity set point was set to 80 % and controlled with ventilation.

RESULTS

GENERAL REGIME BEHAVIOUR

Simulations with the different temperature regimes all reached the targeted 24-hour mean temperature range (18.5±0.5 °C) during winter (TABLE 3). The higher than 18 °C – 19 °C 24 -hour blueprint mean temperature in spring, summer and autumn was due to a natural increase of greenhouse temperature through solar radiation, not directly resulting in a higher energy consumption. Towards summer, greenhouse temperature for the blueprint regime increased to a maximum in June. Results for TI_{24} differed only slightly from that. A slightly higher 24-hour mean temperature was observed in most summer weeks with increasing temperature bandwidth in TI_{24}. $TI_{24,DIF}$ had almost the same realised mean temperature as BP during mid winter but was lower between early spring and late autumn. The yearly variation of 24-hour mean temperature differed only slightly between different temperature bandwidths in TI_{24} but decreased with DIF set point in $TI_{24,DIF}$ (TABLE 4). Realising the DIF set points in $TI_{24,DIF}$ was only possible during winter (FIG. 1). In that case, TI_{24} behaved almost similar to $TI_{24,DIF}$. In winter, temperature dropped during day and increased during night. Later in the year (spring, summer and autumn), achieving a negative DIF was not possible. In these seasons, realised DIF increased to higher positive
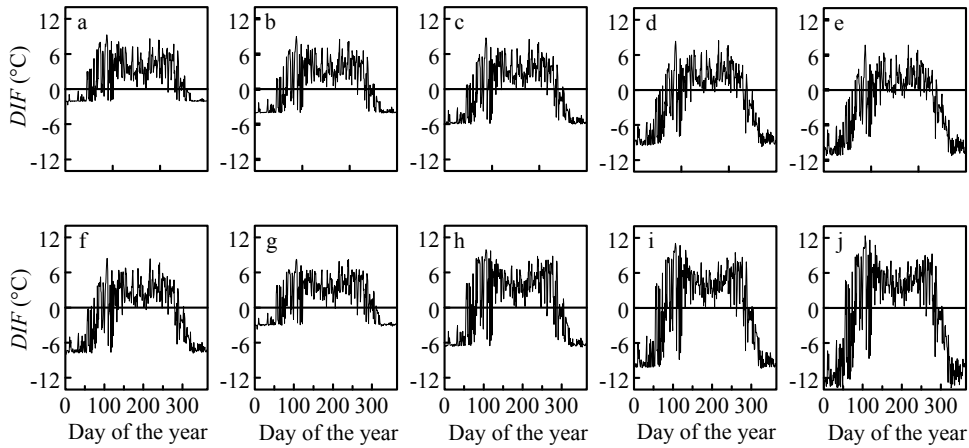
FIGURE 1. Realised *DIF* for simulated temperature regimes for cut chrysanthemum with 24-hour temperature integration with *DIF* settings ($TI_{24,DIF}$) (a - f); with $TI_{24,DIF} - 2$ (a), $TI_{24,DIF} - 4$ (b), $TI_{24,DIF} - 6$ (c), $TI_{24,DIF} - 8$ (d), $TI_{24,DIF} - 10$ (e) and $TI_{24,DIF} - 12$ (f) and with 24-hour temperature integration (TI_{24}) (g - j) with different temperature bandwidths; with $TI_{24} \pm 2$ (g), $TI_{24} \pm 4$ (h), $TI_{24} \pm 6$ (i) and $TI_{24} \pm 8$ (j).

values for TI_{24} compared to a negative *DIF* set point with $TI_{24,DIF}$. In summer, the achieved positive *DIF* was lower than during spring and autumn for all regimes, but mean temperature was higher (FIG. 1, TABLE 3).

TABLE 3. Simulated weekly means of realised temperatures during short-day application for blueprint regime (*BP*), 24-hour temperature integration with 2 °C and 6 °C bandwidths ($TI_{24} \pm 2$, $TI_{24} \pm 6$) and negative *DIF* regimes with a set point difference between average day and night temperatures of 4 °C and 12 °C ($TI_{24,DIF} - 4$, $TI_{24,DIF} - 12$).

Week of the year	BP	$TI_{24} \pm 2$	$TI_{24} \pm 6$	$TI_{24,DIF} - 4$	$TI_{24,DIF} - 12$
			Temperature regime		
1	18.0	18.0	18.1	18.0	18.0
5	18.1	18.0	18.1	18.0	18.0
9	18.5	18.2	18.3	18.0	18.0
13	20.1	19.5	19.3	18.0	18.0
17	19.1	18.6	18.8	18.1	18.0
21	22.5	22.3	22.8	18.4	18.1
25	23.4	23.6	23.9	22.5	21.7
29	22.3	22.4	22.4	21.4	20.5
33	23.6	23.6	23.5	22.9	22.1
37	20.4	20.6	21.9	19.3	19.0
41	19.0	18.4	18.8	18.0	18.0
45	18.3	18.0	18.1	18.0	18.0
49	18.0	18.0	18.1	18.0	18.0

155
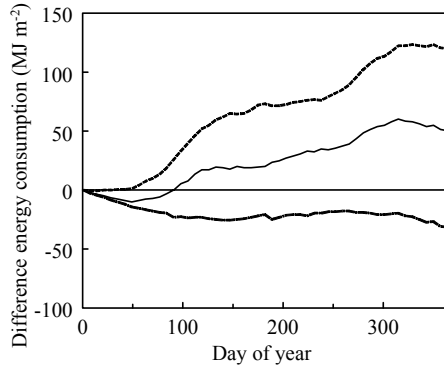
FIGURE 2. Difference in cumulative energy consumption between temperature integration treatments and negative DIF settings with the same potential temperature bandwidths ($TI_{24,DIF} - 4$ and $TI_{24} \pm 2$ (---), $TI_{24,DIF} - 8$ and $TI_{24} \pm 4$ (—), $TI_{24,DIF} - 12$ and $TI_{24} \pm 6$ (---).
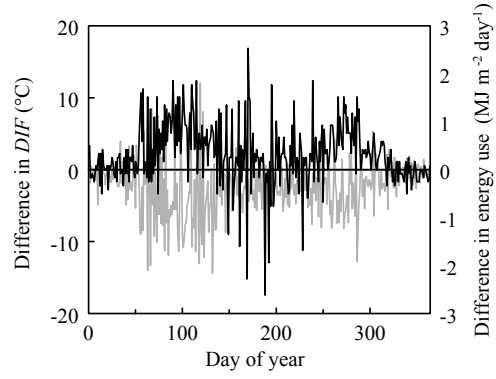
FIGURE 3. Difference in weekly mean DIF (grey line) and difference in energy demand (black line) per day between 24-hour temperature integration with ± 6 °C bandwidth ($TI_{24} \pm 6$) and 24-hour temperature integration with a negative DIF regime with -12 °C DIF set point ($TI_{24,DIF} \pm 12$).

ENERGY SAVING

Annual energy consumption was slightly higher for *BP* compared to BP_{fix} (0.4 %). The two flexible regimes (TI_{24} and $TI_{24,DIF}$) reduced energy consumption compared to the blueprint regime in winter and spring with all applied bandwidths (TABLE 5). Simulations showed that temperature control with TI_{24} and $TI_{24,DIF}$ could decrease annual energy consumption compared to a blueprint regime (TABLE 5). Highest energy saving was achieved in spring and autumn with TI_{24}. Energy consumption was slightly higher for TI_{24} regimes with narrow temperature bandwidths ($\leq \pm 2$ °C) compared to $TI_{24,DIF}$ with a potential similar temperature flexibility of e.g. -4 °C *DIF* in winter and early spring (TABLE 5). The difference in annual energy consumption

TABLE 4. Simulated yearly means ($\overline{T}_{in,real}$, °C) and relative coefficient of variance (CV, %) of realised 24-hour mean temperature for the blueprint regime (*BP*), for 24-hour temperature integration (TI_{24}) and 24-hour temperature integration including negative *DIF* ($TI_{24,DIF}$), with different temperature bandwidths (*b*) and *DIF* settings (DIF_{set}), respectively.

b / DIF_{set}	Temperature regime						
	BP	TI_{24}			$TI_{24,DIF}$		
	± 0.5 °C*	± 2 °C	± 4 °C	± 6 °C	-4 °C	-8 °C	-12 °C
$\overline{T}_{in,real}$	20.05	19.86	19.88	20.07	19.34	19.25	19.06
CV	1.50	1.58	1.62	1.58	1.45	1.34	1.29

*Linear increase of heating and ventilation set points during nighttime with daily global radiation sum (0.25 K per 1 MJ m^{-2} d^{-1} between 12 and 16 MJ m^{-2} d^{-1}) and linear increase during of ventilation set point daytime with outside global radiation (0.5 K per 100 W m^{-2} between 800 to 1200 W m^{-2}).

TABLE 5. Weekly and annual energy consumption (E-cons., MJ m^{-2} week^{-1} and GJ m^{-2} year^{-1}) for different temperature regimes with blueprint regime (BP), 24-hour temperature integration with different temperature bandwidths (b) ($TI_{24} \pm b$) and 24-hour temperature integration with different negative *DIF* set point (DIF_{set}) ($TI_{24,DIF} - DIF_{set}$).

Regime	E-cons. (MJ m^{-2})						E-cons. (GJ m^{-2})
	Week number						1 – 52
	1	6	11	16	21	26	
BP	62.0	49.0	33.7	17.1	8.3	6.5	1.33
$TI_{24} \pm 2$	60.9	46.7	31.3	11.8	7.1	5.9	1.22
$TI_{24} \pm 4$	59.1	44.3	27.8	9.5	7.1	5.9	1.13
$TI_{24} \pm 6$	56.1	42.5	26.6	9.5	7.1	5.9	1.09
$TI_{24} \pm 8$	56.1	42.0	26.0	8.9	7.1	5.9	1.07
$TI_{24,DIF} - 2$	60.3	46.7	30.7	12.4	7.1	7.1	1.23
$TI_{24,DIF} - 4$	58.5	44.9	30.1	12.4	7.1	7.1	1.18
$TI_{24,DIF} - 6$	57.3	43.1	29.0	13.0	7.7	5.9	1.18
$TI_{24,DIF} - 8$	56.7	43.1	29.0	15.4	5.9	6.5	1.18
$TI_{24,DIF} - 10$	55.5	42.5	29.0	16.0	11.2	7.7	1.19
$TI_{24,DIF} - 12$	55.0	42.5	30.1	16.0	11.2	7.1	1.21
$TI_{24,DIF} - 16$	55.5	44.3	32.5	17.1	11.2	8.9	1.27

between TI_{24} and $TI_{24,DIF}$ with the same initial temperature bandwidth, however, increased with increasing temperature bandwidth (FIG. 2). The differences in realised *DIF* and energy consumption between TI_{24} and $TI_{24,DIF}$ for a temperature bandwidth of ±6 °C or –12 °C DIF_{set} were basically negatively correlated (FIG. 3). This indicates that the achievement of a negative *DIF* with $TI_{24,DIF}$ had to be paid by an increase in energy consumption compared to TI_{24}. The highest difference in energy saving between a common TI_{24} and $TI_{24,DIF}$ with the same potential temperature margin was observed in spring and autumn (FIG. 4). With a temperature bandwidth of e.g. ±6 °C in TI_{24}, weekly energy saving could increase to almost 60 % in autumn. With $TI_{24,DIF}$, on the other hand, energy saving was only 32 % and 9 % for e.g. –6 °C and –12 °C DIF_{set} during the same week, respectively.

Energy consumption clearly decreased with increasing temperature bandwidth in TI_{24} for crops grown during winter and early spring (TABLE 5, FIG. 5). The absolute additional benefit, however, decreased with temperature bandwidth. Annual energy consumption decreased with increasing temperature bandwidth for TI_{24}, too, but resulted in an optimum annual energy saving level between –6 °C and –8 °C DIF_{set} for $TI_{24,DIF}$ (FIG. 6). Similar behaviour was observed with independent 12-week cultivations (FIG. 5). Fitted functions explain the relationship between energy
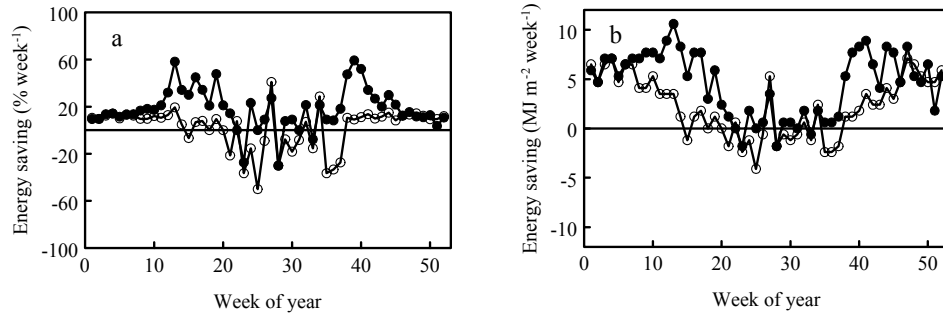
FIGURE 4. Weekly energy saving in percent (a) and in absolute terms (b) of 24-hour temperature integration with a temperature bandwidth of ±6 °C ($TI_{24} \pm 6$, ●) and 24-hour temperature integration with a negative *DIF* setting of –12 °C ($TI_{24,DIF} - 12$, ○) compared to the blueprint regime (*BP*).

consumption and temperature bandwidth or *DIF* set point for separate cultivations and a complete year (FIG. 5 and FIG. 6, respectively). Energy consumption decreased exponentially with temperature bandwidth with TI_{24} annually and in winter and spring ($x_1 + x_2 \cdot \exp(-b/x_3)$). Quadratic responses were found for TI_{24} in summer and for with $TI_{24,DIF}$ in all seasons. At the crossing point of one pair of related functions for TI_{24} and $TI_{24,DIF}$, energy consumption was the same for TI_{24} and $TI_{24,DIF}$ with the same potential temperature bandwidth. This was ±2.4 °C for TI_{24} or –4.8 °C *DIF*_set annually, and ±4.2 °C / –8.4 °C, ±1.8 °C / –3.6 °C, ±0.3 °C / –0.6 °C, ±0.3 °C / –0.6 °C for independent 12-week cultivations with plantings 01 January, 01 March, 01 May and 01 July, respectively. During spring and autumn, relative energy saving was the highest for TI_{24} and the difference to $TI_{24,DIF}$ increased. In these seasons temperature increased during day and decreased during night to achieve the targeted 24-hour mean temperature almost without heating for TI_{24}. A typical spring and autumn day is illustrated in FIG. 7. In TI_{24} most energy consumption was then due to CO_2 dosage. In contrast, $TI_{24,DIF}$ resulted in ventilation
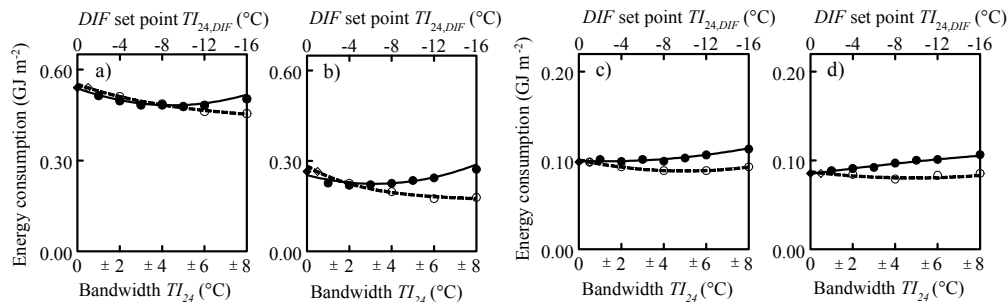
FIGURE 5. Cumulative energy consumption (GJ m^{-2}) for separate 12-week cut chrysanthemum cultivation with planting on 01 January (a), 01 March (b), 01 May (c) and 01 July (d) for blueprint regime (*BP*) regarding temperature bandwidth (⬅) or *DIF* (⬅), 24-hour temperature integration with different temperature bandwidths (TI_{24}, ↓) and 24-hour temperature integration with different negative *DIF* set point ($TI_{24,DIF}$, ⬇); with curve fittings for TI_{24} (---) and $TI_{24,DIF}$ (—).
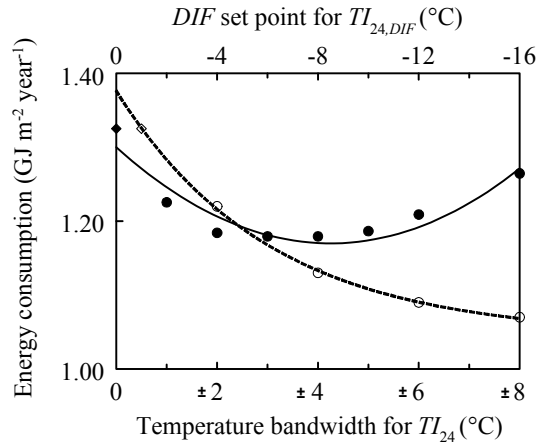
FIGURE 6. Annual cumulative energy consumption (GJ m^{-2}) for blueprint regime (*BP*) regarding temperature bandwidth (⬅) or *DIF* (⇐), 24-hour temperature integration with different temperature bandwidths (TI_{24}, ↓) and 24-hour temperature integration with different negative *DIF* set point ($TI_{24,DIF}$, ⬇); with exponential and polynomial curve estimations for annual energy consumption for TI_{24} (---, $E_{TI_{24}} = 1.045 + 0.332 \cdot \exp(-b/3.032)$, R^2 = 0.99) and $TI_{24,DIF}$ (—, $E_{TI_{24,DIF}} = 0.0018 \cdot DIF_{set}^2 + 0.0306 \cdot DIF_{set} + 1.299$, R$^2 = 0.89$).

during the whole day period to reduce the temperature level to achieve a negative *DIF*. Heating pipes had to warm up the greenhouse during nighttime to compensate for the relative cool day to achieve the targeted 24-hour mean temperature. Due to that, energy consumption was more than two times higher for $TI_{24,DIF}$ with a set point of –12 °C *DIF* than for TI_{24} with ±6 °C temperature bandwidth (FIG. 7). Towards the end of the night period the energy consumption increased for $TI_{24,DIF}$ with DIF_{set} of –12 °C, because the cumulative heat demand at that moment was higher than the capacity of the heat buffer.
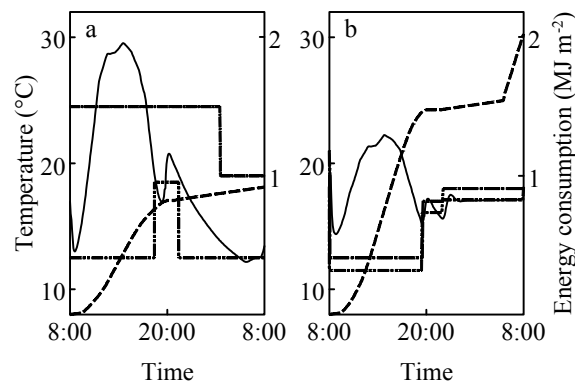
FIGURE 7. Simulations of realised greenhouse temperature (—), ventilation set point (- - -) and heating set point (- - - -), and daily cumulative energy consumption (- - -) for 24 hours from day 85 to 86 of the year for 24-hour temperature integration with ±6 ºC bandwidth ($TI_{24} \pm 6$) (a) and 24-hour temperature integration with negative *DIF* regime with a set point of –12 ºC *DIF* ($TI_{24,DIF} \pm 12$) (b).

159

DISCUSSION

Simulated annual energy consumption for the blueprint regime (1.33 GJ m^{-2} year^{-1}) was close to that reported for cut chrysanthemum practice (1.41 or 1.55 GJ m^{-2} year^{-1})[174, 175], which supports the validity of the simulations. The small differences can occur from many factors as e.g. differences in the blueprint regimes, greenhouse structures or equipment. Simulations showed that energy consumption was reduced compared to a blueprint regime with both dynamic temperature regimes (TI_{24} and $TI_{24,DIF}$). The most crucial aspect of applying TI_{24} is the achievement of the desired 24-hour mean temperature to ensure to keep crop growth, development and quality as with regular temperature control[39]; whereas the most crucial aspect of $TI_{24,DIF}$ is the simultaneous achievement of 24-hour mean temperature and the targeted negative DIF. The different approaches led to differences in greenhouse climate and energy consumption in some moments and resulted in the same in others. Between spring and autumn, TI_{24} could compensate warm days with high peak temperatures by cool nights and therefore refrain from heating, as it is the aim with temperature integration[42]. In contrast, $TI_{24,DIF}$ aimed to cool down daytime temperature to be able to warm up the greenhouse during night to achieve a negative DIF. This is necessary when stem-elongation should be reduced by temperature control[23]. The highest absolute energy savings were possible in winter with heating under energy screens as is commonly known[39, 56]. During the cold season, $TI_{24,DIF}$ behaved almost similar to TI_{24}. An imbalance between the lengths of day and night in $TI_{24,DIF}$ during the short-day period, however, led to wider actual temperature bandwidths with $TI_{24,DIF}$ than with TI_{24}. In $TI_{24,DIF}$, an 11 hours day period had to compensate 13 hours night, whereas a fixed lower boundary of $\overline{T}_{targ,24} - b$ was used in TI_{24}. This led to lower energy demand for $TI_{24,DIF}$ compared to TI_{24} with narrow potential temperature bandwidths. This effect, however, was overruled by the effect of a higher temperature flexibility with TI_{24} compared to $TI_{24,DIF}$ when temperature bandwidths were wider. The second effect was only stronger when outside climate was too mild to cool down greenhouse temperature below the heating set point without ventilation.

Under mild climate conditions with $TI_{24,DIF}$, vents were opened for long periods during day to reduce the air temperature to achieve the targeted negative DIF. During night, heating and therefore energy had to be used to compensate that. With TI_{24}, on the other hand, the optimum temperature trajectory for energy saving was continuously calculated and set points were adjusted accordingly. Vents were kept closed during day and less nighttime heating was used compared to $TI_{24,DIF}$.

When outside day temperature was cold enough to cool down the greenhouse below the heating set point without ventilation, TI_{24} and $TI_{24,DIF}$ had the same energy consumption. Then, heating had to be used during daytime for both regimes.

In spring, summer and autumn, the two regimes behaved completely different compared to winter. Relatively highest energy savings could be achieved with TI_{24} in

spring and autumn according to the expectations with temperature integration[39, 56], because then the freedom for temperature fluctuation in TI_{24} has it's highest benefit. Accordingly, the disadvantage for energy demand of a negative *DIF* compared to TI_{24} was highest during these seasons.

CONCLUSIONS

It is concluded that TI_{24} and $TI_{24,DIF}$ can be applied in winter with similar impact on energy saving demand when using an energy screen. In spring and autumn, however, negative *DIF* restricts temperature integration in its potential for energy saving. When applying a negative *DIF* for stem length control, the increasing energy costs compared to TI_{24} have to be taken into account. Simulations showed that between –6 °C and –8 °C DIF_{set} annual energy saving was maximised when applying $TI_{24,DIF}$. However, for a more detailed decision whether to apply TI_{24} or $TI_{24,DIF}$ with which temperature bandwidth or DIF_{set}, the actual cultivation period is the most important criterion. Controlling stem length with a negative *DIF* in spring and autumn has the highest additional costs, almost no negative *DIF* control is possible in summer, and during winter TI_{24} and $TI_{24,DIF}$ result in an almost similar greenhouse climate. During the coldest periods in the year, a very low negative DIF_{set} of –12 °C or –16 °C can be more advantageous for energy saving than a higher one. With less extreme winter temperatures, however, such an extreme DIF_{set} increases energy consumption. For the best decision what kind of temperature control regime to use at which time of the year, a well performing crop quality model for cut chrysanthemum[26, 27] would be needed. A dynamic crop growth and quality model connected to an economical model estimating the monetary value of stem-length in comparison to the energy costs could then be used for decision support.

3.5 Temperature integration and *DIF* in cut chrysanthemum

O. Körner & H. Challa
Temperature integration and *DIF* in cut chrysanthemum
Journal of Horticultural Science and Biotechnology (in press)

ABSTRACT

To reduce energy consumption in greenhouses temperature integration can be used. However, the temperature integration principle considers only average temperatures and does not comply with the *DIF* concept (difference between mean day temperature and mean night temperature). With *DIF*, stem elongation, one of the major quality aspects of many crops, can be controlled. Short compact plants can be achieved by a negative *DIF* (average night temperature > average day temperature). In spring, summer and autumn temperature integration usually results in positive *DIF* and therefore longer stems. The aim of this study was to investigate whether temperature integration and *DIF* could be applied simultaneously. Greenhouse temperature fluctuates with temperature integration. During spring or autumn it is difficult to obtain short compact plants by a negative *DIF* with regular temperature integration. In this research, temperature integration was therefore modified by applying two independent integration regimes, one for daytime and one for nighttime while a zero

DIF was set. Simulations and experiments with standard temperature control, regular and modified temperature integration showed that temperature integration and *DIF* could be applied simultaneously, while energy consumption and stem elongation were reduced.

INTRODUCTION

In Dutch greenhouse horticulture, production costs and energy consumption are becoming more and more important. The greenhouse industry is aiming at low energy greenhouse concepts while keeping yield and quality on a high level. One possibility to reduce energy consumption is to control mean rather than instantaneous temperature leaving a wide bandwidth between heating and ventilation temperature set points. This concept is widely known as temperature integration principle[167]. Temperature integration can easily be applied in greenhouses by refraining from climate control. Greenhouses can heat up through solar radiation during day when ventilation is reduced. Temperature can drop during night with reduced heating to achieve the targeted mean temperature. In general, the temperature integral can be maintained at its desired level while heating is shifted to periods of lower costs[36]. In winter when daytime solar radiation is low and greenhouses do not heat up naturally, energy consumption can be reduced by 12 % – 15 % when heating is shifted to night under energy screens[39, 55]. In autumn or spring 30 % – 40 % energy saving is possible during sunny days, when greenhouses can heat up during day and consequently no or only marginal heating during night is required[39, 56].

Temperature integration is a tool to decrease energy consumption, but it can conflict with other goals in climate control. Prices for ornamental crops as cut chrysanthemum are often related with external quality (e.g. stem and internode length, leaf number, leaf area, flower-number, -size and -mass)[238]. One of the main aspects in this matter is the achievement of short compact chrysanthemum plants[26]. To reduce internode length to achieve short compact plants, environmental unfriendly chemical growth inhibitors could be used[75]. For environmental reasons, this has to be reduced in the same way as energy consumption[74, 231, 232]. Therefore, the *DIF* concept (difference between average day temperature, DT and average night temperature, NT)[73] is largely applied. Negative *DIF* (i.e. NT > DT) results in short internodes and compact plants whereas positive *DIF* results in the opposite[74]. However, a positive *DIF* usually occurs with *TI* between spring and autumn in moderate climates such as in The Netherlands. Then, greenhouse temperature increases during day and decreases during night and due to that internodes elongate. The effect of temperature on stem elongation, nevertheless, is still not fully understood and this leads to uncertainties of temperature control[74, 75]. It was repeatedly reported that internode elongation responds to independent effects of DT and NT[74, 231]. However, if it is possible to integrate this

effect over time has not been reported in literature. Because plant development in general with its underlying processes as e.g. leaf unfolding rate depends on mean temperature[68] and can be integrated over time, it could be hypothesised that stem elongation as morphological parameter may respond to timely integrated effects of DT and NT. Then, *TI* could be modified and joined with the *DIF* concept. It could be possible to compensate warm days by cool days and warm nights by cool nights (not days by nights and *vice versa*). Then, a certain zero or negative mean *DIF* could probably be maintained.

The main aim of this study was to reduce energy consumption while achieving short compact cut chrysanthemum plants. A first evaluation of a regime to simultaneously control temperature with *TI* and *DIF* is introduced to show future possibilities for climate control in chrysanthemum. The regime consists of completely independent sub-regimes of mean day and mean night temperatures over several days and a zero *DIF*. It is presented and tested with simulations and greenhouse experiments.

MATERIALS AND METHODS

Three different climate regimes were investigated in simulations and in greenhouse experiments. A reference blueprint climate regime according to commercial practice (*BP*), a regular temperature integration regime (*TI*) and a temperature integration regime including a zero *DIF* treatment (TI_{DIF}) were investigated with respect to energy consumption, greenhouse climate, crop growth and development and stem elongation.

REFERENCE CLIMATE REGIME

In practice, the temperature regime is established according to the grower's experience and expectations of optimal crop growth, yield, quality etc.[207] and possibilities to translate those by the climate computer[237]. Usually, ventilation temperature set points (temperature where the vents start opening) increase with instantaneous radiation or daily radiation sum. In *BP* initial heating and ventilation set points were respectively set to 18.5 °C and 19.5 °C during day and 19.5 °C and 20.5 °C during night for greenhouse experiments, and to 18.5 °C and 19.5 °C for day and night for simulations. The daytime ventilation set point increased by instantaneous global radiation outside the greenhouse (0.5 K per 100 W m^{-2} between 800 and 1200 W m^{-2}). Nighttime heating and ventilation set points increased by global daily radiation sum of the preceding light period (0.25 K per 1 MJ m^{-2} d^{-1} between 12 and 16 MJ m^{-2} d^{-1}).

TEMPERATURE INTEGRATION

A regular temperature integration procedure with a six day temperature averaging period was applied, because *TI* with an averaging period of several days has a higher possibility for energy saving. A six-day averaging period is applicable for many ornamental crops such as roses and cut chrysanthemum[239]. Temperature bandwidths (margin between heating and ventilation set point for temperature control) of ±2 °C, ±4 °C, ±6 °C and ±8 °C were applied for separate simulations and greenhouse experiments. Temperature during each day (24 hours) compensated deviations of average temperature during the preceding five days. The procedure used a receding horizon of 24 hours, i.e. each new 24-hour period the preceding 5 day period was evaluated and compensated at day six of the integration period. Temperature history older than five days was not taken into account for control. Target mean temperature for each 24-hour period ($T_{set,24}$) for day six (d_{24}^{+1}) was calculated at the beginning of each day to achieve the overall targeted mean temperature (T_{targ}) over the complete integration interval (t_{int}, i.e. averaging period). $T_{set,24}$ was calculated by the difference of the accumulated 24-hour mean record of previously realised temperatures ($\overline{T}_{real}$) during the past five 24-hour periods (d_{24}) and the desired temperatures ($\overline{T}_{des}$) over t_{int} (EQ. 1).

$$T_{set,24}(d_{24}^{+1}) = \sum_{1}^{t_{int}} \overline{T}_{des}(d_{24}) - \sum_{1}^{t_{int}-1} \overline{T}_{real}(d_{24}) \qquad [1]$$

Actual heating and ventilation set points were calculated from $T_{set,24}$, the given temperature bandwidth and the difference between realised and targeted mean temperatures over the six-day averaging period. A proportional back-regulation of the temperature bandwidth towards $T_{set,24}$ to achieve T_{targ} was used (CHAPTER 3.1).

TEMPERATURE INTEGRATION AND ZERO *DIF*

The *DIF* concept was connected with temperature integration to form a new temperature regime (TI_{DIF}). Temperature integration regimes with an averaging period of six days or six nights were applied for DT and NT, respectively. The difference between average DT and average NT was set to 0, i.e. a zero *DIF*. Target mean temperatures for daytime and nighttime, $T_{set,day}$ and $T_{set,night}$ were calculated at the beginning of the actual day or night time similar to EQ. 1.

$$T_{set,day}(d^{+1}) = \sum_{1}^{t_{int}} \overline{T}_{des}(d) - \sum_{1}^{t_{int}-1} \overline{T}_{real}(d) \qquad [2]$$

$$T_{set,night}(n^{+1}) = \sum_{1}^{t_{int}} \overline{T}_{des}(n) - \sum_{1}^{t_{int}-1} \overline{T}_{real}(n) \qquad [3]$$

with daytime period (*d*), nighttime period (*n*), subsequent daytime (d^{+1}) and subsequent nighttime (n^{+1}).

<div align="center">SIMULATIONS</div>

The three regimes (*BP, TI* and *TI*$_{DIF}$) were implemented in a simulation model of the greenhouse crop system developed in the technical software environment MATLAB$^{®}$ (version 6.0, MathWorks, Natick, MA, USA). This model functioned as a set point generator (SPG). The SPG was coupled with a greenhouse climate and control model[105] (CCM) of a typical 1-ha Venlo-type greenhouse with a single glass cover (transmission for diffuse radiation of 78.5 %) and a blackout screen. A representative one-year reference climate data set for De Bilt[177] (The Netherlands, lat. 52 °N) was used for simulations on yearly dynamics of greenhouse climate and energy consumption. Temperature, relative humidity and CO_2 concentration inside the greenhouse and outside global radiation were calculated by the CCM and were input to the SGR. The SGR provided temperature set points for heating and ventilation, relative humidity, CO_2 concentration and screening to the CCM. Data were exchanged between SGR and CCM in a simulation time step of five minutes. The internal time step for climate simulation in the CCM was two minutes. Simulations were performed for four different planting dates (day 61, 121, 182 and 246 of the year) for a 12-week cut chrysanthemum cultivation for the three mentioned temperature regimes. *TI* and *TI*$_{DIF}$ were simulated with temperature bandwidths of ±2 °C, ±4 °C and ±6 °C. RH was set at 80 % and CO_2 was dosed to 1000 µmol mol^{-1} during day when ventilation was closed and outside global radiation was above 40 W m^{-2} and otherwise to a minimum of 350 µmol mol^{-1}.

<div align="center">GREENHOUSE EXPERIMENTS</div>

<u>Experimental lay-out:</u> Three experiments (EXPT. 1, EXPT. 2 and EXPT. 3) were performed in four almost identical greenhouse compartments (12.8 x 12.0 m) within a multi-span Venlo-type greenhouse at Wageningen University, The Netherlands (lat. 52 °N). The compartments A, B, C and D were neighbouring each other in an ascending row from A (west) to D (east). Greenhouse compartments A, B and C consisted of one outside wall (south) and greenhouse compartment D of two outside (east and south) and two inside walls.

Different *TI* bandwidths with optimal heating and ventilation set points (CHAPTER 3.1) where compared to each other in EXPT. 1. *TI* with temperature bandwidths of ±2 °C, ±4 °C, ±6 °C and ±8 °C was applied in greenhouse compartments B, A, C and D, respectively. The desired set point of the 24-hour mean temperature was the same as that of a simultaneous simulated reference regime. In EXPT. 2, *TI* with ±6 °C

TABLE 1. Simulated average realised greenhouse temperature ($\overline{T}_{real}$, °C) for a 12-week cut chrysanthemum cultivation with different planting dates (DOP) for the reference climate regime (*BP*, including average heating set point ($\overline{T}_{heat}$), and temperature integration (*TI*) and temperature integration with zero *DIF* (TI_{DIF}) with three different temperature bandwidths (*b*). Targeted six-day mean temperature for temperature integration was 19.0 °C, heating and ventilation set points for *BP* were initially set to 18.5 °C and 19.5 °C, respectively.

			Temperature regime					
	BP		*TI*			TI_{DIF}		
b (°C)	±0.5*		±2	±4	±6	±2	±4	±6
DOP	$\overline{T}_{heat}$	$\overline{T}_{real}$				$\overline{T}_{real}$		
1	18.50	18.7	18.9	18.9	18.8	19.0	18.8	18.8
61	18.50	20.3	19.7	19.4	19.3	19.7	19.6	19.5
121	18.51	23.4	22.7	22.2	21.9	21.9	21.9	21.9
182	18.51	23.2	22.6	22.1	21.8	21.9	21.9	21.9
246	18.50	19.6	19.3	19.1	18.9	19.3	19.2	19.0

*Linear increase of daytime temperature ventilation set point by instantaneous outside global radiation (0.5 K per 100 W m^{-2} between 800 and 1200 W m^{-2}) and nighttime heating and ventilation set points by outside global daily radiation sum of the preceding light period (0.25 K per 1 MJ m^{-2} d^{-1} between 12 and 16 MJ m^{-2} d^{-1})

temperature bandwidth was applied in greenhouse compartments A and C, and *BP* was applied in greenhouse compartments B and D. $\overline{T}_{des}$ for *TI* was made equal to the average of the two *BP* compartments. In EXPT. 3, TI_{DIF} with ± 6 °C temperature bandwidths for separate day and night and *BP* were applied in greenhouse compartments B and C, respectively. Because flower initiation in chrysanthemum is very sensitive to temperature fluctuations, temperature set points for *TI* and TI_{DIF} were set according to the reference regime until the first flower bud was clearly visible (i.e. ca. three weeks).

Plant material and climate conditions: Cut chrysanthemum plants 'Reagan Improved' obtained from a commercial propagator (Fides Goldstock Breeding, Maasland, The Netherlands) were transplanted in four (EXPT. 1 and EXPT. 2) and two greenhouse compartments (EXPT. 3) on 24.08.2001 (EXPT. 1), 06.02.2002 (EXPT. 2) and 06.09.2000 (EXPT. 3) at a density of 64 plants m^{-2}. Greenhouse compartments consisted of eight parallel soil beds (each 1.13 x 10.25 m) and plants were treated with an 18-hour long-day period until plants had 16 leaves. After that, short day of 13 hours night period was induced with blackout-screens. Compartments were heated with upper and lower heating pipes and equipped with pure CO_2 supply. CO_2 was set to a minimum of 350 μmol mol^{-1} in EXPT. 1. CO_2 in EXPT. 2 and EXPT. 3 was controlled according to ventilation and radiation. A minimum of 350 μmol mol^{-1} CO_2 was maintained when vents were open and below an outside global radiation (I_{out}) threshold of 40 W m^{-2}. When vents were closed and I_{out} was higher than 40 W m^{-2}, a

concentration of 1000 μmol mol^{-1} CO_2 was maintained. Relative humidity (RH) in the greenhouses was controlled with ventilation. RH was between 79 and 98 % in all experiments and treatments. Temperature, RH and CO_2 concentration were automatically recorded every five minutes by a commercial computer system (VitaCo, Hoogendoorn, Vlaardingen, The Netherlands). In greenhouse compartments of EXPT. 2 and 3, assimilation light (SON-T AGRO, Philips, Eindhoven, The Netherlands) with 9.6 W m^{-2} photosynthetic active radiation (PAR) was used throughout the light period when outside global radiation fell below 150 W m^{-2} and switched off again at 200 W m^{-2}. No assimilation light was used in EXPT. 1.

Energy consumption of greenhouse compartments B and C was calculated by measuring water flux in the heating pipes with an electromagnetic flowmeter (MagMaster, ABB Kent-Taylor Ltd., Cambridgeshire, England) and temperature difference between in and out flux to the greenhouse compartments (isolated PT 100 thermometers mounted on the heating-pipes with thermoconductive gel). Data were measured every 10 seconds and averaged over 5 minutes and stored in a data logger (Hewlett Packard, Englewood, CO, USA) between day of year 38 − 108 and 261 − 311 for EXPT. 2 and EXPT. 3, respectively.

Weekly harvest of 24, 12 and 12 plants (EXPT. 1, EXPT. 2 and EXPT. 3, respectively) distributed over six planting beds was performed. Fresh- and dry weight (drying oven at 105 °C for two cycles of 16 hours) of leaves, stems and flowers, and stem length, leaf number and flower number from each plant was evaluated. Leaf area was measured with a leaf area meter (LI 3100, LI-COR, Lincoln, NE, USA).

RESULTS

GENERAL REGIME BEHAVIOURS

Simulated and measured greenhouse temperature differed only little between the two temperature integration treatments (TABLE 1 and TABLE 2). Average simulated greenhouse temperature generally decreased with temperature bandwidth in *TI* (TABLE 1). In TI_{DIF}, this was only observed in early spring and late autumn. Measured mean greenhouse temperature decreased with temperature bandwidth in *TI* from ±4 °C to ±8 °C, too (TABLE 2). The temperature decrease, however, was small. Averages of 0.13 °C and 0.13 °C with *TI* (EXPT. 1 and simulations, respectively) and 0.07 °C with TI_{DIF} per ±1 °C temperature bandwidth was found (TABLE 1 and TABLE 2). Towards summer, simulated greenhouse temperature with the reference regime increased more than *TI* and TI_{DIF}.

Simulations showed that the difference in realised *DIF* between *TI* and TI_{DIF} strongly increased with increasing temperature bandwidth in spring (FIG. 1). The opposite was

TABLE 2. Realised average greenhouse temperature during the experimental period in greenhouses with planting day (DOP) for a reference climate regime (BP), temperature integration with different temperature bandwidths (b) and temperature integration with zero DIF ($TI_{\pm 2,DIF}$, $TI_{\pm 4,DIF}$, $TI_{\pm 6,DIF}$). Targeted six-day mean temperature for temperature integration was calculated from BP (EXPT. 2 and 3) or from a simulated blueprint regime (EXPT. 1).

		Climate regime					
		BP	TI				TI_{DIF}
b (°C)		±0.5	±2	±4	±6	±8	±6
EXPT.	DOP						-
1	236/01	-	19.6	19.8	19.4	19.3	-
2	37/02	20.3	-	-	19.7	-	-
3	249/00	20.0	-	-	-	-	20.0

observed in summer. Then, realised DIF with TI and TI_{DIF} differed only slightly with high temperature bandwidths. In both seasons, realised DIF changed only little with temperature bandwidth in TI_{DIF}. With TI, DIF strongly increased in winter and little in summer.

Experiments showed that mean 6-day, mean 6-night temperatures and DIF differed only slightly between BP and TI_{DIF} (FIG. 2). When TI was applied without concerning about DIF, there was a strong difference between day and night temperatures and a remarkable DIF of up to 10 towards spring. Mean temperatures over 6 days or 6 nights did not differ significantly between the respective reference regime and TI or TI_{DIF}.

INFLUENCE OF TEMPERATURE REGIMES ON PLANTS

The difference in total accumulated dry weight of chrysanthemum plants between TI_{DIF} and BP was less than 1 % in the greenhouse experiment (TABLE 3). Also dry weight distribution, leaf area index and specific leaf area were only slightly affected. TI had a distinct influence on stem length (EXPT. 1, TABLE 4; EXPT. 2, FIG. 3). Stem length and mean internode length increased with increasing temperature bandwidth for temperature integration (TABLE 4). Using two independent temperature integration regimes for day- and nighttime with a zero mean DIF treatment (TI_{DIF}) did result in a much lower stem length increase compared to the reference temperature regime (BP) (FIG. 3). In EXPT. 3, stem elongation rate was higher in the first weeks of cultivation for both temperature regimes (TI_{DIF} and BP) compared to TI and BP in Exp. 2 (FIG. 3). Leaf unfolding rate in the first weeks was only slightly lower in EXPT. 2. Leaf number as indicator for final plant development was only slightly influenced by temperature bandwidth of TI (TABLE 4).
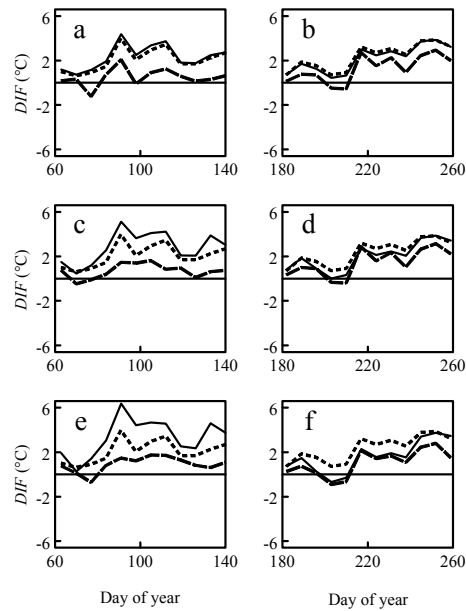
FIGURE 1. Simulated weekly *DIF* averages in greenhouse cut chrysanthemum cultivation during two different 12-week cultivation periods (planting day of year 61, a, c, e; planting day of year 182, b, d, f). With temperature integration (*TI*, ——) and temperature integration with zero *DIF* (TI_{DIF}, – – –) with three different temperature bandwidths of ±2 °C (a, b), ±4 °C (c, d) and ±6 °C (e, f) and a reference temperature regime according to commercial practice (*BP*,----).

ENERGY CONSUMPTION

Simulations showed that energy consumption was lower for *TI* and TI_{DIF} for almost all investigated planting dates compared to *BP* (TABLE 5). Only in summer, energy consumption with TI_{DIF} with ±2 °C and ±4 °C temperature bandwidths was slightly higher than *BP*. Energy consumption decreased with temperature bandwidth for *TI* and TI_{DIF} for all planting dates. This decrease was most pronounced in spring and autumn. The highest absolute energy savings were also observed with spring plantings. Compared to *BP*, 22 % energy could be saved with regular *TI* and 15 % for *TI* with zero *DIF* for a 12-week cultivation with ±6 °C temperature bandwidth. Energy saving compared to *BP* was also found for TI_{DIF} and *TI* in greenhouse experiments in autumn and spring, respectively (TABLE 6). +

DISCUSSION

Mean temperature of the reference regime was higher in simulations for spring and autumn cultivations. This, however, did not directly contribute to higher energy consumption. Heating set point of *BP* was only little influenced by radiation.

171
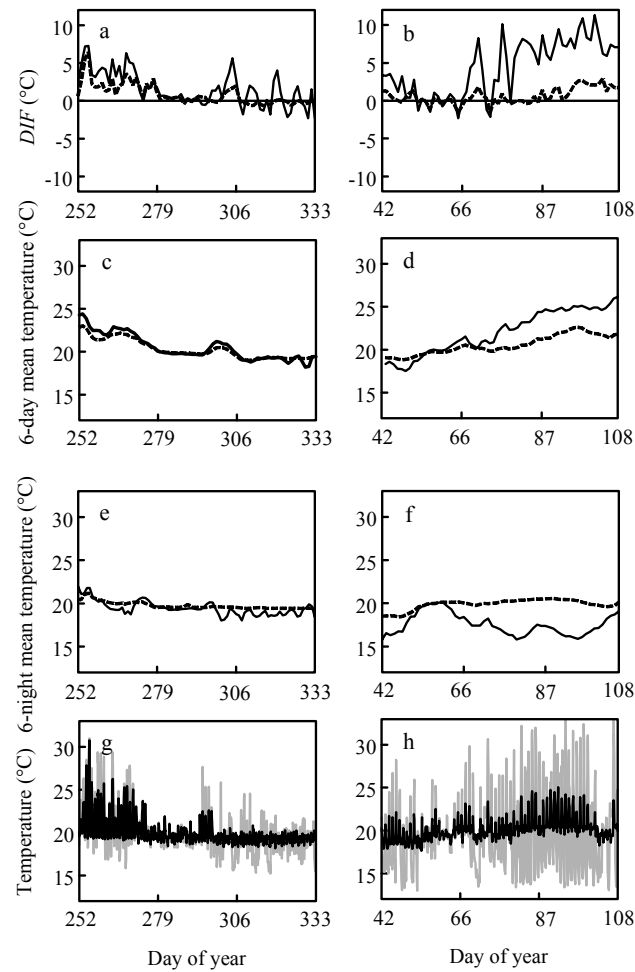
FIGURE 2. Measured climate-data of EXPT. 2 with regular temperature integration (*TI*) (b, d, f, h) and EXPT. 3 with temperature integration and zero *DIF* (*TI*$_{DIF}$) (a, c, e, g) of *DIF* (a, b), 6-day mean temperature (c, d), 6-night mean temperature (e, f) and one-hour greenhouse mean temperature (g, h) for the complete cultivation periods. Data are given for a reference climate control greenhouse (*BP*) (broken line or black) and temperature integration greenhouse (*TI* or *TI*$_{DIF}$) (non-broken line or grey). Data from EXPT. 2 are means of two greenhouses each, data from EXPT. 3 are from one greenhouse each.

TABLE 3. Dry weight of main-stems, side-stems, main-leaves, side-leaves and flowers, and leaf area (LAI) and specific leaf area (SLA) of temperature integration regime with zero *DIF* (*TI*$_{DIF}$) and reference temperature regime (*BP*) at the end of EXPT. 3.

Regime	Dry weight (g m^{-2})					LAI (-)	SLA (cm^{-2} g^{-1})
	Main-Stem	Side-Stems	Main-Leaves	Side-Leaves	Flowers		
BP	224	29	149	17	106	5.9	350
TI$_{DIF}$	218	33	147	14	108	5.8	366
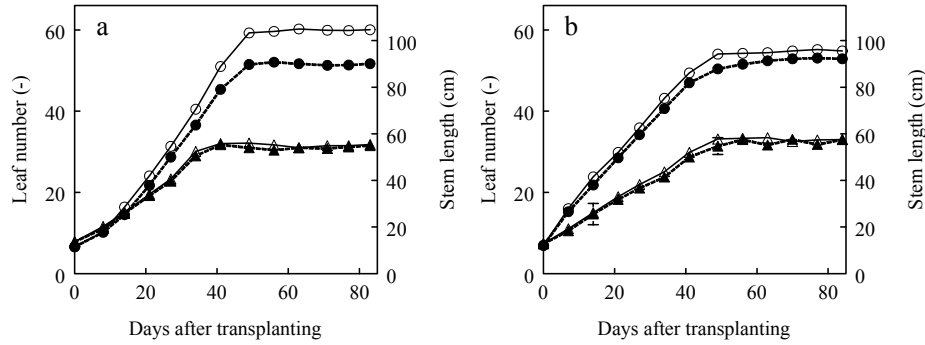
FIGURE 3. Influence of regular temperature integration (*TI*) (a, open symbols; △, ○) and temperature integration with zero *DIF* (*TI*$_{DIF}$) (b, open symbols; △, ○) on leaf number (△, ▲) and stem length (○, ●) compared to a reference climate regime (*BP*) (closed symbols; ▲, ●) of cut chrysanthemum 'Reagan Improved'. Data were taken from two greenhouse compartments for each treatment of 12 plants each (evenly distributed) (a) and from one greenhouse for each treatment of 15 evenly distributed greenhouse plants each (b). Vertical bars indicate standard error of mean larger than symbols.

TABLE 4. Final stem length, mean internode length and leaf number of cut chrysanthemum controlled by temperature integration (*TI*) with an averaging period of 6 days with different temperature bandwidths (*b*) at the end of Experiment 1, with standard error of the mean (SEM).

	Length (cm)		Number
b (°C)	Stem ± SEM	Internodes ± SEM	Leaves ± SEM
±2	93.4 ± 0.6	3.04 ± 0.04	30.8 ± 0.3
±4	93.2 ± 0.4	3.02 ± 0.03	30.9 ± 0.3
±6	98.8 ± 0.4	3.14 ± 0.03	31.6 ± 0.3
±8	97.2 ± 0.4	3.08 ± 0.04	31.5 ± 0.3

TABLE 5. Simulated total energy consumption (MJ m^{-2}) for a 12-week cut chrysanthemum cultivation with different planting dates (DOP) for the reference climate regime (*BP*), temperature integration (*TI*) and temperature integration with zero *DIF* (*TI*$_{DIF}$) with different temperature bandwidth (*b*).

	Climate regime						
	BP	*TI*			*TI*$_{DIF}$		
b (°C)	±0.5*	±2	±4	±6	±2	±4	±6
DOP							
61	267	245	221	209	256	242	227
121	79	70	64	61	76	75	69
182	66	59	58	58	68	68	65
246	300	285	274	260	295	287	276

*Linear increase of daytime temperature ventilation set point by instantaneous outside global radiation (0.5 K per 100 W m^{-2} between 800 and 1200 W m^{-2}) and nighttime heating and ventilation set points by outside global daily radiation sum of the preceding light period (0.25 K per 1 MJ m^{-2} d^{-1} between 12 and 16 MJ m^{-2} d^{-1}).

TABLE 6. Measured energy consumption with six day averaging period and bandwidth of ±6 °C compared to the reference regime (*BP*) for cultivation of cut chrysanthemum in EXPT. 2 and 3 with different day of years (DOY).

Experiment	Measuring period (DOY)	Energy consumption (MJ m^{-2})			Energy saving compared to *BP* (%)
		BP	*TI*	*TI$_{DIF}$*	
EXPT. 2	38 – 108	250.8	191.7	-	23.5
EXPT. 3	261 – 311	86.9	-	67.9	22.0

The higher greenhouse temperature with *BP* was therefore due to natural temperature increase through increasing solar short wave radiation in spring. In *TI* and *TI$_{DIF}$*, warm periods were later compensated by cool periods, whereas temperature set points could not drop below 18.5 °C with *BP*. With *TI* and *TI$_{DIF}$*, mean temperature was closer to the targeted mean temperature of 19 °C than with *BP*. The new regime with simultaneous temperature control according to *TI* and *DIF* resulted in a good performance controlling mean day and mean night temperature over 6 days or night. Because this regime compensated days by days and nights by nights, temperature was more restricted than with regular temperature integration. Therefore, the differences between day and night temperatures were lower with *TI$_{DIF}$* than with *TI*. This resulted in a lower realised *DIF* for the new regime compared to regular temperature integration. The resulting decrease in stem length difference between a reference regime and *TI$_{DIF}$* compared to *TI* was therefore rather due to a decrease in the difference between day and night temperature with *TI$_{DIF}$* than due to integration of the effects of NT and DT on stem elongation. The hypothesis that the *DIF* effect on stem elongation could be integrated over several days could not be proven. For that, well-planned experiments in climate chambers would be necessary. This research, however, could point out that temperature integration and *DIF* could be controlled simultaneously to achieve shorter chrysanthemum plants while saving energy. Final stem length of plants treated with *TI$_{DIF}$* and *BP* in EXPT. 3 was almost the same, but stems were longer than those controlled with *BP* in EXPT. 2 (FIG. 2). Next to temperature, stem elongation is affected by other climatic factors as light intensity, light quality, photoperiod, relative humidity and CO_2 concentration[26]. Different cultivation periods may be the reasons for that. Variation between young plant batches could be a reason, too. Differences were already visible after the first week of cultivation. Final stem length was probably higher because of the high initial elongation rate.

It can be stated that the independent day and night temperature integration regime is a promising step to more sustainable cut chrysanthemum cultivation by reducing the use of growth retardants and energy without loss of visible quality. Application of this regime, however, is only possible in regions with variable weather conditions as in The Netherlands. With more stable climatic regions with e.g. a constant succession of warm days and cool nights temperatures could not be compensated and this would result in a normal temperature regime.

In this research, only a zero *DIF* was investigated. Stems in all treatments were still longer than plants with high quality market value of 75 – 80 cm in The Netherlands[174]. Further research should therefore focus on simultaneous negative *DIF* and *TI* treatments to investigate if stem elongation could be reduced strongly while saving energy. Only then, the two aims of energy saving and reduction of chemicals in Dutch horticulture as two major targets[175] could be reached by climate control.

ACKNOWLEDGEMENTS

3.6 Synthesis – Climate control for sustainable plant production

O. Körner, H. Challa & G. van Straten

ABSTRACT

A combined greenhouse climate and control model was used to study energy consumption in year round cut chrysanthemum cultivation. In this paper the idea is to investigate the combined effect of different previously developed regimes to find the best regime regarding energy saving and plant quality for different seasons. Temperature integration (TI), flexible humidity and DIF (difference average day and average night temperature) regimes were adapted from earlier papers. TI with a regular 24-h averaging period (TI_{24}), TI with two nested temperature averaging periods of 24 hours and 6 days (TI_n, subscript 'n' for nested), and a combination of TI_n respecting the DIF concept ($TI_{n,DIF}$) to control stem elongation were simulated. TI_{24} and TI_n were also combined with a flexible humidity regime. The regimes were compared to a blueprint temperature regime (BP). Energy saving screen control was applied with all regimes. The TI regimes were simulated with three temperature bandwidths (b) (±2 °C, ±4 °C and ±6 °C) and three DIF set points (0 °C, –6 °C and –12 °C DIF) were used with $TI_{n,DIF}$. Energy consumption and temperature were

evaluated for different seasons within a year round cultivation assuming 12-weeks for one period from planting until harvest. Absolute highest energy saving was achieved throughout the year when temperature integration was combined with flexible humidity regime. The winter months are the most important in that issue as already 28 % of annual energy consumption can be saved within 12 winter weeks. In winter with a fixed RH set policy only (i.e. 80 %) and temperature bandwidth of ±2 °C, absolute energy saving compared to BP for one period (planting 1 January) was highest with $TI_{n,DIF}$ (62 MJ m^{-2}, 12 % at -12 °C DIF), then TI_n (49 MJ m^{-2}, 9 %) and TI_{24} (38 MJ m^{-2}, 7 %). In spring or autumn in relative sense the largest energy saving can be obtained with TI_n of e.g. 28 % with planting 01 March, and then with TI_{24} (16 %) and $TI_{n,DIF}$ (13 %, -6 °C DIF). However, most energy can be saved when temperature integration is combined with a flexible humidity regime. Then 33 % energy saving per year is possible with TI_n (±2 °C temperature bandwidth). If no negative DIF is enforced, the TI_n and TI_{24} regimes led to a positive DIF, with the highest value in spring and autumn. A DIF set point with $TI_{n,DIF}$ of -12 °C consumed less energy than -6 °C and 0 °C DIF in winter, in spring and autumn -6 °C DIF was lowest and 0 °C DIF was lowest in summer.

INTRODUCTION

The greenhouse industry nowadays aims at reducing energy consumption. This can be achieved with advanced greenhouse technique and new materials[10]. To support that, different energy saving climate regimes were designed. These regimes, however, differ in their energy saving potential and cannot always be applied without concerning other aims in climate control. Our aim was to improve existing regimes by combining features and to evaluate the different regimes with simulations to find the best combination concerning energy saving and plant quality for each season in year round cut chrysanthemum cultivation.

The most common climate control measure for energy saving is the temperature integration concept[41, 167, 168] (TI), which is mostly applied with an averaging period of 24 hours[39, 59] (TI_{24}). More freedom for energy saving, however, can be achieved when the TI averaging period is expanded[52, 57]. With averaging periods of several days in regular TI, nevertheless, distinguishing short- and long-term processes is not a concern. Temperature integration takes only the slowly responding plant responses into account, but fast responses as photosynthesis are not optimised. Distinguishing different time constants was suggested for improved climate control[133, 207]. A modified TI regime (TI_n) that allows to distinguish short- and long-term processes was designed in CHAPTER 3.1 by nesting TI_{24} and several-day TI. TI_n allows more flexibility in the short-term (24-hours) while respecting the long-term (several days) temperature boundaries.

The applicability of TI_{24}, regular TI over several days or TI_n in climate control, however, differs between seasons. A good strategy for one season may not minimise energy consumption for all seasons throughout the year; e.g. temperature in winter at moderate latitudes is easy to control with TI_{24} by just shifting heating to nighttime under energy screen[39, 55]. Then, longer integration periods are not more beneficial. The strategy changes in spring and autumn when greenhouse temperature naturally heat up during day and cool down during night or when warm and cool days interchange. TI with a several-day averaging period can then be applied with highest benefits. In summer on the other hand, greenhouse temperature is difficult to control due to passive ventilation (as common in The Netherlands) and most energy is then consumed due to humidity control, CO_2 supply or night heating. TI can then lead to a higher CO_2 consumption (with above ambient CO_2 concentration set point) through higher ventilation rate during day.

In addition to that, other climate control aims can counteract with TI in one season but support it in an other. One of the main disadvantages on chrysanthemum quality when applying TI in spring and autumn is stem elongation increase. This is because TI usually leads to a positive DIF (difference between average day and average night temperature) (CHAPTER 3.5), which favours stem elongation[16, 23, 74]. With cut chrysanthemum and most pot plants, nevertheless, compact plants with short internodes are targeted. In winter, a negative DIF is achieved with TI when heating is shifted to the night under energy screens. In order to avoid excessive stem elongation, environmental unfriendly growth inhibitors are used when DIF is not applied[75]. To reduce energy consumption and the use of chemical growth inhibitors at the same time, regular temperature integration and a zero DIF set point were combined in CHAPTER 3.5 (TI_{DIF}). With that regime, day and night temperatures were averaged over the integration interval and controlled independently to attain an integrated DIF. With TI_{DIF} with a setting of zero DIF as opposed to positive DIF resulting from regular TI, stem length could be reduced slightly, but energy consumption was higher compared to regular TI. To further decrease energy consumption and stem length in this paper, we combined TI_{DIF} with TI_n ($TI_{n,DIF}$) and extended the DIF set point to –6 or –12 °C DIF.

The main restriction in energy saving possibilities with temperature integration regimes is humidity control. The fixed set points for humidity control used in common practice counteract the positive effect of TI on energy consumption throughout the year as shown in CHAPTER 3.2. Vents open at lower temperatures than required for TI or heating decreases relative humidity or both. A flexible humidity regime for energy saving with TI was therefore designed (CHAPTER 3.2). In this paper, also TI_{24} and TI_n were combined with flexible humidity control to $TI_{24,RH_{flex}}$ and $TI_{n,RH_{flex}}$, respectively.

CHAPTER 3.6

The aim was to find the best regime concerning energy consumption while respecting plant growth and quality. To increase energy saving, optimal screen control was implemented in TI_n, $TI_{n,DIF}$ and $TI_{n,RH_{flex}}$, that was not done originally in CHAPTER 3.1. All regimes (TI_{24}, TI_n, $TI_{n,DIF}$, $TI_{24,RH_{flex}}$ and $TI_{n,RH_{flex}}$) were compared to a blueprint regime according to commercial practice with 80 % relative humidity set point or flexible humidity regime (BP, $BP_{RH_{flex}}$). Regimes were implemented in a set point generator programme combined with a greenhouse climate and control model and evaluated regarding energy consumption and temperature (i.e. DIF) in different seasons.

MATERIALS AND METHODS

REFERENCE TEMPERATURE REGIME

BP as in CHAPTER 3.4 was used. Heating and ventilation set points were initially set to 18.0 °C and 19.0 °C, respectively. Daytime ventilation set points increased linearly with outside global radiation level (0.5 K per 100 W m^{-2} between 800 to 1200 W m^{-2}) and nighttime heating and ventilation set points increased linearly with daily global radiation sum of the previous daytime period (0.25 K per 1 MJ m^{-2} d^{-1} between 12 and 16 MJ m^{-2} d^{-1}). RH was set to 80 %.

24-HOUR TEMPERATURE INTEGRATION

A temperature integration procedure with a 24-hour averaging period (TI_{24}) was applied according to CHAPTER 3.4. To achieve comparable mean temperatures with TI_{24} as in BP, constantly the same 24-hour mean target temperature range ($\overline{T}_{targ,24}$) of 18.5±0.5 °C as used for heating and ventilation temperature for BP was applied. During each 24-hour cycle, temperature could fluctuate freely between the calculated heating and ventilation temperature set points (T_h, T_v). Initial T_h and T_v ($T_{h,init}$, $T_{v,init}$) were first determined from $\overline{T}_{targ,24}$ and the temperature bandwidth (b).

$$T_{v,init} = \overline{T}_{targ,24} + b \tag{1}$$

$$T_{h,init} = \overline{T}_{targ,24} - b \tag{2}$$

T_h and T_v were recalculated every 5 minutes. At the beginning of each new 24-hour period (t_1, 8:00 a.m.) a sequence of subsequent 24 hourly greenhouse temperatures were simulated with forecasted weather and a simple static greenhouse model within $T_{h,init}$ and $T_{v,init}$ (CHAPTER 3.4). Weather forecast was assumed to be ideal (i.e. a 100 % fit between forecasted and later realised weather). The mean of the expected temperature over 24-hours ($\overline{T}_{24}^+$) was updated every five minutes with realised

180

greenhouse temperature up till then ($\overline{T}'_{24}{}^+$). T_h and T_v were then determined to achieve $\overline{T}_{\text{targ},24}$ at the end of the 24-hour period as follows. Initial temperature set points were used when $\overline{T}'_{24}{}^+$ was inside the allowed temperature range; otherwise heating or ventilation temperature set point was adjusted to the value of the original blueprint ($\overline{T}_{\text{targ},24} \pm 0.5$ °C).

$$T_v = \begin{cases} T_{v,\text{init}} & \text{if } \overline{T}'_{24}{}^+ \leq \overline{T}_{\text{targ},24} + 0.5 \\ T_{v,\text{init}} - b + 0.5 & \text{if } \overline{T}'_{24}{}^+ > \overline{T}_{\text{targ},24} + 0.5 \end{cases} \qquad [3]$$

$$T_h = \begin{cases} T_{h,\text{init}} & \text{if } \overline{T}'_{24}{}^+ \geq \overline{T}_{\text{targ},24} - 0.5 \\ T_{h,\text{init}} + b - 0.5 & \text{if } \overline{T}'_{24}{}^+ < \overline{T}_{\text{targ},24} - 0.5 \end{cases} \qquad [4]$$

When $\overline{T}'_{24}{}^+$ was smaller than $\overline{T}_{\text{targ},24} - 0.5$, the possibility of shifting heating to night-time under the screen for energy saving was taken into account. This was realised by calculating the new expected 24-hour mean $\overline{T}'_{24}{}^+$ by assuming that the nighttime temperature during the closure of the screen was b degree higher. The energetically optimal subsequent 24-hour course for T_h was then calculated.

NESTED 24-HOUR / 6-DAY TEMPERATURE INTEGRATION

Nested temperature integration (TI_n; CHAPTER 3.1) was modified from regular TI with a six-day averaging period and combined with TI_{24}. Each 24-hour period was treated independently and nested within the six-day averaging period (t_{int} = 6 days in this case). A target 24-h mean temperature window rather than a fixed target temperature as in regular TI was used as control criterion (CHAPTER 3.1). Temperature was allowed to fluctuate provided that the 24-h average temperature remained within the specified six-day boundaries (see CHAPTER 3.1). A receding horizon of 1 day was used, i.e. the preceding 5-day period was evaluated at the beginning of each new day (t_1, 8:00 a.m.) and compensated at day six ($d_{24}{}^{+1}$) of t_{int}. Temperature history older than five days was not taken into account for control. 24-hour target mean temperature ($\overline{T}_{\text{targ},24}$) for $d_{24}{}^{+1}$ was calculated at t_1.

$$^{*)}\ \overline{T}_{\text{targ},24}(d_{24}{}^{+1}) = \sum_{j=1}^{t_{\text{int}}} \overline{T}_{\text{des}}(d_{24}{}^{j-t_{\text{int}}}) - \sum_{j=1}^{t_{\text{int}}-1} \overline{T}_{\text{real}}(d_{24}{}^{j-t_{\text{int}}}) \qquad [5]$$

with 24-hour means of previously realised temperatures ($\overline{T}_{\text{real}}$) during the past five 24-hour periods (d_{24}) and the desired mean temperatures ($\overline{T}_{\text{des}}$) for each day of the six-day period.

$^{*)}$ The notation $d_{24}{}^{+1}$ indicates the current 24-hour period. The notation $d_{24}{}^{j}$ (j = -5, ..., +1) is used to indicate the jth 24-hour period, respectively, before (negative j) or after (positive j).

Too extreme temperatures were avoided by soft and hard boundaries that were treated with a temperature-time dose-response (CHAPTER 3.1). Two types of thresholds (hard and soft) represented the limits. Temperature was allowed to exceed the soft boundary (30 °C or 14 °C for ventilation and heating, respectively) for a certain amount of time that depended on the absolute temperature value. When temperature exceeded the soft boundary, the dose was recorded. A maximum duration (30 min) at the hard boundary temperatures (34 °C and 10 °C, upper and lower, respectively) was set and an exponential response was assumed (CHAPTER 3.1). Heating and ventilation temperatures for the dose response ($T_{h,dose}$, $T_{v,dose}$) were initially set to the absolute thresholds and adjusted to the soft boundary after dosage was completed. The soft boundary value was then used as set point for the duration of a refresh time of 6 h and was then reset to the more extensive hard limit.

As in TI_{24}, the possibility of shifting heating to nighttime under the screen was taken into account by simulating the optimal temperature trajectory. T_v and T_h were calculated from $\overline{T}_{targ,24}$, b and the difference between realised and targeted mean temperatures over t_{int}. A proportional back-regulation for heating and ventilation set points of the temperature bandwidth towards $\overline{T}_{targ,24}$ to achieve the target six-day mean temperature was used (f_h and f_v for T_h and T_v, respectively); f_h and f_v were related to the difference between realised and targeted six-day mean temperature ($\Delta\overline{T}$, CHAPTER 3.1).

$$f_h = \frac{b}{2} + \frac{b}{2} \cdot \frac{t_{int}}{M}\left(1 - e^{\frac{\Delta\overline{T}}{r_h}}\right) \qquad [6]$$

$$f_v = \frac{b}{2} + \frac{b}{2} \cdot \frac{t_{int}}{M}\left(1 - e^{-\frac{\Delta\overline{T}}{r_v}}\right) \qquad [7]$$

The dimension factor M was chosen equal to 1 day. Factors for the strength of back regulation for heating and ventilation (r_h and r_v, respectively) were used; r_h and r_v were equally set to 1.7, 2.9 and 4.7 for ±2 °C, ±4 °C and ±6 °C temperature bandwidth, respectively. The final set points could then be determined.

$$T_v = \begin{cases} T_{v,dose} & if \quad \overline{T}'_{24}{}^+ \le \overline{T}_{targ,24} + b - f_v \\ \overline{T}_{targ,24} + b - f_v & if \quad \overline{T}'_{24}{}^+ > \overline{T}_{targ,24} + b - f_v \end{cases} \qquad [8]$$

$$T_h = \begin{cases} T_{h,dose} & if \quad \overline{T}'_{24}{}^+ \ge \overline{T}_{targ,24} - b + f_h \\ \overline{T}_{targ,24} - b + f_h & if \quad \overline{T}'_{24}{}^+ > \overline{T}_{targ,24} - b + f_h \end{cases} \qquad [9]$$

NESTED 24-HOUR / 6-DAY TEMPERATURE INTEGRATION AND *DIF*

Temperature control on the difference between average temperature during daytime (DT) and average temperature during nighttime (NT) is commonly called *DIF* (DT – NT). The control was extended to an average *DIF* over the duration of the *TI* averaging period ($DIF_{t_{int}}$) and combined with *TI* (see CHAPTER 3.5).

In the present research, TI_n was coupled with *DIF* ($TI_{n,DIF}$). Two separate parallel running averaging periods for daytime and nighttime were applied within TI_n. Target mean temperatures for daytime and nighttime, $\overline{T}_{targ,day}$ and $\overline{T}_{targ,night}$ were calculated at the beginning of the actual day or nighttime similar to EQ. 5.

$$^{**)}\ \overline{T}_{targ,day}\left(t_{day}^{\ +1}\right) = \sum_{j=1}^{t_{int}} \overline{T}_{des}\left(t_{day}^{\ j-t_{int}}\right) - \sum_{j=1}^{t_{int}-1} \overline{T}_{real}\left(t_{day}^{\ j-t_{int}}\right)$$

$$\overline{T}_{targ,night}\left(t_{night}^{\ +1}\right) = \sum_{k=1}^{t_{int}} \overline{T}_{des}\left(t_{night}^{\ k-t_{int}}\right) - \sum_{k=1}^{t_{int}-1} \overline{T}_{real}\left(t_{night}^{\ k-t_{int}}\right)$$

[10]

$DIF_{t_{int}}$ was set to 0 °C, –6 °C and –12 °C ($DIF_{t_{int},set}$) for separate simulations. $\overline{T}_{des}$ for day- and nighttime ($T_{des}(t_{day})$, $T_{des}(t_{night})$, respectively) were set as function of $\overline{T}_{des}$, number of daytime hours and nighttime hours (h_{day} , h_{night}) and $DIF_{t_{int}}$.

$$\overline{T}_{des}\left(t_{day}\right) = \overline{T}_{des} + \frac{DIF_{t_{int},set}}{24/(24-h_{day})}$$

$$\overline{T}_{des}\left(t_{night}\right) = \overline{T}_{des} - \frac{DIF_{t_{int},set}}{24/(24-h_{night})}$$

[11]

FLEXIBLE HUMIDITY REGIME

A process based humidity regime focussing on separate humidity affected plant processes as calcium deficiencies, plant water stress, crop growth, crop development and airborne fungus diseases (CHAPTER 3.2) was added to *BP* ($BP_{RH_{flex}}$), TI_{24} ($TI_{24,RH_{flex}}$) and TI_n ($TI_{n,RH_{flex}}$).

GREENHOUSE CLIMATE MODEL

Climate regimes were implemented in a simulation model with the technical software environment MATLAB® (version 6.0, MathWorks, Natick, MA, USA) that functioned as a set point generator (SPG; CHAPTERS 3.1 and 3.4). Greenhouse temperature, relative humidity (RH) and CO_2 concentration inside the greenhouse and outside global radiation were input with a fixed time step of 5 minutes. The SPG was coupled

---

**)The notation $t_{day}^{\ +1}$ and $t_{night}^{\ +1}$ indicate the current day or night period. The notations $t_{day}^{\ j}$ and $t_{night}^{\ k}$ (j = -5, ..., +1; k = -5, ...+1) are used to indicate the jth and k^{th} day or nighttime period, before or (negative j or k) or after (positive j or k).

with a greenhouse climate and control model[105] (CCM). With the CCM the inner greenhouse climate was controlled by a replica of commercially available climate controllers. The CCM provided simulations for a 1-ha Venlo-type greenhouse with single glass cover with diffuse short-wave radiation transmission of 78.5 %. It controlled greenhouse climate through heating and ventilation, and simulated energy consumption with a 2-minute time step. Set points for heating, ventilation and CO_2 concentration were calculated by the SPG and sent as input to the CCM. The CCM returned simulated greenhouse climate (RH, air temperature and CO_2 concentration), while using the received set points for control of heating and ventilation.

SIMULATIONS

Greenhouse cut chrysanthemum cultivation was simulated for a year round cultivation as it is common practice in The Netherlands, but no assimilation light was used. For this, 25 % of the greenhouse area was assumed under long-day (daytime 6:00 a.m. – 0:00 a.m.) and 75 % under short-day. Short-day was induced with a blackout screen. An energy saving screen was used during long day. The respective screen was unfolded between 7 p.m. and 8 a.m. or whenever outside radiation was zero. A representative one-year reference climate data set for De Bilt[177] (The Netherlands, lat. 52 °N) was used for simulations on yearly dynamics of greenhouse climate and energy consumption. The reference year consisted of a typical Dutch climate data set with hourly values of air temperature, relative humidity, direct and diffuse global radiation, CO_2 concentration, wind speed, wind direction and soil temperature. Gas was burned for CO_2 supply with the heater. Excess heat was stored in a heat buffer of 120 m^3. When the buffer was completely filled, CO_2 supply stopped. For all simulations, the CO_2 set point was 400 μmol mol^{-1}. Different temperature bandwidths of ± 2 °C, ± 4 °C and ± 6 °C were applied for separate simulations for TI_{24}, TI_n, $TI_{n,DIF}$ and $TI_{n,RH_{flex}}$. $TI_{n,DIF}$ was simulated with 0 °C, –6 °C and –12 °C DIF. Set point for RH (i.e. upper limit) was 80 % with TI_{24}, TI_n and $TI_{n,DIF}$. Energy consumption and temperature were evaluated for year-round cultivation. Different seasons were evaluated from year - round cultivations assuming 12-weeks for one period from planting until harvest.

RESULTS

GENERAL REGIME BEHAVIOUR AND ENERGY SAVING

In order to check the mean temperature achieved with the various strategies against the blue print, 4-week temperature means were computed as shown in TABLE 1.

TABLE 1. 4-weekly and annual temperature means during short-day application for blueprint regime (*BP*) and temperature integration regimes with ±2 °C bandwidths and fixed relative humidity set point of 80 %.

Week	Temperature regime					
	BP	TI_{24}	TI_n	$TI_{n,0DIF}$	$TI_{n,-6DIF}$	$TI_{n,-12DIF}$
1 – 4	18.0	18.0	18.2	18.0	18.0	18.1
5 – 8	18.1	18.0	18.2	18.2	17.9	18.2
9 – 12	18.5	18.2	18.4	18.2	18.0	18.0
13 – 16	19.8	19.3	18.9	18.8	18.2	18.3
17 – 20	20.2	19.7	19.3	19.1	18.4	18.5
21 – 24	23.1	23.1	21.6	21.5	21.5	21.5
25 – 28	23.4	23.2	22.1	22.0	21.9	21.9
29 – 32	22.7	22.8	21.4	21.4	21.4	21.4
33 – 36	22.1	22.1	20.6	20.8	20.5	20.5
37 – 40	19.8	19.3	18.8	18.7	18.2	18.3
41 – 44	18.7	18.2	18.4	18.2	18.0	18.0
45 – 48	18.1	18.0	18.2	18.1	18.0	18.1
49 – 52	18.0	18.0	18.0	18.0	17.9	18.2
1 – 52	20.3	19.8	19.4	19.3	19.1	19.4

Mean greenhouse temperature during winter differed only little between the temperature regimes. In spring, summer and autumn, temperature was lower with temperature integration regimes compared to *BP*. In these seasons, mean temperature decreased with increasing freedom for short-term temperature fluctuation with *BP*, TI_{24} and TI_n in ascending order. Three typical days (winter, spring and summer) controlled with *BP*, TI_{24} or TI_n are illustrated in FIG. 1. In winter, climate is controlled with heating only and then most energy is consumed for all regimes. With TI_{24} and TI_n, heating can be shifted to nighttime using a screen to save energy (TABLE 2). In spring on the other hand, heating during night can be reduced strongly with temperature integration when greenhouses heat up during daytime to more than common values as with the blueprint (FIG. 1, d to f). This is more pronounced with more freedom for temperature fluctuation as with TI_n compared to TI_{24}, accordingly most energy is then saved with TI_n or with $TI_{n,DIF}$ with low *DIF* set point (FIG. 1 f and TABLE 2). Although only one day was shown in each season, the respective days were representative. In summer, greenhouse are difficult to control and with temperature integration no energy saving can be achieved. In the contrary, due to the fixed CO_2 set point of 400 µmol mol^{-1} that is also maintained when no heating is used (i.e. with using the heat-buffer), slightly more energy is used with TI_n in the summer

185
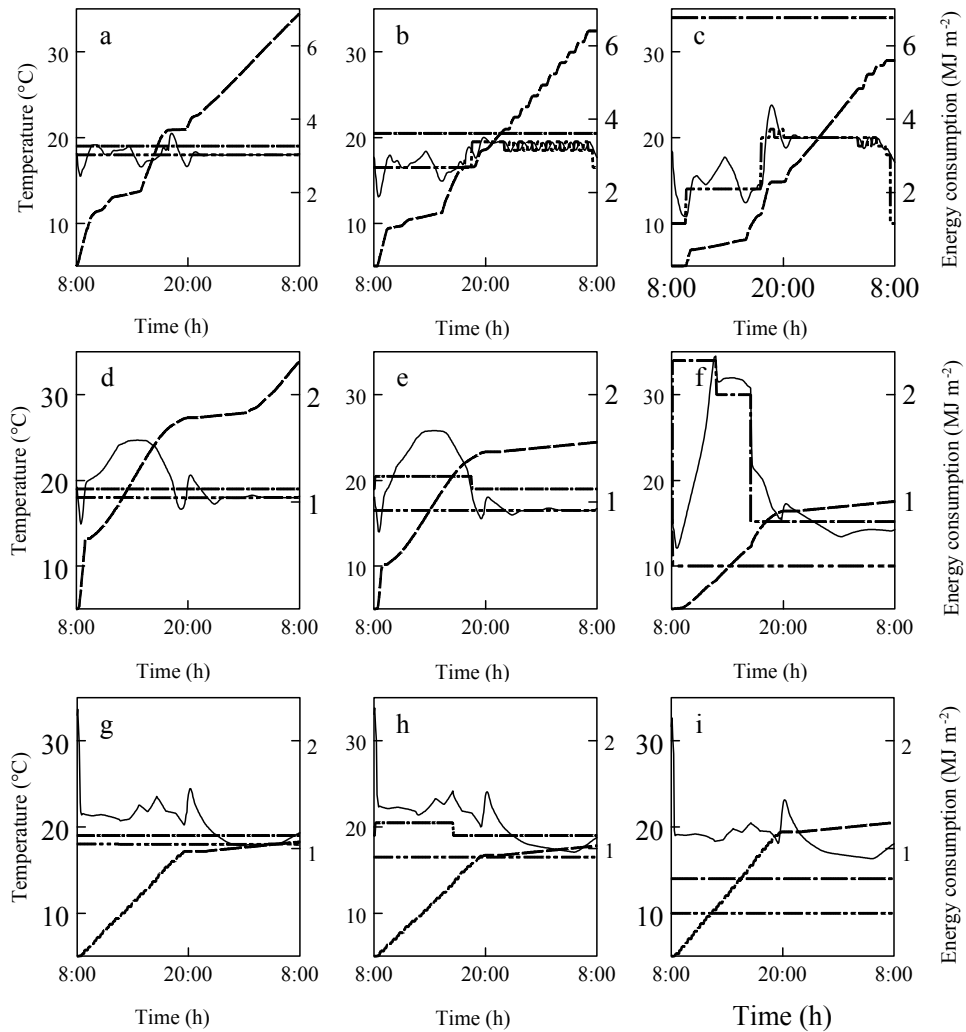
FIGURE 1. Realised greenhouse temperatures (——), heating set points (----), ventilation set points (---) and energy consumption (---) for a typical winter day (day 10 of the year) (a, b, c), a typical spring day (day 90 of the year) (d, e, f) and a typical summer day (day 176 of the year) (g, h, i) with *BP* (a, d, g), TI_{24} (b, e, h) ($b = \pm 2\ °C$) and TI_n (c, f, i) ($b = \pm 2\ °C$).

months (TABLE 2, FIG. 1, g − i). This is due to the higher ventilation rate compared to *BP* and TI_{24}. In FIG. 2 the weekly energy consumption of the various *DIF* regimes at different bandwidths were correlated to each other. Over all, there was a strong correlation. Comparing different $TI_{n,DIF}$ regimes with each other showed that energy consumption depended mainly on the *DIF* set point rather than the applied temperature bandwidth; with a tendency to have lower energy consumption at more negative *DIF*, although the effect is mainly occurring in periods of the year with high energy consumption (FIG. 2b).

TABLE 2. Energy consumption (MJ m^{-2}) for 12-week cultivations with different climate regimes and for a complete year (GJ m^{-2}): blueprint regime (*BP*), temperature regimes with ±2 °C temperature bandwidths (TI_{24}, TI_n and $TI_{n,DIF}$). Set points of 0 °C, –6 °C and –12 °C *DIF* were applied for $TI_{n,DIF}$. The lowest energy consumption is indicated with bold fonts.

Regime	Planting date					
	01 Jan	01 Mar	01 May	01 Jul	01 Sep	Year*)
						(GJ m^{-2})
BP	524	267	100	89	264	1.27
TI_{24}	487	223	**96**	**88**	227	1.17
TI_n	475	**190**	97	101	**202**	**1.10**
$TI_{n,0DIF}$	516	241	107	104	242	1.26
$TI_{n,-6DIF}$	475	229	108	110	229	1.17
$TI_{n,-12DIF}$	**462**	235	109	111	233	1.15

*) Yearly values are not the sum of the 12-week simulations

TABLE 3. Energy consumption (MJ m^{-2}) for 12-week cultivations and for a complete year (GJ m^{-2}) with different climate regimes with flexible humidity control (RH_{flex}): blueprint regime ($BP_{RH_{flex}}$), temperature regimes with ±2 °C temperature bandwidths ($TI_{24,RH_{flex}}$ and $TI_{n,RH_{flex}}$). The lowest energy consumption is indicated with bold fonts.

Regime	Planting date					
	01 Jan	01 Mar	01 May	01 Jul	01 Sep	Year*)
						(GJ m^{-2})
$BP_{RH_{flex}}$	424	194	100	87	205	1.03
$TI_{24,RH_{flex}}$	388	166	**88**	**81**	170	0.93
$TI_{n,RH_{flex}}$	**353**	**119**	95	101	**138**	**0.85**

*) Yearly values are not the sum of the 12-week simulations
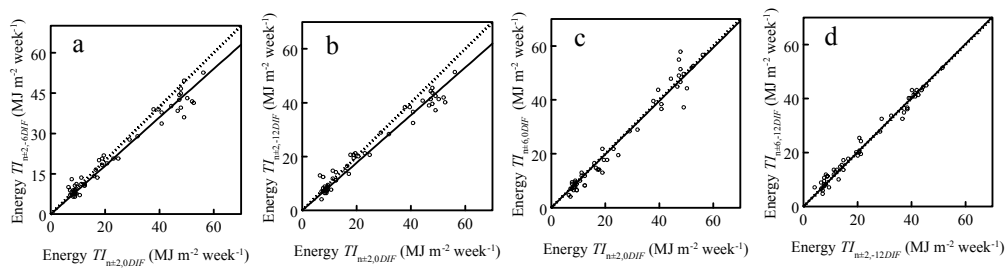
FIGURE 2. Comparison of weekly energy consumption with $TI_{n,DIF}$ regimes with different temperature bandwidths (*b*) and *DIF* set points with linear regression (—) and[$f(x) = x$] (---): a) 0 °C *DIF* compared to –6 °C *DIF* (*b*=±2 °C, R^2=0.96); b) 0 °C *DIF* compared to –12 °C *DIF* (*b* = ±2 °C, R^2 = 0.96); c) *b* = ±2 °C compared to *b* = ±6 °C (0 °C *DIF*, R^2 = 0.96); d) *b* = ±2 °C compared to *b* = ±6 °C (–12 °C *DIF*, R^2 = 0.98).

187
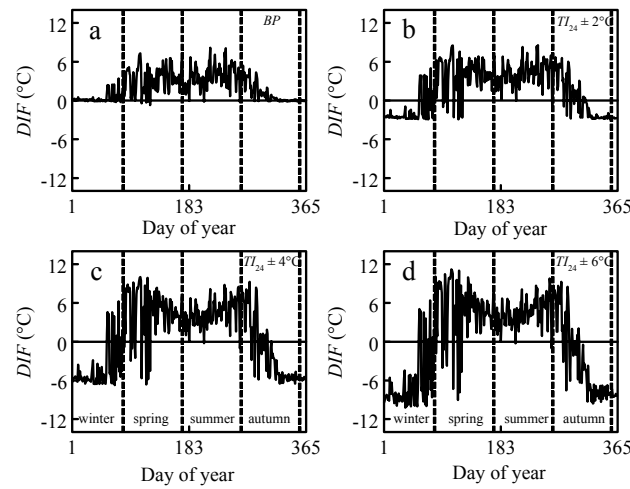
FIGURE 3. Attained *DIF* for blueprint regime (*BP*, a), and 24-hour temperature integration (TI_{24}) with temperature bandwidths of ±2 °C (b), ±4 °C (c) and ±6 °C (d).

When temperature control was combined with a flexible humidity control, energy consumption dropped with all temperature regimes during all periods (TABLES 2 and 3). Absolute the highest energy reduction in one period compared to *BP* could then be achieved applying TI_{n} with flexible humidity control during winter (TABLE 3). Because this period was responsible for 42 % of the annual energy consumption of *BP*, it had a strong effect of annual savings. Applying $TI_{n,RH_{flex}}$ only during the first 12 weeks of the year reduced annual energy consumption by 28 % compared to *BP*. When $TI_{n,RH_{flex}}$ was applied throughout the year, annual energy saving compared to TI_{n} with 80 % RH set point was 23 % for ±2 °C temperature bandwidth and 33 % compared to *BP* (TABLES 2 and 3).

DIF

Attained *DIF* decreased with temperature bandwidth for TI_{24} in winter (FIG. 3). In spring, more extreme *DIF* values (positive and negative) were attained with higher bandwidths. Then high and low *DIF* values interchanged between days and *DIF* fluctuated. In late spring and summer, attained *DIF* was similar for all bandwidths with TI_{24} but slightly higher with TI_{24} than with *BP*. Attained *DIF* with TI_{n} (b = ±2 °C) was lower than TI_{24} in winter and higher in spring and autumn (FIG. 3 and FIG. 4). With increasing bandwidth, attained *DIF* with TI_{n} strongly fluctuated in winter and autumn (FIG. 4). Averaging *DIF* over six-day balanced these fluctuations. With TI_{24} or TI_{n}, *DIF* was not controlled. When *DIF* was actually controlled (i.e. the average *DIF* in $TI_{n,DIF}$), the targeted *DIF* set point was attained in winter with 0 and
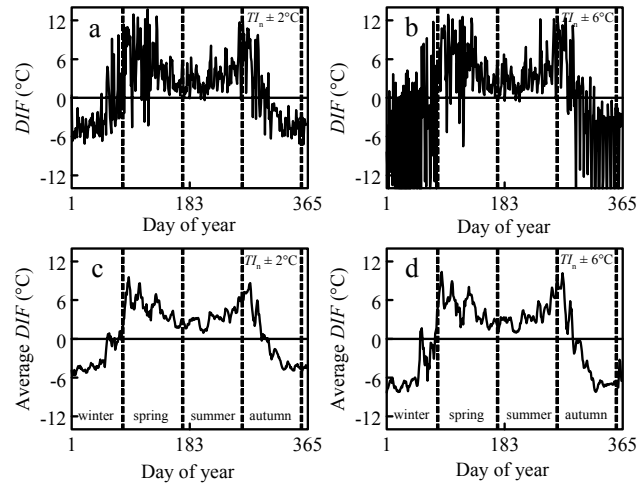
FIGURE 4. Attained *DIF* (a, b) and attained average *DIF* over the six-day averaging period ($DIF_{t_{int}}$) (c, d) with the nested temperature integration regime with temperature bandwidth of ±2 °C (a, c) and ±6 °C (b, d) .
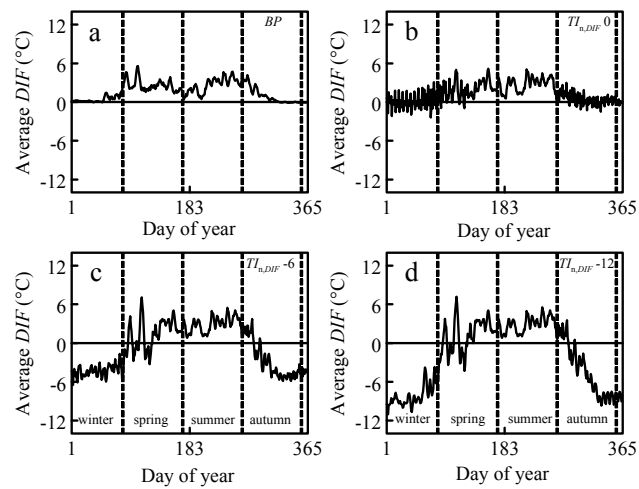
FIGURE 5. Averaged *DIF* over the six-day averaging period ($DIF_{t_{int}}$) with the blueprint regime (a) and nested temperature integration regimes with different *DIF* set points with temperature bandwidth of ±2 °C: $TI_{n,DIF}$ with 0 °C *DIF* (b), $TI_{n,DIF}$ with −6 °C *DIF* (c), and $TI_{n,DIF}$ with −12 °C *DIF* set point (d).

−6 °C *DIF* similar to TI_n (FIG. 5). In spring, the difference between TI_n and $TI_{n,DIF}$ was most pronounced. Although the targeted *DIF* set point with $TI_{n,DIF}$ was not achieved then, values were much lower than with TI_n .

DISCUSSION

GREENHOUSE CLIMATE AND CONTROL SIMULATOR

When comparing regimes with simulations, the validity of the greenhouse model[105] is of major importance. The same model was applied earlier (CHAPTERS 3.1, 3.2, 3.4 and 3.5) and simulations with a blueprint temperature regime showed a good fit with experimental measured energy consumption for tomato and cut chrysanthemum and with an experimentally validated greenhouse climate model[175]. In this study, it was assumed that the greenhouse model remained close to reality when flexible climate regimes were applied, because the underlying model processes were purely physical processes and its parameters were well validated.

MEAN TEMPERATURE

A drop of 1 % temperature set point generally decreases greenhouse energy consumption by 10% [240]. When comparing greenhouse climate regimes on energy consumption, equalising greenhouse temperature of the different regimes with the comparble blueprint regime are therefore of major importance. The reference regime was chosen with a rather low heating temperature set point (18 °C), a constant CO_2 set point of 400 µmol mol^{-1}, and with screen-closing whenever outside radiation was zero. This was a low energy-consuming regime already as it consumed only 1.27 GJ m^{-2} year^{-1} as compared to blueprint regimes in commercial practice that were reported to have energy consumption of 1.41 and 1.55 GJ m^{-1} year^{-1} [174, 175]. This made the selected blueprint a suitable lower limit in evaluating energy regimes.

In winter, greenhouse temperatures differed only slightly between the different evaluated temperature regimes. During this season, greenhouse heating was achieved due to gas-burning only. When solar radiation increased towards spring, average greenhouse temperature increased more with more rigid temperature regimes. While, for instance with the most rigid regime (BP) the average temperature could be maintained at the lower limit in winter with greenhouse heating. When greenhouses heat up naturally during day through solar radiation to higher temperatures than the heating or even ventilation temperature set point, BP was not able to keep the targeted temperature level. In contrast, with the flexible temperature regimes, when temperature exceeded the targeted temperature during day, night temperature could drop to compensate this, which is a clear advantage. The difference in average temperature between BP and the flexible temperature regimes was therefore not primarily leading to higher energy consumption. In general, attained temperature was closer to the target range (18 °C – 19 °C) with temperature integration than with the blueprint.

Heat-loss factor

When flexible temperature control (TI_{24}, TI_n or $TI_{n,DIF}$) was applied, energy consumption could be reduced as a consequence of shifting the heating to times when the greenhouse heat loss factor was reduced[30, 36]. The first measure was performed during cold periods by calculating the optimal temperature trajectory when the screen-factor was taken into account. Then it is most beneficial to shift heating to the night[39]. This measure was not implemented in earlier reported simulations with the nested TI regime.

When this regime was applied without concerning the energetically optimal heat-loss factor (i.e. no calculated optimal heating trajectory taking the screen into account), more energy was consumed with a tomato cultivation than with a blueprint regime (Chapter 3.1). Also when the regime was adapted for simulations with cut chrysanthemum including screens[215], no optimal temperature trajectory taking the blackout screens into account was implemented. In that report, energy consumption for a 12-week period with planting 01 January was 4 % higher with nested temperature integration compared to a blueprint. Our results showed an annual energy saving of 15 % ($b = \pm 4$ °C) compared to the blueprint. This was still lower than the reported 18 % [39]. There, however, the regime was tested with more heat demanding crops (rose and sweet pepper) and higher target temperatures during winter increase energy saving using an energy screen.

Nested and 24-hour temperature integration

To improve the nested TI regime for winter conditions, we implemented the screen-factor for temperature compensation in TI_n as described. With that, nighttime heating was simulated before the night period to attain the best temperature trajectory concerning energy consumption. This was not taken into account in the original regime (Chapter 3.1). A further improvement in this paper was screen unfolding whenever outside radiation was zero. By only doing that, energy consumption during the first 12 weeks of the year was 3 % lower for the blueprint regime (data not presented).

Simulations have shown that TI_n was not the best choice for all cultivation periods as it was still not implemented optimally. Heating was obviously also shifted from cool nights under an energy screen to the daytime afterwards. The result of that were strongly fluctuating average achieved DIF values. When TI_n was compared to TI_{24} with higher bandwidths in winter, more energy was consumed with TI_n than with TI_{24}. Temperature bandwidths had only little effect on energy consumption with TI_n, whereas a strong effect was observed with TI_{24} in winter, spring and autumn. This was probably due to the extended temperature flexibility during the 24-hour period with TI_n that already covered most energy saving possibilities and therefore only

little additional profit was gained with higher six-day temperature bandwidths (CHAPTER 3.1).

TI_n was applied with an averaging period of several days. This contributed to energy saving. This was obvious when comparing TI_{24}, $TI_{n,DIF}$ and TI_n with plantings in March. With $TI_{n,DIF}$, averaging cycles to day and night were applied separately. This strongly reduced the benefit of the extension of the 24-hour temperature boundaries as can be seen in TABLES 2 and 3.

NESTED TEMPERATURE INTEGRATION AND *DIF*

In winter, TI_{24} and regular *DIF* regimes with a 24-hour averaging period ($TI_{24,DIF}$) have similar behaviours and energy consumptions (CHAPTER 3.4). Energy consumption can be reduced by both regimes when heating is shifted mainly to the nighttime using screens. With *DIF* this trajectory is set as fixed target and with TI_{24} is calculated as the most energy efficient strategy. The actual energy saving potential depends then on how much greenhouse temperature can drop naturally during daytime. A regime with a low daytime heating set point can only save energy compared to a regime with a higher set point when greenhouse temperature would naturally drop (no artificial heat source) below the higher one. During winter, between –9 °C and –10 °C $DIF_{t_{int}}$ was the lowest to achieve. A set point of –12 °C $DIF_{t_{int}}$ had therefore a lower energy consumption than –6 °C $DIF_{t_{int},set}$, but –10 °C $DIF_{t_{int},set}$ would probably result in the same. Although, occasionally lower values than –12 ºC *DIF* were attained with TI_n ($b = \pm6$ °C, FIG. 4 b). $TI_{n,DIF}$ had a lower energy consumption when the *DIF* set point was very low, because then also attained $DIF_{t_{int}}$ was lower (FIG. 5). Compensating temperatures of different day and night periods was possible, but reduced energy saving compared to TI_{24} and TI_n. Compared to *BP*, 13 % energy could be saved with $TI_{n,DIF}$ ($b = \pm2$ °C). Energy can therefore be saved with the $TI_{n,DIF}$ regime but more saving is possible with other dynamic temperature regimes.

$TI_{n,DIF}$ with –12 °C *DIF* set point was the best choice for energy saving in winter, but not in other seasons. The restricted freedom for temperature flexibility to independent day and night cycles restricted energy saving during the rest of the year. In spring and autumn, TI_n showed it's highest benefit. Then, different features within TI_n yielded maximum energy saving.

ACHIEVING NEGATIVE *DIF*

In winter and autumn, cold days could be used to cool down the greenhouses during days to attain the necessary degrees of freedom for controlling night heating to simultaneously achieve a negative *DIF* and the targeted mean temperature. In summer, the achievement of a negative *DIF* was not possible. Although, the

ventilation temperature set point was very low and vents were opened maximal to drop greenhouse temperature during day, mean daytime greenhouse temperature actually increased to values above the mean 24-hour target temperature. There were no degrees of freedom left for heating up the greenhouse during night to achieve the desired negative *DIF*. Because attained *DIF* during summer was almost the same for each temperature regime, *DIF* for stem-length control cannot be used during summer.

HUMIDITY REGIME

To drop energy consumption for the whole year the flexible humidity regime (CHAPTER 3.2) can be applied regardless season and temperature regime. It has the highest additional value with temperature integration in winter, spring and autumn. Traditional RH control counteracts the positive effect of *TI* on energy consumption in these seasons[39]. Vents will open at lower temperatures than required for temperature integration or heating is employed to decrease relative humidity, or both. This problem is even more pronounced in future highly insulated greenhouses[180].

ENERGY PRODUCING MEASURES

The high ventilation-rates in summer in combination with CO_2 supply by burning fuel were responsible for a higher energy consumption with TI_n and $TI_{n,DIF}$. Through the higher than ambient CO_2 set point of 400 μmol mol^{-1}, CO_2 supply and energy consumption (gas was burned with the heater for CO_2 supply) increased when vents were open. Because a proportional ventilation control to the difference between actual greenhouse temperature and ventilation temperature was applied, a lower ventilation set point lead to higher energy consumption during summer. A more advanced control for CO_2 supply to optimise between additional energy costs and CO_2 benefit for growth should therefore be recommended.

CONCLUSIONS

Most energy can be saved when temperature integration is combined with a flexible humidity regime (with a temperature bandwidth of ±2 °C, 33 % energy saving compared to the blueprint regime). The winter months are the most important in that respect as already 28 % annual energy consumption can be saved within 12 winter weeks. Also the achievement of a negative *DIF* for crop quality control) is then the easiest. In winter, daytime heating set point should be as low as possible to be able to shift as much as possible energy to periods of lower costs during the night with an unfolded screen.

During spring or autumn energy saving and the achievement of negative *DIF* are contrasting aims. In these seasons, the nested *TI* regime has its highest benefit

compared to all other regimes. *TI* with a several-day averaging period and temperature bandwidths as large as possible should be applied for energy saving. For *DIF* control, temperature integration and negative *DIF* can be joined and energy consumption and stem elongation can be reduced simultaneously compared to the blueprint. The actual value of the desired *DIF* plays an important role and the ability to naturally drop greenhouse temperature during the day to achieve the desired *DIF* is of most importance. The desired *DIF* must be adjusted to the season to get the maximum benefit between energy saving and stem-length control.

During summer, temperature integration as applied here has no profit. In that season, a more sophisticated CO_2 supply control is necessary to save energy.

CHAPTER 4

DISCUSSION AND CONCLUSION

4.1 GENERAL DISCUSSION

In the presented thesis, it was aimed to design sustainable climate regimes for greenhouse cultivation that were based on crop tolerance and crop needs. The starting point of this research was a more general concept aiming at a complete sustainable greenhouse system[9]. In this concept, new materials and new technology should be merged with a more advanced climate control concept based on optimal greenhouse climate control[32–34] to maximise energy saving and reductions of chemical biocide use. Optimal control with an explicit goal function automatically results in a non-fixed climate, within boundaries determined by crop tolerance. This means that the planned sustainable greenhouse system[9] depends on non-fixed climate regimes and is therefore different from current commercial practice.

In optimal control, increasing the degrees of freedom for temperature and humidity is highly beneficial. Optimal control has an economic goal function that consists of the expected benefit of the harvested crop minus the integrated costs of resources like heat and CO_2. The economical criterion is used to find a control path and the associated trajectories of the various states as temperature, humidity and CO_2 concentration of the greenhouse air that is best adapted to the actual prevailing conditions[241]. This procedure requires a model of the greenhouse as well as the crop. Since crop models are not yet able to correctly predict crop development and crop quality, constraints are used to ensure that the system states remain within tolerable bounds. Thus, the development of greenhouse climate control strategies that aim at creating more flexibility of the temperature and humidity states as performed in this

thesis is beneficial to the optimisation and fits well within the context of the complete Dutch solar greenhouse concept. The core of this thesis, however, has the current greenhouse technology as starting point, because there are many options for increasing sustainability by flexibilisation of the climate control regime in existing systems. As it is reported in the yearly survey of LEI[7, 10, 242], computerised climate control is broadly accepted among greenhouse growers. Climate computers have the highest degree of penetration of all technical measures contributing to energy saving, With a degree of penetration of 96 % in 2001 and a rather constant increase of 2.1 % per year, an almost complete coverage of all greenhouse nurseries with climate computers could be expected by 2004. In addition, some important technical equipment for reducing energy consumption, as e.g. movable screens, is widely spread and degree of penetration of most technical equipment constantly increases with an average of almost 2 % per year[7]. While the infrastructure is present it is, however, questionable whether the equipment is used in the best possible way. Climate is controlled conservatively in most greenhouses, as the slow progress of the use of regular temperature integration reveals. The acceptance of temperature integration among growers is low and did not increase in the last three years. Temperature integration with a certain software package was only 6 % in 1998 [242] and even decreased to 5 % in 1999 and 2000 [7, 10]. There is obviously much unused potential for energy saving with existing technique. Before more advanced technique as the complex Dutch solar greenhouse can be realised, existing technique should be evaluated first on its potential for energy saving with climate control. Rather than just creating the basis for optimal climate control, the approach in this thesis has been to develop various regimes that can be applied in current commercial greenhouse systems with only little adjustments.

A kind of optimisation procedure by only using the classical controllers and using their existing set point control has been proposed earlier [243]. The idea of leaving the classical controller structure intact has been adopted in this thesis. Only set points for relative humidity, temperature and CO_2 concentration were concerned and sent from a set point generator to the climate computer. The latter was responsible for controlling vents and heating valves in order to realize the desired climate. This is a major difference to the optimal control approach were the controlled states are the result of direct operation of the actuators such as the percentage vent opening and percentage heating pipe valve opening. The regimes described in the present thesis act therefore on a higher aggregation level.

Within these regimes, the crop was put central and it was aimed to increase energy saving while creating a climate that contributes to reducing biocide use. A crop based sustainable climate regime applicable for current greenhouse technology and creating the basis for future more advanced climate control was aimed at. However, creating flexibility is not a matter of just adjusting the settings, but can only be achieved by

respecting the different plant morphological and developmental parameters. In order to bring this out clearly, a crop was chosen that is sensitive to climate fluctuations and that needs to be treated carefully to achieve positive economical return.

The ornamental crop cut chrysanthemum was put central. In contrast to most vegetable crops, cut chrysanthemum is sold as a complete plant with stems, leaves and flowers. Therefore, climate control has to be performed in order to achieve a plant that fulfils the market demands. External quality is determined among others by temperature, radiation, CO_2 and relative humidity[26]. It can be hypothesised that when the designed climate is applicable for cut chrysanthemum, it could be applied for other crops with only little adjustments. In addition, chrysanthemum is the second most important cut flower in The Netherlands[174] and has the third highest biocide input after lily and rose[244]. Although the use of insecticides and acaricides decreased between 1994 and 1997 in Dutch chrysanthemum greenhouses, consumption of fungicides and chemical growth regulators increased[245]. Decreasing biocide use in cut chrysanthemum is therefore of major importance. Cut chrysanthemum was therefore assumed extraordinary suitable for climate control research for sustainable crop production in greenhouses.

In this thesis, the different aspects of climate control were treated independently first and then it was tried to combine them to a complete climate regime, denoted as nested temperature integration including a *DIF* treatment and process based humidity control in the synthesis CHAPTER 3.6. Basically, a modular regime was designed consisting of temperature integration, *DIF* control and process based humidity regime. Sub-regimes can be used independently or merged. This is one of the main advantages of the reported design. Also regimes can be applied in practice with using only a commercial greenhouse climate computer. A set point generator system similar to the software used in CHAPTER 3.3 to control the greenhouse climate in the experiments is the only additional need for using the described regimes.

TEMPERATURE CONTROL

The temperature regime consisted of a modified temperature integration regime and different approaches to handle the *DIF* aspect to control stem elongation. It was found that temperature integration and negative *DIF* can only be applied simultaneously with either reduced energy saving or increased use of chemical growth inhibitors. However, the in The Netherlands commonly used chemical daminocide can cause e.g. cancer and has further environmental consequences that are partly unknown[174]. Between 1994 and 1997 its use in chrysanthemum greenhouses increased by 20 % [245]. Its reduction is therefore of major importance. If this is to be achieved by negative *DIF*, the extra energy demand will provoke more CO_2 emission. Since CO_2 emission only recently decreased below the levels of 1990 [7], but a stronger decrease should be achieved (though no independent CO_2 emission rule exist for greenhouse

horticulture), an trade off problem exists. This problem could not be solved within the present thesis, although a joined temperature integration and zero *DIF* regime was proposed and successfully tested in CHAPTER 3.5. Moreover, when this regime was extended to a negative *DIF* as done in CHAPTER 3.6, simulations did show that it is, in fact, possible to reduce energy consumption while simultaneously attaining a negative *DIF*. However, the energy saving was modest and the targeted *DIF* set point was not fully reached in spring and early autumn. In these seasons, the regime was a compromise between two contrasting regimes, temperature integration and *DIF*. Temperature integration is partly based on the premise that heating is performed at times with lowest costs and that other times benefit from that through less heat requirement. In some periods of the year, as in spring and autumn, one can almost completely refrain from heating when natural solar radiation is utilised optimally. This is realised by almost no ventilation during the day and accordingly no or only little heating is required during cooler periods (usually nighttime). Hence, a positive *DIF* is attained with temperature integration in these seasons. A negative *DIF* regime counteracts that. With negative *DIF*, just the opposite temperature trajectory is targeted; temperature must drop during day in order to be able to heat up the greenhouse during night to respect the mean temperature restriction. A negative *DIF* is only set to reduce internode elongation, thus avoiding the need for chemical growth retardants. With a positive *DIF*, however internodes elongate even more, thus provoking an increased application of growth retardants. On the other hand, when stem-length is controlled with negative *DIF*, energy saving diminishes and CO_2 emission increases compared to temperature integration. Therefore, depending on the control regime, either more energy is consumed or more chemical growth retardant are applied in spring and autumn. As a first step towards solution of this problem a well performing crop quality model is needed[26]. When combining this with an economical-model and a greenhouse climate model, the optimal control approach could be used to find the best compromise. However, current quality and morphology models for crops are not mature enough, and are also not in a form that is feasible for climate control. Solving this optimisation remains problematic and other solutions should be found. A completely different approach would be to convince the market to accept longer stems which would probably occur when chemical growth inhibitors would be completely forbidden. Another option is genetic modification, but environmental problems of that are difficult to assess.

In the present situation, the decision whether to apply temperature integration with or without negative *DIF* restriction has to be decided per season (as was shown in CHAPTERS 3.4 and 3.6). In winter, a negative *DIF* does not restrict temperature integration when screens are used. Since about 2/3 of the growers have a movable screen[7] and this number constantly increases, it is assumed that the acceptance of temperature integration including heating to the night time when screens are unfolded

as described in CHAPTERS 3.4 and 3.6 is not restricted by commonly existing greenhouse technology. In summer, temperature control is difficult and temperature integration is not profitable. Then, energy consumption is low and CO_2 supply is the main energy consumer and negative *DIF* cannot be achieved.

A positive achievement of the temperature control strategy as developed here is the extended temperature range that is attained by a short and a long term integration period. Also the proposed temperature time and dose response contributed to more temperature flexibility. Although this regime was tested with experiments (including process based humidity control), and only little negative consequences were observed, tuning of the control model was not done. The approach is based on justifiable but still rather arbitrary functions. The next step must be to establish the hard and the soft limits as used in CHAPTER 3.1. This thesis could not solve the long lasting demand on establishing the temperature and time ranges over which integration can occur as was noted 15 years ago[65]. The presented design is, however, a further step in the development of feasible temperature integration regimes. Although the real boundaries are still unknown, it could be shown that much higher boundaries than currently applied are acceptable without detrimental effects to the crop. A general theoretical design rather than a mature approach was shown. To really establish the best possible boundaries empirically, large amounts of experiments must be done, probably for each crop and also for different cultivars.

One of the main disadvantages within cut chrysanthemum cultivation remains. Temperature integration can probably not be applied during all cultivation stages. This aspect was not investigated further. In the majority of this research, cut chrysanthemum was used as a model crop and it was not aimed to solve all plant specific problems. This is the reason why the existing developmental stage dependent temperature control approach[56] was used in the experiment in CHAPTER 3.3. When temperature integration as proposed here is applied with commercial chrysanthemum growers, the cultivation system needs to be changed such that different developmental stages can receive independent temperature control. This, however, is probably difficult to realise. Although the temperature control strategies developed in this thesis do not take into account a dependency on developmental stage, and therefore may not be useful for the entire cultivation period of this crop as it is cultivated nowadays, the flexible temperature regime can be applied for crops like tomato where is was actually designed for in CHAPTER 3.1.

CO_2 CONTROL

Simulations on energy consumption were performed with a validated greenhouse climate and control model[105]. Within the simulations, gas was burned for CO_2 supply. A heat storage tank with 120 m^3 ha^{-1} was used to store excess heat. With that

capacity, the tank was slightly bigger than the mean buffer size of 103 m^3 ha^{-1} as recently (year 2000) used in commercial practice in The Netherlands[7]. The buffer size in commercial practice increases quickly[7] and the 120 m^3 ha^{-1} used for simulations are therefore realistic for an average greenhouse in 2003. In The Netherlands, 58 % of the growers are burning gas for CO_2 production, even when there is no heat demand[7]. This however, consumes energy (CHAPTERS 3.4 and 3.6). In the nested temperature integration regime (CHAPTER 3.1), CO_2 was supplied for maximised crop photosynthesis with a maximum CO_2 set point of 1000 μmol mol^{-1} when vents were closed. Due to the extended vent closure, CO_2 supply is needed, otherwise greenhouse CO_2 concentration drops to low levels and photosynthesis is reduced strongly. Obviously, this increased energy consumption in summer, because heating demand is low with regular temperature control and it is even lower with temperature integration (CHAPTERS 3.4 and 3.6).

In the presented regime (nested temperature integration), CO_2 control was implemented in a rather heuristic way. The CO_2 supply rate was only taken into account as a switch-on switch-off control, using a set point of 350 and 1000 μmol mol^{-1} CO_2 when vents were open or closed, respectively. A more advanced approach combining simulated photosynthesis and greenhouse ventilation rate[66] would probably improve that regime. However, to this end a well performing crop photosynthesis model is needed. As was shown in CHAPTERS 2.2 and 2.4, existing crop photosynthesis models differ considerably in their predictive ability at temperatures occurring with the nested temperature integration regime. The model used in the nested temperature integration was the most promising at high temperatures (CHAPTER 2.4), but still discrepancies remain. These problems need to be solved before additional benefits can be expected from more advanced CO_2 control.

HUMIDITY CONTROL

The process based humidity regime contributed strongest to energy saving. Although the comparing relative humidity set point of 80 % was probably on the low side, high savings were also achieved compared to 85 % and 90 % relative humidity set point. The regime was designed for cut chrysanthemum only, for other plants a new set of rules must be defined. It was largely based on functions for which parameters were set in a more or less arbitrary way, so that this module needs to be tuned, too. Although experiments have shown that this regime did not result in negative consequences for the plants, the hard boundaries have not been tested. The process based humidity regime showed, nevertheless, that a fixed relative humidity set point could be changed with benefit to a more dynamic regime. This regime is

extraordinary useful to support temperature integration, but thanks to the modular set-up of the designed system it can also be used with regular temperature control.

<div align="center">IMPLEMENTATION OF THE DYNAMIC REGIME IN PRACTICE</div>

Dynamic temperature and humidity regimes as proposed were able to increase the degrees of freedom for climate control strongly. It could be shown that annual energy consumption could decrease by more than 1/3 when dynamic temperature and dynamic humidity regimes were combined (CHAPTER 3.6). With that combination crop dry yield increased by 39 % in a spring-experiment (CHAPTER 3.3), but with | 23.5 % energy saving was less than expected from simulations. In the simulations, nevertheless, the developmental stage dependent temperature control was not taken into account. When this period of about 25 % of the time would be excluded from temperature integration in the simulations, similar savings would be obtained. With that result, the energy efficiency target would have been reached easily. The experimental observations cannot be extrapolated to a complete year, because the experimental period was only three months. In addition, statistical evidence does not exist with only one experiment. The only way to obtain a more general view is by simulations. This is the reason why such simulations -with the standard year- were performed in CHAPTER 3.6.

In 2001, energy efficiency index was 52 % of the values from 1980 and to fulfil the convenant, the energy efficiency-index has to be decreased by an additional 17 % until 2010. A major part of this (10 %) can be achieved with standard estimated greenhouse technological development[28]. The remaining could easily be achieved with the kind of climate control as investigated in this thesis. This, however, requires that growers adapt the new policies. In practice, existing energy saving options remain largely unused and growers even apply-probably unnecessary- energy consuming measures. One example is the minimum-pipe temperature for dehumidification in the morning. In CHAPTER 3.2 and 3.3, the process based humidity regime showed that morning condensation does not harm the plant when leaves dry in a certain time-span (regarding fungi). Large amounts of energy can be saved but acceptance by the growers is necessary. As the reluctant acceptance of temperature integration reveals, the introduction of new climate regimes among the growers remain difficult. Although the grower-oriented organisation *Applied Plant Research* (PPO) has published several reports including that subject in The Netherlands[37, 40, 59, 239, 246, 247] and many articles in Dutch professional magazines were basically advising temperature integration[46, 54, 58, 246, 248–250], acceptance has even become less. The presented regimes include more dynamics than regular temperature integration and dynamic humidity regimes are not existing nowadays. Apparently, growers hesitate to trust this if it is not absolutely necessary from an energy saving point of view. The example about the acceptance of temperature integration shows that additional work

in the area of technology transfer and grower behaviour is needed before the present research can be seen as being a contribution to energy saving in greenhouse horticulture. On the other hand, perhaps due to different marketing, in Denmark the so called INTELLIGROW® system[136, 222, 251], a dynamic temperature control regime based on simple photosynthesis models was probably the reason that Danish growers commonly apply dynamic climate regimes. Also, government policy plays a significant part in achieving energy saving.

4.2 CONCLUSIONS

Current greenhouse technique contains high unused capacities for energy saving. The energy efficiency target for 2010 can be achieved with current technology and in combination with the presented dynamic climate regimes including nested temperature integration and process based humidity control. With that combination, annual energy consumption could decrease by more than 1/3.

The dynamic humidity regime can be applied without negative consequences for plants. Temperature can either be controlled with temperature integration, temperature integration restricted by a negative *DIF* or with regular temperature regime. Both main dynamic regimes (humidity and temperature) need still to be tuned for optimal performance.

In winter most energy can be saved when temperature integration is combined with screen control and process based humidity regime. Then, 28 % of the annual energy consumption can be saved compared to a blueprint regime according to commercial practice within only 12 weeks.

Temperature integration can be combined with a (negative) *DIF* regime to simultaneously achieve short – compact plants (reduce chemical growth inhibitors) and a reduction in energy consumption. This is however, a compromise. An optimisation problem between the two regimes aiming at sustainable greenhouse horticulture remains. This can only be solved when detailed models for crop quality,

development and growth will become available. The designed regimes can be applied in commercial greenhouses with only little adjustment. The only additional expense is a computer functioning as set point generator, and a suitable interface with the existing climate computer. In addition, the achieved degrees of freedom for two main states (temperature and humidity) form a promising perspective for future optimal greenhouse climate control. Dynamic climate regimes within current greenhouse technology can easily achieve the required 35 % energy efficiency index in 2010 relative to 1980, but acceptance of growers is the largest difficulty.

4.3 CONTRIBUTION OF THE THESIS

The present research presents designs for different climate regimes. Important steps were made towards a more efficient greenhouse climate control:

1) Crop photosynthesis models were evaluated at conditions expected with more sustainable climate regimes. It was shown with experimental evidence that theoretical considerations on the temperature- CO_2 effects in a crop that are based on theoretical models scaling up leaf photosynthesis to the crop level, are valid. It was shown that regular models can be applied up to 28 °C, but with higher temperatures modifications are needed. This can probably be achieved with an improved stomata model.

2) The well-known temperature integration principle was enriched with two nested time-frames and a temperature-dose response. The temperature flexibility could increase strongly when a low long-term temperature bandwidth was used. Parameters as the temperature hard limits and dose-response time, however, have yet to be supported with further experimental evidence.

3) A new approach to control relative humidity based on the underlying processes was introduced. This idea builds upon earlier ideas to use set points for transpiration[189, 252]. In the current approach, the major humidity affected processes were evaluated and general rules were formulated. From that, a control regime was designed. This regime forms a milestone in dynamic climate control, because it largely enhances dynamic temperature control, and contributes significantly to energy saving. The new regime was shown to be applicable in greenhouse cultivation

with cut chrysanthemum, although partly based on assumptions. For other crops, this approach can be used easily by determining the crop specific parameters.

4) Temperature integration without a *DIF* restriction was extensively compared to temperature integration with *DIF* restriction. Energy consumption with different settings was quantified. It was shown that an optimisation problem exists in spring and summer. To elucidate this, a joined temperature integration and *DIF* regime over several days was designed and tested. The use of an average *DIF* over several days rather than a *DIF* within 24-hours was proposed. In times and climate regions when cold and warm days interchange, this approach can increase energy saving and decrease final plant stem length simultaneously. The general optimisation problem, nevertheless, could not be solved.

6) A general basis for a more sustainable greenhouse horticulture in conjunction with optimal climate control was created through largely increasing the degrees of freedom for climate control.

REFERENCES

1. Charlson, R.J., S.E. Schwartz, J.M. Hales, R.D. Cess, J.A. Coakley, J.E. Hansen, and D.J. Hoffmann, 1992. Climate forcing by anthropogenic aerosols. Science, 255, 423-430

2. Fletcher, S.R., 2001. Global climate change: the Kyoto protocol. National Council for Science and the Environment, Washington DC, USA

3. NEIC, 2002. Greenhouse gases, global climate change, and energy. National Energy Information Center (NEIC)

4. Tweede-Kamer, 2003. Effectiviteit energiebesparingsbeleid in de glastuinbouw. (Efficiency energy-saving policy in greenhouse horticulture). Tweede Kamer der Staten-Generaal, vergaderjaar 2002-2003, 28 780, 2, Den Haag, The Netherlands, 62pp., (in Dutch)

5. RIVM, 2001. Milieubalans 2001. (Equilibrium of the environment 2001). Rijksinsituut voor Volksgezondheid en Milieu (RIVM), Kluwer, Den Haag, The Netherlands, (in Dutch)

6. Heuvelink, E., 1996. Dry matter partitioning in tomato: Validation of a dynamic simulation model. Annals of Botany, 77, 71-80

7. Van der Knijff, A., J. Benninga, J. Nienhuis, and N. Van Der Velden, 2002. Energie in de glastuinbouw van Nederland; Ontwikkelingen in de sector en op de bedrijven t/m 2001. (Energy in greenhouse horticulture in The Netherlands; Development in the sector and on the companies intil 2001). LEI, Den Haag, The Netherlands, 63pp., (in Dutch)

8. Productschap-Tuinbouw, 2002. Tuinbouwgids. Wegwijs in de Nederlandse tuinbouw. (Guide to horticulture. Direction in Dutch horticulture), Zoetermeer, The Netherlands, 63pp., (in Dutch)

9. Bot, G.P.A., 2001. Developments in indoor sustainable plant production with emphasis on energy saving. Computers and Electronics in Agriculture, 30, 151-165

10. Bakker, R., A. Van der Knijff, and N.J.A. Van der Velden, 2001. Energie in de glastuinbouw van Nederland. Ontwikkelingen in de sector en op de bedrijven t/m 2000. (Energy in greenhouse horticulture in The Netherlands; Development in the sector and on the companies intil 2000). LEI, Den Haag, The Netherlands, 62pp., (in Dutch)

11. Pluimers, J.C., 2001. An environmental system analysis of greenhouse horticulture in the Netherlands, Ph.D. Thesis, Wageningen University, The Netherlands, 181pp.

12. LNV, 1992. Meerjarenafsprak tussen de Nederlandse Glastuinbouwsector en de Staat vertegenwoordigt door de Ministers van EZ en LNV over verbetering van energie-efficiëntie. (Several-year agreement between the Dutch greenhouse horticultural sector and the government represented by the ministers from EZ and LNV to improve energy efficiency), Den Haag, The Netherlands, (in Dutch)

REFERENCES

13. LNV, 1997. Convenant Glastuinbouw en Milieu, 1995-2010 met integrale milieu taakstelling. (Declaration of intent greenhouse horticulture and environment, 1995-2010 with integral environmental targets). Ministry of Agriculture, Nature management and Fisheries (LNV), Den Haag, 187pp., (in Dutch).

14. Schroën, G.J.M., T. Kok, and G.H. Horeman, 2000. Voortgangsrapportage 1999. Bestuurovereenkomst Uitvoring Meerjarenplan Gewasbescherming. (Progress report 1999. Management agreement executing several year plan for plant protection). Ministerie van Landbouw, Natuurbeheer en Visserij (LNV), Ede, The Netherlands, 37pp., (in Dutch)

15. Kresten-Jensen, H.E., 1994. Effects of duration and degree of pulse-DIF temperatures on plant height and flowering of *Kalanchoë blossfeldiana* v. Poelln. Scientia Horticulturae, 59, 45-54

16. Cuijpers, L.H.M. and J.V.M. Vogelezang, 1992. DIF and temperature drop for short day pot plants. Acta Horticulturae, 327, 25-32

17. Cockshull, K.E., F.A. Langton, and C.R.J. Cave, 1995. Differential effects of different DIF treatments on chrysanthemum and poinsettia. Acta Horticulturae, 378, 15-25

18. Moe, R., 1994. Morphogenetic effects of temperature and the control of plant height by day/night temperature alternations, in The scientific basis of poinettia production, E. Stromme, Editor, The Agr. University of Norway: Aas, 65-72

19. Ueber, E. and L. Hendriks, 1992. Effects of intensity, durartion and timing of a temperature drop on the growth and flowering of *Euphorbia pulcherrima* WILLD. Ex Klotzsch. Acta Horticulturae, 327, 33-40

20. Strøm, M. and R. Moe, 1997. DIF affects internode and cell extension growth and cell number in *Campanula isophylla* shoots. Acta Horticulturae, 435, 17-24

21. Torre, S. and R. Moe, 1998. Temperature, DIF and photoperiod effects on the rhythm and rate of stem elongation in *Campanula isophylla* Moretti. Scientia Horticulturae, 72, 123-133

22. Myster, J., R. Moe, and O. Junttila, 1995. Does diurnal temperature fluctuations (DIF) regulate internode lengths mediated through the biosynthetic formation of GA1 in *Begonia X hiemalis* Fotch. Acta Horticulturae, 378, 123-128

23. Bertram, L., 1992. Stem elongation of *Dendranthema* and tomato plants in relation to day and night temperatures. Acta Horticulturae, 327, 61-69

24. Jacobson, B.M. and D.H. Willits, 1998. Developing relationships between environmental variables and stem elongation in chrysanthemum. Transactions of the ASAE, 41, 825-832

25. Steinbacher, F., F. Walz, and W. Horn, 1993. Ein Modell für das Längenwachstum von Topfchrysanthemen. (A model for elonagtion growth of pot chrysanthemum). Gartenbauwissenschaft, 58, 149-153, (in German)

26. Carvalho, S.M.P. and E. Heuvelink, 2001. Influence of greenhouse climate and plant density on external quality of chrysanthemum (*Dendranthema grandiflorum* (Ramat.) Kitamura): First steps towards a quality model. Journal of Horticultural Science and Biotechnology, 76, 249-258

27. Schouten, R.E., S.M.P. Carvalho, E. Heuvelink, and O. Van Kooten, 2002. Modelling of temperature-controlled internode elongation applied to chrysanthemum. Annals of Botany, 90, 353-359

28. Bakker, R., 1999. Effect van kasconstructie op het toekomstige energiegebruik in de glastuinbouw. (Effects of greenhouse construction on future energy consumption in greenhouse horticulture). LEI, Den Haag, The Netherlands, 58pp., (in Dutch)

29. Santamouris, M., C.A. Balaras, E. Dascalaki, and l.M. Vallindras, 1994. Passive solar agricultural greenhouses: a worldwide classification and evaluation of technologies and systems used for heating purposes. Solar Energy, 53, 411-426

30. Bailey, B.J., 1985. Wind dependent control of greenhouse temperature. Acta Horticulturae, 174, 381-386

31. Bredenbeck, H., 1989. Energy saving greenhouse systems with solar energy. Acta Horticulturae, 245, 300-303

32. Tap, R.F., 2000. Economic-based optimal control of greenhouse tomato crop production. Ph.D. Thesis, Wageningen University, The Netherlands, 127pp.

33. Gal, S., A. Angel, and I. Seginer, 1984. Optimal control of greenhouse climate: methodology. European Journal of Operations Research, 17, 45-56

34. Van Henten, E.J., 1994. Greenhouse climate management: an optimal control approach.Ph.D Thesis, Wageningen Agricultural University, The Netherlands, 329pp.

35. Van Straten, G., 1999. Acceptance of optimal operation and control methods for greenhouse cultivation. Annual Reviews in Control, 23, 83-90

36. Lacroix, R. and R. Kok, 1999. Simulation-based control of enclosed ecosystems - a case study: determination of greenhouse heating setpoints. Canadian Agricultural Engineering, 41, 175-183

37. Buwalda, F., B. Eveleens, and R. Wertwijn, 1999. Mogelijkheden voor energiebesparing door temperatuurintegratie bij siergewassen. Effecten van lichtniveau, temperatuurniveau en wachttijd op de integratiecapaciteit van Ficus, Kalanchoë, Gerbera en Roos. (Possibilities for energy saving with temperature integration in ornamental plants. Effects of radiation level, temperature and time on integration capacity of ficus, kalanchoë, gerbera en rose). Proefstation voor Bloemisterij en Glasgroenten, Aalsmeer, The Netherlands, 103pp., (in Dutch)

38. Van den Berg, G.A., 1987. Influence of temperature on bud break, shoot growth, flower bud atrophy and winter production of glasshouse roses. Ph.D. Thesis, Agricultural University Wageningen, The Netherlands, 170pp.

39. Rijsdijk, A.A. and J.V.M. Vogelezang, 2000. Temperature integration on a 24-hour base: a more efficient climate control strategy. Acta Horticulturae, 519, 163-169

40. Buwalda, F., B. Eveleens, and R. Wertwijn, 1999. Mogelijkheden voor energiebesparing door temperatuurintegratie bij siergewassen. Een inventarisatie van kritische processen bij zes sierteeltgewassen. (Possibilities for energy saving with temperature integration in ornamental plants. A survey of critical processes in six ornamental plants). Proefstation voor Bloemisterij en Glasgroenten, Aalsmeer, The Netherlands, 64pp., (in Dutch)

41. Cockshull, K.E., D.W. Hand, and F.A. Langton, 1981. The effects of day and night temperature on flower initiation and development in chrysanthemum. Acta Horticulturae, 125, 101-110

42. Miller, W.B., R.W. Langhans, and L.D. Albright, 1985. Plant growth under averaged day/night temperatures. Acta Horticulturae, 174, 313-326

43. Hendriks, L. and H.C. Scharpf, 1987. Neue Gewächshaus-Technik bedingt neue Regelstrategien. (New greenhouse technology requires new control strategies). Gb+Gw, 24, 872-878, (in German)

44. Hendriks, L. and K. Müller, 1988. Temperaturschwankungen tolerierbar? (Temperature fluctuations acceptable?). Gb+Gw, 37, 1578-1579, (in German)

45. Menne, A., 1992. Reaktionen einiger Zierpflanzen auf mehrtägige Fluktuationen von Temperatur und Lichtintensität. (Reactions of some ornamental plants on temperature and light fluctuations over several days). Ph.D. Thesis, Universität Hannover, Germany, 128pp., (in German)

46. Maaswinkel, R., 2001. Ook bij chrysant ruimte voor temperatuurintegratie. (Also with chrysanthemum possibilities for temperature integration). Vakblad voor de Bloemisterij, 43, 88-89, (in Dutch)

47. Liebig, H.P., 1988. Temperature integration by kohlrabi growth. Acta Horticulturae, 230, 371-380

48. Fink, M., 1993. Effects of short-term temperature fluctuations on plant growth and conclusions for short-term temperature optimization in greenhouses. Acta Horticulturae, 328, 147-150

49. Krug, H. and H.P. Liebig, 1980. Diurnal thermoperiodism of the cucumber. Acta Horticulturae, 118, 83-94

50. Slack, G. and D.W. Hand, 1983. The effect of day and night temperatures on the growth, development and yield of glasshouse cucumbers. Journal of Horticultural Science, 58, 567-573

51. De Koning, A.N.M., 1988. More efficient use of base load heating with a temperature integrating control programme. Effect on development, growth and production of tomato. Acta Horticulturae, 229, 233-237

52. De Koning, A.N.M., 1990. Long term temperature integration of tomato. growth and development under alternating temperature regimes. Scientia Horticulturae, 45, 117-127

53. Bakker, J.C. and J.A.M. Van Uffelen, 1988. The effect of diurnal temperature regimes on growth and yield of glasshouse sweet pepper. Netherlands Journal of Agricultural Science, 36, 201-208

REFERENCES

54. Heij, G., 1998. Temperatuurintegratie werkt ook bij paprika. (Temperature integration also applicable in sweet pepper). Groenten en Fruit / Glasgroenten, 13, 12-13, (in Dutch)

55. Bailey, B.J. and I. Seginer, 1989. Optimum control of greenhouse heating. Acta Horticulturae, 245, 512-418

56. Ludolph, D. and L. Hendriks, 1989. Dynamische Regelstrategien - Grenzen und Möglichkeiten. (Dynamic control strategies - boundaries and possibilities). Zierpflanzenbau, 4, 150-154, (in German)

57. Buwalda, F., A.A. Rijsdijk, J.V.M. Vogelezang, A. Hattendorf, and L.G.G. Batta, 1999. An energy efficient heating strategy for cut rose production based on crop tolerance to temperature fluctuations. Acta Horticulturae, 507, 117-125, (in Dutch)

58. Verdegaal, J., 1999. Twijfels over temperatuurintegratie zijn niet terecht. (Doubts about temperature integration are not justified). Vakblad voor de Bloemisterij, 25, 44-45, (in Dutch)

59. Rijsdijk, A.A., J.V.M. Vogelezang, G.J.L. Van Leeuwen, F.R. Van Noort, G. Heij, G.E. Mulderij, J. De Hoog, and H. Jasperse, 1998. Temperatuurintegratie op eetmalbasis. (Temperature integration over 24-hours). Proefstation voor Bloemisterij en Glasgroenten, Aalsmeer, The Netherlands, 73pp., (in Dutch)

60. Sigrimis, N., A. Anastasiou, and N. Rerras, 2000. Energy saving in greenhouses using temperature integration: a simulation survey. Computers and Electronics in Agriculture, 26, 321-341

61. Seginer, I., C. Gary, and M. Tchamitchian, 1994. Optimal temperature regimes for a greenhouse crop with a carbohydrate pool: A modelling study. Scientia Horticulturae, 60, 55-80

62. Tchamitchian, M. , B. Montbroussous, B. Jeannequin, and R. Martin-Clouaire, 1998. SERRISTE: daily greenhouse climate set-point determination for tomatoes. Paper read at Mathematical and control applications in agriculture and horticulture, at Hannover, Germany.

63. Tchamitchian, M. and I. Ioslovich, 2000. Equivalence of the temperature integral and the carbon balance concepts in plants: utility for control. Acta Horticulturae, 519, 171-180

64. Bellamy, L.A. and B.A. Kimball, 1986. CO_2 enrichment duration and heating credit as determined by climate, in Carbon dioxide enrichment of greenhouse crops, H.Z. Enoch and B.A. Kimball, Editors, CRC Press Inc.: Boca Raton, 167-197

65. Cockshull, K.E., 1988. The integration of plant physiology with physicle changes in the greenhouse climate. Acta Horticulturae, 229, 113-129

66. Bakker, J.C., 1985. A CO_2 control algorithm based on simulated photosynthesis and ventilation rate. Acta Horticulturae, 174, 387-392

67. Challa, H. and A.H.C.M. Schapendonk, 1986. Dynamic optimalization of CO_2 concentration in relation to climate control in greenhouses, in Carbon dioxide enrichment of greenhouse crops, H.Z. Enoch and B.A. Kimball, Editors, CRC Press Inc.: Boca Raton, 181

68. Karlsson, M.G., R.D. Heins, J.E. Erwin, and R.D. Berghage, 1989. Development rate during four phases of chrysanthemum growth as determined by preceding and prevailing temperatures. Journal of the American Society of Horticultural Science, 114, 234-240

69. Moe, R., 1989. Regulere planthoyden med dag-/nattemperatur. (Controlling plant heights with day/-night temperature). Gartneryrket, 8, 17-19, (in Norwegian)

70. Amsen, M.G., L.H. Jacobsen, and J.J. Brondum, 1990. Negative DIF: the effect of temperature drop prior to daybreak on internode length of young tomato seedlings. Tidsskrift-for-Planteavl., 94(5), 503-506.

71. Langton, F.A. and K.E. Cockshull, 1997. Is stem elongation determined by DIF or by absolute day and night temperatures? Scientia Horticulturae, 69, 229-237

72. Moe, R. and R.D. Heins, 1990. Control of plant morphogenesis and flowering by light quality and temperature. Acta Horticulturae, 272, 81-89

73. Erwin, J.E., R.D. Heins, and M.G. Karlsson, 1989. Thermomorphogenesis in *Lilium longiflorum*. American Journal of Botany, 76, 47-52

74. Carvalho, S.M.P., E. Heuvelink, R. Cascais, and O. Van Kooten, 2002. Effect of day and night temperature on internode and stem length in cut chrysanthemum: Is everything explained by DIF? Annals of Botany, 90, 111-118

75. Langton, F.A., 1998. Regulation of stem extension by temperature, in Genetic and environmental manipulation of horticultural crops, K.E. Cockshull, D. Gray, G.B. Seymour, and B. Thomas, Editors, CABI Publishing: New York, 191-203

76. Hendriks, L. and E. Ueber, 1995. Alternative methods of regulating the elongation growth of ornamental plants: A current assessment. Acta Horticulturae, 378, 159-167

77. Van Koot, Y. , and W. Van Ravestijn. 1963. The germination of tomato pollen on the stigma. Paper read at 16th International Horticultural Congress.

78. Bakker, J.C., 1991. Analysis of humidity effects on growth and production of glasshouse fruit vegetables. Ph.D. Thesis, Wageningen Agricultural University, The Netherlands, 155pp.

79. Kerssies, A., 1994. Epidemiology of Botrytis spotting on gerbera and rose flowers grown under glass. Ph.D. Thesis, Wageningen Agricultural University, The Netherlands, 131pp.

80. Holder, R. and K. Cockshull, 1990. Effects of humidity on the growth and yield of glasshouse tomatoes. Journal of Horticultural Science, 65, 31-39

81. Jolliet, O., B.J. Bailey, D.J. Hand, and K. Cockshull, 1993. Tomato yield in greenhouses related to humidity and transpiration. Acta Horticulturae, 328, 115-124

82. Ho, L.C., R. Belda, M. Brown, J. Andrews, and P. Adams, 1993. Uptake and transport of calcium and the possible causes of blossom-end rot in tomato. Journal of Experimental Botany, 44, 509-518

83. Cook, R.T.A., 2001. First report in England of changes in the susceptibility of *Puccinia horiana*, the cause of chrysanthemum white rust, to triazole and strobilurin fungicides. Plant Pathology, 50, 792

84. Dirkse, F.B., M. Dil, R. Linders, and I. Rietstra, 1982. Resistance in white rust (*Puccinia horiana* P. Henning) of chrysanthemum to oxycarboxin and benodanil in the Netherlands, in Mededelingen Fuculteit Landbouwwetenschap Rijksuniversiteit Gent, Gent, Belgium, 793-800

85. De Gelder, A., 2000. Vaststellen van grenswaarden voor luchtvochtigheid bij energiebesparende kasklimaatregeling met behoud van kwaliteit in sierteeltproducten. (Determining air humidity boundaries for energy saving greenhouse climate control respecting quality of ornamental plant products). Proefstation voor Bloemisterij en Glasgroenten, Aalsmeer, The Netherlands, 32pp., (in Dutch)

86. Bot, G.P.A., 1992. New greenhouse production control strategy. Acta Horticulturae, 312, 95-100

87. Körner, O., and H. Challa. 2001. Climate control regime for cut chrysanthemum in a solar greenhouse. Paper read at 38. Gartenbauwissenschaftliche Tagung, 28.02. - 02.03.2001, at Osnabrück, Germany.

88. Berry, J. and O. Björkmann, 1980. Photosynthetic response and adaptation to temperature in higher plants. Annual Review of Plant Physiology, 31, 491-543

89. Heuvelink, E., 1996. Tomato growth and yield: quantitative analysis and synthesis. Ph.D. Thesis, Wageningen Agricultural University, The Netherlands, 326pp.

90. Van Keulen, H. and E. Dayan, 1993. TOMGRO - a greenhouse-tomato simulation model. CABO-DLO, Wageningen, 48pp.

91. Gijzen, H., 1992. Simulation of photosynthesis and dry matter production of greenhouse crops. CABO-DLO, Wageningen, The Netherlands, 69pp.

92. Stanghellini, C., 1987. Transpiration of greenhouse crops. Ph.D. Thesis, Wageningen Agricultural University, The Netherlands, 150pp.

93. Tarnopolsky, M. and I. Seginer, 1999. Leaf temperature error from heat conduction along thermocouple wires. Agricultural and Forest Meteorology, 93, 185-194

94. Thornley, J.H.M., 1976. Mathematical models in plant physiology. Academic Press (Inc.), London, UK, 318pp.

95. Goudriaan, J., 1977. Crop Micrometereology: A simulation study. Pudoc, Wageningen, The Netherlands

96. Goudriaan, J. and H.H. Van Laar, 1994. Modelling potential crop growth processes. Kluwer, Dordrecht, The Netherlands, 238pp.

97. Farquhar, G.D., S. Von Caemmerer, and J.A. Berry, 1980. A biochemical model of photosynthetic CO_2 assimilation in leaves of C3 species. Planta, 149, 78-90

R<small>EFERENCES</small>

98. Gijzen, H., 1994. Ontwikkeling van een simulatiemodel voor transpiratie en wateropname en van een integral gewasmodel. (Development of a simulation model for transpiration and water uptake and an integral crop model). AB-DLO, Wageningen, The Netherlands, 90pp.

99. SAS, 1994. SAS/STAT guide for personal computers. SAS Institute Inc., Cary, NC, USA

100. Cannell, M.G.R. and J.H.M. Thornley, 1998. Temperature and CO_2 responses of leaf and canopy photosynthesis: a clarification using the non-rectangular hyperbola model of photosynthesis. Annals of Botany, 82, 883-892

101. Long, S.P., 1991. Modification of the response of photosynthetic productivity to rising temperature by atmospheric CO_2 concentrations: Has its importance been underestimated? Plant, Cell and Environment, 14, 729-739

102. Stanghellini, C., 1988. Microclimate and transpiration of greenhouse crops. Acta Horticulturae, 229, 405-410

103. Körner, O. and H. Challa, 2003. Design for an improved temperature integration concept in greenhouse cultivation. Computers and Electronics in Agriculture, 39, 39-59

104. Körner, O. and H. Challa, 2003. Process based humidity control regime for greenhouse crops. Computers and Electronics in Agriculture, in press

105. De Zwart, H.F., 1996. Analyzing energy-saving options in greenhouse cultivation using a simulation model. Ph.D. Thesis, Wageningen Agricultural University, The Netherlands, 236pp.

106. Nederhoff, E.M. and J.G. Vegter, 1994. Photosynthesis of stands of tomato, cucumber and sweet pepper measured in greenhouses under various CO_2-concentrations. Annals of Botany, 73, 353-361

107. Hao, X. and A.P. Papadopoulus, 1999. Effects of Supplementary Lighting and Cover Materials on Growth, Photosynthesis, Biomass Partitioning, Early Yield and Quality of Greenhouse Cucumber. Scientia Horticulturae, 80, 1-18

108. Wolfe, D.W., 1991. Low temperature effects on early vegetative growth, leaf gas exchange and water potential of chilling-sensitive and chilling-tolerant crop species. Annals of Botany, 67, 205-212

109. Stanghellini, C. and J.A. Bunce, 1993. Response of photosynthesis and conductance to light, CO_2, temperature and humidity in tomato plants acclimated to ambient and elevated CO_2. Photosynthetica, 29, 487-497

110. Bunce, J.A., 2000. Acclimation of photosynthesis to temperature in eight cool and warm climate herbaceous C3 species: Temperature dependence of parameters of a biochemical photosynthesis model. Photosynthesis Research, 63, 59-67

111. Heissner, A., 1997. Der CO_2-Gaswechsel von Paprikapflanzen in Abhängigkeit von der Bestrahlungsstärke, der CO_2-Konzentration, der Lufttemperatur und dem Dampfdrucksättigungsdefizit der Luft: Messungen und Modell. (CO_2 gas-exchange of sweet-pepper plants depending on irradiation, CO_2 concentration, air temperature and vapour pressure deficit: Measurements and model). Gartenbauwissenschaft, 62, 78-90, (in German)

112. Dutton, R.G., J. Jiao, M.J. Tsujita, and B. Grodzinski, 1988. Whole plant CO_2 exchange measurements for nondestructive estimation of growth. Plant Physiology, 86, 355-358

113. Boonen, C., R. Samson, K. Janssen, H. Pien, R. Lemeur, and D. Berckmans, 2002. Scaling the spatial distribution of photosynthesis from leaf to canopy in a plant growth chamber. Ecological Modelling, 156, 201-212

114. Van Iersel, M.W. and B. Bugbee, 2000. A multiple chamber, semicontinuous, crop carbon dioxide exchange system: design, calibration, and data interpretation. Journal of the American Society of Horticultural Science, 125, 86-92

115. Miller, D.P., G.S. Howell, and J.A. Flore, 1996. A whole plant, open gas-exchange system for measuring net photosynthesis of potted woody plants. Hort Science, 31, 944-946

116. Gijzen, H., J.G. Vegter, and E.M. Nederhoff, 1990. Simulation of crop photosynthesis: Validation with cucumber, sweet pepper and tomato. Acta Horticulturae, 268, 71-80

117. Hand, D.W., 1973. A null balance method for measuring crop photosynthesis in an airtight daylit controlled-environment cabinet. Agricultural Meteorology, 12, 259-270

118. Dayan, E., I. Zipori, H.Z. Enoch, D. Shmue, and P. Gefen, 1985. A system for measuring photosynthesis and respiration rates of crops in commercial size greenhouses. Acta Horticulturae, 174, 505-512

119. Hand, D.W., G. Clark, M.A. Hannah, J.H.M. Thornley, J. Warren-Wilson, and J.W. Wilson, 1992. Measuring the canopy net photosynthesis of glasshouse crops. Journal of Experimental Botany, 43, 375-381

120. Hand, D.W., J. Warren Wilson, B. Acock, and J.W. Wilson, 1993. Effects of light and CO_2 on net photosynthetic rates of stands of aubergine and Amaranthus. Annals of Botany, 71, 209-216

121. Zekki, H., C. Gary, A. Gosselin, and L. Gauthier, 1999. Validation of a photosynthesis model through the use of the CO_2 balance of a greenhouse tomato canopy. Annals of Botany, 84, 591-598

122. Jarvis, D.G. and J. Catsky, 1971. General principles of gasometric methods and the main aspects of installation design, in Plant Photosynthetic Production, Z. Sestak, J. Catsky, and D.G. Jarvis, Editors, Dr. W. Junk N.V.: The Hague, 49-111

123. Lake, J.V., 1966. Measurement and control of the rate of carbon dioxide assimilation by glasshouse crops. Nature, 209, 97-98

124. Scholtens, R., and A. Van 't Ooster. 1994. Performance and accuracy of methods for measuring natural ventilation rates and ammonia emission from naturally ventilated livestock houses. Paper read at Agricultural Engineering Society at Milano

125. Van 't Ooster, A., 1993. Tracergasexperimenten. (Experiments with tracer gas), in Meetmethode NH_3-emissie uit stallen, E.N.J. Ouwerkerk, Editor, Ministerie van Landbouw, Natuurbeheer en Visserij, Dienst Landbouwkundig Onderzoek: Wageningen, The Netherlands, 73-84, (in Dutch)

126. Acock, B., K.E. Cockshull, D.W. Hand, and J.W. Wilson, 1978. The use of airtight, daylit, controlled-environment cabinets for fundamental and applied physiological studies of canopy photosynthesis. Phytotronic Newsletter, 17, 7-10

127. Hansen, J.M. and K. Høgh-Schmidt, 1996. A computer controlled chamber system designed for greenhouse microclimatic modelling and control. Acta Horticulturae, 440, 310-315

128. Goudriaan, J., H.H. Van Laar, H. Van Keulen, and W. Louwerse, 1985. Photosynthesis, CO_2 and plant production, in Wheat Growth and Modelling, W. Day and R.K. Atkins, Editors, NATO ASI, 107-122

129. Spitters, C.J.T., 1986. Separating the diffuse and direct component of global radiation and its implication for modeling canopy photosynthesis. Part II. Calculation of canopy photosynthesis. Agricultural and Forest Meteorology, 28, 231-242

130. Bot, G.P.A., 1983. Greenhouse climate : from physical processes to a dynamic model. Ph.D. Thesis, Wageningen Agricultural University, The Netherlands, 240pp.

131. Gijzen, H. and J. Goudriaan, 1989. A flexible and explanatory model of light distribution and photosynthesis in row crops. Agricultural and Forest Meteorology, 48, 1-20

132. Nederhoff, E. and J.G. Vegter, 1994. Canopy photosynthesis of tomato, cucumber and sweet pepper in greenhouses: measurements compared to models. Annals of Botany, 73, 421-427

133. Van Straten, G., H. Challa, and F. Buwalda, 2000. Towards user accepted optimal control of greenhouse climate. Computers and Electronics in Agriculture, 26, 221-238

134. Van Straten, G., L.G. Van Willigenburg, and R.F. Tap, 2002. The signifcance of crop co-states for receding horizon optimal control of greenhouse climate. Control Engineering Practice, 10, 625-632

135. Lee, J.H., 2002. Analysis and simulation of growth and yield of cut chrysanthemum. Ph.D. Thesis, Wageningen University, The Netherlands, 120pp.

136. Aaslyng, J.M., N. Ehler, P. Karlsen, and E. Rosenqvist, 1999. Intelligrow: A component based greenhouse climate control system for decreasing energy consumption. Acta Horticulturae, 507, 35-41

137. Bertin, N. and E. Heuvelink, 1993. Dry-matter production in a tomato crop: comparison of two simulation models. Journal of Horticultural Science, 68, 995-1011

138. Tatsumi, M. and Y. Hori, 1970. Studies on the photosynthesis of vegetable crops II. Effect of temperature on the photosynthesis of young plant of vegetables in relation to light intensity. Bulletin of the Horticultural Research Station, Japan, Series A, 181-188

139. Enoch, H.Z. and R.G. Hurd, 1977. Effect of light intensity, carbon dioxide concentration and leaf temperature on gas exchange of spray carnation plants. Journal of Experimental Botany, 28, 84-95

140. Drake, B.G., M.A. Gonzàlez-Meler, and S.P. Long, 1997. More efficient plants: a consequence of rising atmospheric CO_2? Annual Review of Plant Physiology and Plant Molecular Biology, 48, 609-639

REFERENCES

141. Nilwik, H.J.M., 1980. Photosynthesis of whole sweet pepper plants 1. Response to irradiance and temperature as influenced by cultivation conditions. Photosynthetica, 14, 373-381

142. Al-Khatib, K. and G.M. Paulsen, 1999. Crop physiology and metabolism: high temperature effects on photosynthetic processes in temperate and tropical plants. Crop Science, 39, 119-125

143. Long, S.P., C.P. Osborne, and S.W. Humphries, 1997. Photosynthesis, rising atmospheric CO_2 concentration and climate change, in Scope 56: Global Change, A. Bremeyer, D.O. Hall, and J. Melillo, Editors, Wiley: Chichester, UK

144. Acock, B., 1991. Modelling canopy photosynthesis response to carbon dioxide, light interception, temperature, and leaf traits, in Modeling crop photosynthesis - from biochemistry to canopy, CSSA Special Publication, American Society of Agronomy and Crop Science Society of America, 41-55

145. Seginer, I., 1993. Crop models in greenhouse climate control. Acta Horticulturae, 328, 79-98

146. Ito, T., 1971. Photosynthetic activity of vegetable plants and its horticultural significance. II. the time course of photosynthesis in the tomato plant as influenced by some external and internal factors, especially by water and starch contents in the leaf. Journal of the Japanese Society for Horticultural Sciences, 40, 41-47

147. SAS, 2000. SAS/STAT guide for personal computers. SAS Institute Inc., Cary, NC, USA

148. McCree, K.J., 1972. Test of current definitions pf photosynthetically active radiation against leaf photosynthesis data. Agricultural Meteorology, 10, 443-453

149. Laing, W.A., W.L. Ogren, and R.H. Hageman, 1974. Regulation of soybean net photosynthetic CO_2 fixation by the interaction of CO_2, O_2, and ribulose 1,5-diphosphate carboxylase. Plant Physiology, 54, 678-685

150. Acock, B., D.W. Hand, J.H.M. Thornley, and J. Warren Wilson, 1976. Photosynthesis in stands of green peppers, an application of empirical and mechanistical models to controlled-environment data. Annals of Botany, 40, 1293-1307

151. Hand, D.W., 1988. Effects of atmospheric humidity on greenhouse crops. Acta Horticulturae, 229, 143-158

152. Johnson, I.R. and J.H.M. Thornley, 1984. A model of instantaneous and daily canopy photosynthesis. Journal of Theoretical Biology, 107, 531-545

153. Giaglaras, P., M. Baille, and A. Baille, 1995. Net photosynthesis response to light and air CO_2 concentration of *Begonia × hiemalis*: whole plant measurements and modelling. Scientia Horticulturae, 63, 83-100

154. Collatz, G.J., J.T. Ball, C. Grivet, and J.A. Berry, 1991. Physiological and environmental regulation of stomatal conductance, photosynthesis and transpiration: a model that includes a laminar boundary layer. Agricultural and Forest Meteorology, 54, 107-136

155. Kim, S.H. and J.H. Lieth, 2003. Parametrization and testing of a coupled model of photosynthesis conductance for greenhouse rose crop. Acta Horticulturae, 593, 113-120

156. Nederhoff, E.M., 1994. Effects of CO_2 concentration on photosynthesis, transpiration and production of greenhouse fruit vegetable crops. Ph.D. Thesis, Wageningen Agricultural University, The Netherlands, 213pp.

157. Von Caemmerer, S. and G.D. Farquhar, 1981. Some relationships between the biochemistry of photosynthesis and the gas exchange of leaves. Planta, 153, 376-387

158. Medlyn, B.E., E. Dreyer, D. Ellsworth, M. Forstreuter, P.C. Harley, M.U.F. Kirschbaum, X. Le Roux, P. Montpied, J. Strassemeyer, A. Walcroft, K. Wang, and D. Loustau, 2002. Temperature response of parameters of a biochemically based model of Photosynthesis. II. A review of experimental data. Plant, Cell and Environment, 25, 1167-1179

159. Bernacchi, C.J., E.L. Singsaas, C. Pimentel, A.R. Portis, and S.P. Long, 2001. Improved temperature response functions for models of Rubisco-limited photosynthesis. Plant, Cell and Environment, 24, 253-259

160. Jones, H.G., 1998. Stomatal control of photosynthesis and transpiration. Journal of Experimental Botany, 49, 387-398

161. Jarvis, A.J. and W.J. Davies, 1998. The coupled response of stomatal conductance to photosynthesis and transpiration. Journal of Experimental Botany, 49, 399-406

162. Harley, P.C., R.B. Thomas, J.F. Reynolds, and B.R. Strain, 1992. Modelling photosynthesis of cotton grown in elevated CO_2. Plant, Cell and Environment, 15, 271-282

163. Ball, J.T., I.E. Woodrow, and J.A. Berry, 1987. A model predicting stomatal conductance and its contribution to the control of photosynthesis under different environmental conditions, in Progress in Photosynthesis Research, J. Biggins, Editor, Martinus Nijhoff: Dordrecht, The Netherlands, 221-224

164. Farquhar, G.D. and S.C. Wong, 1984. An empirical model of stomatal conductance. Australian Journal of Plant Physiology, 11, 191-209

165. Tap, R.F., L.G. Van Willigenburg, and G. Van Straten. 1996. Receding horizon optimal control of greenhouse climate based on the lazy man weather prediction. Paper read at 13th IFAC World Congress, at San Francisco, USA.

166. Kaniuga, Z., B. Sochanowicz, J. Zabek, and K. Krzystyniak, 1978. Photosynthetic apparatus in chilling-sensitive plants. 1. Reactivation of Hill reaction activity inhibited on the cold and dark storage of detached leaves and intact plants. Planta, 140, 121-128

167. Hurd, R.G. and C.J. Graves, 1984. The influence of different temperature patterns having the same integral on the earliness and yield of tomatoes. Acta Horticulturae, 148, 547-54

168. Langhans, R.W., M. Wolfe, and L.D. Albright, 1981. Use of average night temperatures for plant growth for potential energy savings. Acta Horticulturae, 115, 31-37

169. Rietze, E. and H.J. Wiebe, 1989. Limits of a short-term temperature decrease as a base for on-line control. Acta Horticulturae, 248, 345-348

170. Sato, S., M.M. Peet, and J.F. Thomas, 2000. Physiological factors limit fruit set of tomato (*Lycopersicon esculentum* Mill.) under chronic, mild heat stress. Plant, Cell and Environment, 23, 719-726

171. Larcher, W. and M. Bodner, 1980. Dosisletalität-Nomogramm zur Charakterisierung der Erkältungsempfindlichkeit tropischer Pflanzen. (Dose-lethality nomogram for evaluating susceptibility to chilling in tropical plants). Angewandte Botanik, 54, 273-278, (in German)

172. De Zwart, H.F., 1993. Determination of direct transmission of a multispan greenhouse using vector algebra. Journal of Agricultural Engineering Research, 56, 39-49

173. De Jong, T., 1990. Natural ventilation of large multi-span greenhouses. Ph.D. Thesis, Wageningen Agricultural University, The Netherlands 116pp.

174. Spaargaren, J.J., 2002. Jaarrond chrysanthen - teelt en achtergronden. (Year-round chrysanthenmums - cultivation and background), 3 ed., Ir. J.J. Spaargaren, Aalsmeer, The Netherlands, 253pp.

175. Woerden, S.C. and J.P. Bakker, eds, 2000. Kwantitatieve Informatie voor de Glastuinbouw 2000-2001. (Quantative information about the greenhoue sector 2001-2001)., Proefstation voor Bloemisterij en Glasgroenten, Naaldwijk, The Netherlands, 188pp., (in Dutch)

176. Körner, O., H. Challa, and R.J.C. Van Ooteghem, 2003. Modelling temperature effects on crop photosynthesis at high radiation in a solar greenhouse. Acta Horticulturae, 593, 137-144

177. Breuer, J.J.G. and N.J. Van de Braak, 1989. Reference year for dutch greenhouses. Acta Horticulturae, 248, 101-108

178. De Koning, A.N.M., 1989. The effect of temperature on fruit growth and fruit load of tomato. Acta Horticulturae, 248, 229-336

179. Jewett, T.J. and W.R. Jarvis, 2001. Management of the greenhouse microclimate in relation to disease control: a review. Agronomie, 21, 351-366

180. Bakker, J.C. and H.F. De Zwart, 1999. Minimumbuis ondermijnt temperatuurintegratie. (Minimum-pipe temperature control counteracts temperature integration). Vakblad voor de Bloemisterij, 48 (23), 28-29, (in Dutch)

181. Kranz, J., 1996. Epidemiologie der Pflanzenkrankheiten. (Epidemiology of plant diseases). 1 ed. Ulmer, Stuttgart, 413pp., (in German)

182. Mortensen, L.M., 1986. Effect of relative humidity on growth and flowering of some greenhouse plants. Scientia Horticulturae, 29, 301-307

183. Mortensen, L.M., 2000. Effects of air humidity on growth, flowering, keeping quality and water relations of four short-day greenhouse species. Scientia Horticulturae, 86, 299-310

REFERENCES

184. Hand, D.W., F.A. Langton, M.A. Hannah, and K. Cockshull, 1996. Effects of humidity on the growth and flowering of cut-flower chrysanthemums (*Dendranthema grandiflora* Tzvelev). Journal of Horticultural Science, 71, 227-234

185. Gislerød, H.R. and P.E. Nelson, 1989. The interaction of relative humidity and carbon dioxide enrichment in the growth of Chrysanthemum x morifolium Ramat. Scientia Horticulturae, 38, 305-313

186. Bakker, J.C., G.W.H. Welles, and J.A.M. Van Uffelen, 1987. The effects of day and night humidity on yield and quality of glasshouse cucumbers. Journal of Horticultural Science, 62, 361-368

187. Bakker, J.C., 1990. Effects of day and night humidity on yield and fruit quality of glasshouse tomatoes (*Lycopersicon esculentum* Mill.). Journal of Horticultural Science, 65, 323-331

188. Nederhoff, E., 1998. Coping with low air humidity. New Zealand Commercial Grower, 53 (1), 17-18.

189. Stanghellini, C. and W.T.M. Van Meurs, 1997. Crop transpiration: A greenhouse climate control parameter. Acta Horticulturae, 245, 384-388

190. Huber, L. and T.J. Gillespie, 1992. Modeling leaf wetness in relation to plant disease epidemiology. Annual Review of Plant Phytopathology, 30, 553-577

191. Uchida, T., 1983. Studies on epidemiology and control of chrysanthemum white rust, caused by *Puccinia horiana* P. Henn.. Bulletin of the Yamanashi Agricultural Experiment Station, Futaba, Yamanashi, Japan, 105pp.

192. Krebs, E.K., 1991. Krankheiten und Schädlinge durch Temperatur begrenzen. (Limiting diseases and pests by temperature). Gb+Gw, 39, 1942-1945, (in German)

193. Horst, R.K. and P.E. Nelson, 1997. Compendium of chrysanthemum diseases, Cornell University, NY, USA. American Phytopathological Society (APS Press), St. Paul, USA, 62pp.

194. Dickens, J. and R. Potter, 1983. Spraying for white rust. Grower, 100 (18), 35-37.

195. D' Aulerio, A.Z. and S. De Polzer, 1982. (Il crisantemo e le sue principali malattie crittogamiche. (Chrysanthemums and their main fungal diseases). Informatore di Ortoflorofrutticoltura, 23, 7-12, (in Italian)

196. Meneses, J.F., A.A. Monteiro, and P.E. Abreu, 1994. Influence of two different natural ventilation methods on greenhouse climate, tomato production and Botrytis control. Plasticulture, 101, 3-12

197. Nederhoff, E., 1997. High humidity and plant diseases. New Zealand Commercial Grower, 52 (4), 18.

198. Nederhoff, E., 1997. How to use RH and other humidity measures. New Zealand Commercial Grower, 52 (2), 40.

199. Kerssies, A., 1993. *Botrytis cinerea* en echte meeldauw. Het klimaat als bestrijdingsmiddel. (*Botrytis cinerea* and powdery mildew. The climate as biocide). Vakblad voor de Bloemisterij, 48(23), 41-41., (in Dutch)

200. Verhaar, M.A., 1998. Studies on biological control of powdery mildew in cucumber (*Sphaerotheca fuliginea*) and rose (*S. pannosa*) by means of mycoparasites. Ph.D. Thesis, Wageningen University, The Netherlands, 164pp.

201. Watterson, J.C., 1986. Diseases, in The Tomato Crop, J.G. Atherton and J. Rudich, Editors, Chapman and Hall: London, 443-484

202. Liu, H.L., 2001. Management of rose powdery mildew with automatic water sprays. Plant Protection Bulletin Taichung, 43, 7-16

203. Coelho, M.V.S., F.A.C. Cafe, C.A. Lopes, and W.A. Marouelli, 2000. Severity of powdery mildew on hybrid squash under different water depths and nitrogen levels. Fitopatologia Brasileira, 25, 157-160

204. Yarwood, C.E., 1978. Water stimulates *Sphaerotheca*. Mycologica, 70, 1035-1039

205. Sivapalan, A., 1993. Effects of water on germination of powdery mildew conidia. Mycological Research, 93, 71-76

206. Yamaoka, N. and Y. Takeuchi, 1999. Morphogenesis of the powdery mildew fungus in water (4). The significance of conidium adhesion to the substratum for normal appressorium development in water. Physiological and Molecular Plant Pathology, 54, 145-154

207. Challa, H. and G. Van Straten, 1993. Optimal diurnal climate control in greenhouses as related to greenhouse management and crop requirements, in The Computerized Greenhouse, Y. Hashimoto, G.P.A. Bot, W. Day, H.J. Tantau, and H. Nonami, Editors, Academic Press: San Diego, 119-138

208. Monteith, J.L., 1973. Principles of environmental physics. Edward Arnold, London, 241pp.

209. Monsi, M. and T. Saeki, 1953. Über den Lichtfaktor in den Pflanzengesellschaften und seine Beschreibung für die Stoffproduktion. (About the light factor in plant communities and its description for production). Japanese Journal of Botany, 14, 22-52, (in German)

210. Zolnier, S., G.S. Gates, J. Buxton, and C. Mach, 2000. Psychrometric and ventilation constraints for vapor pressure deficit control. Computers and Electronics in Agriculture, 26, 343-359

211. Avissar, R. and Y. Mahrer, 1982. Verification study of a numerical greenhouse microclimate model. Transactions of the ASAE, 25, 1711-1720

212. Zhang, Y., Y. Mahrer, and M. Margolin, 1997. Predicting the microclimate inside a greenhouse: an application of a one-dimensional numerical model in an unheated greenhouse. Agricultural and Forest Meteorology, 86, 291-297

213. Van der Knijff, A., H.F. De Zwart, N.J.A. Van Der Velden, and R. Bakker, 2001. Energieclustering in de glastuinbouw. (Energy clusters in greenhouse horticulture). LEI, Den Haag, The Netherlands, 120pp.

214. Seginer, I., 1981. Economic greenhouse temperatures. Acta Horticulturae, 115, 439-452

215. Körner, O. and H. Challa, 2003. Energy saving climate control regime for greenhouse cut chrysanthemum. Acta Horticulturae, (Proceedings of the XVII International Horticultural Congress. Symposium: Protected Cultivation 2002, in search for structures, systems, and plant materials for sustainable production of greenhouses. Toronto, Canada, August 2002), in press

216. Kempkes, F.L.K. and N.J. Van de Braak, 2000. Heating system position and vertical microclimate distribution in chrysanthemum greenhouse. Agricultural and Forest Meteorology, 104, 133-142

217. Cockshull, K.E. and A.M. Kofranek, 1994. High night temperatures delay flowering, produce abnormal flowers and retard stem growth of cut-flower chrysanthemum. Scientia Horticulturae, 56, 217-234

218. Wilkins, H.F., W.E. Healy, and K.L. Grueber, 1990. Temperature regime at various stages of production influences growth and flowering of *Dendranthema* X *grandiflorum*. Journal of the American Society of Horticultural Science, 115, 732-736

219. Adams, S.R., S. Pearson, and P. Hadley, 1998. The effect of temperature on inflorescence initiation and subsequent development in chrysanthemum cv. Snowdown (*Chrysanthemum x morifolium* Ramat.). Scientia Horticulturae, 77, 59-72

220. Van Ruiten, J.E.M. and J. De Jong, 1984. Speed of flower induction in *Chrysanthemum morifolium* depends on cultivar and temperature. Scientia Horticulturae, 23, 287-294

221. Cockshull, K.E., 1979. Effects of irradiance and temperature on flowering of *Chrysanthemum morifolium* Ramat. in continous light. Annals of Botany, 44, 451-460

222. Rosenqvist, E., C.O. Ottosen, and J.M. Aaslyng, 2001. Let the plant control the climate. FloraCulture International, 5, 28-31.

223. Hansen, J.M., N. Ehler, P. Karlsen, K. Høgh-Schmidt, and E. Rosenqvist, 1996. Decreasing the environmental load by a photosynthetic based system for greenhouse climate control. Acta Horticulturae, 440, 105-111

224. Peet, M.M., D.H. Willits, K.E. Tripp, W.K. Kroen, D.M. Pharr, M.A. Depa, and P.V. Nelson. 1991. CO_2 enrichment responses of chrysanthemum, cucumber and tomato: photosynthesis, growth, nutrient concentrations and yield. Paper read at Impact of global climatic changes on photosynthesis and plant productivity, at New Delhi, India.

225. Marcelis, L.F.M., E. Heuvelink, and J. Goudriaan, 1998. Modelling biomass production and yield of horticultural crops: a review. Scientia Horticulturae, 74, 83-111

226. Gijzen, H., 1995. Short-term crop responses, in Greenhouse climate control, an integrated approach, J.C. Bakker, G.P.A. Bot, H. Challa, and N.J. Van de Braak, Editors, Wageningen Pers: Wageningen, The Netherlands, 16-62

227. Hendriks, L., D. Ludolph, and A. Menne, 1990. Influence of different heating strategies on morphogenesis and flowering of ornamentals. Acta Horticulturae, 305, 9-17

REFERENCES

228. Gislerød, H. and P.V. Nelson, 1997. Effect of relative air humidity and irradiance on growth of Dendranthema X grandiflorum (Ramat.) Kitamura. Gartenbauwissenschaft, 62, 214-218

229. Cockshull, K.E., 1982. Disbudding and its effect on dry matter distribution in *Chrysanthemum morifolium*. Journal of Horticultural Science, 57, 205-207

230. Karlsson, M.G. and R.D. Heins, 1992. Chrysanthemum dry matter partitioning patterns along irradiance and temperature gradients. Canadian Journal of Plant Science, 72, 307-316

231. Pearson, S., P. Hadley, and A.E. Wheldon, 1995. A model of the effect of day and night temperature on the height of chrysanthemum. Acta Horticulturae, 378, 71-80

232. Khattak, A.M. and S. Pearson, 1997. The effect of light quality and temperature on the growth and development of chrysanthemum cvs. Bright Golden Anne and Snowdon. Acta Horticulturae, 435, 113-121

233. Karlsson, M.G., R.D. Heins, J.E. Erwin, R.D. Berghage, W.H. Carlsson, and J.A. Biernbaum, 1989. Temperature and photosynthetic photon flux influence chrysanthemum shoot development and flower. Journal of the American Society of Horticultural Science, 114, 158-163

234. Van de Braak, N.J., 1995. Heating equipment, in Greenhouse climate control, an integrated approach, J.C. Bakker, G.P.A. Bot, H. Challa, and N.J. Van de Braak, Editors, Wageningen Pers: Wageningen, The Netherlands, 171-179

235. Yoo, H. and E. Pak, 1993. Theoretical model of the charging process for stratified thermal storage tanks. Solar Energy, 51, 513-519

236. Miguel, A.A.F., 1998. Transport phenomena through porous screens and openings : from theory to greenhouse practice. Ph.D. Thesis, Wageningen Agricultural University, Wageningen, The Netherlands, 129pp.

237. Tap, R.F., L.G. Willigenburg, and G. Van Straten, 1996. Experimental results of receding horizon optimal control of greenhouse climate. Acta Horticulturae, 406, 229-238

238. Lawson, R.H., 1996. Economic importance and trends in ornamental horticulture. Acta Horticulturae, 432, 226-237

239. Buwalda, F., A.A. Rijsdijk, G.J.L. Van Leuwen, A. Hattendorf, and J.V.M. Vogelezang, 1999. Mogelijkheiden voor energiebesparing door temperatuurintregratie bij siergewassen. Toetsen van een meerdags integrerende temperatuurregeling onder realistische teeltomstandigheden. (Possibilities for energy saving with temperature integration in ornamental plants. (Evaluation of a several-day temperature regime under realistic cultivation methods). Proefstation voor Bloemisterij en Glasgroenten, Aalsmeer, The Netherlands, 34pp., (in Dutch)

240. Tantau, H.J., 1998. Energy saving potential of greenhouse climate control. Mathematics and Computers in Simulation, 48, 93-101

241. Challa, H. and G. Van Straten, 1995. Greenhouse climate control systems, in Greenhouse climate control, J.C. Bakker, G.P.A. Bot, H. Challa, and N.J. Van de Braak, Editors, Wageningen Pers: Wageningen, The Netherlands, 249-261

242. Bakker, R., A. Van der Knijff, N.J.A. Van der Velden, and A.P. Verhaegh, 2000. Energie in de glastuinbouw van Nederland. Ontwikkelingen in de sector en op de bedrijven t/m 1999. (Energy in greenhouse horticulture in The Netherlands; Development in the sector and on the companies until 1999). LEI, Den Haag, The Netherlands, 62pp., (in Dutch)

243. Tantau, H.J., 1993. Optimal control for plant production in greenhouses, in The Computerized Greenhouse, Y. Hashimoto, G.P.A. Bot, W. Day, H.J. Tantau, and H. Nonami, Editors, Academic Press, Inc.: San Diego, 139-152

244. CBS, 2000. Kencijfers tuinbouwgewassen onder glas. (Numbers on crops in greenhouse horticulture). Centraal bureau voor de statistiek, Den Haag, The Netherlands., (in Dutch)

245. Vernooij, C.J.M. and C. Ploeger, 1999. Energie en gewasbescherming op chrysanthebedrijven. (Energy and plant protection at chrysanthemum growers). LEI, Den Haag, 67pp., (in Dutch)

246. Rijsdijk, A.A., 2000. Temperatuurgrenzen aan de teelt van tomaat bij minimaliseren van de gasansluitwaarde. (Temperature limits on tomato cultivation for minmising gas-connection). Proefstation voor Bloemisterij en Glasgroenten, Naaldwijk, The Netherlands, 23pp., (in Dutch)

247. Buwalda, F., 1999. Mogelijkheden voor energiebesparing door temperatuurintegratie bij siergewassen. Literatuuroverzicht. (Possibilities for energy saving with temperature integration in

ornamental plants. Literature survey). Proefstation voor Bloemisterij en Glasgroenten, Aalsmeer, The Netherlands, 57pp., (in Dutch)

248. Boonekamp, G., 2001. Veel besparen met goede plantsturing. (High savings with well performing plant control). Groenten en Fruit, 14, 30-31., (in Dutch)

249. Rijsdijk, A.A., 1998. Temperatuur integreren loont. Vakblad voor de Bloemisterij, 13, 46-48, (in Dutch)

250. Rijsdijk, T., 1998. Energie besparen met temperatuurintegratie. (Energy saving with temperature integration). Groenten en Fruit / Glasgroenten, 13, 10-11, (in Dutch)

251. Rosenqvist, E., 1999. IntelliGrow - a new climate control concept, in Grøn Viden (English edition). Ministeriet for Fødevarer, Landbrug og Fiskeri, Danmarks Jordbrugs Forskning, 8pp.

252. Stanghellini, C. and W.T.M. Van Meurs, 1992. Environmental control of greenhouse crop transpiration. Journal of Agricultural Engineering Research, 51, 297-311

SUMMARY / SAMENVATTING / ZUSAMMENFASSUNG

SUMMARY

The concern about anthropogenic *greenhouse gas* emission affecting the Earth's climate increases. In 1992 and 1997 negotiations took place on the control of emissions of greenhouse gases and a convention to reduce *greenhouse gas* emission was signed by the industrial nations. One of the most important greenhouses gases is carbon dioxide (CO_2) and it's atmospheric concentration must be reduced to prevent global warming. In The Netherlands, the industry was split into sectors to reduce fossil energy consumption, the main contributor to CO_2 emission. The agricultural sector was a major *greenhouse gas* emitter with more than 10 % of the Dutch national in 2000. One third of that was CO_2 of which and 80 % was attributed to greenhouse horticulture. In 1997, the Dutch greenhouse sector and the government signed the *declaration of intent on greenhouse horticulture and environment*, the successor of an earlier signed agreement from 1992. In the agreement, energy efficiency (energy consumption per unit produce) was aimed to improve with 50 % by 2000 and 65 % by 2010 relative to 1980 and to increase sustainable energy sources by 4 %. Targets for reducing biocides emission were formulated, too. Until 2010 biocides should be reduced by 72 % and 88 % for ornamentals and vegetables, respectively, relative to the mean value of the period between 1984 and 1988. Within biocides, fungicides and plant growth retardants are most important in greenhouse horticulture.

To improve the environmental aspects in greenhouse horticulture, measures have to be taken to reduce the environmental impact on one side and to keep crop production on a high level in terms of mass and quality on the other side. Energy efficiency was improved in the last years, but it was not enough to fulfil the target. To compensate that, the energy efficiency index must decrease even stronger. Energy consumption can probably be reduced strongly by new greenhouse materials and technique. On the other hand, existing greenhouse technique could probably be used to reduce energy consumption with only little adjustments. This could be done by more advanced climate regimes. In the present situation, climate regimes are commonly rigid. More flexibility for the three major greenhouse climate states (temperature, humidity and CO_2 concentration) can probably increase energy saving. Climate regimes can be developed that protect plants from high humidity on the one side and that keep a high temperature flexibility on the other. The present thesis therefore aimed at reduction of energy consumption and biocide use by designing and analysing several flexible control regimes, employing existing climate control possibilities using set points of commercial climate computers. The resulting dynamic climate regimes could then be used for more advanced greenhouse climate control.

To control greenhouse climate optimally to temperature, humidity and CO_2 concentration, a partly model-based approach was chosen. The starting point in CHAPTER 2 was therefore to design and calibrate a crop gross photosynthesis model for the use in more extreme climate conditions as they were expected when more flexibility in temperature and humidity was allowed. With this model, crop gross photosynthesis (P_{gc}) must be well predicted at a range

of temperatures. In CHAPTER 2.1, three versions with increasing complexity of leaf photosynthesis simulation models were evaluated with simulations in a canopy photosynthesis model under extreme temperature conditions. There were substantial differences between the three models, especially at high temperatures and high radiation, irrespective of the CO_2 level. The most complex leaf photosynthesis model that was based on biochemical equations and where a simple stomata model was added resulted in the most promising P_{gc} prediction.

The results attained in CHAPTER 2.1 were only theoretically based. To test whether the model with the most promising P_{gc} prediction was truly the best and if any model can be used for reliable P_{gc} prediction, P_{gc} measurements must be compared to model predictions. For this, a well performing measuring system is necessary. This was designed and calibrated with a cut chrysanthemum crop in CHAPTER 2.2. The measuring system was re-build from two identical free-standing semi-closed greenhouses and could measure crop photosynthesis at a range of CO_2 concentrations and different constant temperatures, various constant photosynthetic photon flux densities (PPFD) and natural light. To resemble a sideless and endless crop canopy for model validation, CO_2 net exchange measurements were recalculated with a geometric crop photosynthesis model taking light penetration into the sides of the crop into account.

The measuring system was used in CHAPTER 2.3 to determine cut chrysanthemum crop photosynthesis at 23, 28 and 33 °C and at 400, 700 and 1000 µmol mol CO_2 concentrations. Data were fitted to the negative exponential light response curve for canopies and P_{gc} was then predicted for 300, 600, 900 and 1200 µmol m^{-2} s^{-1} PPFD and for the three applied temperatures. A quadratic curve was fitted to the predicted P_{gc}-temperature responses to determine the temperature that maximises photosynthesis at the different PPFD levels. An increase in the maximum P_{gc} temperature from 400 to 1000 µmol mol^{-1} CO_2 of at least 1 °C, 3.5 °C and 4.5 °C at 600, 900 and 1200 µmol m^{-2} s^{-1} PPFD, respectively, was found. The obtained measurements were compared to model predictions in CHAPTER 2.4 from the biochemical based leaf photosynthesis model with and with fixed stomata resistance. Only small differences were observed at 23 °C. At 28 °C, the model with a low constant stomata resistance had a better prediction of P_{gc}. At higher temperatures, this model overestimated P_{gc}. The model with calculated stomata resistance had a good prediction (only slightly underestimating P_{gc}) and also temperature that maximises photosynthesis was reasonable good.

This model was used for implementation to the climate regimes that were designed and evaluated in CHAPTER 3. First, a more flexible temperature regime was designed in CHAPTER 3.1. The well-known temperature integration principle was used as starting point. Using temperature integration a certain mean temperature is maintained within upper and lower limits over specified time intervals. The maximum integration interval and temperature bandwidth for high quality crops are still fairly unknown. The concept in fact is based on empiricism and fixed temperature bandwidths and integration intervals are commonly used. This concept was slightly refined by two dependent (nested) integration intervals. A regime with a wider short-term (24-hour) temperature bandwidth while maintaining the restrictions of a narrow long-term temperature integration (several days) was designed. The regime existed further of a temperature-dose response and maximisation of crop gross photosynthesis employing the model with a simple predicted stomata resistance as evaluated in CHAPTER 2.4.

The temperature regime was tested with simulations using a validated greenhouse climate and control model. Greenhouse climate, energy consumption and P_{gc} were simulated for complete years with different parameter settings for tomato as model crop. With the modified

regime compared to regular temperature integration, with the same ±2 °C long-term temperature bandwidth 4.5 % (normal secure settings) or up to 9 % (extreme settings) more energy could be saved (on a yearly basis).

When applying flexible temperature control, humidity is a limiting factor for energy saving. With temperature integration, heating and ventilation are minimised leading to more temperature fluctuations. In this situation with reduced ventilation and heating, relative humidity increases when temperature drops and *vice versa*. The low fixed set points for humidity control used in common practice counteract the positive effect of dynamic temperature control on energy consumption. Vents open at lower temperatures than required for temperature integration, or heating is employed to decrease the relative humidity, or both. A dynamic humidity regime to support the dynamic temperature regime was therefore developed in CHAPTER 3.2. The regime was based on the response of the underlying cut chrysanthemum crop processes that are affected by greenhouse atmospheric humidity (plant water stress, calcium deficiencies, crop growth, crop development and fungal diseases). Greenhouse performance with this humidity regime and different temperature regimes were simulated with respect to greenhouse climate, energy consumption and photosynthesis. Compared to a fixed 80 % relative humidity set point, annual energy consumption of a year-round cut chrysanthemum cultivation could be reduced by 18 %. When also regular temperature integration was used, energy saving could increase up to 27 % for a separate 12-week cultivation in spring.

The newly developed regimes for dynamic temperature control (CHAPTER 3.1) and dynamic humidity control (CHAPTER 3.2) were combined in CHAPTER 3.3 and evaluated with greenhouse experiments with cut chrysanthemum. A commercial greenhouse climate computer was used for set point realisation. Different temperature bandwidths for the modified temperature integration regime of ±2 °C, ±4 °C, ±6 °C and ±8 °C were compared with the combined regime and to a blueprint climate regime. Crop development was only delayed with ±8 °C temperature bandwidth. The best regime with respect to plant development, growth and energy saving was the combined regime with ±6 °C temperature bandwidth. No negative consequences of high humidity were observed, but a strong increase in dry weight of all plant organs. However, two negative points could be made: 1) A developmental stage dependent temperature control must be applied during the ca. first three weeks of the short-day period (i.e. week 4 - 6 of cultivation) such that temperature control must be rigid in this period. In commercial cut chrysanthemum greenhouses, however, different developmental stages are grown together. This is the bottleneck of the applied regime since application of this dynamic regime is only possible when also the growing system changes. 2) With a *free* dynamic temperature regime as it was suggested in CHAPTER 3.1, a positive difference between the average day-temperature and the average night-temperature (*DIF*) is commonly attained in spring, summer and autumn. This leads to stem elongation in many crops (especially chrysanthemum) and this yields lower plant quality and decreased market value.

In commercial cut chrysanthemum cultivation, chemical growth retardants are used to control stem elongation. A negative *DIF* set point (i.e. higher night than day temperature) can be used to attain shorter and more compact stems and by that reducing the application of chemical growth retardants. To quantify the additional energy costs with either certain negative *DIF* set points or temperature integration with a 24-hour averaging interval, simulations were performed for chrysanthemum cultivations with a greenhouse climate and control simulator in CHAPTER 3.4. Temperature was either controlled for energy saving with 24-h temperature integration or was restricted by a negative *DIF* regime. Energy consumption was reduced by both regimes compared to a blueprint regime according to commercial

practice when heating was shifted to nighttime using a screen in winter. With increasing weather fluctuations in spring and autumn, weekly energy reduction with 24-hour temperature integration (±6 °C temperature bandwidth) without *DIF* restriction could increase to more than 60 %. When this was restricted by e.g. −6 °C *DIF*, only 37 % energy was saved. Energy saving decreased with decreasing *DIF* set point. In general, the *DIF* restriction reduced energy demand compared to the blueprint, and energy saving was higher when no *DIF* restriction was applied. The actual cultivation period is the most important criterion to decide whether to apply a *DIF* restriction. Controlling stem length with negative *DIF* in spring and autumn has the highest additional energy costs, but has a beneficial effect of reduced stem elongation. Almost no negative *DIF* control is possible in summer and during winter, temperature integration with and without *DIF* restriction resulted in similar realised greenhouse climate.

In the simulation research of CHAPTER 3.4, temperature integration with an averaging period of only 24 hours was compared to a regular *DIF* regime. A *DIF* regime is actually a modification or restriction of 24-hour temperature integration. The effect of temperature on stem elongation, nevertheless, is still not fully understood and this leads to uncertainties of temperature control. If it is possible to integrate the *DIF* effect over time is not known.

It was hypothesised that stem elongation may respond to time integration effects of day-temperature and average night-temperature. Temperature integration with a six-day averaging period was therefore combined with *DIF*. Then warm days could be compensated by cool days and warm nights by cool nights (not days by nights and *vice versa*). In CHAPTER 3.5, temperature integration was therefore modified by applying two independent integration regimes, one for daytime and one for nighttime while a zero *DIF* was set. Simulations and experiments with standard temperature control, regular and modified temperature integration showed that temperature integration and *DIF* could be applied simultaneously, while energy consumption and stem elongation were reduced.

The research in CHAPTER 3.5 was done with regular temperature integration and only a zero *DIF* was used. In CHAPTER 3.6, the reported designs from earlier Chapters were connected with the combation of *DIF* and 6 day temperature integration regime of CHAPTER 3.5 and the regime was extended to -6 °C and -12 °C *DIF*. The earlier used greenhouse climate and control model was applied for simulations. Absolute highest energy saving was achieved throughout the year when the dynamic temperature regime (CHAPTER 3.1) was combined with flexible humidity regime (CHAPTER 3.2). Then, 33 % energy saving per year was predicted with a 6-day (long-term) temperature bandwidths of ±2 °C. Here, the winter months were the most important. In spring or autumn, in relative sense the largest energy saving can be obtained with the dynamic temperature regime.

If no negative *DIF* was enforced, the dynamic temperature regimes led to a positive *DIF*, with the highest value in spring and autumn. Simulations showed again that it is possible to reduce energy consumption while simultaneously attaining a negative *DIF*. However, the decreased degrees of freedom for temperature control resulted in decreased energy saving possibilities when a *DIF* restriction was applied within temperature integration.

It was found that temperature integration and negative *DIF* can only be applied with reduced energy saving. Otherwise the application of chemical growth inhibitors will increase to control stem elongation in chrysanthemum. Since CO_2 emission and biocide reduction is targeted likewise, a trade off problem exists, that could not be solved within the present thesis. In the present situation, the decision whether to apply temperature integration with or without negative *DIF* restriction has to be decided per season.

In 2001, energy efficiency index was 52 % of the values from 1980. To fulfil the signed convenant, the energy efficiency-index has to be decreased by an additional 17 % until 2010. A major part of this (10 %) can be achieved with standard estimated greenhouse technological development. The remaining could easily be achieved with the climate control as investigated in this thesis. For that, the process based humidity regime alone (CHAPTER 3.2) would be sufficient. This, however, requires that growers adapt the new policies. Because growers hesitate to use dynamic climate regimes, additional work in the area of technology transfer needed before the present research can be extended and implemented in pratice. The here presented regimes could only then be seen as contribution to energy saving in greenhouse horticulture.

SAMENVATTING

De zorg om broeikasgassen die zijn ontstaan door menselijke handelen en het wereldklimaat kunnen beïnvloeden, neemt onafgebroken toe. In de jaren 1992 en 1997 zijn tussen de industrielanden onderhandelingen ter controle van deze gassen gevoerd. In Kyoto was door deze landen een contract ondertekend om emissievermindering te realiseren. Een van de belangrijkste gassen is kooldioxide (CO_2). Om de wereldwijde opwarming te verminderen moet die concentratie in de atmosfeer gereduceerd worden.

In de strijd om reductie van fossiele brandstof (hoofdveroorzaker van CO_2 emissies) wordt de hele Nederlandse industrie in sectoren ingedeeld, waarvan de agrarische een belangrijk positie inneemt. In het jaar 2000 was deze sector goed voor 10 % van de nationale emissie van broeikasgassen, waarvan een derde CO_2 was. Al in 1997 ondertekenden de Nederlandse glastuinbouwsector en de regering het *convenant glastuinbouw en milieu*. Dit convenant was het vervolg op een in 1992 ondertekende overeenkomst. Het doel van deze overeenkomsten was het verbeteren van de energie-efficiënte (gebruikt hoeveelheid energie per eenheid product) tot 2000 en 2010 ten opzichte van 1980 met respectievelijk 50 % en 65 %. Verder zou -in lijn met dit convenant- het gebruik van milieuvriendelijke energie met 4 % toenemen. Ook zijn er doelen voor reductie van chemicaliën geformuleerd. Deze zouden tot het jaar 2010 binnen de sector sierplantenteelt met 72 % en binnen de sector groenteteelt met 88 % teruggebracht worden (gebaseerd op de gemiddelde waarde tussen 1984 en 1988). In de kassenteelt zijn fungicide en groeiremmers de meest gebruikte chemicaliën. Het is dan ook van groot belang de toepassing daarvan te reduceren. Voor de verbetering van de milieuvriendelijkheid van de tuinbouwsector moeten maatregelen worden. Ten eerste om die CO_2 emissie en de applicatie van chemicaliën te verminderen; ten tweede om de productie zowel qua massa als in kwaliteit op een hoog niveau te houden.

In de laatste jaren is de energie-efficiënte wel verbeterd, maar deze verbetering was onvoldoende om het doel te bereiken. Om dit alsnog te kunnen doen, moet de energie-efficiënte nog meer verbeterd worden gedurende de jaren tot 2010. Dit kan mogelijk door toepassing van nieuwe kassenmaterialen en verbeterde technieken. Maar ook met de bestaande techniek zou het energieverbruik in kassen verlaagd kunnen worden. Hier zouden verbeteringen van bestaande klimaatregelingen een waardevol bijdrage kunnen leveren. De inflexibele strategieën voor klimaatcontrole kunnen door verhoogde flexibiliteit van de drie belangrijkste kasklimaatfactoren (temperatuur, vocht en CO_2 concentratie) in het voordeel van energiebesparing worden aangepast. Dit proefschrift heeft de doelstelling energie- en chemicaliënverbruik in kassen door het ontwerpen en analyseren van flexibele kasklimaat regelstrategieën te verminderen. Bestaande techniek kan dan gehandhaafd blijven (b.v. door de mogelijkheden van de kasklimaatcomputer te benutten). De zo ontstane strategieën kunnen dan voor geavanceerdere klimaatregelaars benut worden.

Om temperatuur, vocht en CO_2 concentratie goed te controleren, is een deels modelgebaseerde aanpak gekozen. In HOOFDSTUK 2 is daarom een gewasfotosynthesemodel voor applicatie in extreme kasklimaten zoals die bij dynamische kasklimaatregeling verwacht

227

wordt, getoetst. In HOOFDSTUK 2.1 zijn drie bladfotosyntesemodellen met toenemende complexiteit onder extreme temperatuurcondities als onderdeel van een gewasfotosynthesemodell geëvalueerd. Tussen die drie modellen waren vooral bij hoge temperatuur duidelijke verschillen te zien. Het model met de hoogste complexiteit (gebaseerd op biochemische vergelijkingen en met een eenvoudig huidmondjesweerstands-model) was het meest belovend.

De resultaten uit HOOFDSTUK 2.1 zijn alleen theoretisch. Om het beste model te vinden moet de gemeten gewasbrutofotosynthese (P_{gc}) worden vergeleken met simulaties. Een goed werkend systeem is daarvoor noodzakelijk. In HOOFDSTUK 2.1 is daartoe een systeem ontworpen en gekalibreerd. Testmetingen zijn met vegetatief groeiende snijchrysanten gedaan. Meting van CO_2 uitwisseling was bij verschillende CO_2 concentraties en temperaturen zoals bij constante en variabele lichtcondities met een maximale foutmarge van 5 % mogelijk. Om simulaties met metingen te kunnen vergelijken, moet bij een klein gewasoppervlakte met zijlicht rekening gehouden worden. Om dit goed te kunnen schatten, is een geometrisch gewasfotosynthesemodel ontworpen en getoetst.

In HOOFDSTUK 2.3 is met dit systeem de CO_2 uitwisseling bij snijchrysanten gemeten (bij 23, 28 en 33 °C en 400, 700 en 1000 µmol mol^{-1} CO_2). De gegevens zijn verder met de negatief-exponentieel lichtresponse-curve gefit en verder is P_{gc} bij 300, 600, 900 en bij 1200 µmol m^{-2} s^{-1} PPFD voor de drie toegepaste temperaturen geschat. Om de temperatuur te vinden die P_{gc} onder verschillende lichtniveaus maximeert, is een kwadraat functie aan de geschatte P_{gc}-temperatuur verhouding gepast. Deze waarde steeg tenminste 1 °C, 3,5 °C of 4.5 °C bij 600, 900 of 1200 µmol m^{-2} s^{-1} met het klimmen van de lucht CO_2 concentratie van 400 naar 1000 µmol mol^{-1}.

In HOOFDSTUK 2.4 zijn de in HOOFDSTUK 2.3 gedane metingen met simulaties vergeleken. Daarbij wordt het bovengenoemde biochemische model gebruikt (met zowel constante als ook gesimuleerde huidmondjesweerstand). Bij 23 °C waren slechts marginale verschillen te zien. Bij 28 °C waren de modelsimulaties met een lage en constante huidmondjesweerstand beter. Bij hogere temperaturen overschatte dit model de gemeten waardes. Onder deze omstandigheden waren simulaties met een berekende huidmondjesweerstand beter.

Het model kon in de in HOOFDSTUK 3 beschreven dynamische regelstrategieën geïmplementeerd worden. Eerst is een dynamisch temperatuurregime ontworpen (HOOFDSTUK 3.1) waarbij temperatuurintegratie het beginpunt vormde. Met temperatuurintegratie wordt temperatuur op dynamische wijze gestuurd. Temperatuur mag vergaand fluctueren als een bepaalde temperatuurgemiddelde in een bepaald tijdinterval wordt bereikt. Deze methode is een algemeen geaccepteerde standaard, alhoewel de maximale integratietijd en de maximale temperatuurbandbreedte om gelijke plantenontwikkeling en kwaliteit te waarborgen, vrij onbekend zijn. Het concept temperatuurintegratie is vooral empirisch. Normaal worden vaste temperatuurbandbreedten en integratieperioden ingeschakeld. In dit proefschrift is het concept temperatuurintegratie gemodificeerd. In plaats van vaste temperatuurbandbreedten en integratieperioden is een systeem met een korte en een lange termijn temperatuurintegratie ontwikkeld. De korte termijn integratie (24 uur) heeft bredere temperatuurbanden, maar bij de lange termijn (meerdere dagen) is dit beperkt. In deze strategie zijn verder een temperatuur dose-response concept en een module voor maximalisatie van gewasbrutofotosynthese geïmplementeerd. Daarvoor wordt dit in HOOFDSTUK 2 genoemde fotosynthesemodel gebruikt.

Het regime is met behulp van een gevalideerd kasklimaat- en controlemodel (KASPRO) getoetst. Kasklimaat, energieconsumptie en tomaatgewasfotosynthese zijn met verschillende instellingen voor hele jaren gesimuleerd. De simulaties toonden aan dat -vergeleken met

normale temperatuurintegratie- energie kon worden bespaard (4.5 % met normale en veilige instellingen en tot 9 % met extreme instellingen).

Bij dynamische temperatuurregeling is vocht een limiterende factor voor energiebesparing. Met temperatuurintegratie worden verwarming en ventilatie geminimaliseerd en daaruit volgen hogere temperatuurfluctuaties en dus fluctuaties van relatief vocht (RV). De in de praktijk gebruikte (lage) vaste instellingen voor RV beïnvloeden het temperatuurintegratie-regime negatief. Het openen van ramen bij lagere temperatuur is dan noodzakelijk wanneer alleen de temperatuurintegratie wordt gebruikt om RV te verlagen. Soms worden verwarming en ventilatie tegelijk gebruikt. Om temperatuurintegratie te steunen en niet tegen te werken is een dynamische RV controle strategie voor chrysanten ontwikkeld (HOOFDSTUK 3.2). Die is gebaseerd op de door RV beïnvloede processen (stress, calciumtekort, plantengroei en – ontwikkeling, en schimmelziektes). Net als bij het modificeerde tempertuurintegratie concept zijn ook hier kasklimaat, energieconsumptie en fotosynthese met KASPRO gesimuleerd. Vergeleken met een constante streefwaarde van 80 % RV kon met het dynamische vochtregime op jaarbasis 18 % energiebesparing berekend worden. In een tijdsspanne van 12 weken (een volledige chrysantencultuur) in het voorjaar kon, in combinatie met een normale temperatuurintegratie-regime, 27 % energie bespaard worden.

De twee nieuw ontwikkelde strategieën voor temperatuursturing (HOOFDSTUK 3.1) en vochtsturing (HOOFDSTUK 3.2) zijn in HOOFDSTUK 3.3 met elkaar gecombineerd en in experimenten met vier verschillende langetermijn temperatuurbandbreedten (±2 °C, ±4 °C, ±6 °C en ±8 °C) geëvalueerd. Verder is een in de praktijk gebruikte standaardstrategie met het gecombineerde regime vergeleken. Plantenontwikkeling was alleen bij 8 °C vertraagd, en een bandbreedte van ±6 °C was optimaal voor groei, energieconsumptie en ontwikkeling. Negatieve consequenties door te hoge vochtgehalte waren niet te zien, maar een sterke droogstof toename werd wel geconstateerd. Twee opmerkingen moeten desondanks gemaakt worden: 1) Omdat chrysanten gevoelig zijn voor temperatuurfluctuaties in de eerste drie weken van de korte dag, kan temperatuurintegratie in deze tijd niet toegepast worden. In de commerciële chrysantenteelt vinden echter alle ontwikkelingsstadia in een kas plaats. Een temperatuursturing die inspeelt op de verschillende stadia is om die rede niet mogelijk. Dit is een zwak punt van de hier ontwikkelde strategie. Het dynamische temperatuurregelsysteem kan bij chrysanten alleen gebruikt worden als het hele cultuursysteem wijzigt. 2) Met toenemende flexibiliteit van de temperatuursturing kan tussen voorjaar en najaar een zogenoemd positief *DIF* ontstaan. *DIF* (*DIF*ferentie tussen het dag- en het nacht-temperatuurgemiddelde) kan bij een groot aantal planten (vooral bij chrysanten) de stengellengte beïnvloeden. Een negatief *DIF* remt stengelstrekking en een positief *DIF* verhoogt dit. Een lange hoofdtak leidt echter tot een lage kwaliteit en een lage marktwaarde. In de commerciële chrysantenteelt worden groeiremmers gebruikt om de taklengte te beïnvloeden, maar dit is te omzeilen als temperatuursturing met een negatief *DIF* gedaan wordt. Om de extra energiekosten van dit soort regime te vergelijken met temperatuurintegratie (integratieperiode van een etmaal) en te kwantificeren, zijn simulaties met het kasklimaatmodel KASPRO gemaakt. Vergeleken met de standaardstrategie wordt het energieverbruik in de wintermaanden gelijktijdig met *DIF* en temperatuurintegratie verlaagd. Bij toenemende temperatuur fluctuaties in het voorjaar en najaar kon de wekelijkse energieconsumptie met temperatuurintegratie (±6 °C) tot 60 % verlaagd worden. Als b.v. een *DIF* waarde van –6 °C toegepast werd, kon op hetzelfde tijdstip slechts 37 % energie bespaard worden. Als de nagestreefde *DIF* lager was, waren de energiebesparingmogelijkheden nog minder. In het algemeen waren de energiebesparingmogelijkheden door een negatieve *DIF* streefwaarde ten behoeve van temperatuurintegratie gereduceerd. Vergeleken met een standaard regime kon echter ook met

DIF energie bespaard worden. Bij de beslissing over de toepasbare temperatuurstrategie (temperatuurintegratie met of zonder *DIF* benadering) is de actuele cultuurperiode (seizoen) de belangrijkste factor. Taklengtes sturen door een negatief *DIF,* zorgt voor extra kosten in het voorjaar en het najaar; in de zomer is er geen controle met negatief *DIF* mogelijk. In het winter zijn er geen verschillen tussen temperatuurintegratie en *DIF*.

In het simulatie-experiment in HOOFDSTUK 3.4 is alleen etmaal-temperatuurintegratie met *DIF* vergeleken. Het *DIF* regime is daadwerkelijk een modificatie of restrictie van de etmaal-temperatuurintegratie. Het effect op taklengte is echter nog niet volledig bekend en dit leidt tot onzekerheden in de temperatuursturing. Het is niet bekend of de *DIF* effecten ook over meerdere dagen geïntegreerd kunnen worden. Daarom is in HOOFDSTUK 3.5 de hypothese gedaan dat stengelstrekking op geïntegreerde effecten van dag- en nachttemperatuur reageren. In dit hoofdstuk zijn temperatuurintegratie met een zesdaagse interval met een nieuw *DIF* concept gecombineerd. De integratieprocedure voor dag en nacht zijn in onafhankelijke sturingen geïmplementeerd. Voor toetsing van deze strategie met simulaties en in kasexperimenten is een streefwaarde van 0 °C *DIF* gekozen. Energieconsumptie kon significant verlaagd worden en de planten waren niet duidelijk langer dan met een standaardregime.

Omdat de experimenten in HOOFDSTUK 3.5 alleen met de normale temperatuurintegratie gedaan zijn (enkel met 0 °C *DIF),* is de strategie in HOOFDSTUK 3.6 met streefwaarden van – 6 °C en –12 °C *DIF* uitgebreid. Verder zijn hier de ontwerpstrategieën van de vorige hoofdstukken gecombineerd. Ook daarbij is het kasklimaatmodel KASPRO voor een simulatiestudie gebruikt. Absoluut de hoogste energiebesparingen zijn met een combinatie van het temperatuurregime uit HOOFDSTUK 3.1 en het vochtregime uit HOOFDSTUK 3.4 behaald. Over een heel jaar gezien kon met een langetermijn temperatuurbandbreedte van slechts ±2 °C 33 % energie worden bespaard; de grootste besparing was te zien in de wintermaanden. Met de dynamische regeling kunnen, relatief gezien, in het voorjaar en in het najaar de hoogste hoeveelheden energie bespaard worden. Dan wordt bij temperatuurintegratie zonder *DIF* restrictie een positief *DIF* behaald. Wederom is aangetoond dat het mogelijk is om korte planten met minder chemicaliën (dus met negatief *DIF* sturing) wel degelijk een energiebesparing te realiseren. De negatief *DIF* restricties leiden desondanks tot minder energiebesparing dan met het pure dynamische temperatuurregime uit HOOFDSTUK 3.1.

Temperatuurintegratie en een negatief *DIF* kunnen alleen tegelijkertijd gestuurd worden als een vermindering van energiebesparing geduld wordt. Anders leidt een puur temperatuurintegratie regime tot een toename van chemische groeiremmers in de chrysantenteelt. Omdat CO_2 emissies en chemicaliën tegelijkertijd verlaagd moeten worden, bestaat er een optimalisatieprobleem. Dit kon in dit proefschrift niet opgelost worden.

In 2001 was de eerder genoemde energie-efficiënte index 52 % ten opzichte van 1980. Om het uiteindelijke doel van 65 % te bereiken moet deze tussen 2001 en 2010 met nog eens 17 % verlaagd worden. Een groot deel daarvan (10 %) kan met de standaardontwikkeling in de kassentechniek bereikt worden. Het resterende zou met de hier gepresenteerde klimaatregelstrategieën eenvoudig te realiseren zijn, zodat in principe het dynamische vochtregime (HOOFDSTUK 3.2) al voldoende zou zijn. Het optimalisatieprobleem tussen reductie van chemicaliën en energie door temperatuursturing speelt dan geen rol.

Voordat een dynamisch regime in de praktijk geïmplementeerd kan worden, is acceptatie door de telers van uiterst belang. Omdat veel telers aarzelen, is verbetering in kennisoverdracht en voorlichting noodzakelijk. Pas als dynamische regelstrategieën vergaand geaccepteerd zijn in de praktijk, kunnen de hier gepresenteerde strategieën geëxpandeerd

worden. Dan pas zou dit proefschrift daadwerkelijk als belangrijke bijdrage voor energiebesparing in de glastuinbouw beschouwd kunnen worden.

ZUSAMMENFASSUNG

Anthropogene Gas-Emissionen, die das globale Klima beeinflussen, nehmen stetig zu. Aus dieser Sorge heraus führten die Industrienationen in den Jahren 1992 und 1997 Verhandlungen zur Emissionverminderung und unterzeichneten mit dieser Zielsetzung den Vertrag von Kyoto. Hierin wurde Kohlendioxid (CO_2) als eines der wichtigsten Gase bezeichnet, dessen athmosphärische Konzentration reduziert werden sollte.

Mit dem Ziel das Verbrennen von fossile Stoffen (die Hauptverursacher von CO_2 Emissionen) zu reduzieren, wurde daher der gesamte niederländische Industriesektor in Untersektoren eingeteilt. Von diesen nimmt der Agrarsektor eine Schlüsselposition ein, u.a. da dieser allein im Jahr 2000 mit mehr als 10 % an der gesamten anthropogenen Gas-Emission beitrug (ein Drittel davon CO_2). Von dem CO_2 - Anteil hatten 80 % ihren Ursprung im Gewächshausgartenbau. Schon früher, 1997, einigten sich der niederländische Gewächshausgartenbausektor und die Regierung, Massnahmen zur Verbesserung der Umweltfreundlichkeit im Gewächshausgartenbau zu treffen, und unterzeichneten das *Abkommen Gewächshausgartenbau und Umwelt*. Diese Absichtserklärung war die Folge eines bereits fünf Jahre zuvor unterzeichneten Vertrages dieser beiden Parteien mit der Zielsetzung, die Energieeffizienz (Energieverbrauch pro Einheit Produkt) zu verbessern. In den Abkommen verpflichtete man sich, die Energieeffizienz ausgehend von 1980 mit 50 % bis 2000 und 65 % bis 2010 zu verbessern. Weiterhin sollten umweltfreundliche Energiequellen mit 4 % zunehmen und Chemikalienapplikationen im Allgemeinen verringert werden. Dieses sind im Gewächshausgartenbau v.a. Fungizide und Wachstumshemmer. Bis 2010 soll deren Anwendung innerhalb des Zierpflanzensektors mit 72 % und innerhalb des Gemüsesektors mit 88 % vermindert werden (basiert auf den Mittelwert von 1984 bis 1988).

Um die Umweltfreundlichkeit des Gewächshausgartenbausektor zu verbessern, müssen daher Massnahmen getroffen werden, die zum einen CO_2 Emissionen und die Anwendung von Chemikalien verringern und die zum anderen die Produktion sowohl in der Masse als auch in der Qualität auf dem gegenwärtig hohen Standard halten.

Die Energieeffizienz konnte in den vergangenen Jahren verbessert werden, aber nicht ausreichend um das gesteckte Ziel zu erreichen. Um dieses bis 2010 dennoch zu realisieren, muss die Energieeffizienz in den nächsten Jahren noch drastischer verbessert werden.

Der Energieverbrauch wird durch neue Gewächshausmaterialien und Technik stark reduziert werden können, allerdings wären möglicherweise auch mit bestehender Gewächshaustechnik (Stand 2003) ausreichende Möglichkeiten gegeben. Klimaregelstrategien könnten durch höhere Flexibiliät der drei wichtigsten Gewächshausklimafaktoren (Temperatur, Luftfeuchte und CO_2 Konzentration) zugunsten von Energieeinsparung verbessert werden.

Diese Dissertation hat die Verminderung des Energieverbrauches und die Reduzierung der Applikation von Chemikalien im Gewächshausgartenbau durch Klimaregelung zum Ziel.

Hierbei sollten flexiblere Regelstrategien entworfen und analysiert werden, mit der Pflanze im zentralen Blickfeld. Ausgangspunkt ist der derzeitig technische Standard mit den bestehende Klimareglern, die in existierenden Klimaregelcomputern implementiert sind. Die resultierenden dynamischen Strategien könnten aber auch für noch fortschrittlichere Regelsysteme benutzt werden.

Um Temperatur, Luftfeuchte und CO_2 Konzentration optimal zu kontrollieren, wurde eine teils modelbasierte Arbeitsweise gewählt. Der Ausgangsspunkt in KAPITEL 2 war deswegen das Design und die Kalibrierung eines Models zur Simulation von Gewächs-bruttofotosynthese (P_{gc}) zur Anwendung in extremen Klimabedingungen, so wie sie mit flexiblerer Temperatur- und Luftfeuchtesteuerung im Gewächshaus erwartet werden können. Mit diesem Model sollte P_{gc} weiträumig beschrieben werden.

In KAPITEL 2.1 wurden drei Blattfotosynthesemodell-Versionen mit zunehmender Komplexität unter extremen Temperaturbedingungen als Untermodelle eines Gewächsfotosynthesemodels evaluiert. Zwischen den drei Modellen konnten v.a. bei hoher Temperatur deutliche Unterschiede festgestellt werden. Das Modell mit der höchsten Komplexität (basiert auf biochemischen Gleichungen und mit einem einfachen Spaltöffnungswiderstandsmodell) war am vielversprechensten.

Die Ergebnisse von KAPITEL 2.1 sind jedoch rein theoretisch. Um das tatsächlich qualitativ beste Model zu finden, müssen P_{gc} Messungen mit Modellsimulationen verglichen werden. Ein gut funktionierendes Messsystem ist dafür notwendig. Ein solches System wurde in KAPITEL 2.2 entworfen und kalibriert. Das System wurde aus existierenden freistehenden Gewächshäusern umgebaut. Testmessungen konnten mit vegetativ kultivierten Schnittchrysanthemen durchgeführt werden. CO_2 Austausch war bei einer Reihe von CO_2 Konzentrationen, verschiedenen konstanten Temperaturen und konstanten und variablen Lichtbedingungen mit einer Genauigkeit von 95 % messbar. Um Simulationen mit Messungen vergleichen zu können, muss bei einer kleinen Gewächsoberfläche der Seitenlichteinfall berücksichtigt werden, wofür ein geometrisches Gewächsfotosynthesemodell entworfen und getestet wurde.

In KAPITEL 2.3 ist der CO_2 Austausch von Chrysanthemen bei 23, 28 und 33 °C und 400, 700 und 1000 µmol mol^{-1} CO_2 mit diesem System gemessen. Aus diesen Messdaten konnte P_{gc} berechnet werden. Potentielle Maximumfotosynthese und die Lichtnutzungseffizienz der negativ-exponentielle Funktion wurde von den Messwerten berechnet. Hieraus wiederum konnte P_{gc} bei 300, 600, 900 und 1200 µmol m^{-2} s^{-1} PPFD bei den drei angewendeten Temperaturen geschätzt werden. Um die Temperatur zu finden, die P_{gc} bei verschiedenen Lichtniveaus maximiert, wurde eine quadratische Funktion an das geschätzte P_{gc}-Temperatur Verhältnis berechnet. Ein Anstieg dieser Temperatur von mindestens 1 °C, 3,5 °C oder 4,5 °C bei 600, 900 oder 1200 µmol m^{-2} s^{-1} wurde bei einem Anstieg des CO_2 Gehaltes der Gewächshausluft von 400 nach 1000 µmol mol^{-1} aus den Messungen geschätzt.

In KAPITEL 2.4 wurden die in KAPITEL 2.3 durchgeführten Messungen mit Simulationen verglichen. Dazu diente das oben genannte biochemische Modell (mit sowohl konstantem als auch mit simuliertem Spaltöffnungswiderstand). Bei 23 °C konnten nur geringe Unterschiede gefunden werden. Bei 28 °C schätzte das Modell mit niedrigem konstanten Spaltöffnungswiderstand die gemessenen P_{gc}-Werte besser. Bei höherer Temperatur jedoch, überschätzte das Modell die gemessenen Daten. Unter diesen Umständen hatten Simulationen mit berechnetem Spaltöffnungswiderstand eine bessere Annäherung an die Messdaten; auch die Schätzung des P_{gc} maximierenden Temperaturwertes war zufriedenstellend.

Das evaluierte Modell konnte in die in KAPITEL 3 beschriebenen dynamischen Regelstrategien implementiert werden, wobei zuerst Temperatur behandelt wurde

(KAPITEL 3.1). Die bekannte Temperaturintegration wurde hierbei als Ausgangspunkt benutzt. Bei Temperaturintegration darf Temperatur weitgehend frei fluktuieren, wenn eine bestimmte Mitteltemperatur nach einem bestimmten Zeitinterval erzielt wird. Auch wenn diese Methode weit verbreitet ist, sind maximaler Integrationszeitraum sowie maximale Temperaturbandbreiten, um gleichbleibende Pflanzenentwicklung und -qualität zu gewährleisten, relativ unbekannt. Das Konzept ist v.a. auf empirischen Experimenten basiert und im allgemeinen werden feste Temperaturbandbreiten und Integrationszeiträume verwendet. Das Temperaturintegrationskonzept wurde in dieser Arbeit modifiziert. Anstelle fester Eistellungen wurde ein System entwickelt, in dem ein Kurzzeitintervall in ein Langzeitintervall eingebettet ist. Das Kurzzeitintervall (24 Stunden) besitzt erweiterte Temperaturbanden, wobei die Beschränkungen des Langzeitintervalls (mehrere Tage) berücksichtigt werden müssen. Weiterhin sind ein *Temperatur Dosis-Respons Konzept* und ein Modul zur Fotosynthesemaximierung implementiert. Für das letztere ist das in KAPITEL 2 evaluierte Modell verwendet.

Die Strategie wurde mit Hilfe eines validierten Gewächshausklima- und Steuerungsmodells getestet. Für komplette Jahre sind Gewächshausklima, Energieverbrauch und Tomatengewächsfotosynthese bei verschiedenen Einstellungen simuliert. Es konnte gezeigt werden, dass im Vergleich zur regulärer Temperaturintegration mehr Energie eingespart werden kann (4,5 % mit normalen sicheren Einstellungen und bis zu 9 % mit extremeren Einstellungen).

Bei dynamischer Temperatursteuerung ist Luftfeuchte ein limitierender Faktor zur Energieeinsparung. Bei der dynamischen Temperaturintegration werden Heizung und Lüftung minimiert und daraus folgen höhere Temperaturschwankungen und folglich Schwankungen der relativen Luftfeuchte (RH). Die in der Praxis gewöhnlich benutzten (niedrigen) festen Einstellungen für RH steuern der Temperaturintegrationsstrategie entgegen. Lüftungsklappen öffnen bei niedrigerer Temperatur als es bei Temperaturintegration allein notwendig wäre, oder es wird geheizt um RH im Gewächshaus zu senken. In manchen Fällen werden Heizung und Lüftung auch gleichzeitig angewendet. Um Temperaturintegration zu unterstützen (und nicht entgegenzuwirken), wurde eine dynamische Strategie zur Luftfeuchtekontrolle entwickelt (KAPITEL 3.2). Diese beruht auf den grundlegenden durch RH beeinflussten Prozessen bei Gewächshauschrysanthemen (Stress, Kalziummangel, Wachstum und Entwicklung der Pflanzen, sowie Pilzbefall). So wie schon mit dem modifierten Temperaturintegrationskonzept wurden auch hier Gewächshauklima, Energieverbrauch und Fotosynthese simuliert. Im Vergleich zu einem konstanten *set point* von 80 % RH konnte der Jahresenergieverbrauch mit der neuen Strategie mit 18 % gesenkt werden. In einem 12-Wochen Zeitraum (vollständige Kulturperiode eines Chrysanthemen-Satzes) im Frühjahr konnte der Energieverbrauch in Verbindung mit regulärer Temperaturintegration auf 63 % sinken.

Die beiden neuentwickelten Strategien zur Temperatur- (KAPITEL 3.1) und Luftfeuchtesteuerung (KAPITEL 3.2) wurden in KAPITEL 3.3 miteinander kombiniert und in Experimenten mit vier verschiedenen langzeit Temperaturbandbreiten (±2 °C, ±4 °C, ±6 °C und ±8 °C) evaluiert. Weiterhin wurde eine praxisübliche Standardstrategie mit dem kombinierten Konzept verglichen. Pflanzenentwicklung war lediglich bei ±8 °C verzögert, und eine Bandbreite von ±6 °C war optimal im Hinblick auf Wachstum, Energieverbrauch und Entwicklung. Negative Konsequenzen durch zu hohe Luftfeuchte konnten nicht beobachtet werden, aber eine starke Trockenmassenzunahme aller Pflanzenorgane war signifikant. Zwei Anmerkungen müssen jedoch gemacht werden: 1) Weil Chrysanthemen empfindlich auf Temperaturschwankungen in den ersten drei Wochen des Kurztages reagieren, kann Temperaturintegration in dieser Zeit nicht angewendet werden.

In kommerziellen Chrysanthemenbetrieben werden allerdings alle Entwicklungsstadien im selben Gewächshaus kultiviert. Eine von den Entwicklungsstadien abhängige Temperatursteuerung, so wie in der Literatur vorgeschlagen, ist daher nicht gegeben. Das ist einer der schwachen Punkte des hier entwickelten Konzeptes. Die dynamische Temperaturregelung kann bei Chrysanthemen nur angewendet werden, wenn sich das Anbausystem ändert; 2) Mit der dynamischen Temperatursteuerung kann es zwischen Frühjahr und Herbst zu einem sogenannten positiven *DIF* kommen. *DIF* (*DIF*ferenz zwischen gemittelter Tag- und gemittelter Nachttemperatur) kann bei vielen Pflanzen (v.a. Chrysanthemen) die Streckung der Stengel beeinflussen. Ein negativer *DIF* Wert verringert die Stengelstreckung und ein positver erhöht sie. Ein langgestreckter Stengel führt zu einer minderen Qualität und einem geringen Marktwert.

Im kommerziellen Chrysanthemenanbau werden chemische Wachstumshemmer zur Steuerung der Stengelstreckung gehandhabt, welches umgangen werden kann wenn Temperatursteuerung mit dem negativen *DIF* Konzept durchgeführt wird. Um die zusätzlichen Energiekosten solch einer Steuerungs im Vergleich zu der flexibleren Temperaturintegration (24-Stunden Zeitintervall) zu quantifizieren, wurden Simulationen mit dem schon in KAPITEL 3.1 und KAPITEL 3.2 verwendetem Gewächshausmodell durchgeführt (KAPITEL 3.4). Im Vergleich zur Standardstrategie wurde der Energieverbrauch im Winter gleichermassen mit *DIF* und Temperaturintegration vermindert. Mit zunehmenden natürlichen Temperaturschwankungen im Frühjahr und Herbst konte der wöchentliche Energieverbrauch mit Temperaturintegration (±6 °C) bis zu 60 % gesenkt werden. Wenn z.B. ein *DIF* Wert von –6 °C eingestellt wurde, konnten im gleichen Zeitraum nur 37 % Energie gespart werden. Mit einer niedrigeren *DIF* Einstellung nahmen in diesen Jahreszeiten die Energiesparmöglichkeiten ab. Im allgemeinen reduzierte eine *DIF* Einstellung die Energiesparmöglichkeiten der Temperaturintegrationsstrategie, aber im Vergleich zum Standard konnte der Energieverbrauch auch mit *DIF* gesenkt werden. Ob Temperatur mit Temperaturintegration oder mit *DIF* gesteuert werden soll, ist von der aktuellen Kulturperiode (d.h. Jahreszeit) abhängig. Stengellängenkontrolle durch *DIF* hat die höchsten Zusatzkosten im Frühjahr und im Herbst, im Sommer ist keine Stengellängenreduktion mit *DIF* möglich. Im Winter hingegen unterscheiden sich Temperaturintegration und *DIF* nicht.

In dem Simulationsexperiment von KAPITEL 3.4 wurde Temperaturintegration nur mit einem 24 Stunden Intervall mit *DIF* verglichen. Das *DIF* Regime ist tatsächlich eine Modifikation oder Restriktion des 24-Stunden-Temperaturintegrationsregimes. Der Effekt von Temperatur auf die Stengellänge ist jedoch noch nicht vollständig bekannt. Das führt zu Unsicherheiten in der Temperatursteuerung. Auch die Möglichkeit *DIF* Effekte über meherere Tage und Nächte zu integrieren, ist unbekannt. In KAPITEL 3.5 wurde die Hypothese aufgestellt, dass Stengelstreckung auf integrierte Effekte von Tag- und Nachttemperatur reagiert. Temperaturintegration mit einem sechs Tage Intervall wurden hier mit einem neuartigem *DIF* Konzept kombiniert. Unabhängige Integrationsprozeduren für Tag und Nacht konnten in ein Steuerungssystem implementiert werden. In diesem System wurde ein *DIF set point* von 0 °C eingestellt und in Gewächshausexperimenten sowie mit Simulationen erfolgreich getestet. Energieverbrauch konnte gesenkt werden und Pflanzen waren nicht deutlich länger als mit einer Standardstrategie.

Da die Experimente in KAPITEL 3.5 nur mit regulärer Temperaturintegration und mit lediglich 0 °C *DIF* durchgeführt wurden, ist die Strategie in KAPITEL 3.6 zu –6 °C und –12 °C erweitertert worden. Weiterhin sind die Strategien aus den vorangegangenen Kapiteln miteinander kombiniert. Das schon vorher wiederholt verwendete Gewächshausklima- und Kontrollmodell wurde hier erneut für eine Simulationsstudie verwendet. Absolut die höchsten Energieeinsparungen wurden erzielt wenn das in KAPITEL 3.1 entworfene

Temperaturregelkonzept mit der in KAPITEL 3.2 konzipierten dynamischen Luftfeuchtestrategie kombiniert wurde. Der Jahresenergieverbrauch konnte mit einer langzeit Temperaturbandbreite von nur ±2 °C mit 33 % gesenkt werden, woran die Wintermonate den grössten Anteil hatten. Relativ können jedoch mit der dynamische Steuerung im Frühjahr und Herbst die höchsten Energiemengen gespart werden. In diesen Jahreszeiten führten die dynamischen Strategien (ohne negative *DIF* Restriktion) zu einem positiven *DIF*. Wiederum zeigten Simulationen, dass es möglich ist, Energie zu sparen und gleichzeitig ein negativen *DIF* zu erzielen. Die *DIF* Restriktionen führten allerdings erneut zu verringerten Energiesparmöglichkeiten des modifizierten Temperaturintegrationregimes aus KAPITEL 3.1.

Temperaturintegration und eine negative *DIF* Einstellung können nur gleichzeitig angewendet werden wenn eine verringerte Energieeinsparung in Kauf genommen wird. Andererseits führt eine pure Temperaturintegrationssteuerung zu einer Zunahme von chemischen Wachstumshemmern im Chrysanthemenanbau. Weil sowohl CO_2 Emissionen und Chemikalien gleichermassen verringert werden sollten, besteht ein Optimierungsproblem. Dieses konnte in der hier vorliegenden Dissertation nicht gelöst werden.

Im Jahre 2001 war der zu Beginn erwähnte Energieeffizienzindex 52 % des Wertes von 1980. Um das gesteckte Ziel (35 % des Wertes von 1980) zu erreichen muss der Index bis zum Jahre 2010 weitere 17 % sinken. Ein grosser Teil (10 %) kann mit der geschätzten Standardentwicklung in der Gewächshaustechnik erreicht werden. Der restliche Teil könnte mit den hier vorgestellten Klimaregelstrategien leicht erreicht werden, so dass im Prinzip die dynamische Luftfeuchteregelung (KAPITEL 3.2) ausreichend wäre. Bei dieser Strategie spielt das Optimierungsproblem zwischen *DIF* und Temperaturintegration keine Rolle. Die Praxisimplementation dieser Strategie verlangt jedoch eine hohe Anbauerakzeptanz. Weil viele Anbauer hierbei allerdings zögerlich sind, ist zusätzliche Arbeit im Technologietransfer notwendig. Erst wenn dynamische Regelstrategien in der Praxis weiträumig Akzeptanz finden, können die hier vorgestellte Strategien ausgebaut und in die Praxis implementiert werden. Erst dann wird diese Arbeit als Beitrag zur Energieeinsparung im Gewächshausgartenbau gesehen werden können.

CURRICULUM VITAE (NEDERLANDS)

Oliver Körner werd op 12 september 1971 in Hannover, Duitsland, geboren. Nadat hij zijn VWO diploma in het voorjaar van 1992 behaalde aan het *Ganztagsgymnasium Barsinghausen*, begon hij in het zelfde jaar aan de studie tuinbouwplantenteelt aan de Universiteit Hannover. Het kandidaatsexamen (*Vordiplom*) met de vakken biometrie, bodemkunde, communicatie theorie en plantengenetica werd in het najaar 1994 behaald. Daarnaar werkte hij zes maanden aan teelt en selectie methodieken van kiwifruit aan het *Mount Albert Research Centre* in Auckland, Nieuw Zeeland. Later werkte hij ook aan verschillende onderzoeksprojecten om wetenschappelijke werkervaring op te doen, bijvoorbeeld aan het effect van verhoogd CO_2 op bladmorfologie aan het *Department of Plant Sciences* van de *Cornell University* in de VS (juli – september 1996); operations research en bedrijfskunde aan de vakgroep tuinbouweconomie van de Universiteit Hannover (oktober 1995 – juli 1996) en met verschillende projecten aan de vakgroep Groenteelt van deze universiteit (oktober 1996 – maart 1998). Verder heeft hij inzicht gekregen in technisch engineering via het *Institut für Stadthydrologie* (instituut voor stadshydrologie) te Hannover (oktober 1996 - maart 1998). Zijn doctoraalexamen met de bijvakken fruitteelt en planten genetica en hoofdvakken biometrie, systeemtheorie, groenteelt en bedrijfskunde van de Universiteit Hannover behaalde hij in oktober 1998. Zijn studie werd met een zes maanden durend afstudeervak (van april tot september 1998) aan de toenmalige vakgroep Tuinbouwplantenteelt van de toenmalige Landbouwuniversiteit Wageningen afgerond. Tussen januari 1999 en maart 2003 was hij werkzaam aan deze universiteit (nu Wageningen Universiteit) aan de vakgroep Agrarische Bedrijfstechnologie binnen het departement Agrotechnologie en Voedingswetenschappen. De resultaten van het onderzoek dat hij gedurende deze aanstelling uitvoerde, zijn geïllustreerd in dit proefschrift.

Sinds april 2003 werkt Oliver Körner als onderzoeker aan Den Kgl. Veterinær og Landbohøjskole (Koninklijke Veterinair en Landbouwuniversiteit) in Kopenhagen, Denemarken.

238

CURRICULUM VITAE (ENGLISH)

Oliver Körner was born in Hanover, Germany, on 12th September 1971. After he finished high school at the *Ganztagsgymnasium Barsinghausen* in spring 1992, he started studying horticultural sciences at the University of Hanover, Germany, in the same year. The B.Sc. level was attained in 1994 with majors in biometry, soil science, communication theory, and genetics and plant breeding. After that, he worked for six months on breeding and selection methods of kiwifruit species at the Mount Albert Research Centre in Auckland, New Zealand. He also worked in several research projects to gain scientific work experience as e.g. on the effect of elevated CO_2 on leaf morphology at the Department of Plant Sciences at Cornell University, Ithaca, NY, USA (July – September 1996); operations research and business administration at the Department of Horticultural Economics at University of Hanover (October 1995 – July 1996); and within several projects at the Department of Vegetable Sciences at University of Hanover (October 1996 – March 1998); he also got some insight into technical engineering with the *Institut für Stadthydrologie* (Urban Hydrological Engineering Society) in the same town (October 1996 - March 1998). His M.Sc. in Horticultural Sciences from University of Hanover was completed in 1998 with minors in pomology and plant genetics; and majors in biometry, systems theory, vegetable science and management in organisations. The final six months of his study were completed with his M.Sc. – thesis at the Department of Horticulture at the Wageningen Agricultural University, The Netherlands. Between January 1999 and March 2003 he was employed by the same University (now called Wageningen University) working in the Department Agrotechnology and Food Sciences with the Farm Technology Group. Results of his research during this time are illustrated in this thesis.

Currently since April 2003, Oliver Körner is researching at the Royal Veterinary and Agricultural University in Copenhagen, Denmark.

PRESENT ADDRESS OF THE AUTHOR

The Royal Veterinary and Agricultural University
Department of Agricultural Sciences
Section Horticulture
Højbakkegård Allé 21
2630 Taastrup
Denmark

240